

# **Radiocarbon Dating of Kimberley Rock Art**

**Damien Geoffrey Finch**

**ORCID: 0000-0002-9447-5685**

**Submitted in total fulfilment of  
the requirements of the  
degree of Doctor of Philosophy**

**September 2020**

**School of Earth Sciences**

**The University of Melbourne**

## **Abstract**

Throughout the world, ancient rock art records some of the earliest attempts at complex human communication. However, constraining the age of older rock art has remained a largely intractable scientific problem thereby limiting our ability to integrate rock art into the rest of the archaeological record.

Researchers have studied the globally significant Aboriginal rock art in the Kimberley region of Western Australia for more than 40 years and have comprehensively documented a sequence of rock art stylistic periods. It has long been thought that the oldest styles in this sequence date back to the Pleistocene but only two such dates, relating to identifiable motifs, have been published and both are problematic.

The surviving pigment in paintings of all but the most recent Kimberley rock art style contains no material that can be radiometrically dated. There are, however, mineral accretions and mud wasp nests in the same Kimberley rock shelters that house rock art and, occasionally, these under or overlie paintings. This study explores the development of radiocarbon dating techniques to reliably date remnant mud wasp nests found to be in contact with rock art.

Recently constructed mud wasp nests were collected and analysed to understand the source and age of carbon-bearing material they contain. Unburned plant material and charcoal were found in similar volumes, but charcoal is the carbon-bearing constituent most likely to provide a reliable radiocarbon age for old nests. Old wasp nests were analysed using a wide range of techniques to determine how taphonomic processes alter their physical and chemical composition. These results guided experimentation with pretreatment methods designed to remove sources of carbon contamination while preserving as much of the carbon in the original charcoal as possible. A total of 120 old mud wasp nests were prepared for radiocarbon dating of which 75 contained sufficient carbon for measurement. The distribution of the 75 ages indicated nests were built quasi-continuously over, at least, the last 20,000 years.

The motifs in contact with the 75 nests were classified into one of the six main Kimberley rock art stylistic periods by two subject matter experts. Just 3 nests overlay motifs from each of the Cupules and Wanjina periods suggesting only that some motifs in these styles are older than 7,200 years and 500 years, respectively. The 4 dates available for each of the Static Polychrome and Painted Hand periods permit a very tentative hypothesis for their chronology while the 16 dates relating to Irregular Infill Animal Period (IIAP) motifs and the 20 dates for Gwion motifs provide a more secure estimate.

The concise hypothesis proposed for the chronology of the Kimberley rock art styles is that the IIAP style was in use from at least 17,000 to 13,000 years ago. It was followed by the Gwion period from 13,000 – 12, 000 years ago and then the Static Polychrome period 11,000 to 9,000 years ago. The Painted Hand period followed at around 8,500 to 9,000 years ago.

## **Declaration**

This is to certify that

- (i) the thesis comprises only my original work towards the PhD except where indicated in the preface;
- (ii) due acknowledgement has been made in the text to all other material used;
- (ii) the thesis is fewer than the 100,000 words in length, exclusive of tables, maps, bibliographies and appendices

---

Damien Geoffrey Finch



## Preface

This thesis contains material that is published and material that has been submitted for publication.

Chapter 2 was published by *Quaternary Geochronology* on 5<sup>th</sup> March 2019:

**Finch, D.**, A. Gleadow, J. Hergt, V. A. Levchenko and D. Fink (2019). "New developments in the radiocarbon dating of mud wasp nests." *Quaternary Geochronology* **51**: 140-154, doi:10.1016/j.quageo.2019.02.007.

Chapter 3 was published by *Science Advances* on 5<sup>th</sup> February 2020:

**Finch, D.**, A. Gleadow, J. Hergt, V. A. Levchenko, P. Heaney, P. Veth, S. Harper, S. Ouzman, C. Myers and H. Green (2020). "12,000-Year-old Aboriginal rock art from the Kimberley region, Western Australia." *Science Advances* **6**(6):eaay3922, doi:10.1126/sciadv.aay3922.

Chapter 4 was submitted to *Nature Human Behaviour* on 13<sup>th</sup> July 2020 and sent out for peer review on 15<sup>th</sup> July 2020:

**Finch, D.**, A. Gleadow, J. Hergt, P. Heaney, H. Green, C. Myers P. Veth, S. Harper, S. Ouzman and V. A. Levchenko (2020). "Ages for Australia's oldest rock paintings."

The contributions of co-authors for Chapter 2 were provided to the journal as a "Credit author statement" at the time of submission and are as recorded below:

**Damien Finch:** Methodology, Conceptualization, Resources, Investigation, Formal Analysis, Writing - Original Draft, Writing - Review & Editing. *Andrew Gleadow:* Funding acquisition, Resources, Project administration, Supervision, Writing – Review & Editing. *Janet Hergt:* Funding acquisition, Resources, Supervision, Writing – Review & Editing. *Vladimir Levchenko:* Methodology, Investigation, Resources, Formal Analysis, Project administration, Supervision, Writing – Review & Editing. *David Fink:* Funding acquisition, Methodology, Resources, Formal Analysis, Project administration, Supervision

The co-author contributions for Chapters 3 and 4 are as noted in the "Authors contributions" section of those manuscripts. The contributions of University of Melbourne supervisors Prof. Andrew Gleadow and Prof. Janet Hergt and ANSTO supervisor Dr Vladimir Levchenko were those normally provided by advisors to a

PhD student, including logistical and financial support, assistance during field work, assistance during data acquisition and interpretation, discussions on research strategy and comments on written work. The research design, execution, sample collection, sample processing (up to combustion stage), calibration and interpretation of results, statistical modelling, and writing of the manuscripts was the work of the present author.

The candidate is the sole author of all other chapters which are unpublished material apart from the publications listed below and included as appendices.

Appendix 3 includes details of three co-authored publications. The first was published by the Journal of Archaeological Science: Reports on 18<sup>th</sup> July 2017. The present author performed the mineralogical analysis of the X-ray Diffraction data.

Green, H., A. Gleadow, **D. Finch**, J. Hergt and S. Ouzman (2017). "Mineral deposition systems at rock art sites, Kimberley, Northern Australia - Field observations." Journal of Archaeological Science-Reports **14**: 340-352, doi: 10.1016/j.jasrep.2017.06.009.

The second paper was published by Data in Brief on 18<sup>th</sup> July 2017. The present author provided the mineralogical analysis of the XRD data.

Green, H., A. Gleadow and **D. Finch** (2017). "Characterisation of mineral deposition systems associated with rock art in the Kimberley region of northwest Australia." Data in Brief, doi: 10.1016/j.dib.2017.08.029

The third paper was published by the Journal of Archaeological Method and Theory on 2<sup>nd</sup> August 2020. The present author identified a suitable wasp nest sample under relevant rock art, collected the sample (D755, OZW423U2), performed sample pretreatment and interpreted the radiocarbon age.

Delannoy, J.-J., B. David, K. Genuite, R. Gunn, **D. Finch**, S. Ouzman, H. Green, P. Veth, S. Harper and R. J. Skelly (2020). "Investigating the Anthropic Construction of Rock Art Sites Through Archaeomorphology: the Case of

Borologa, Kimberley, Australia." Journal of Archaeological Method and Theory: 1-39, doi: 10.1007/s10816-020-09477-4.

This research was funded by Australian Research Council Linkage Projects LP130100501 and LP170100155 and co-funded by the Kimberley Foundation Australia and Dunkeld Pastoral Co Pty Ltd. The author was supported by an Australian Postgraduate Award and an AINSE Post Graduate Research Award. The Kimberley Foundation provided additional funding for equipment to establish a radiocarbon pretreatment facility at the University of Melbourne.

## Acknowledgements

It was the Kimberley rock art itself that prompted me to start this PhD journey. Like many other visitors to the Kimberley, I was awestruck when I first saw these ancient paintings 10 years ago. So, first of all, I acknowledge the artists, the First People of Australia. I would defy even the most cynical to stand in the same place they stood and to look at what they created, without wondering who they were and what they wanted to say (and when!). It is a very great privilege to work in those same rock shelters with the descendants of the artists, the Dambimangari and Balanggarra/Kwini people. In particular, the senior elders Augustine Unghango and Ambrose Chalarimeri who placed their trust in a bunch of crazy scientists from the other side of the continent. It was also a privilege and a delight to spend time on country with the younger Balanggarra Traditional Owners and future leaders particularly Ian Waina, Scott and Adrian Unghango, Gareth, Ethan and Lucas Karadada, and Uriah Waina. I am also grateful for the help and support of Donny and Kenny Woolagoodja, and Wayne Oobagooma on Dambimangari land.

It was a courageous individual, Russell Willis, that I thank for being brave enough to lead small groups of (sometimes less experienced!) bushwalkers into some of the most remote parts of the Kimberley. After two of Russell's Kimberley "Walkabouts" I was so intensely curious to know more that I spent a couple of years studying Archaeological Science at ANU where Tony Barham, Sue O'Connor, Tristen Jones, Sally Brockwell, Uli Troitzsch and Rainer Grun gave so generously of their expertise, enthusiasm and support. These early mentors then introduced me to other leaders in Australian archaeology who were equally generous and supportive: thank you Peter Veth, Jill Huntley, Darrell Lewis, Bert Roberts, Max Aubert and Jo McDonald.

Having formed the view that we know too little about all but the most recent few hundred years of the history of people in Australia, I sought out opportunities to uncover some more answers. A bit of luck always helps: my lucky break came when Andy Gleadow and Janet Hergt courageously agreed to supervise me as a somewhat unconventionally qualified PhD candidate. While I started with a clear idea of what I wanted to do, I had no idea of how to make it happen. Fortunately for me, Andy and

Janet are two of the most experienced science researchers and teachers in the country and were up for the challenge. Janet and Andy's wise council and very gentle nudges helped bring me back on track as I journeyed through the often difficult terrain that is a PhD research project. Together with my ANSTO supervisor, Vlad Levchenko, they have demonstrated great patience and I am most grateful for their enduring support.

Fieldwork in the Kimberley is logistically challenging and not without significant risks. Helen Green has led the charge for the UoM team in the 7 field trips undertaken since we started in 2015. We were most fortunate to have unwavering assistance in the field from the Dunkeld Pastoral Company represented by the wonderful Susan Bradley, Cecilia Myers, and staff at Theda and Doongan Stations. Our fieldwork was only possible with the best of support from our Camp Manager Paul Hartley as well as Nick Sundblom, Robin Maher, Sue Ball, Peter Turnbull, Joc Schmiechen, Traudl Tan, Michi Maier and Peter Kendrick. Special thanks also to the UWA archaeologists who recorded the field context of many of our samples, particularly Peter Veth, Sven Ouzman and Sam Harper.

After 5 years of fieldwork for the Rock Art Dating team there is a small group, the *RADicals*, that have spent months together scrambling around rock shelters looking for samples, eating lunch too early, and re-inventing song lyrics. Thanks to my fellow *RADicals* for the best of times: C Myers, Pauline Heaney, Helen Green, Nick Sundblom, Paul Hartley and Ian Waina.

Like most other PhD candidates, I relied heavily on the deep technical expertise of research staff and laboratory specialists provided so generously by Abaz Alimanovic, Jon Woodhead, Alan Greig, Liz Goodall, Jay Black and Graham Hutchinson at the University of Melbourne and Alan Williams, Fiona Bertuch and Bin Yang at ANSTO.

My immediate and extended family have been somewhat abandoned as I pursued this quest but have always provided support when it was needed most. None more so than my wife Kryz. In our partnership of 40 years we have tackled all manner of challenges together; this is our latest.

# Table of contents

<b>Abstract .....</b>	<b>ii</b>
<b>Declaration .....</b>	<b>iv</b>
<b>Preface .....</b>	<b>v</b>
<b>Acknowledgements .....</b>	<b>viii</b>
<b>Table of contents .....</b>	<b>x</b>
<b>List of figures.....</b>	<b>xv</b>
<b>List of tables .....</b>	<b>xvii</b>
<b>Chapter 1 Introduction .....</b>	<b>1</b>
1.    The research rationale .....	1
1.1    Previous research .....	5
1.2    Research aims .....	13
1.3    Approach.....	14
1.3.1    Fieldwork planning.....	14
1.3.2    Site and sample selection.....	15
1.3.3    Mineralogical analysis .....	16
1.3.4    Elemental analysis .....	17
1.3.5    Sample pre-treatment.....	17
1.3.6    Radiocarbon dating.....	17
1.3.7    Documentation, Analysis and Interpretation of results .....	17
1.4    Thesis outline .....	17
1.5    References .....	20
<b>Chapter 2 Development of radiocarbon dating method for mud wasp nests ....</b>	<b>26</b>
2.1    Abstract .....	27
2.2    Introduction.....	28
2.3    Approach.....	29
2.4    Methods.....	30
2.4.1    Field sampling .....	30
2.4.2    Mineralogical and Elemental Analysis.....	30
2.4.3    Physical pretreatment.....	31

2.4.4	Chemical pretreatment.....	32
2.5	Results.....	34
2.5.1	Modern mud wasp nests .....	34
2.5.2	Old mud wasp nests .....	38
2.6	Discussion .....	53
2.6.1	Charcoal as a target for dating nests .....	53
2.6.2	Alternative Methods .....	55
2.6.3	Sources of uncertainty .....	56
2.6.4	Anomalous results .....	56
2.6.5	Age distribution of dated nest samples .....	57
2.7	Conclusion .....	59
2.8	Acknowledgements .....	61
2.9	References .....	62
2.10	Supplementary Information .....	67
2.10.1	Routine methods .....	67
2.10.2	Micro-CT scan of old wasp nest.....	68
2.10.3	Calibrated radiocarbon dates for modern wasp nest fractions.....	70
2.10.4	Modern wasp nest AMS measurements .....	71
2.10.5	References – Supplementary Information .....	73
	<b>Chapter 3 Radiocarbon age estimates for the Gwion Period .....</b>	<b>74</b>
3.1	Abstract .....	75
3.2	Introduction.....	76
3.3	Results.....	79
3.3.1	Age constraints for Gwion motifs.....	79
3.4	Discussion .....	81
3.4.1	Theoretical determination of art periods.....	81
3.4.2	Age range hypothesis for the Gwion style.....	83
3.4.3	Allowance for inbuilt age of charcoal .....	85
3.5	Results in context .....	87
3.6	Materials and Methods.....	89
3.6.1	Sample collection.....	89
3.6.2	Radiocarbon age measurements .....	90
3.6.3	Motif classification .....	91

3.6.4	Probability functions for motif ages .....	92
3.7	Acknowledgements .....	94
3.7.1	Funding .....	94
3.7.2	Author contributions .....	94
3.7.3	Competing interests: .....	95
3.7.4	Data and materials availability .....	95
3.8	Supplementary Materials: .....	96
3.8.1	Figure 3-S1 Relationship between age of nest and associated motif...96	
3.8.2	Text 3-S1. Calibrated age modelling code .....	96
3.8.3	Figure 3-S2. Photographs and illustrative interpretations .....	98
3.8.4	Table 3-S1. Radiocarbon age determinations on wasp nests.....	100
3.8.5	Table 3-S2. Radiocarbon pretreatment methods and ages.....	102
3.9	References .....	104
<b>Chapter 4 Radiocarbon age estimates for the Irregular Infill Animal Period</b>		<b>108</b>
4.1	Abstract: .....	109
4.2	Introduction .....	110
4.3	Results .....	113
4.3.1	Minimum age constraints .....	114
4.3.2	Maximum age constraints .....	116
4.3.3	Reliability considerations .....	118
4.3.4	Age bracket for macropod motif.....	119
4.4	Hypothesised IIAP age range.....	122
4.5	Conclusions .....	124
4.6	Acknowledgements: .....	127
4.6.1	Funding .....	127
4.6.2	Authors contributions: .....	127
4.6.3	Data and materials availability .....	128
4.7	Methods: .....	129
4.7.1	Sample Collection.....	129
4.7.2	Motif Classification .....	129
4.7.3	Sample Preparation and Age Measurement.....	129
4.7.4	Statistical Model and Code .....	130
4.8	Supplementary Information .....	132



4.9	References .....	139
<b>Chapter 5 Radiocarbon age estimates for the Cupule and more recent art periods 144</b>		
5.1	Introduction .....	144
5.2	Cupules and Grooves .....	145
5.3	Possible IIAP motifs .....	147
5.4	Possible Gwion motifs .....	149
5.5	Static Polychrome motifs .....	150
5.6	Painted Hand motifs .....	153
5.7	Wanjina motifs .....	155
5.8	Motifs of indeterminate style .....	156
5.9	Conclusion .....	156
5.10	Supplementary Data .....	160
5.11	References .....	162
<b>Chapter 6 Modelling the chronology of the Kimberley rock art sequence .....163</b>		
6.1	Modelling art period chronologies .....	163
6.1.1	Using wasp nest dates as age constraints.....	163
6.1.2	Modelling different sample sizes.....	167
6.1.3	Modelling for declining nest volume with age .....	168
6.1.4	Modelling with a small number of wasp nest ages.....	170
6.1.5	What is a “good” estimate?.....	174
6.2	A hypothesis for the chronology of the Kimberley rock art sequence.....	175
6.3	References .....	179
<b>Chapter 7 Conclusion.....180</b>		
7.1	Mud wasp nests - observations .....	180
7.1.1	Modern mud wasp nests .....	180
7.1.2	Old mud wasp nests .....	181
7.1.3	Field sampling .....	182
7.2	Radiocarbon pretreatment.....	182
7.2.1	Physical pretreatment.....	183
7.2.2	Chemical pretreatment.....	183
7.2.3	Reliability Score .....	183
7.3	Radiocarbon age measurements.....	184

7.4	Motif classification .....	184
7.5	Modelling rock art periods from wasp nest dates .....	185
7.6	Hypothesised Kimberley rock art sequence chronology.....	186
7.7	Future work .....	189
7.8	References .....	191
<b>Appendix 1 Photographs of the sampled motifs, .....</b>		<b>192</b>
<b>Appendix 2 Tables of radiocarbon measurements of old wasp nests .....</b>		<b>205</b>
<b>Appendix 3 Additional published work.....</b>		<b>213</b>

# List of figures

Figure 1-1 Map Kimberley region of Western Australia.....	2
Figure 1-2 Kimberley Rock Art Styles .....	3
Figure 1-3 Multi-generational mud wasp nests.....	10
Figure 2-1 Light fraction of a typical modern wasp nest.....	35
Figure 2-2 Nest diagenesis for two of the most common wasp species .....	39
Figure 2-3 High density wasp nest areas. ....	40
Figure 2-4 Mineralised wasp nest stump .....	41
Figure 2-5 Distribution of Ca, K, P and S in a mineralised nest.....	42
Figure 2-6 SEM imaging of D018 .....	43
Figure 2-7 Histogram of the mass, as collected, of all old wasp nests .....	46
Figure 2-8 Mass of sample combusted vs carbon mass after combustion. ....	47
Figure 2-9 Median calibrated age of wasp nest samples .....	53
Figure 2-10 Calibrated ages for nests from site DR015.....	59
Figure 2-S1 Mineralised wasp nest sample D459.....	69
Figure 2-S2 Calibrated radiocarbon date ranges for Modern Wasp Nests .....	70
Figure 3-1. Mud wasp nest samples and their development sequence .....	78
Figure 3-2. Summary of Gwion related ages .....	80
Figure 3-3. Hypothetical ages of nests overlying and underlying motifs .....	82
Figure 3-4. Gwion motif age ranges. ....	84
Figure 3-5. Probability distributions for age constraints for Gwion motifs.....	85
Figure 3-6. Hypothesised age range for the Gwion style.....	87
Figure 3-S1. Histogram of ages of 75 mud wasp nests.....	96
Figure 3-S2. Photograph and illustration of dated Gwion motifs .....	98
Figure 4-1. Map of Kimberley showing coastline change over time.....	112
Figure 4-2. Minimum ages for 10 motifs from overlying wasp nest ages. ....	115

Figure 4-3. Maximum ages for 5 motifs from 6 underlying was nest ages. ....	117
Figure 4-4. Macropod motif DR015_10 .....	120
Figure 4-5. Calibrated ages used to constrain age for motif DR015_10.....	122
Figure 4-6. Age constraints for IIAP motifs. ....	124
Figure 4-S1. Dated IIAP motifs (excluding DR015_10) .....	136
Figure 4-S2. Context for boomerang stencil motif DR013-09 .....	137
Figure 4-S3. Macropod motif DR015_10 sample locations. ....	138
Figure 5-1 Mud wasp nests inside grooves and cupules.....	146
Figure 5-2 Possible IIAP motifs and associated age constraints .....	148
Figure 5-3 Possible Gwion motifs and associated age constraints .....	150
Figure 5-4 Static Polychrome possible motifs - locations and ages .....	151
Figure 5-5 Painted Hand possible motifs - locations and ages .....	154
Figure 5-6 Wanjina motifs - locations and ages .....	155
Figure 5-7 Motifs of indeterminate style - locations and ages.....	156
Figure 5-8 Age constraints for older motif styles. ....	158
Figure 5-9 Age constraints for younger motif styles .....	159
Figure 6-1 Probability density functions representing possible age ranges.....	164
Figure 6-2 Spdfs derived from randomly generated ages of 1000 nests.....	166
Figure 6-3 Spdfs from different sized sets of randomly generated nest ages .....	168
Figure 6-4 Age distribution of 2000 nests with ages randomly generated .....	169
Figure 6-5 Fifteen sets of Spdfs from 12 over- and 5 under-art nest ages.....	170
Figure 6-6 Gaps/overlaps from 100 simulations - art period 11 – 9 ka, .....	172
Figure 6-7 Gaps/overlaps from 100 simulations - art period 10.1 – 9.9 ka .....	173
Figure 6-8 Hypothesised chronology of the Kimberley rock art sequence.....	178
Figure 7-1 Hypothesised chronology of the Kimberley rock art periods .....	188

# List of tables

Table 2-1 Analysis of carbon in modern wasp nests .....	35
Table 2-2 Radiocarbon ages for modern wasp nests.....	37
Table 2-3 Major elements, in weight % oxides, from XRF analysis.....	44
Table 2-4 Percentage weight of carbon and sulphur in old wasp nests .....	45
Table 2-5 Old wasp nests with multiple analysed fractions.....	48
Table 2-6 Old wasp nests with multiple dated fractions.....	49
Table 2-7 Dated modern and ancient carbon pseudo-nest samples .....	51
Table 2-S1 Radiocarbon measurements for modern wasp nest .....	71
Table 2-S2 Mineral composition of old wasp nests - XRD results.....	72
Table 3-S1. Radiocarbon ages for nests associated with Gwion motifs .....	101
Table 3-S2. Radiocarbon pretreatment methods and ages (uncalibrated) .....	103
Table 4-1. Calibrated radiocarbon ages for macropod motif DR015_10 .....	119
Table 4-S1. Radiocarbon age measurements associated with IIAP motifs.....	133
Table 4-S2. Stylistic classification of IIAP motifs .....	134
Table 5-1 Stylistic classification of 24 motifs .....	145
Table 5-2 Radiocarbon pretreatment and carbon isotope measurements .....	160

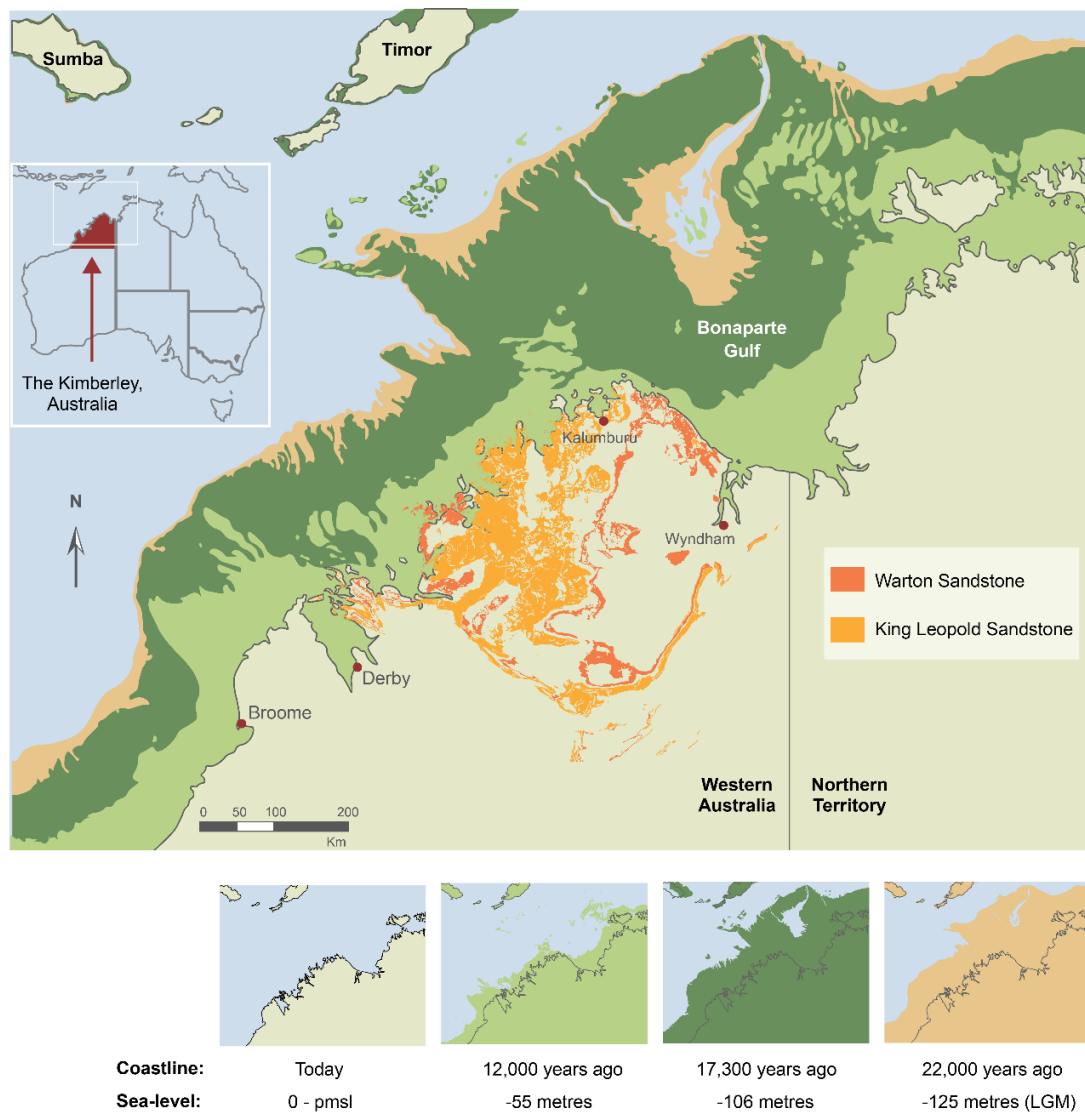
# **Chapter 1 Introduction**

## **1.1 The research rationale**

Strong claims have been made for both the antiquity and archaeological importance of rock art in the Kimberley region of Western Australia (Figure 1-1). Even with limited scientific research into Kimberley rock art to date, some researchers have concluded that it represents one of the greatest concentrations of rock art in the world (Aubert 2012: 573) and that it is the oldest rock art in the world (Morwood 2002: 19). Others argue that northern Australian rock art is also the world's most complex repertoire (Watchman 1998: 67, Flood 2004: 166).

While the relative chronological sequence of Kimberley rock art styles is still being refined to accommodate Aboriginal preferences for nomenclature and the findings from more recent field observations, there is broad agreement with the sequence proposed by Grahame Walsh in his major publications (1994a, 2000). A simplified version of the main styles, with more modern nomenclature, is shown as Figure 1-2.

Archaeological excavations in the Kimberley have established that ochre was being used in the earliest stages of human occupation of Australia about 40,000 years ago (O'Connor and Fankhauser 2001). Some 700 kilometres to the east, in Arnhem Land, an excavated rock fragment, that may have been part of a painted or drawn charcoal motif, was dated to around 28 ka (David et al. 2012) so there is reason to believe that rock painting was a cultural practice in the region during the Pleistocene. There is, however, very little direct evidence of paintings that have survived from that time. One review of rock art dating in Australia came to the conclusion that "there is still a dearth of reliably dated rock art from Australia." (David et al. 2013: 8). An earlier review focussed on the Kimberley region and concluded that "at the moment, there is no substantial evidence to support a Pleistocene age for the rock art." (Aubert 2012: 577). This lack of progress is not because the subject is considered to be of little consequence, rather, the challenge is the inability to date artwork directly and a need to date bracketing events with improved precision and accuracy.



**Figure 1-1** Kimberley region of Western Australia showing the coastline today (0 present mean sea level – pmsl), at 12 ka, at 17.3 ka and at 22 ka during the Last Glacial Maximum (LGM)(Whiteway 2009, Williams et al. 2018). The main rock art sites are found on the Warton and King Leopold Sandstone geological units (Donaldson 2007, White and Ferland 2015).



### Pecked Cupule

Also called: Rock Markings, *Pit & Groove Period*.



### Irregular Infill Animal

The earliest visible Kimberley rock art paintings

Also called: *Archaic Period*, *Irregular Infill Animal Period*.



### Gwion

Also called: *Kujon*, *Kira Kiro*, *Diangargun*, *Bradshaws*.



### Static Polychrome

Also called: *Wararrajai*, *Missing/Straight Part*, *Clothes Peg Figures*.



### Painted Hand

Also called: *Clawed Hand*, *Compartment Infill Period*.



### Wanjina

Also called: *Regular Infill Period*, *Polychrome Art Period*.

**Figure 1-2** Kimberley Rock Art Styles from oldest (top) to youngest (bottom).  
Adapted from Veth et. al (2017)



The late Mike Morwood stated that, in Australia, rock art is the most common surviving evidence of symbolic systems that we cannot ignore if we want to understand how cultures have developed here (2002: xi). One model, seeking to explore the evolution of human cultural capacities, positions figurative art as an example of the highest order of cultural capacity that reliably transmits cultural concepts from one generation to the next (Haidle et al. 2015:61). An example of the potential impact of rock art dating is the 40 ka minimum age estimate for rock art in Sulawesi (Aubert et al. 2014). For the first time, this evidence challenged the prevailing view that figurative rock painting originated in Europe. It allows the possibility that this high order cultural capacity may have originated in Africa before *Homo sapiens* began migrations to Europe and Asia. Alternatively, this capacity may have developed independently in Europe and Southeast Asia and, perhaps, other places including Australia (Aubert et al. 2014: 226, Tacon et al. 2014: 1062). Dating of the earliest Australian figurative rock art could also make a significant contribution to the study of human evolution (Roebroeks 2014) and would help to address some unsupported speculation about the origin of Kimberley rock art that arises from time to time.

In the wider community, there is an appetite for interpretations of rock art and its antiquity. Unfortunately, in the absence of facts, some have speculated wildly. Wilson recalls the widespread publicity given to popular writer, Erich von Daniken, who claimed in the 1970's that figures in Kimberley paintings in the Wanjina style were extra-terrestrials (2006: 16). More serious is the controversial interpretation of the provenance of Gwion period paintings from the Kimberley as being "non-Aboriginal". Motivation for such interpretations has been attributed to a desire to disassociate modern Aboriginal people from the paintings as part of a political process to oppose Native Title land claims (McNiven 2011). In spite of a lack of evidence to support this notion of "non-Aboriginal" authorship it arose again more recently in the context of the debate about the proposal to recognise First Australians in the Australian Constitution. Senator David Leyonhjelm made the erroneous assertion that some anthropologists had cast doubt over whether Australian Aboriginals were the first occupants of Australia (Westaway 2015, Yaxley 2015).

Watchman (1998: 67) takes a more positive outlook and points to the importance of establishing the origins of Aboriginal artistic traditions for the relevance it would have to “Aboriginal identity and heritage issues”. More specifically, they note that establishing reliable chronologies is not just a question of solving a scientific riddle, but that it is a chance to establish “...the antiquity of the specifically Aboriginal vision of the world, as encoded in their own rock paintings and engravings”. Firm chronologies would be of great benefit, more generally, to help communicate the depth of this cultural heritage to the non-Aboriginal population.

Only when the ages of individual phases in the Kimberley rock art sequence are quantitatively dated, will it be possible to integrate this powerful evidence of Aboriginal cultural activity into the archaeological, and palaeoenvironmental record with confidence.

## **1.2 Previous research**

The stylistic chronology established for Kimberley rock art describes a rich and varied body of petroglyphs (pounded, abraded, engraved, or drilled grooves and holes) and pictographs (paintings, drawings, stencils, beeswax figures) created over thousands of years (Welch 1993, Walsh 1994b: 71, Walsh 2000: VIII). One small, more recent part of the sequence contains figures executed with carbon-bearing material such as beeswax or charcoal but most motifs are painted using red, yellow and white ochres that contain no significant concentrations of carbon (Watchman 1997, Ward et al. 2001). This literature review, therefore, considers the previous application of radiocarbon dating techniques to this type of rock art and, in particular, research into radiocarbon dating of carbon-bearing material that is found to under or overlie rock art.

No dating technique has so far been successfully applied to a range of motifs from any of the older Australian rock art styles. A 2010 survey counted 432 direct dates from 92 sites published for Australian rock art (Langley and Tacon 2010). Almost half of the dates are for beeswax figures, probably because they are one of the few types amenable to radiocarbon dating. The earliest recorded beeswax figures are from Arnhem Land and the Kimberley at around 4000 BP (Aubert 2012: 574). The record is biased toward the present because beeswax becomes more brittle with age and is

unlikely to survive on exposed rock surfaces (Langley and Tacon 2010: 72, David et al. 2013: 4). Langley and Tacon state that just 37 of the ages obtained were in the Pleistocene (2010: 72); a conclusion very much at odds with that of Aubert (2012) for the Kimberley. Unfortunately, details are provided on only a few of the 37 dates so it is not possible to reconcile the different accounts, but there is certainly ongoing debate about even these few.

While it is generally agreed that the Carpenter's Gap site in the Kimberley is one of the sites establishing human occupation of Australia prior to 40,000 years ago (Hiscock 2008: 34) there is less agreement that "this is the earliest evidence for rock art anywhere in the world" (Morwood 2002: 19) or at least in Australia (Flood 2004: 7). The debate about a piece of painted slab found in between strata radiocarbon dated to  $33,600 \pm 500$  BP (above) and  $42,800 \pm 1850$  BP (below) centres around what constitutes evidence of art rather than the accuracy of the ages. Even if it is accepted that the paint is an allochthonous ochre, this is not sufficient for Aubert: "a robust interpretation of Pleistocene rock art would require a recognisable motif as ochre was not exclusively used to produce rock art" (2012:574). On this basis, the 3 cm rock fragment offered as evidence by David et. al. (2012) is also insufficient to justify their claim that it represents the "oldest confirmed pictograph in Australia." Excavated fragments containing pigment will always be contentious unless they can be directly matched to a motif still evident on the shelter wall or they are large enough to contain an unambiguously non-utilitarian anthropic design.

Another long running debate in the dating of rock art relates to early work in the Kimberley, using optically stimulated luminescence (OSL) dating, published in Nature in 1997 (Roberts et al. 1997). The residual stump of a mud-wasp nest (labelled as KERC4), reported as overlying a Gwion style rock painting (formerly known as Bradshaw paintings), was dated to around 16,400 years old. Bednarik (2010: 99) dismisses the estimate as "unlikely to be correct", mainly because the style of rock art in question was believed to be in the range of 1400 – 4000 years BP, citing evidence from just one site in the north Kimberley. This misrepresents the results from that particular site in that they are qualified in the article title as being "Preliminary Results" and the conclusion the authors actually draw is that "the AMS  $^{14}\text{C}$  estimates

currently available show that early Bradshaw paintings are at least about 4000 years old – but may be much older” (Watchman et al. 1997: 25).

In Aubert’s review of Kimberley rock art dates he, too, takes issue with the KER4/5 dates, mainly on the basis that he does not believe that Roberts adequately established that the KER4 nest unambiguously overlaid the Gwion painting (2012: 575). David et al. come to the opposite conclusion: they support the OSL dates for KER4 and KER5 as representing the “oldest generally accepted age for a pigment rock image in Australia” (2013: 7).

Despite the ongoing debates, some key results are evident from this work. One is that wasp nests can survive in open Kimberley rock shelters for 20,000 to 30,000 years (Roberts et al. 1997, Yoshida et al. 2003). Another is that Watchman et al. (1997), at least, has been successful in deriving minimum age estimates on Kimberley rock art using radiocarbon dating of mineral accretions. A further observation is that great care is required when removing samples to be able to convincingly establish the relationship between the paint layer and the under or overlying accretion or nest. The ability of mud wasp nests to survive so long is one of the key reasons they have been considered for their radiocarbon dating potential. Consequently, research specifically relating to mud wasp nests is considered below before returning to the question of the dating potential of mineral accretions.

Mud wasp nests occur commonly throughout the world, so it is unsurprising that researchers have attempted to obtain radiocarbon age determinations on their organic content. Carbon can be incorporated into the nest in a number of ways. The mud collected from creeks and water holes (Naumann 1983: 137, Roberts et al. 1997) may contain pollen that has a carbon content of about 50% (Brown et al. 1989:206, Chester and Prior 2004:725). Charcoal fragments may also have been washed or blown into the same mud. Once constructed, the nest is provisioned with spiders or caterpillars and old nests may contain their fossilised remains (Smith 1979:183, Naumann 1983:135). Mineralised nests will also be subject to many of the same geochemical processes as rock shelter walls so carbon bearing mineral accretions can also be expected on the outer surface of nests in shelters where such accretions form. Of these

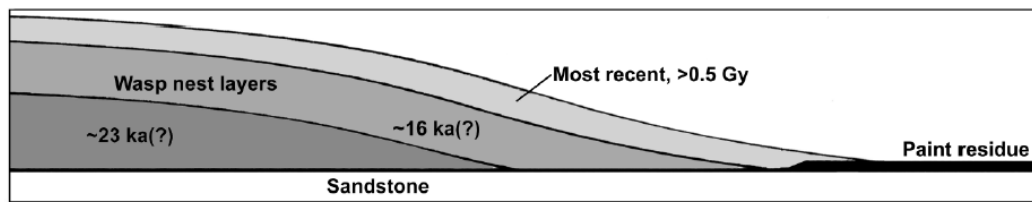
potential sources of carbon, it is pollen that has been most widely researched. Radiocarbon dating of pollen in lake sediment cores has been used in palaeoenvironmental studies. Reports vary as to how much pollen is required from these cores for radiocarbon dating. In one example, Long et al.(1992) report taking two days to manually sort 500 µg of pollen (using a microcapillary), each grain weighing between 0.01 to 0.2 µg, with 100-200 µg of carbon required for a reliable Accelerator Mass Spectrometry (AMS)  $^{14}\text{C}$  date. Where larger fossil spruce pollen are available then only 200-500 grains were required to make up the reported minimum AMS sample of 22 µg of carbon in 1989 (Brown et al. 1989:206). Researchers using smaller pine pollen required 10,000 grains to produce a sample containing the ~70 µg of carbon they considered as necessary for reliable AMS dating (Mensing and Southon 1999: 4). More recently, Neulieb et al. (2013:1145) reported that 200 – 2000 conifer pollen grains were required to make a viable sample size. The ANTARES AMS at the Australian Nuclear Science and Technology Organisation (ANSTO) in Sydney can readily process samples containing 10 µg of carbon and employing a specialised microfurnace, produce age estimates for samples containing as little as ~5 µg of carbon (Smith et al. 2010a, Smith et al. 2010b). Allowing for the wide range of figures quoted, the implication is that a minimum of a few hundred pollen grains would be required for samples processed at ANSTO.

Some experimentation in Australia suggests it may be difficult to obtain wasp nest samples that contain sufficient pollen. Two Kimberley nests, from two different nest building species (*Sceliphron laetum* and *Abispa* spp.) yielded 1-2 mg of pollen from 1 g of mud (i.e. 0.1 – 0.2%) but an indurated *Sceliphron formosum* nest contained no apparent pollen (Roberts et al. 1997: 698). The same report observed that *S. formosum* nests are those typically found overlying paintings of the older styles (1997: 699). In other research in the Kimberley, radiocarbon dating of pollen from a small nest yielded an age of ~30 ka but the authors observed that “Most small nests, however, contain insufficient pollen for AMS  $^{14}\text{C}$  dating” (Yoshida et al. 2003:1274).

The reliability of radiocarbon dating of pollen has been called into question with reports of differences found between age estimates derived using other reliable dating

techniques such as varve chronology and discrepancies between dates on pollen and  $^{14}\text{C}$  dates on botanical macrofossils found in the same part of the core (Long et al. 1992, Mensing and Southon 1999, Kilian et al. 2002, Neulieb et al. 2013). Although many potential causes are identified to account for these discrepancies, the main issue seems to be with pollen from marine sources or lake sediments in limestone areas. Pollen found in mineralised wasp nests is not subject to this type of aquatic environment but some limited potential remains for old, reworked, pollen to be mixed with mud subsequently collected by wasps in a manner analogous to pollen reworking as proposed to explain some anomalous dates from sediment cores (Neulieb et al. 2013).

Another cautionary note on dating of mud wasp nests comes from the debate mentioned previously regarding the OSL age estimate for KERC4/5. Bednarik (2014: 225) comments on nest morphology stating that “It is well known that mud-dauber wasps prefer to construct nests on the remains or stumps of pre-existing nests...” and he cites Naumann that “Mud-dauber wasps prefer to build nests on the stumps of abandoned ones (Naumann 1983)” (ibid). But Bednarik overstates Naumann’s evidence. Naumann, observed in the behaviour of one *S. laetum* wasp that “The observation (see above) of the female investigating an abandoned nest during its search for a nesting site suggests that a female is more likely to build a nest near existing nests.” (1983: 135). Aubert (2012:576) also cites Naumann observing “mud-dauber wasps prefer to build nests near existing nests and on the stumps of abandoned nests, rather than on a bare rock surface (Naumann, 1983; Waterhouse, 1991), but Waterhouse says only that “*Sceliphron laetum* tend to build their nests near existing nests...” (1991: 225). So assertions about the preference for wasps to build on top of earlier generations of nests are based on very little evidence, but if it does happen then there is the risk that samples from different parts of a wasp nest will yield different age estimates as suggested by Bednarik (2014: 225 Figure 1). Therefore, even if a particular nest is clearly observed to be over or under paint, if the sample removed for analysis is from another part of the nest, it might represent a different generation of construction and therefore have no relationship to the age of the painting (Figure 1-3).



**Figure 1-3.** From Figure 1 in Bednarik (2014:225) demonstrating the risk posed by multi-generational nests. A date based on a sample that included all layers of the nest would be much older than the age of that part of the nest overlying paint. The presumed “constraint” on the timing of the artwork would therefore be incorrect.

Apart from mud wasp nests, the other major targets for radiocarbon dating of Kimberley rock art are the mineral accretions that have formed under or over paint layers or inside petroglyphs (e.g. Green et al. 2017). There is a very large body of work published on rock coatings and their potential for palaeoenvironmental analysis, rock art dating and conservation (e.g. Dorn and Dragovich 1990, Dragovich 1994, Dietzel et al. 2008, Gorbushina and Broughton 2009, Gershtein et al. 2017). Unfortunately, much of this is of doubtful application in the tropical Kimberley environment: the substantial work of Dorn, Liu and Krinsley (e.g. Krinsley et al. 1990, Liu 1994, Dorn 1998, Liu and Broecker 2008, Dorn 2009, Dorn and Krinsley 2011, Krinsley et al. 2013) has a particular focus on the dry desert climates where much of their work is based. Research into accretions on monuments in the polluted environments of Europe and in limestone caves is unlikely to explain the specific geochemistry of rock shelters in the Kimberley sandstone country. Alan Watchman (e.g. 1994, 1996, 1997, 2000a, 2014), however, has a 25-year record of research that is more directly relevant to this region. Key findings from his work, and that of other local researchers are reviewed below.

A point made by many researchers, in different ways, is that dating of the carbon content of mineral accretions is only useful if the provenance of the carbon can be securely established. Watchman (2000b: 270) concluded “Unidentified organic matter is not a reliable medium for dating because the relationship between the carbon compounds of unknown origin and the event being dated is uncertain.” Gillespie (1997:436) criticises plasma oxidation and laser ablation techniques as they both release carbon from indeterminate sources. Bednarik also lends support to this view (2002:1218): “It should be of concern that in most cases so far published we

have in effect obtained bulk samples from what were described as rock varnish deposits, without any indication of what the target substances were, or from what precisely the carbon dates were secured.” Aubert (2012) is similarly critical: “In general, the problems are so severe with radiocarbon dating of rock art that, unless the source of carbon can be identified and isolated prior to analysis, radiocarbon dates on related art and/or associated mineral deposits should be taken as of unknown accuracy.”

Geochemically closed systems address part of the carbon provenance uncertainty by providing an assurance that new or old carbon cannot contaminate the source of carbon in an accretion layer once it is sealed by subsequent layers. Accretions are said to be “closed” to carbon if it is not possible for carbon to enter or exit the accretion once it has been formed. Not all rock coatings can be said to be closed systems, and late recognition of this fact eroded confidence in some earlier radiocarbon age determinations (Dorn 1997, Bednarik 2000:107). Oxalate-rich crusts, found throughout Australia (Watchman 1990), are an attractive target because they have been found to be closed and the most commonly found oxalate mineral, whewellite, is stable and insoluble (Watchman et al. 2005, Smith et al. 2009:192). It is also possible to use a straightforward chemical process, acidified permanganate oxidation, to selectively extract calcium oxalate from samples with other potential sources of carbon such as carbonates, charcoal, or other organic material (Gillespie 1997:432, Hedges et al. 1998:38, Mazel and Watchman 2003:61, Cole and Watchman 2005:664). Watchman (1993) had also advocated the use of a focused laser extraction technique (FLECS) as well as micro-excavation of specific accretion layers to extract carbon for dating purposes. Advantages claimed for FLECS were that the use of a lower energy laser beam could avoid ionisation of the sample and subsequent isotopic fractionation while allowing accurate and precise selection of the area to be sampled (2000a:38). It is not entirely clear why Watchman and others did not persist with the FLECS method but in his PhD thesis Watchman notes that “The major problem with the laser system is the lack of volume of carbon-bearing substances under the focused beam, a matter limited by the surface area of the cross-sections, so that not enough gas is produced to make graphite targets.” (1996:193).



The micro-excavation technique holds more promise now as precise micromilling is an established practice in geochronological analysis of speleothems (Drysedale et al. 2012). In a comparison of microdrilling, micromilling and laser ablation for stable isotope sampling of speleothems the researchers concluded: “Laser ablation analysis represents the fastest technique, but its spatial resolution... and precision ... is second to micromilling (and microdrilling, respectively)” (Spötl and Matthey 2006). Precise micro-milling of specific accretionary layers, alone, does not guarantee a reliable age estimate. Crusts are subject to differential erosion, re-deposition and micro-fissuring (e.g. from the action of microcolonial fungi whose hyphae may penetrate crust laminae) such that discontinuities at a micro and macro scale are created (Watchman 2000a: 39, Gorbushina 2007: 1614, Dorn et al. 2013: 66). Such areas need to be identified by microscopic examination and avoided during sampling but even then multiple samples within the same layer should be analysed to obtain a reliable result (Watchman 2000b: 271). Bednarik takes this a step further and advocates “methodological pluralism” (Bednarik 2000:108) whereby an age estimate would draw on radiocarbon dating of organic and mineral material as well as other dating methods.

Although there is near universal agreement that the provenance of carbon in a sample must be known, some level of uncertainty can be tolerated, particularly when minimum and maximum ages are being estimated. While the aim is always to minimise the potential for new (e.g. modern charcoal) and old (e.g. geological calcite) carbon contamination of the sample to be analysed, some types of contamination can be tolerated more readily than others. A 1% contamination of a sample with ancient material, containing no  $^{14}\text{C}$ , will produce an error of 80 years, irrespective of the age of the sample. The same level of contamination (1%) from a source of modern carbon will, however introduce an error that varies with the age of the sample: a 50 ka BP sample will appear to be just 35.5 ka BP, but a 12 ka BP sample will test as 11.7 ka BP (Wood 2015: 63). A significant observation here is that any level of modern carbon contamination does not invalidate a minimum age estimate, it just makes it less useful in that it is further removed from the actual age.

Given the depth and relevance of Alan Watchman's experience in radiocarbon dating of rock art his concluding thoughts on this subject in his thesis are worth repeating here:

"Dating rock art is expensive and time consuming, requiring the collection of many samples, followed by detailed microscopic and mineralogical analyses, ....Taking a single sample from rock art encapsulated by silica in the hope of dating the art is also undesirable because there is no way of knowing if the radiocarbon determination is accurate.....Preliminary results from a number of rock art sites show that much more systematic work is necessary, such as collecting amorphous silica coatings off-art and on-art, and radiocarbon dating larger samples to establish site and regional rates of silica deposition. Internal consistency, or stratigraphic conformity, of the dating results can also be obtained by determining ages for carbon-bearing substances in a series of laminations from bottom to top in a cross-section, associated with art and off-art. Therefore, future rock art dating work should focus on particular sites where certain stylistic representations are well documented and where the archaeological associations between organics in silica and paint layers can be precisely defined." (1996:194).

### **1.3 Research aims**

The high level objective for this thesis is to generate absolute age estimates for the previously defined stylistic sequence of Kimberley rock art. There is a particular emphasis on the earlier, pre-Wanjina, styles because there are so few dates for the older art and the age of the earliest figurative art is germane to questions of human development in a global context.

An important subordinate objective is to understand the carbon-bearing constituents of mud wasp nests; both those included in nests when they are built and any carbon contamination that may be incorporated subsequently. This will include a mineralogical analysis required to guide development of radiocarbon pretreatment methods to retain the preferred source of carbon for dating while removing carbon contamination. Statistical methods will be devised to estimate the age ranges for art periods from the maximum and minimum age constraints provided by wasp nest dates. Ultimately, a quantitative, chronological hypothesis for the main Kimberley rock art styles will be advanced as an initial framework, to be refined over time with further radiometric age data.

## **1.4 Approach**

The previous studies described above suggest two main approaches to obtain radiocarbon age estimates on Kimberley rock art. One is to date specific organic inclusions in wasp nests such as pollen, charcoal, and the remains of insect exoskeletons. The other is to precisely extract dateable carbon from closed mineral accretions, particularly those containing calcium oxalates. Understanding that all such age determinations represent maximum or minimum age estimates for the rock art they relate to, careful design of sampling strategies is required to maximise the chance of obtaining well constrained age estimates for individual rock art styles. In addition, detailed study of the composition and structure of the samples is required to understand the nature of their constituents and assess any potential contamination. To this end, the approach taken in this study is considered under each of the main steps in the experimental process:

- Pre-fieldwork planning
- Site and sample selection in the field
- Mineralogical analysis of samples
- Elemental analysis of samples
- Sample pretreatment
- Radiocarbon dating
- Analysis and documentation of results

### **1.4.1 Fieldwork planning**

The objective of the fieldwork is to generate sufficient dateable samples to provide estimates of the ages for each of the main styles – understanding that many samples will prove to be unsuitable for a range of reasons and that a statistically robust result is required to produce well constrained age estimates.

Pre-fieldwork planning involved desktop research to identify areas and sites where the target rock art styles are most readily accessed. Careful inspection of photographs taken by earlier visitors to Kimberley rock art locations was used to help identify sites with mineral accretions and mud wasp nests. Sources of these photographs include bushwalkers (particularly customers and guides of Willis Walkabouts), the

publications of Mike Donaldson and Grahame Walsh, independent rock art researchers (e.g. Joc Schmiechen, Darrell Lewis and Lee Scott-Virtue) and project team member Cecilia Myers. Some of these researchers also have site records that include details of insect nests and mineral accretions.

#### **1.4.2 Site and sample selection**

The factors listed below were identified as being important considerations for site selection and to target samples within rock art sites. They were used for that purpose for the initial 2015 Dry Season fieldwork.

- *Motif style*: Age determinations relating to motifs that are clearly of a specific style/period are more useful than motifs of uncertain classification. For the reasons mentioned earlier it is the older, well defined styles that are of higher priority, i.e. Naturalistic (or Irregular Infill Animal Period), Gwion (or Kiro Kiro), Static Polychrome (previously, Clothes Peg Figures).
- *Size of potential samples*: Larger samples provide greater potential for multiple dating techniques to be applied to a single specimen. OSL probably requires a mud wasp nest sample at least 3-4mm thick, and ~10-15mm in diameter. Older nests reportedly contain less pollen so larger samples are preferable and will also allow some of the external surface to be removed to minimise the chance of contamination from modern pollen.
- *Bracketed age estimates*: A motif that has mud wasp nests (or mineral accretions) both underneath and on top of the pigment represents a particularly valuable target as it offers the potential for both a minimum and maximum age estimate.
- *Number of potential samples on the same motif*: If large samples are unavailable then preference should be given to a motif that has more than one potentially datable nest stump or mineral accretion.

- *Presence of multiple motifs of the same style in clear association:* A large panel with multiple datable motifs, that appear to have been painted at around the same time (because they are all of the same style, forming a group “scene”, with similar material goods etc) may provide a statistically more robust age estimate.
- *Ability to characterise the immediate geochemical environment:* An ideal site is one where it is possible to characterise the complex mineralogical, geochemical, isotopic and geomicrobiological systems operating on rock faces and determine the characteristics and origin of crusts, varnish pigments, and other surface coating materials. Most of these aspects are the focus of investigation by other members of the Kimberley rock art dating project (e.g., uranium-series dating) but the outputs of their research will support the radiocarbon age determinations.

These objectives were revised for subsequent field seasons as additional objectives were explored. These include an improved understanding about the sources of carbon contained in the mud collected by wasps for nest construction and the morphology, age and size distribution of nests found on rock shelter walls.

### **1.4.3 Mineralogical analysis**

X-ray diffraction (XRD) has been the primary method used to determine the mineralogy of wasp nests and mineral accretions. XRD results are used to identify samples containing whewellite for radiocarbon dating and uranium concentrating minerals, such as newberyite, for uranium series dating. XRD was also used to understand the composition of wasp nests and how they are mineralised over time. Preparation of thin sections and polished sections was undertaken to enable the identification of the components of wasp nests and accretions.

Fourier transform infrared spectroscopy (FTIR) has been used on 24 crusts and coating samples (collected pre-2015) to understand the amorphous mineral and organic content.

#### **1.4.4 Elemental analysis**

Elemental analysis was used to support mineralogical analysis and to provide quantitative data not available from XRD (particularly for the amorphous content of samples). X-ray fluorescence (XRF) was employed where large samples (>500 mg) were available.

#### **1.4.5 Sample pre-treatment**

Initially, project partner, ANSTO made available their radiocarbon pretreatment laboratory and associated training and supervision. Subsequently, a pretreatment facility was fabricated within the School of Earth Sciences at the University of Melbourne. This facility was used to record, clean, grind and then chemically pre-treat wasp nest samples. Pretreated samples were then combusted and graphitised at ANSTO.

#### **1.4.6 Radiocarbon dating**

ANSTO AMS facilities were employed to measure the carbon isotope ratios of the prepared graphite targets. Choice of a particular accelerator was determined based on machine availability, size of the carbon sample, and measurement accuracy required.

#### **1.4.7 Documentation, Analysis and Interpretation of results**

Statistical methods were developed for the analysis of the sets of the radiocarbon age determinations relating to each particular rock art style. Data were also analysed to understand more about the age distribution of wasp nests found in rock shelters. The results of these approaches are then used to constrain the ages, where possible, of particular art styles of the Kimberly.

### **1.5 Thesis outline**

This chapter reviews the literature available at the start of this study in 2015. It describes the approaches that appeared to be most likely to lead toward a useful method for dating Kimberley rock art. The review also identifies the problems encountered by other researchers and the comprehensive nature of the evidence that would be needed as part of the development of a robust methodology.

The main sections of Chapters 2, 3, and 4 either have been published or are under review in peer-reviewed international journals. Chapter 2 (Methodology) was published in *Quaternary Geochronology* in March 2019. Chapter 3 (Gwion period) was published in *Science Advances* in February 2020. Chapter 3 (Irregular Infill Animal Period) was sent out for review by *Nature Human Behaviour* in July 2020. While care was taken to logically apportion unique content across the three manuscripts, some repetition, particularly in background and methods, is necessarily unavoidable.

Chapter 2 describes the development of the methods used to secure radiocarbon age estimates of mud wasp nests. It reports on the analysis and dating of modern wasp nests to identify the most promising sources of carbon that are likely to persist for millennia in old nests. An important result from the work on modern nests is the determination of the inbuilt or inherited carbon age. For old wasp nests, the methods used for field sampling, physical and chemical pretreatment, and AMS measurement are described. The results from experimentation with, and analysis of, 120 old mud wasp nests are discussed in detail and the ages of the 75 old nests successfully radiocarbon dated are reviewed. Sources of potential error and uncertainty in the results are identified and considered in light of some early anomalous results.

The ages determined for 24 mud wasp nests in contact with 21 Gwion motifs are presented in Chapter 3. The procedure developed to classify motifs into one of the 6 main Kimberly rock art styles (Figure 1-2) is detailed and the methods used in the field to confidently establish the context of the wasp nest sample in relation to pigment from the motif are described. The chapter then discusses the theoretical basis by which wasp nest dates can be used to infer the absolute chronology for a rock art stylistic period using the Gwion period as an example. Basic statistical concepts are used to propose a method that employs the age estimates for the 24 nests to determine the period during which Gwion motifs were commonly painted.

In Chapter 4 the 27 radiocarbon dates on wasp nests in contact with pigment from 16 Irregular Infill Animal Period (IIAP) motifs are reviewed. The age of one IIAP macropod motif is very well constrained by dates on three nests underlying the large motif and another three dates from overlying nests. In total, the data suggest a more

prolonged period of production for motifs in this style when compared to the Gwion period. Some other possible ramifications of the timing determined for the IIAP and Gwion periods are discussed.

Chapter 5 reviews the dates for samples associated with motifs from the four other main Kimberley rock art styles: Cupules/Grooves, Static Polychrome, Painted Hand and Wanjina. Age constraints for motifs that are less confidently classified to any style are also discussed. Wasp nest dates related to seven possible IIAP or Gwion motifs are considered to test the idea that the age might be used to determine the art period the motif belongs to.

Chapter 6 fully develops the probabilistic model that is used to derive absolute age ranges for individual art periods from any datable material found underlying or overlying rock art motifs. While the general concept is introduced in Chapter 3, here the model is developed in more detail and then tested using Monte Carlo data simulations. Randomly generated age constraints are analysed to understand the patterns of probability density functions produced by art periods of different durations. Further simulations are run to identify how these patterns vary as the number of samples is reduced. The final section of the chapter uses the probabilistic model to define a hypothesis for the chronology of the six main periods of the Kimberley rock art sequence. Although there is little evidence, at this stage, to support any estimates for the youngest and oldest periods in the sequence, in particular, the hypothesis is proposed as a framework to be reinforced or adjusted as further age constraints become available. Chapter 7 concludes by summarising the main findings of the study and suggests areas for further research.



## 1.6 References

Aubert, M. (2012). "A review of rock art dating in the Kimberley, Western Australia." Journal of Archaeological Science **39**(3): 573-577.

Aubert, M., A. Brumm, M. Ramli, T. Sutikna, E. W. Saptomo, B. Hakim, M. J. Morwood, G. D. van den Bergh, L. Kinsley and A. Dosseto (2014). "Pleistocene cave art from Sulawesi, Indonesia." Nature **514**(7521): 223-227.

Bednarik, R. G. (2000). Some problems with 'direct dating' of rock pictures. Advances in dating Australian rock-markings : papers from the first Australian Rock-Picture Dating Workshop. G. Ward and C. Tuniz. Lucas Heights, Sydney, Melbourne : Australian Rock Art Research Association, 2000. **Occasional AURA publication: no. 10**: 120.

Bednarik, R. G. (2002). "The Dating of Rock Art: a Critique." Journal of Archaeological Science **29**(11): 1213-1233.

Bednarik, R. G. (2010). "Australian rock art of the Pleistocene." Rock Art Research **27**(1): 95-120.

Bednarik, R. G. (2014). "Mud-wasp Nests and Rock Art." Rock Art Research **31**(2): 225-231.

Brown, T. A., D. E. Nelson, R. W. Mathewes, J. S. Vogel and J. R. Southon (1989). "Radiocarbon dating of pollen by accelerator mass spectrometry." Quaternary research (USA) **32**(2): 205 - 212.

Chester, P. I. and C. A. Prior (2004). An AMS 14C Pollen-Dated Sediment and Pollen Sequence from the Late Holocene, Southern Coastal Hawke's Bay, New Zealand, Department of Geosciences University of Arizona.

Cole, N. and A. Watchman (2005). "AMS dating of rock art in the Laura Region, Cape York Peninsula, Australia – protocols and results of recent research." Antiquity **79**: 661-678.

David, B., B. Barker, F. Petchey, J.-J. Delannoy, J.-M. Geneste, C. Rowe, M. Eccleston, L. Lamb and R. Whear (2012). "A 28,000 year old excavated painted rock from Nawarla Gabarnmang, northern Australia." Journal of Archaeological Science.

David, B., J.-M. Geneste, F. Petchey, J.-J. Delannoy, B. Barker and M. Eccleston (2013). "How old are Australia's pictographs? A review of rock art dating." Journal of Archaeological Science **40**(1): 3-10.

Dietzel, M., H. Kolmer, P. Pölt and S. Simic (2008). "Desert varnish and petroglyphs on sandstone – Geochemical composition and climate changes from Pleistocene to Holocene (Libya)." Chemie der Erde - Geochemistry **68**(1): 31-43.

Donaldson, M. (2007). Introduction and overview of Kimberley rock art. Rock Art of the Kimberley. M. Donaldson and K. Kenneally. Perth, Kimberley Society: 158.

- Dorn, R. (2009). Desert Rock Coatings. Geomorphology of Desert Environments. A. Parsons and A. Abrahams, Springer Netherlands: 153-186.
- Dorn, R. I. (1997). "Constraining the age of the Coa valley (Portugal) engravings with radiocarbon dating." Antiquity **71**(271): 105-115.
- Dorn, R. I. (1998). Rock coatings, Elsevier Science & Technology Books.
- Dorn, R. I. and D. Dragovich (1990). "Interpretation of Rock Varnish in Australia: case studies from the arid zone." Australian Geographer **21**(1): 18-32.
- Dorn, R. I. and D. Krinsley (2011). "Spatial, temporal and geographic considerations of the problem of rock varnish diagenesis." Geomorphology **130**(1-2): 91-99.
- Dorn, R. I., D. H. Krinsley, K. A. Langworthy, J. Ditto and T. J. Thompson (2013). "The influence of mineral detritus on rock varnish formation." Aeolian Research **10**: 61-76.
- Dragovich, D. (1994). "Fire, climate, and the persistence of desert varnish near Dampier, Western Australia." Palaeogeography, Palaeoclimatology, Palaeoecology **111**(3-4): 279-288.
- Drysdale, R. N., B. T. Paul, J. C. Hellstrom, I. Couchoud, A. Greig, P. Bajo, G. Zanchetta, I. Isola, C. Spötl, I. Banerjee, E. Regattieri and J. D. Woodhead (2012). "Precise microsampling of poorly laminated speleothems for U-series dating." Quaternary Geochronology **14**(0): 38-47.
- Flood, J. (2004). Archaeology of the Dreamtime: the story of prehistoric Australia and its people. Marleston, Gecko Books.
- Gershtein, E. C., M. Willis, S. L. Black, A. M. Castañeda, T. Buonasera, C. W. Koenig, J. Shipp and D. Nadel (2017). "High-resolution mapping and analysis of shiny grooved rock surfaces: The case study of the Skiles Shelter, Lower Pecos, Texas." Quaternary International **439, Part B**: 69-82.
- Gillespie, R. (1997). "On human blood, rock art and calcium oxalate: Further studies on organic carbon content and radiocarbon age of materials relating to Australian rock art." Antiquity **71**(272): 430-437.
- Gorbushina, A. A. (2007). "Life on the rocks." Environmental Microbiology **9**(7): 1613-1631.
- Gorbushina, A. A. and W. J. Broughton (2009). "Microbiology of the Atmosphere-Rock Interface: How Biological Interactions and Physical Stresses Modulate a Sophisticated Microbial Ecosystem." Annual Review of Microbiology **63**(1): 431-450.
- Green, H., A. Gleadow, D. Finch, J. Hergt and S. Ouzman (2017). "Mineral deposition systems at rock art sites, Kimberley, Northern Australia - Field observations." Journal of Archaeological Science-Reports **14**: 340-352.

Haidle, M. N., M. Bolus, M. Collard, N. Conard, D. Garofoli, M. Lombard, A. Nowell, C. Tennie and A. Whiten (2015). "The Nature of Culture: an eight-grade model for the evolution and expansion of cultural capacities in hominins and other animals." Journal of anthropological sciences = Rivista di antropologia : JASS / Istituto italiano di antropologia **93**: 43-70.

Hedges, R. E. M., C. Bronk Ramsey, G. J. Van Klinken, P. B. Pettitt, C. Nielsen-Marsh, A. Etchegoyen, J. O. F. Niello, M. T. Boschin and A. M. Llamazares (1998). "Methodological issues in the C-14 dating of rock paintings." Radiocarbon **40**(1): 35-44.

Hiscock, P. (2008). Archaeology of Ancient Australia. Oxon, Routledge.

Kilian, M. R., J. van der Plicht, B. van Geel and T. Goslar (2002). "Problematic 14C-AMS dates of pollen concentrates from Lake Gosciarz (Poland)." Quaternary International **88**(1): 21-26.

Krinsley, D., J. Ditto, K. Langworthy, R. I. Dorn and T. Thompson (2013). "Varnish microlaminations: new insights from focused ion beam preparation." Physical Geography **34**(3): 159-173.

Krinsley, D. H., R. I. Dorn and S. W. Anderson (1990). "Factors that interfere with the age-determination of rock varnish." Physical Geography **11**(2): 97-119.

Langley, M. C. and P. S. C. Tacon (2010). "The Age of Australian Rock Art: A Review." Australian Archaeology **71**: 70 - 73.

Liu, T. (1994). Visual Laminations in Rock Varnish: A New Paleoenvironmental and Geomorphic Tool in Drylands Research. Doctor of Philosophy PhD, Arizona State University,.

Liu, T. and W. S. Broecker (2008). "Rock varnish evidence for latest Pleistocene millennial-scale wet events in the drylands of western United States." Geology **36**(5): 403-406.

Long, A., O. K. Davis and J. De Lanois (1992). "Separation and 14C dating of pure pollen from lake sediments: nanofossil AMS dating." Radiocarbon **34**(3): 557-560.

Mazel, A. and A. Watchman (2003). "Dating Rock Paintings in the uKhahlamba-Drakensberg and the Biggarsberg, KwaZulu-Natal, South Africa." Southern African Humanities **15**: 59-73.

McNiven, I. (2011). "The Bradshaw debate: lessons learned from critiquing colonialist interpretations of Gwion Gwion rock." Australian Archaeology **72**(June 2011): 35-44.

Mensing, S. A. and J. R. Southon (1999). "A simple method to separate pollen for AMS radiocarbon dating and its application to lacustrine and marine sediments." Radiocarbon **41**(1): 1-8.

Morwood, M. J. (2002). Visions from the Past: The Archaeology of Australian Aboriginal Art. Washington, D.C., Smithsonian Institution Press.

Naumann, I. D. (1983). The biology of mud nesting Hymenoptera (and their associates) and Isoptera in rock shelters of the Kakadu region, Northern Territory. The Rock Art Sites of Kakadu National Park - Some Preliminary Research Findings for their Conservation and Management. D. Gillespie. Canberra, Australian National Parks and Wildlife Service: 127 - 189.

Neulieb, T., E. Levac, J. Southon, M. Lewis, I. Florin Pendea and G. L. Chmura (2013). "Potential Pitfalls of Pollen Dating." Radiocarbon **55**(2): 1142-1155.

O'Connor, S. and B. Fankhauser (2001). Art at 40,000 bp? One step closer: an ochre covered rock from Carpenter's Gap Shelter 1, Kimberley Region, Western Australia. Histories of old ages: essays in honour of Rhys Jones. A. Anderson, I. Lilley and S. O'Connor. Canberra, Pandanus Books, Research School of Pacific and Asian Studies The Australian National University: 287-300.

Roberts, R., G. Walsh, A. Murray, J. Olley, R. Jones, M. Morwood, C. Tuniz, E. Lawson, M. Macphall, D. Bowdery and I. Naumann (1997). "Luminescence dating of rock art and past environments using mud-wasp nests in northern Australia." Nature **387**(6634): 696-699.

Roebroeks, W. (2014). "Archaeology: Art on the move." Nature **514**(7521): 170-171.

Smith, A. (1979). "Life strategy and mortality factors of *Sceliphron laetum* (Smith) (Hymenoptera: Sphecidae) in Australia." Australian Journal of Ecology **4**(2): 181-186.

Smith, A. M., Q. Hua, A. Williams, V. Levchenko and B. Yang (2010a). "Developments in micro-sample <sup>14</sup>C AMS at the ANTARES AMS facility." Nuclear Instruments and Methods in Physics Research Section B: Beam Interactions with Materials and Atoms **268**(7-8): 919-923.

Smith, A. M., B. Yang, Q. A. Hua and M. Mann (2010b). "Laser-heated microfurnace: gas analysis and graphite morphology." Radiocarbon **52**(2): 769-782.

Smith, M. A., A. Watchman and J. Ross (2009). "Direct Dating Indicates a Mid-Holocene Age for Archaic Rock Engravings in Arid Central Australia." Geoarchaeology-an International Journal **24**(2): 191-203.

Spötl, C. and D. Mathey (2006). "Stable isotope microsampling of speleothems for palaeoenvironmental studies: A comparison of microdrill, micromill and laser ablation techniques." Chemical Geology **235**(1-2): 48-58.

Tacon, P. S. C., N. H. Tan, S. O'Connor, X. Ji, G. Li, D. Curnoe, D. Bulbeck, B. Hakim, I. Sumantri, T. Heng, S. Im, S. Chia, K.-N. Khuon and K. Soeung (2014). "The global implications of the early surviving rock art of greater Southeast Asia." Antiquity **88**(342): 1050-1064.

Veth, P., C. Myers, P. Heaney and S. Ouzman (2017). "Plants before farming: The deep history of plant-use and representation in the rock art of Australia's Kimberley region." Quaternary International.

Walsh, G. (1994a). "Bradshaws ancient rock paintings of north-west Australia."

- Walsh, G. L. (1994b). Bradshaws, ancient rock paintings of north-west Australia. Carouge-Geneva, Switzerland, Edition Limitée for the Bradshaw Foundation.
- Walsh, G. L. (2000). Bradshaw art of the Kimberley, Takarakka Nowan Kas Publications.
- Ward, I., A. Watchman, N. Cole and M. Morwood (2001). "Identification of minerals in pigments from Aboriginal rock art in the Laura and Kimberley regions, Australia." Rock art research **18**(1): 15-23.
- Watchman, A. (1990). "A summary of occurrences of oxalate-rich crusts in Australia." Rock Art Research **7**(1): 44-50.
- Watchman, A. (1994). "Radiocarbon dating fatty acids in Holocene siliceous rock surface accretions." Australian Journal of Earth Sciences **41**(2): 179-180.
- Watchman, A. (1996). Properties and dating of silica skins associated with rock art. Doctor of Philosophy, University of Canberra.
- Watchman, A. (1997). Dating the Kimberley rock paintings. Kimberley Society Occasional Paper No. 1, University of Western Australia, Kimberley Soceity.
- Watchman, A. (1998). "Dating rock images in the tropical monsoon region of northern Australia." Australian Aboriginal Studies **1998**(2): 64-70.
- Watchman, A. (2000a). Micro-excavation and laser extraction methods for dating carbon in silica skins and oxalate crusts. Advances in Dating Australian Rock-Markings: Papers from the First Australian Rock-Picture Dating Workshop.
- Watchman, A. (2000b). "A review of the history of dating rock varnishes." Earth-Science Reviews **49**: 261 - 277.
- Watchman, A., S. O'Connor and R. Jones (2005). "Dating oxalate minerals 20–45ka." Journal of Archaeological Science **32**(3): 369-374.
- Watchman, A., P. Tacon and M. Aubert (2014). "Erosion rates and weathering history of rock surfaces associated with Aboriginal rock art engravings (petroglyphs) on Burrup Peninsula, Western Australia, from cosmogenic nuclide measurements." Quaternary Science Reviews **91**: 70-73.
- Watchman, A., G. Walsh, M. J. Morwood and C. Tuniz (1997). "AMS Radiocarbon age estimates for early rock paintings in the Kimberley, N.W.Australia: Preliminary Results." Rock Art Research **14**(1): 18-26.
- Watchman, A. L., R. A. Lessard, A. J. T. Jull, L. J. Toolin and W. Blake (1993). "C-14 dating of laser-oxidized organics." Radiocarbon **35**(2): 331-333.
- Welch, D. M. (1993). Stylistic change in the Kimberley rock art, Australia. Rock art studies: the post-stylistic era or where do we go from here?, Cairns, Oxbow Monograph.

Westaway, M. (2015). Senator Leyonhjelm needs to 'update his knowledge of the science' on anti-Aboriginal origins. P. Veth. Online, Australian Archaeological Association.

White, S. R. and M. A. Ferland (2015). Geological Survey of Western Australia, Kimberley. Geological Information Series. W. A. Department of Mines and Petroleum. Perth.

Whiteway, T. (2009). Australian bathymetry and topography grid. G. Australia. Canberra, Department of Industry, Tourism & Resources. **GeoCat # 67703**: 46.

Williams, A. N., S. Ulm, T. Sapienza, S. Lewis and C. S. M. Turney (2018). "Sea-level change and demography during the last glacial termination and early Holocene across the Australian continent." Quaternary Science Reviews **182**: 144-154.

Wilson, I. (2006). Lost World of the Kimberley. Crows Nest, Sydney, Allen & Unwin.

Wood, R. (2015). "From revolution to convention: the past, present and future of radiocarbon dating." Journal of Archaeological Science **56**: 61-72.

Yaxley, L. (2015). Senator David Leyonhjelm questions if Aboriginals were first occupants of Australia; says it would be 'bizarre' to put into constitution. ABC News. Melbourne, Australian Broadcasting Commission.

Yoshida, H., R. G. Roberts and J. M. Olley (2003). "Progress towards single-grain optical dating of fossil mud-wasp nests and associated rock art in northern Australia." Quaternary Science Reviews **22**(10-13): 1273-1278.

## Chapter 2

# **Development of radiocarbon dating method for mud wasp nests**

This chapter is the author accepted version of the paper published in *Quaternary Geochronology* (2019; 51: 140-154, doi:10.1016/j.quageo.2019.02.007). Individual co-author contributions are as noted in the Preface with the candidate contributing more than 90% of the content of the publication. The paper describes the development of methods aimed at achieving reliable radiocarbon age estimates for mud wasp nest samples collected from Kimberley rock shelters. After the initial field season, it was evident that the availability of suitable mud wasp nest samples was much greater than mineral accretions, so all further development and experimentation was directed toward the former.

### **New developments in the radiocarbon dating of mud wasp nests**

Damien Finch<sup>1</sup>, Andrew Gleadow<sup>1</sup>, Janet Hergt<sup>1</sup>, Vladimir A Levchenko<sup>2</sup>,  
David Fink<sup>2</sup>

<sup>1</sup> The School of Earth Sciences, The University of Melbourne

<sup>2</sup> Australian Nuclear Science and Technology Organisation

## 2.1 Abstract

This paper reports on the development of radiocarbon dating of mud wasp nests to provide age estimates for rock art and other anthropogenic modifications to the surfaces of open rock shelters.

Over 150 rock shelters in the remote Kimberley region of Western Australia were visited in five field seasons. Mud wasp nest samples were collected from 108 sites. Thirty newly constructed wasp nests were collected to understand their initial composition and to determine the major sources of carbon. Charcoal-rich fractions extracted from 9 modern nests were radiocarbon dated and, whilst most were of zero age, some were found to be up to 1000 years old with the mean age being 255 years.

Of the old wasp nest samples, 120 were utilised in the experiments reported here. A variety of different physical and chemical pretreatment methods were explored but small sample sizes and low carbon concentrations limit the range of techniques that can be used in practice. The radiocarbon ages measured on the 75 nest samples that contained sufficient carbon for analysis ranged from Modern to just over 20 cal ka BP. Half of these nests were older than 8 cal ka BP and 20% were older than 11 cal ka BP. Even allowing for the inherent uncertainties due to any inbuilt carbon age, the method is capable of producing useful age estimates for rock art and other features of archaeological interest, in relatively open rock shelters.



## 2.2 Introduction

Rock shelters are often a focus of archaeological excavations as they were favoured sites for habitation and cultural practices. A range of dating techniques are available to analyse associated organic material or sediments thereby providing a chronological context for the excavated sequence. Above ground, people may have created grinding hollows, abraded grooves, cupules, petroglyphs, and pictograms but such features are only rarely amenable to dating with current techniques. Therefore, it is largely impossible to place these features in a temporal context or to make a chronological link to excavated deposits, so the archaeological record of the site is inchoate. Here, we report on the development of a method that can be more widely deployed to provide useful age estimates for such features.

Mud dauber wasps are found throughout the world (Naumann 1983: 134) and their nests are common on rock surfaces. Rock shelters serve as protection for wasp nests, so nests are sometimes found on the same surfaces used by people for rock art and domestic activity. Optically-stimulated luminescence (OSL) dates on quartz grains in mud wasp nests overlying rock art have established that mineralised mud wasp nests can survive in open rock shelters for tens of thousands of years (Roberts et al. 1997, Yoshida et al. 2003). However, the application of OSL is greatly restricted because it requires old wasp nests that are still large enough to shield inner quartz grains from sunlight and such nests are rare (Aubert 2012: 576, Ross et al. 2016: 28). On the other hand, smaller stumps of old, often indurated, nests are relatively abundant.

Mud collected by wasps contains sand, clay, and a variety of organic materials. The carbon composition of wasp nests will change over time as any plant matter in the mud decomposes, the outer surface weathers away, dust accumulates, and, potentially, the nest becomes mineralised. The remnant nest will also be subject to the action of bacteria, algae and fungi (Ridges et al. 2000). The critical challenge in estimating when the nest was constructed is to isolate a source of carbon for which an age can be reliably related to the construction event (Watchman 2000, Bednarik 2002, Aubert 2012). Radiocarbon dates on different organic components (e.g. wood, charcoal, pollen, plant matter) within a sediment sample have been shown to differ significantly because they originate from different sources of different age (Brock et

al. 2010: 625). Early attempts to radiocarbon date a specific component from wasp nests focussed on pollen but older nests were generally found to contain too little pollen for analysis (Roberts et al. 1997, 2000, Yoshida et al. 2003). To determine what other sources of carbon may be more suitable targets for dating we need to understand the carbon-bearing components initially present and then the broad range of diagenetic processes at work, post construction.

The aim of this research was to develop a technique that will provide robust age estimates for the timing of mud nest production and one that can be applied to a wide range of rock shelter surfaces. This paper covers the methodological aspects of radiocarbon dating of mud wasp nests; subsequent reports will demonstrate how the method has been applied to generating specific age estimates for rock art.

### **2.3 Approach**

Open rock shelters in the remote Kimberley region of Western Australia contain an abundance of old mud wasp nests as well as a complex rock art repertoire and other evidence of human occupation (Morwood et al. 1994). More than 150 rock art sites in three Kimberley regions were visited in five field campaigns between 2015 and 2017 (see Green et al. (2017b) for details of the fieldwork areas and relevant geology). During two Wet season trips (February 2016 and March/April 2017), wasps were observed and recorded collecting mud, constructing nests and provisioning nests with prey. Samples from 30 freshly constructed (i.e. modern) wasp nests were collected as well as some of the mud or soil from source material gathered by the wasps. More than 300 old mud wasp nest fragments were collected from 105 rock shelters.

Modern nests were examined to understand the initial composition of nests and sources of carbon within them. Different carbon-bearing fractions were extracted, and radiocarbon dated to ascertain whether nests contain anything other than modern carbon at the time of construction.

Old nests were then studied to determine how diagenesis transforms this carbon and how new sources of carbon may be incorporated into the mineralised nest. Extensive mineralogical and geochemical analyses identified the range of minerals and elemental concentrations present in old nests. The results guided experimentation

with a range of physical and chemical pretreatment processes prior to radiocarbon dating. These experiments tested the trade-off between removing all possible sources of unwanted carbon and preserving sufficient carbon to allow reliable measurement of the age of the sample.

## **2.4 Methods**

### **2.4.1 Field sampling**

Sampling from archaeological sites was approved by relevant local Traditional Owners in the country of the Balangarra and Dambimangarri People and under permits issued by the WA Department of Planning Lands and Heritage (Section 16 Permits 558 and 567).

Most mud wasp nests were removed using a 6mm chisel, sharply tapped with a small hammer and caught in a sheet of aluminium foil. In most cases, the nest would fracture along the same plane as the rock surface, minimising damage to surrounding surfaces. Samples were wrapped in aluminium foil then placed in individual plastic sample bags.

In the laboratory, all samples were photographed and weighed then wrapped in new aluminium foil for longer term storage. This storage foil had either been cleaned with acetone or baked overnight in a muffle furnace at 400°C to remove any potential hydrocarbon lubricant contamination from the foil production process (Klingner et al. 2013).

### **2.4.2 Mineralogical and Elemental Analysis**

Optical microscopy was used to examine the contents of the modern wasp nests. The total carbon and sulphur concentration and isotopic ratios of 5 modern and 13 old nests were determined using a Thermo Finnigan EA 1112 Series Flash Elemental Analyser at the Central Science Laboratory, University of Tasmania (Tables 2-1 and 2-4).

A broad range of analytical techniques were applied to old mud wasp nest samples. Typical nests were selected from those available at the time, where sufficient material was available after preparation of the sample for dating. X-ray diffraction

(XRD) was used on 41 old wasp nests to determine the mineral composition and X-ray fluorescence (XRF) spectrometry on 14 of these nests to determine their major element composition. As XRD does not detect the amorphous content, 13 of the XRD samples were also analysed using XRF to understand the typical non-crystalline composition.

Scanning electron microscopy (SEM), and Laser Ablation Inductively-Coupled-Plasma Mass Spectrometry (LA-ICPMS) were used to understand the distribution and concentration of elements in nest samples. The experimental details of analytical equipment used can be found in Supplementary Information. The equipment and methods used for SEM and LA-ICPMS are described in Green et al. (2017a).

The internal structure of mineralised nests was investigated using prepared sample sections and micro Computed Tomography (micro-CT). Three old wasp nest samples were analysed using the GE Nanotom M micro-CT scanner at the School of Earth Sciences, University of Melbourne. Micro-CT was used to determine the extent to which mineralised wasp nests were open to intrusion from biological or geochemical processes. The output of the process is a three-dimensional model of the sample density.

### **2.4.3 Physical pretreatment**

The aim of physical pretreatment was to remove any possible contamination on exterior surfaces of the sample. For the larger modern wasp nest samples, the outer surfaces were scraped away with a clean scalpel blade then a portion, generally closer to the base of the nest, was removed and lightly ground in a mortar.

A number of different cleaning processes were applied to the old, mineralised wasp nest samples, depending on their size. Large, solid samples had their outer surfaces removed with a clean diamond coated disk in a rotary drill. Medium sized and more fragile pieces had any obvious detritus scraped off with a sterile scalpel blade. Some small and very irregularly shaped samples were cleaned in ultrapure water using an ultrasonic bath. One third of samples were made up of small or very friable pieces with the structure of sand and were given no physical pretreatment. Where possible, the outer surfaces of under art samples (i.e. those nests underlying pigment) were more aggressively removed to further minimise the possibility of modern carbon

contamination. All samples were ground in a clean mortar and placed into a 15ml or 50 ml centrifuge tube, depending on sample size.

## **2.4.4 Chemical pretreatment**

### **2.4.4.1 General pretreatment protocol**

Chemical pretreatment was applied to the ground samples to remove unwanted carbon compounds. Apart from the variations noted in following sections, pretreatment followed the long-established acid-base-acid (ABA) charcoal pretreatment protocol (Devries and Barendsen 1954, Hatté et al. 2001 and Supplementary Information). If the sample remaining after pretreatment was less than about 1 mg it was pipetted directly into a short silica combustion tube, then dried. Larger dried samples, up to 100 mg, were loaded into standard silica combustion tubes.

### **2.4.4.2 Modern mud wasp nests**

A variety of fractions were prepared from modern wasp nests, lightly ground in a mortar. Heavy liquid separation (HLS) using either lithium heteropolytungstate (LST) or sodium polytungstate (SPT) was used on most samples at a density of 2.0 g/cm<sup>3</sup> to separate light and heavy fractions. Light fractions were dissected under a microscope to extract charcoal rich fractions from 11 samples. A plant material fraction for D208 was extracted in the same manner. All fractions then underwent a modified version of the pretreatment protocol outlined in 2.4.4.1. Initially HLS was carried out prior to ABA but in subsequent experiments the order was changed as indicated in the Pretreatment column in Table 2-2. Other fractions extracted from modern nest samples include some where only the first acid step was completed using 2M HCl (identified as “Acid Only” fractions). Two humic fractions (“BaseSol”) were also prepared using the supernatant from the first ABA Base step, resulting from dissolution of the sample in 0.5% NaOH, then precipitation following the addition of 2M HCl. Two samples were pretreated without undergoing HLS and one of these, D215, was split into two aliquots; one received “Acid Only” pretreatment and the other full ABA with a separate “BaseSol” fraction extracted after the first alkali treatment.

#### 2.4.4.3 Old mud wasp nests

In initial experiments, old wasp nest samples received the same general chemical pretreatment process described in 2.4.4.1. For samples processed after the first set of results were acquired, long combustion tubes were used to load a larger mass of pretreated material, up to 300 mg, when suitably large samples were available.

Initial experiments (Sample numbers OZT445 to OZT800) on larger old wasp nest samples used HLS after the final acid step at a density of up to 2.5 g/cm<sup>3</sup> (LST). Samples were centrifuged at 3000 rpm for 20 minutes. Any floating material was pipetted into a separate centrifuge tube then the process was repeated. Extended centrifuge times of up to 60 minutes and speeds of up to 4000 rpm were used if the light fraction appeared to contain too little material after the initial attempts. In later experiments (samples OZU776 to OZW425), HLS was carried out after the first acid treatment using 0.5M HCl. For the final experiments, HLS was carried out after completion of the alkali step and the final acid treatment was changed to 8M or 16M HCl for a duration of at least 30 minutes at room temperature.

To experiment with alternative pretreatment protocols, a selection of some very large samples was treated with concentrated (48%) hydrofluoric acid (HF) mixed with the first HCl acid treatment in ABA processing. After the residue was rinsed, a small portion was pipetted on to a glass slide for inspection under an optical microscope.

To assess levels of potential contamination that may be introduced at any stage from pretreatment through to AMS measurement two types of reference samples were prepared. Simulated modern pseudo-nest material was created using quartz sand (Sigma-Aldrich, acid purified, 40-100 mesh, 84878) mixed with ~0.05% (by weight) ground modern charcoal (OZV994, 103.45 pMC). Simulated ancient nest material was prepared by mixing quartz sand and ~0.3% charcoal prepared from ~8 million-year-old fossil wood (OZO022) from a coal deposit. These two materials are referred to herein as “Modern pseudo-nest” and “Ancient pseudo-nest” samples, respectively.

#### **2.4.4.4 Graphitisation and AMS measurement**

The standard process and equipment used to convert most pretreated samples into graphite targets for accelerator mass spectrometry (AMS) measurement is described by Hua et al (2001, 2004) and in the Supplementary Information. Some 33 samples used the Australian Nuclear Science and Technology Organisation's (ANSTO) microconventional furnace (MCF) facility for ultra-small samples (Yang et al. 2013, Yang and Smith 2016). The carbon isotope ratios were measured using ANSTO's Accelerator Mass Spectrometers (AMS) (Fink et al. 2004, Wilcken et al. 2015).

## **2.5 Results**

### **2.5.1 Modern mud wasp nests**

While weathering and diagenesis transform nest morphology, careful study of the different types of modern nests aids the identification of suitable ancient wasp nests in the field. Original nests can be re-used by other species of wasps and bees so different parts of a remnant nest may have been constructed at different times. Observations of a wide variety of younger nests aids the identification (and avoidance) of such problematic samples.

Out of the 8 fieldwork sessions, wasps were observed collecting mud or building nests only in the two Wet season visits, consistent with Naumann's observation that nesting gradually ceases during the Dry season (1983 :135). Wasps were observed collecting mud from 5 sites, all within rock shelters. Two sites were on the sides of small ephemeral pools of water. Of the other 3 sites, one was a muddy slope in a very dark cavity deep within the rock shelter. As others have also observed (Bednarik 2014: 227), the quartz grains in mud collected without exposure to sunlight may not be "reset" for the purposes of OSL dating so their OSL age would not be the same as the age of the nest. The other two sites were flat areas where sandy soil had accumulated. The soil here was dry and yet the mud ball formed by the wasp (typically 2 -3 mm diameter) was wet. These wasps did not appear to carry water externally to the mud collection site and the volume of water required is significant compared to the size of the wasp (see Supplementary Information video). This suggests the wasp initially ingested water elsewhere before regurgitating it at the point of soil collection, supporting reports of wasps sometimes mixing saliva

with the material collected (Naumann 1983: 156, Polidori et al. 2005 :156 and references therein) and the detection of organic ketones in nests (Bednarik 2014 :226).

**Table 2-1** Analysis of carbon in modern wasp nests

Sample	C%	Corrected $\delta^{13}\text{C}_{\text{PDB}}$
D202	2.58	-23.30
D206	0.76	-9.76
D208	0.39	-22.21
D210	1.47	-16.68
D219	0.85	-21.16
Mean	1.21	-18.62

Modern, single generation nests from 13 different sites were analysed to identify the main sources of carbon, particularly those likely to persist for millennia, to inform development of optimal pretreatment methods for old nests. Elemental analysis of 5 modern nests measured an average carbon concentration of just 1.2% (Table 2-1) and optical microscopy confirmed the major component is quartz sand. HLS was used to remove the quartz and subsequent dissection of light fractions (using a needle under binocular microscope) established that plant material and charcoal were the largest sources of carbon-bearing compounds, by volume (Figure 2-1). Insect sclerites were commonly found but in small volume. Very little pollen was observed in any of the light fractions.



**Figure 2-1** Light fraction of a typical modern wasp nest sorted into charcoal, plant and insect components.



Samples from 19 modern wasp nests and from 2 mud collection sites were radiocarbon dated (Table 2-2). All calibrated radiocarbon ages quoted herein used OxCal version 4.3.2 Bronk Ramsey (2009a, 2017) and the SHCal13 atmospheric curve (Hogg et al. 2013).

Of the 19 individual modern wasp nests dated, 8 contained carbon that was not modern. One of these dates, 2150 - 1750 cal BP (95% probability, 1960 cal BP median) for OZU727U2, was measured using a carbon mass of just 17 $\mu$ g and is considered less reliable, but the other results clearly show an inherited component contributing to a significant inbuilt average radiocarbon age for some newly constructed nests. Where heavy and light fractions from the same nest were dated, it is the heavy fraction that often contains any older carbon. In the light fractions, young plant material was a major component of all 12 and in only 3 samples does older carbon (probably from charcoal) give rise to non-modern average ages of 370, 540 and 700 cal BP (median). The ages measured for 9 charcoal fractions ranged from 0 to 950 cal BP (median probability) with a mean of 255 cal years.

Of the charcoal fractions extracted from two soil samples one was modern and the other was 2,040 years cal BP (median probability).

**Table 2-2** Radiocarbon ages and calibrated median dates for modern wasp nests and 2 associated mud sources. The pretreatment code lists the steps taken in chemical pretreatment in the sequence indicated from left to right. See Supplementary Information for  $\delta^{13}\text{C}$ , pMC and calibrated radiocarbon age ranges.

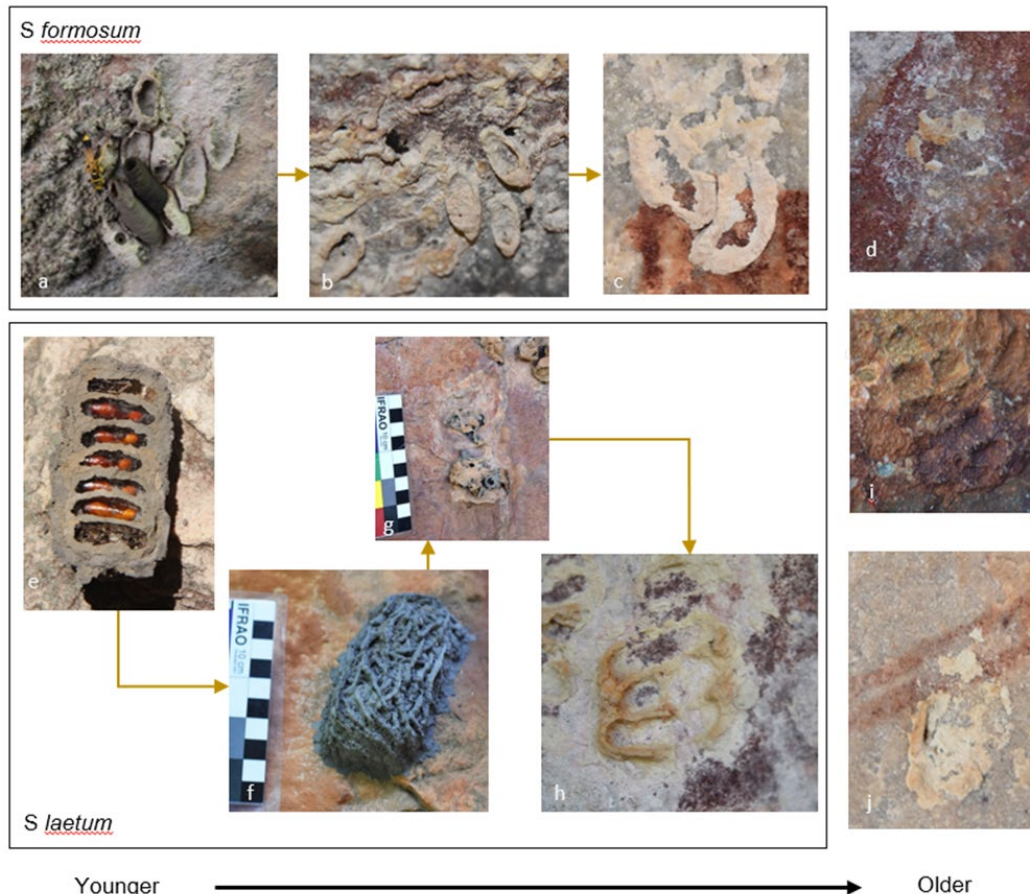
Sample	Laboratory Code	Sample material	Pretreatment	Fraction	$^{14}\text{C}$ Age (BP)	Error ( $1\sigma$ )	Age calBP Median (95.4%)
D202	OZU719	Nest ( <i>S. laetum</i> ?)	HLS - ABA	Charcoal	1,090	50	950
D202	OZU720	Nest ( <i>S. laetum</i> ?)	HLS - ABA	Light	Modern		-
D204	OZU721	Nest ( <i>S. laetum</i> ?)	HLS - ABA	Charcoal	Modern		-
D204	OZU722	Nest ( <i>S. laetum</i> ?)	HLS - ABA	Light	Modern		-
D206	OZU723U1	Nest	HLS - ABA	Light	Modern		-
D206	OZU723U2	Nest	HLS - ABA	Heavy	550	35	530
D207	OZU724	Nest	ABA	All	330	60	380
D208	OZU265	Nest ( <i>S. laetum</i> ?)	HLS - ABA	Charcoal	735	30	650
D208	OZU266	Nest ( <i>S. laetum</i> ?)	HLS - A only	Heavy	1,090	30	950
D208	OZU267	Nest ( <i>S. laetum</i> ?)	HLS - A only	Light	815	25	700
D208	OZU268	Nest ( <i>S. laetum</i> ?)	HLS - ABA	Plant	Modern		-
D208	OZU730U1	Nest ( <i>S. laetum</i> ?)	ABA - HLS	Light	580	35	540
D208	OZU730U2	Nest ( <i>S. laetum</i> ?)	ABA - HLS	Heavy	680	40	600
D208	OZU730U3	Nest ( <i>S. laetum</i> ?)	A	BaseSol	935	20	790
D209	OZU725	Mud balls near D208	ABA	All	Modern		-
D210	OZU269	Nest ( <i>S. laetum</i> ?)	HLS - A only	Light	Modern		-
D211	OZU726U1	Nest ( <i>S. laetum</i> ?)	ABA - HLS	Light	315	25	370
D211	OZU726U2	Nest ( <i>S. laetum</i> ?)	ABA - HLS	Heavy	Modern		-
D212	OZU727U1	Nest	ABA - HLS	Light	Modern		-
D212	OZU727U2	Nest	ABA - HLS	Heavy	2,040	80	1,960
D213	OZU270	Nest ( <i>S. laetum</i> ?)	HLS - A only	Light	Modern		-
D215	OZU271U*	Nest ( <i>S. formosum</i> ?)	A only	All	200	30	190
D215	OZU271U1	Nest ( <i>S. formosum</i> ?)	ABA	All	115	25	70
D215	OZU271U2	Nest ( <i>S. formosum</i> ?)	A	BaseSol	100	50	90
D216	OZU728U1	Nest ( <i>S. laetum</i> ?)	ABA - HLS	Light	Modern		-
D216	OZU728U2	Nest ( <i>S. laetum</i> ?)	ABA - HLS	Heavy	Modern		-
D217	OZU729U1	Nest, resin coated	ABA - HLS	Light	Modern		-
D217	OZU729U2	Nest, resin coated	ABA - HLS	Heavy	Modern		-
D219	OZU272	Nest, resin coated	HLS - A only	Light	Modern		-
D500	OZW346	Nest, <i>eumeninae</i>	A - HLS - BA	Charcoal	825	20	700
D508	OZW344	Nest ( <i>S. laetum</i> ?)	A - HLS - BA	Charcoal	Modern		-
D514	OZW347	Nest ( <i>S. laetum</i> ?)	A - HLS - BA	Charcoal	Modern		-
D632	OZW349	Nest ( <i>S. laetum</i> ?)	A - HLS - BA	Charcoal	Modern		-
D670	OZW350	Nest ( <i>S. laetum</i> ?)	A - HLS - BA	Charcoal	Modern		-
D699	OZW345	Nest ( <i>S. laetum</i> ?)	A - HLS - BA	Charcoal	Modern		-
D516	OZW348	Soil from mud collection site	A - HLS - BA	Charcoal	2,110	25	2,040
D700	OZW351	Dry soil below D699	A - HLS - BA	Charcoal	Modern		-

Age determinations on four fractions derived from sample D208 indicate that all but the plant fraction contained old carbon with the heavy fraction dated to almost 1000 cal BP. The light and charcoal-rich fractions were a few hundred years younger (Table 2-2). While the hand-picked, charcoal-rich fraction is dominated by macroscopic charcoal, smaller charcoal fragments were concentrated in the remaining light fraction, with some mineral coated or impregnated charcoal pieces (Bird et al. 2008: 2703) in the heavy fraction. A different portion (OZU730) of the same D208 nest was pretreated using the full ABA process. The ages for the heavy and light fractions were 540 and 600 cal BP respectively, younger than those of the previously measured portion (OZU266 and OZU267). The precipitated alkali soluble fraction (OZU730U3) for the same sample was dated to 790 cal BP (median) so the removal of this material (humic acid) during ABA processing explains the younger ages for the light and heavy fractions. Given the ages of the other fractions, the source of this humic acid is probably endogenous, diagenetically altered, charcoal rather than exogenous organic material (Ascough et al. 2011: 76).

## **2.5.2 Old mud wasp nests**

### **2.5.2.1 Nest Construction**

Observation of mud wasp nests at more than 150 rock shelters suggests that new nests are quickly transformed due to decomposition and weathering. There are relatively few examples of nests with intact outer surfaces (e.g. Figure 2-2a, e, f). The thin outer “fins” of *S. laetum* nests (Figure 2-2f) and the thin outer cell walls of *S. formosum* nests (Figure 2-2a) weather away rapidly and the initial structure of the nest is lost. The common remnant nest is a distinctive oval shaped stump (e.g. Figure 2-2c, d, h, i) being the thicker, often mineralised mud at the base of the nest. Where mineral accretions have developed on the rock surface (Green et al., 2017b), they can thoroughly indurate and cover old nest stumps (Figure 2-2i).



**Figure 2-2** Nest diagenesis for two of the most common wasp species: *S formosum* (a - c), *S laetum* (e - h). (e) is the underside of a new *laetum* nest showing the characteristic oval shape of cells, two of which are provisioned with spiders and the other 5 having developed to the prepupal stage.

Wasps prefer to build nests in the most protected areas in Kimberley rock shelters, avoiding sunlight and wet areas, as has been reported in the Kakadu region (Naumann 1983: 135). Successive generations of wasps exhibit the same preference so new nests are often constructed on top of old ones in the most favoured locations, thereby creating thick accumulations of multi-generational nests (Figure 2-3). However, in the great majority of cases, such areas are not selected for rock paintings. A typical painted panel will be more exposed and while nest stumps are still found on these surfaces they are usually dispersed and not constructed on top of older nests. Of the 30 modern wasp nests collected only one (Figure 2-2a) appeared to be built on the stumps of old nests. This observation is contrary to reports from other research, where it is stated that wasps prefer to build nests on top of the stumps

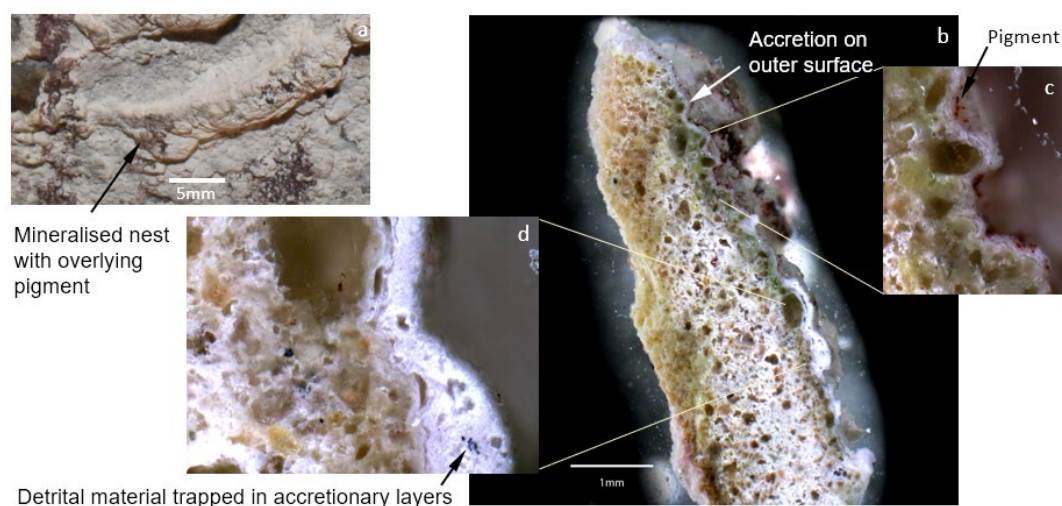
of old nests (Roberts et al. 1997: 698, Bednarik 2014: 227, Ross et al. 2016: 7). This disagreement may be due to views about the minimum acceptable size for a nest sample. For OSL dating, substantially larger samples are required to ensure that the quartz grains have not been exposed to light, post-construction (Roberts et al. 2000: 42). These larger samples are usually only found as multi-generational nests in the more sheltered, highly favoured locations where nest density is very high (Figure 2-3). While large samples are also advantageous for radiocarbon dating, large intact nests are rare compared to the much more common, smaller, nest stumps found on the more exposed painted panels.



**Figure 2-3** High density wasp nest areas. In (c), the location selected for the most recent nest (bottom) is relatively clear of other recently constructed nests and larger nest stumps.

Intact and abandoned nests may be re-used by many species of wasps and bees that do not construct complete, new nests (Naumann 1983: 175). Secondary nest builders often re-work or add mud to reshape the original cells so the ages of material at either end of the nest may be different. Ideally, a sample for dating will be of a single generation nest, not a multi-generation or reworked nest.





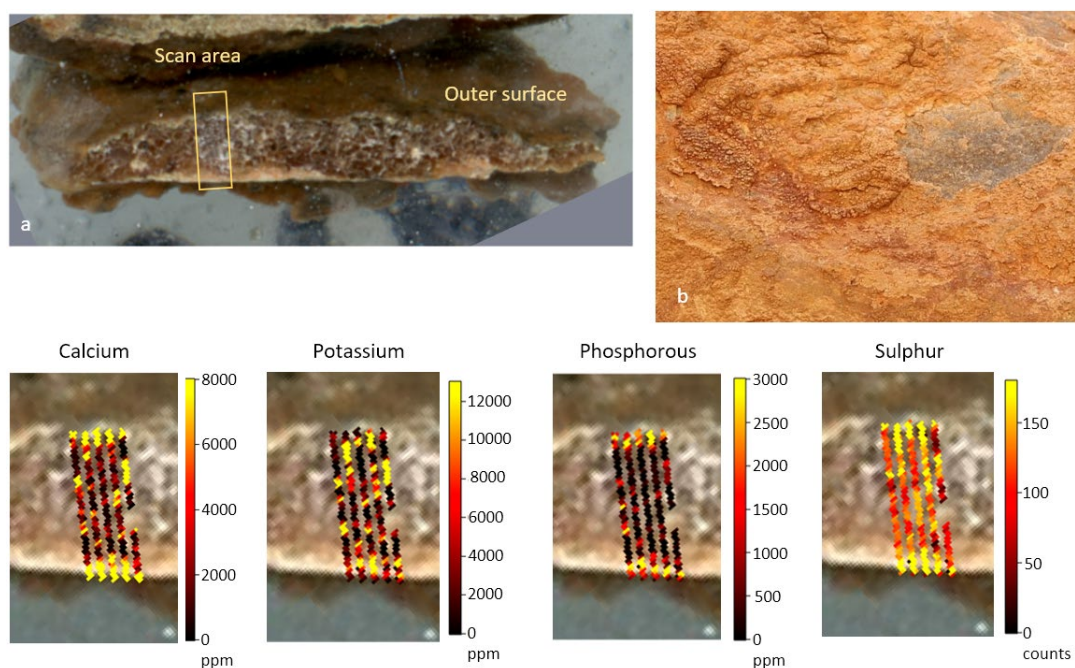
**Figure 2-4** Mineralised wasp nest stump (a) in section (b), with overlying pigment (c), showing detrital material trapped in the accretionary layers(d)

## 2.5.2.2 Nest Composition

### 2.5.2.2.1 Internal structure

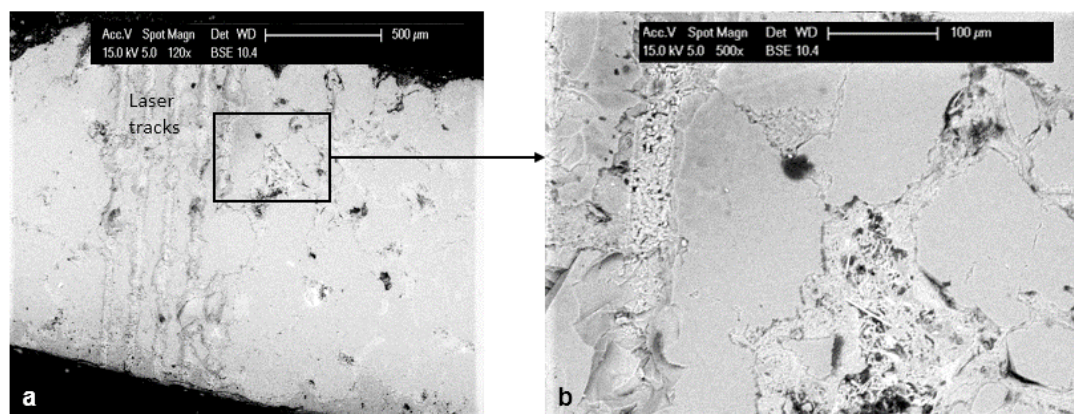
The internal structure of old nests was investigated to understand the potential for new carbon-bearing material to be incorporated into the nest structure.

Optical inspection of polished sections confirmed that heavily indurated nests are coated with accretionary layers (Figure 2-4) and that these layers can trap detrital material (Figure 2-4d), including charcoal. Significant amounts of charcoal embedded in mineral accretions have also been reported from other sites in the Kimberley region (Ford et al. 1994: 61). LA-ICPMS scans of nest sections show high concentrations of accretionary materials on outer surfaces and, sometimes, on the underside where mineral coatings on the rock surface have bonded with the nest (Figure 2-5). For larger sample pieces these coatings were removed mechanically before chemical pretreatment. This is not possible for smaller, and friable samples where chemical pretreatment will remove some sources of exogenous carbon, but not necessarily all of them.



**Figure 2-5** Distribution of Ca, K, P and S in a mineralised nest (D018). Note the warm tones through to yellow indicate increasing concentration in each case. Ca, K and P quantified using calibration against NIST SRM 612 with an estimated precision of elemental concentrations of <5%. S is illustrated on the basis of signal intensity and provides only a qualitative indication of S content.

Examination of polished sections of a range of old nests and micro-CT scans (see Supplementary Information 2.10.2 for an example) show nest interiors to be thoroughly mineralised with few contiguous pore spaces. SEM imaging (e.g. Figure 2-6) shows some voids partly filled with crystalline growths. Across the range of samples imaged, mineralisation had closed off most of the pore space leaving little opportunity for later intrusion of biogenic, aeolian or fluvial contamination. This decrease in porosity is similar to that observed in buried charcoal (Bird et al. 2008: 2705).



**Figure 2-6** SEM imaging of D018, in the area around the LAICPMS scan in Figure 2-5. Crystalline growths evident in interstitial space in expanded view on the right

#### 2.5.2.2.2 XRD

Old nests are dominantly composed of quartz, with subordinate clays from the original mud, together with traces of a range of minerals that are also found in accretions throughout Kimberley rock shelters (Green et al. 2017a, Green et al. 2017b). Of the 39 nests analysed using XRD, only 9 contained major levels (>15% by weight of crystalline content) of phases other than quartz (Supplementary Information Table 2-S2). These included the accretionary sulphate minerals; gypsum, alunite and polyhalite, the phosphates; taranakite and tinsleyite and the oxalate; whewellite. The highest levels of oxalates were observed in heavily indurated nests, similar to Figure 2-2i. The highest levels of phosphates and sulphates are associated with indurated nests from areas with thick surface mineral accretions (e.g. Figure 2-3a and b). Only two nests contained calcite, and only at trace levels. Apart from the insoluble oxalates (whewellite, glushinskite), calcite was the only carbon-bearing mineral detected. It is likely that calcite and the oxalate minerals are present in many samples but at levels below that detectable using XRD (<2 or 3%). One objective of the chemical pretreatment was to ensure that even trace levels of these carbon-bearing minerals were removed prior to radiocarbon dating.



### 2.5.2.2.3 XRF

As XRD does not detect amorphous minerals, the elemental composition of 14 large nest samples were analysed using XRF (Table 2-3).

**Table 2-3** Major elements, in weight % oxides, from XRF analysis. The average MnO% was 0.03% with a maximum of 0.08% in D134. Low total compositions are due to unreported sulphur (particularly D018) and carbon (D025).

Sample	Na <sub>2</sub> O	MgO	Al <sub>2</sub> O <sub>3</sub>	SiO <sub>2</sub>	P <sub>2</sub> O <sub>5</sub>	K <sub>2</sub> O	CaO	TiO <sub>2</sub>	Fe <sub>2</sub> O <sub>3</sub>
D013	0.0	0.2	4.2	85.7	0.4	0.4	0.1	0.4	1.7
D018	3.7	1.5	2.7	57.7	0.5	0.6	12.8	0.1	0.7
D025	0.4	0.3	4.8	76.2	1.4	0.3	0.3	0.3	1.5
D027	0.1	0.1	5.2	86.8	1.3	0.3	0.1	0.4	1.4
D034	4.7	1.2	5.1	63.2	9.7	1.5	3.6	0.4	2.0
D105	2.0	0.6	6.9	78.9	3.2	2.7	0.7	0.4	2.5
D131	2.4	0.4	4.7	77.7	3.8	2.5	0.6	0.5	1.4
D134	4.4	1.3	7.6	67.9	6.7	3.8	3.4	0.5	2.1
D136	0.7	0.3	6.2	81.4	1.2	1.7	0.3	0.5	1.7
D140	0.0	0.1	4.7	81.8	0.1	0.6	0.0	0.6	1.6
D147	1.1	0.5	4.0	83.8	1.2	1.7	0.3	0.3	1.4
D154	4.3	1.8	4.0	69.6	4.9	4.1	2.6	0.2	1.5
D155	1.2	0.6	8.7	75.6	0.8	2.3	0.6	0.5	2.7
PC15-01	0.9	0.3	4.0	82.0	0.3	1.7	0.3	0.4	1.4
Mean:	1.8%	0.7%	5.2%	76.3%	2.5%	1.7%	1.8%	0.4%	1.7%

The XRF elemental analyses are broadly consistent with the XRD mineralogical analyses with no suggestion that other amorphous minerals are present in significant concentrations. The widespread occurrence of iron, albeit at low levels, suggests it may be underrepresented in the mineralogical results. In these analyses, only heavily indurated samples have SiO<sub>2</sub> concentrations less than 80% with Al, P, Na, Ca, K, and S making up most of the balance.

#### 2.5.2.2.4 Elemental Analyser results

The carbon and sulphur content of 13 nests was analysed (Table 2-4) to determine the typical concentrations prior to pretreatment and to complement XRD and XRF results. The average carbon concentration across all 13 samples is 0.65% but this is inflated by the high oxalate concentration in the heavily indurated sample, D019.

The average carbon concentration, excluding D019, is 0.22% and is a more representative estimate of the carbon in old nests. This is significantly less than the average 1.2% carbon measured in modern wasp nests and probably reflects the loss of carbon as CO<sub>2</sub> gas from decayed organic matter in the early stages of nest diagenesis (Trumbore 2009: 49).

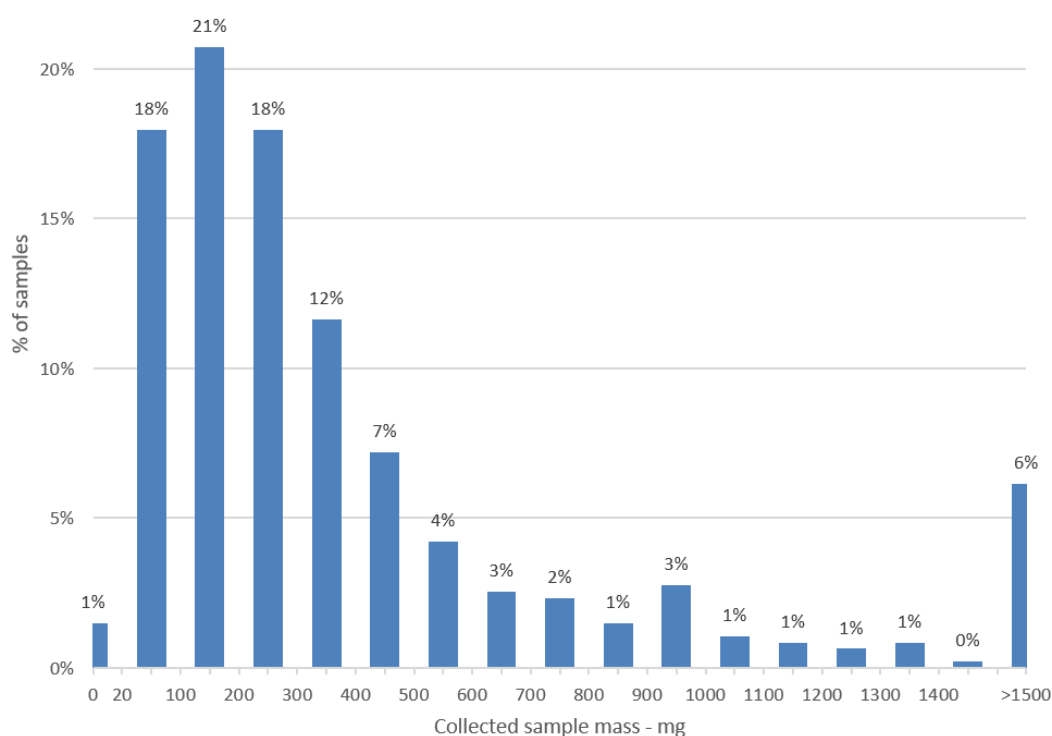
The sulphur concentrations are broadly consistent with the XRD results. The five samples with the lowest sulphur concentrations (from 0.11% to 0.51%) also recorded no sulphate minerals in the XRD analysis. The eight higher sulphur concentration (0.63 – 2.87%) samples all recorded at least trace levels of sulphates in the XRD results.

**Table 2-4** Percentage weight of carbon and sulphur in old wasp nests and isotopic compositions of carbon.

Sample	C%	S%	Corrected $\delta^{13}\text{C}_{\text{PDB}}$
D019	5.75	1.80	-11.4
D105	0.07	2.04	-18.0
D119	0.70	0.11	-20.8
D131	0.11	2.59	-10.6
D134	0.12	2.87	-17.4
D136	0.10	1.87	-12.5
D144	0.15	0.63	-9.9
D147	0.25	1.50	-13.1
D152	0.25	0.35	-13.9
D161A	0.34	0.91	-20.7
D161B	0.21	0.24	-20.6
D168	0.25	0.46	-19.4
D348	0.10	0.51	-14.2
Mean:	0.65	1.22	-15.6

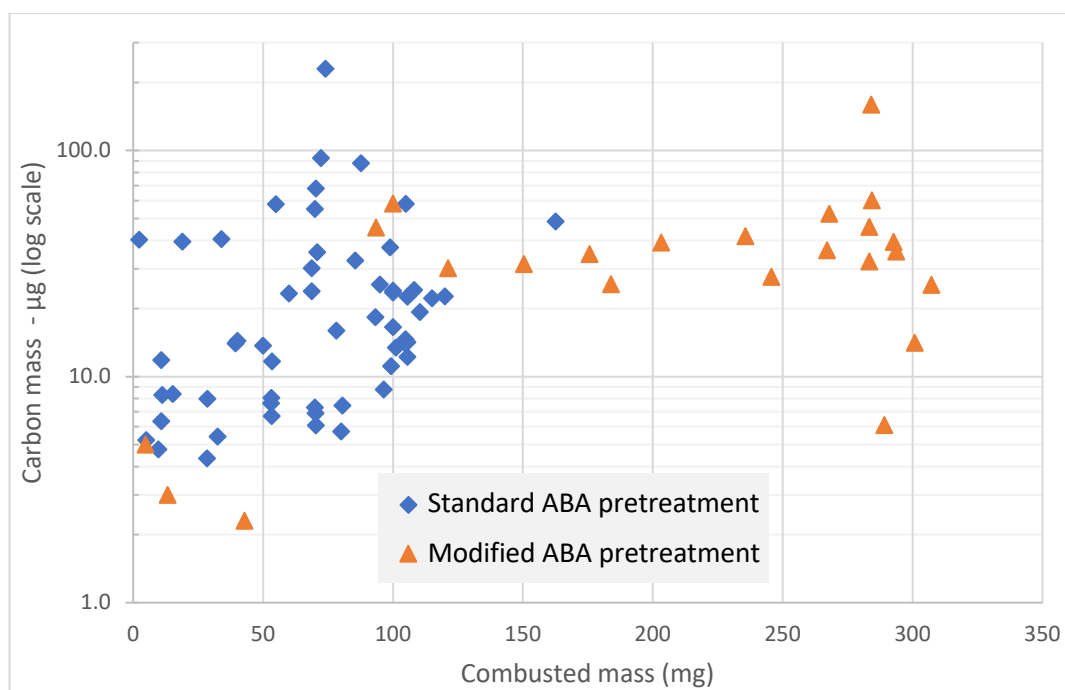
### 2.5.2.3 Pretreatment

#### 2.5.2.3.1 Carbon mass



**Figure 2-7** Histogram of the mass, as collected, of all old wasp nests included in this study

The median mass of all old wasp nests collected is 247 mg with 80% of samples having a mass of less than 570 mg (Figure 2-7). Of all the old wasp nests collected, 120 have been prepared for radiocarbon dating so far. A total of 175 sample fractions were prepared from these 120 samples. Initially, samples were pretreated using a standard ABA protocol (Standard ABA series in Figure 2-8). About 40% of these fractions yielded less than 12 $\mu$ g C after combustion (or failed during graphitisation) and were not measured. Experiments using HLS were then undertaken with the initial aim of improving the percentage of samples that produced sufficient carbon for dating.



**Figure 2-8** Mass of sample combusted vs carbon mass after sample combustion.

#### 2.5.2.3.2 Heavy liquid separation

To improve the yield, experiments were conducted using HLS, on the assumption that charcoal would be concentrated in the light fraction providing the specific gravity was less than that of quartz (c.  $2.6 \text{ g/cm}^3$ ). In practice, microscopic inspection of the heavy fractions suggested that they also contained a significant amount of microscopic charcoal. This was confirmed when both light and heavy fractions from 23 samples were combusted. The average amount of carbon in the heavy fractions ( $28 \mu\text{g}$ ) was very similar to that in the light fractions ( $31 \mu\text{g}$ ). Separations starting at a specific gravity of 1.2 and increasing up to  $2.5 \text{ g/cm}^3$  established that the quantity of floating material (mostly charcoal) increased with density, suggesting pyrogenic carbon at varying degrees of mineralisation was present. This result in mud wasp nests mirrors that found to occur in soils where pyrogenic carbon becomes attached to and impregnated with soil minerals over time (e.g. Brodowski et al. 2005, Bird et al. 2008, Bird et al. 2015). While HLS was only partly successful in concentrating charcoal into the light fraction, dating the separate fractions provided important insights into the carbon sources within the samples.

**Table 2-5** Old wasp nests with multiple analysed fractions using initial pretreatment process. The sample code is constructed from a short site identifier, followed by a number to identify the painted motif and then the number of the sample collected (on that motif, at that site) in the format “SITE\_MOTIF-NEST”. Sample OZT797U2 has a measured  $\delta^{13}\text{C}$  of -22.5‰, all other samples are assumed to be -25‰.

Sample Code*	Laboratory Code	Pretreatment Sequence	Fraction	C mass $\mu\text{g}$	$^{14}\text{C}$ years BP	Error ( $1\sigma$ )	Rel. Score	Single Nest?
DR006_05-1	OZT801U2	ABA - HLS	Light	18	Modern		2	Y
DR006_05-1	OZT801U1	ABA - HLS	Heavy	13	3,110	140	1	Y
DR013_09-1	OZT797U*	ABA	All	48	11,530	80	5	N
DR013_09-1	OZT797U2	ABA - HLS	Light	110	16,930	100	7	N
DR013_09-1	OZT797U1	ABA - HLS	Heavy	26	15,940	160	3	N
DR013_11-1	OZT798U2	ABA - HLS	Light	51	4,920	80	7	N
DR013_11-1	OZT798U1	ABA - HLS	Heavy	20	11,350	150	3	N
DR015_06-1	OZT799U*	ABA	All	24	2,260	100	3	N
DR015_06-1	OZT799U1	ABA - HLS	Heavy	12	9,460	170	1	N

Initially, 4 heavy/light fraction pairs were dated after the standard ABA pretreatment followed by HLS (Table 2-5). The results show some large differences between ages of the heavy and light fractions of the same sample, with the heavy fraction usually older. Only very large samples produced enough carbon for these experiments. Such samples often comprise nests of very different ages so extreme differences in the ages of the heavy and light fractions are feasible. Even so, some of the samples were clearly from a single generation nest (“Single Nest?” = Y in Table 2-5) so this is not the only cause. It may also be the case that the carbon masses were too low to produce reliable age estimates, so experiments were conducted on further samples using different pretreatment protocols (Table 2-6).

**Table 2-6** Old wasp nests with multiple dated fractions using a range of modified pretreatment processes (except OZT447, OZT444, OZT455; included for comparison only).

Sample Code	Laboratory Code	Pretreatment Sequence	Fraction	C mass $\mu$ g	<sup>14</sup> C years BP	Error (1 $\sigma$ )	Rel. Score	Single Nest?
DR013_06-1	OZT447	ABA	All	15	15,350	200	3	N
DR013_06-1	OZU776U1	A-HLS-BA(8M)	Light	27	10,820	120	7	N
DR013_06-1	OZU776U2	A-HLS-BA(8M)	Heavy	33	11,340	90	7	N
DR013_11-1	OZU777U1	A-HLS-BA(8M)	Light	43	1,370	610	8	N
DR013_11-1	OZU777U2	A-HLS-BA(8M)	Heavy	40	11,170	80	8	N
DR013_11-1	OZW354	A-HF-HLS-BA(8M)	Light	11	15,780	200	5	N
DR013_11-1	OZW355	A-HF-HLS-BA(8M)	Heavy	13	10,190	110	5	N
DR015_04-2	OZU778U1	A-HLS-BA(8M)	Light	17	7,010	90	5	N
DR015_04-2	OZU778U2	A-HLS-BA(8M)	Heavy	51	10,010	80	8	N
DR015_10-2	OZU779U1	A-HLS-BA(8M)	Light	42	14,200	110	9	N
DR015_10-2	OZU779U2	A-HLS-BA(8M)	Heavy	47	14,390	100	8	N
DR015_10-7	OZW379	A-HLS-BA(8M)	Light	11	4,690	90	2	N
DR015_10-7	OZW380	A-HLS-BA(8M)	Heavy	33	10,730	70	4	N
DR015_14-4	OZU780U1	A-HLS-BA(8M)	Light	11	12,420	150	5	N
DR015_14-4	OZU780U2	A-HLS-BA(8M)	Heavy	49	13,450	90	8	N
DT1207_01-1	OZW382	A-HLS-BA(8M)	Light	17	2,380	80	5	Y
DT1207_01-1	OZW383	A-HLS-BA(8M)	Heavy	21	6,870	70	6	Y
DT1207_12-1	OZW388	A-HLS-BA(8M)	Light	15	5,260	80	5	Y
DT1207_12-1	OZW389	A-HLS-BA(8M)	Heavy	22	8,240	80	6	Y
FW014_01-1	OZT444	ABA	All	93	5,820	70	8	Y
FW014_01-1	OZT455	ABA	All	87	5,150	70	7	Y
FW014_01-1	OZW352	A-HF-HLS-BA(8M)	Light	61	1,895	40	7	Y
FW014_01-1	OZW353	A-HF-HLS-BA(8M)	Heavy	13	2,560	70	3	Y
KG002_02-1	OZU781U1	A-HLS-BA(8M)	Light	120	13,030	80	9	N
KG002_02-1	OZU781U2	A-HLS-BA(8M)	Heavy	44	10,010	60	7	N
KG021A_02-2	OZU782U1	A-HLS-BA(8M)	Light	56	16,940	120	9	N
KG021A_02-2	OZU782U2	A-HLS-BA(8M)	Heavy	47	12,970	80	7	N
KG028A_03-1	OZU785U1	A-HLS-BA(8M)	Light	25	12,590	200	6	N
KG028A_03-1	OZU785U2	A-HLS-BA(8M)	Heavy	41	11,750	80	7	N

The first experiment used a concentrated (8M or 16M HCl) final acid treatment in place of 2M HCl. Hedges et al (1998: 36) found that “routine acid treatment” did not remove all oxalate from two pigment samples and Armitage et al (2001: 474) concluded that an anomalous result on a pigment date was due to incomplete removal of oxalates and/or carbonates. To test whether the 8/16M final acid step in the ABA process was removing acid soluble carbon, about 20% of the HCl supernatant was removed and dried down in small combustion tubes. The small tube was then combusted inside a larger sealed silica tube. The amount of carbon in 14 of these “acid soluble fractions” was measured to be in the range of 2.4 to 7.8µg with a mean of 5.3µg. This fraction may include up to 6µg of exogenous carbon as the inner/outer tube combustion method is known to be more susceptible to contamination, but 5 samples contained more than 7µg of carbon suggesting it cannot all be from contamination. The implication is that at least a third of samples contained 5 to 10 µg of acid soluble carbon in the final acid supernatant that was not removed in the first acid treatment. To ensure complete removal of oxalates, all subsequent samples (with Lab Codes following OZU272) used 8 or 16 M HCL in the final acid step.

Other changes to the pretreatment process included the use of larger combustion tubes when more than 100 mg of pretreated sample was available. The larger tubes were loaded with up to 300 mg of sample so many more contained enough carbon for AMS measurement (Figure 2-8).

#### **2.5.2.4 Quality Control**

In addition to chemical procedural blanks routinely used at ANSTO, five “modern” and “ancient” pseudo-nest samples were analysed to check for potential contamination introduced during pretreatment (Table 2-7). The 3 modern pseudo-nest analyses recorded pMC values within one standard deviation of the modern charcoal (OZV994) used to make this pseudo-nest material. This confirms that no significant undetected old carbon contamination occurred in the pretreatment process. Of the two old pseudo-nest analyses, one had no significant modern carbon contamination but the other had enough contamination to reduce the measured age

to 42.7 – 41.7 cal ka BP. No specific source was identified for this abnormal result but given that routine blanks and standards showed no such contamination it is most likely that it occurred due to human error during ABA processing. More frequent use of an ancient pseudo-nest reference sample is recommended as an additional check for potential contamination during the earlier stages of sample processing.

**Table 2-7** Dated modern and ancient carbon pseudo-nest samples

Laboratory Code	Sample Description	Pretreatment Sequence	Fract ion	C mass $\mu\text{g}$	$\delta^{13}\text{C}$ ‰	Error (1 $\sigma$ ) $\pm$	percent Modern Carbon	Error (1 $\sigma$ ) $\pm$	$^{14}\text{C}$ years BP ( $\pm 1\sigma$ )
OZV994	Modern charcoal only	ABA	All	-	-28.5	0.1	103.45	0.27	Modern
OZW340	Modern pseudo-nest	A-HLS-BA(8M)	Light	31			103.46	0.59	Modern
OZW342	Modern pseudo-nest	A-HLS-BA(8M)	Light	63			102.72	0.49	Modern
OZW363	Modern pseudo-nest	A-HF-BA(16M)	All	52			103.44	0.44	Modern
OZW362	Dead pseudo-nest	A-HF-BA(16M)	All	265	-24.5	0.4	0.07	0.04	>52600
OZW424U2	Dead pseudo-nest	ABA(16M)	All	210			0.89	0.04	37,940 ( $\pm 350$ )

### 2.5.2.5 Reliability Assessment

The preceding results and analysis identified three factors that affect the reliability of the ages measured: (i) mass of carbon analysed, (ii) ability to remove surface contamination and (iii) use of strong acid to remove all oxalates and carbonates. The nature of these factors means they cannot readily be quantified and included in a statistical error calculation. Nonetheless, an age estimate is more, or less likely to approximate the construction date of the nest depending on these factors (and potentially others). To record and summarise these differences a “Reliability Score” was devised and has been calculated for each AMS measurement reported herein. In this context, a more reliable age estimate is one that is closer to the true date of construction of the mud wasp nest.

The Reliability Score is the sum of semi-quantitative sub-scores for each of the three factors: carbon mass, physical pretreatment and chemical pretreatment. The score is an open-ended scale but, with current processes, the most reliable measurement

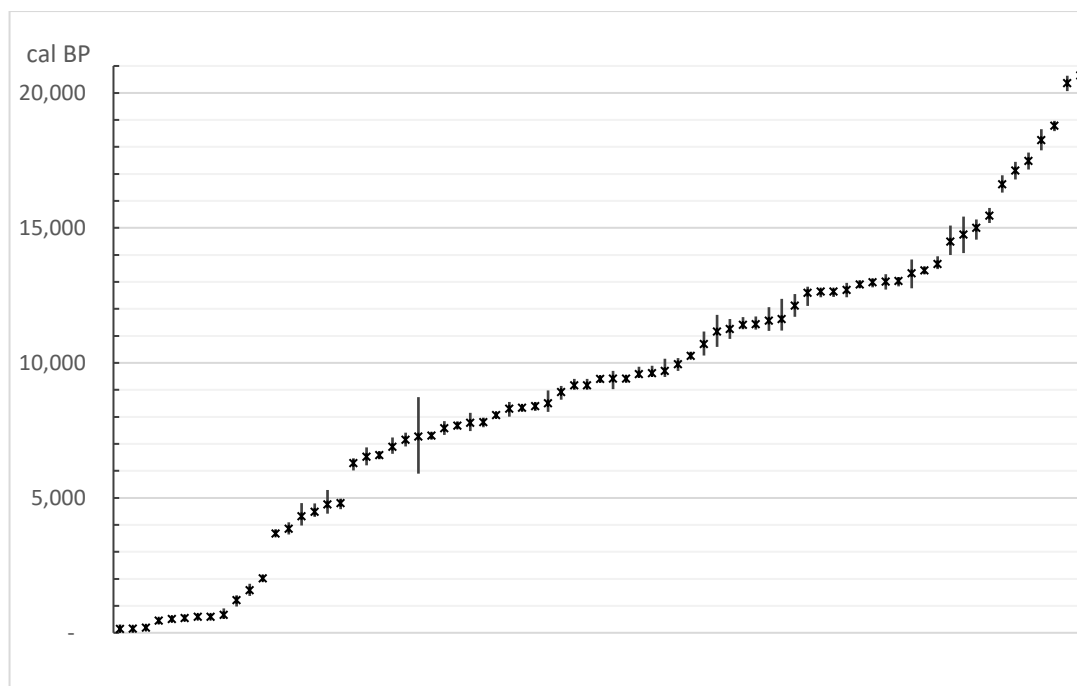


scores a 10 (5+3+2, as follows). Half of the score weighting is for the mass of carbon analysed. Samples with < 12 µg C score zero, 1 for those between 12 and <20 µg, 2 for 20 to <30 µg and so on up to a score of 5 for samples of 50 µg or more. Optimal physical pretreatment scores a maximum of 3 for samples where the entire external surface can be ground off. At the other extreme, sand like samples that cannot be ground, scraped or ultrasonicated score a zero. The maximum score for chemical pretreatment is 2 when the protocol involving the use of 8/16M HCl is employed to generate a light fraction, and a score of zero applies to heavy fractions where oxalates may not have been completely removed.

The Reliability Scores listed in Tables 2-6 and 2-7 serve to identify results that may have an “anomalous sample composition” (sensu Taylor and Southon 2012: 979). As a relative scale, it is intended as an aid to subsequent analysis of the relationship between the date as measured and the underlying or overlying rock art. For example, experiments on the multi-generation nest sample DR013\_06-1, from underneath pigment, yielded 3 age estimates (top 3 rows of Table 2-6) so the question arises as to which date to use as a maximum age for the overlying pigment. An earlier date of 15,350 yr BP on part of the sample has a score of 3 and is discounted as less reliable in favour of a date of 10,820 yr BP on a light fraction with a score of 7. The heavy fraction, measured at 11,340 yr BP, also has a score of 7 so there is certainly charcoal of different ages in this sample, but it is the youngest charcoal that defines the maximum age for the overlying pigment. Hence the 10,820 yr BP date is selected as the most relevant maximum age for this sample.

#### **2.5.2.6 Wasp nest age determinations**

Of the 120 old nests processed to date, a total of 75 old wasp nest samples were successfully radiocarbon dated; 45 nests contained too little carbon for AMS measurement. Where multiple fractions from the same nest have been measured, one has been selected as the most appropriate as outlined in section 2.5.2.5. Measured wasp nest ages range from Modern to just over 20 cal ka BP. The results will be presented in detail elsewhere in the context of their relationship to rock art, but they are summarised graphically in Figure 2-9 simply to illustrate the range and estimated precision of ages obtained using the methods detailed here.



**Figure 2-9** Median calibrated age (x) of wasp nest samples and 95.4% probability range (bar) (OxCal v4.3.2 SHCal13)

## 2.6 Discussion

The variations observed in the age of carbon in modern nests and the dates of different fractions prepared from old nests raise some key issues that are discussed in more detail below.

### 2.6.1 Charcoal as a target for dating nests

Analysis of the composition of the modern wasp nests suggested that charcoal was the main source of carbon likely to survive for long periods. Charcoal will generally be present in sediment collected by mud wasps. Currently, an average of 30% of the North Kimberley is burnt each year in bushfires (Vigilante et al. 2004) so pyrogenic carbon is abundant in this environment. The palaeoenvironmental record also suggests significant levels of burning, at least since people first arrived (Kershaw 1986: 48, Proske et al. 2014: 172). While plant material is another major carbon-bearing component in mud collected by wasps, it rapidly oxidizes to CO<sub>2</sub> and less stable organic compounds (Trumbore 2009: 49), some of which have a mean residence time in soils of just weeks to months (Kuzyakov 2006: 428).

Carbon isotope measurements on 5 modern nests (Table 2-1) point to short-lived grasses as a significant source of the organic content. The mean  $\delta^{13}\text{C}$  value of -15.6‰ is significantly greater than the -26‰ expected for  $\text{C}_3$  trees and shrubs. This suggests pyrogenic carbon from the locally abundant  $\text{C}_4$  grasses (probably spinifex at -12‰  $\delta^{13}\text{C}$ ) or sedges (e.g. a regional Cyperaceae measured at -9.6‰  $\delta^{13}\text{C}$ ) are a major component of carbon in many nests (McWilliam and Mison 1974, Hattersley 1983, Wooller et al. 2005) in the Kimberley region. Ford et al. (1994: 62) studied the micromorphology of charcoal found in pigments from rock shelter walls in the Kimberley and also concluded the source was spinifex rather than wood.

Charcoal from these short-lived grasses will have a negligible inbuilt age prior to combustion and will usually be microscopic in scale, given the fine structure of grasses. It is also unlikely that wood in this region would have a significant inbuilt age, prior to combustion. The vegetation in the northern Kimberley Plateau is mostly savanna with eucalyptus woodlands, tall grasses and spinifex (Bowman et al. 2010: 205, Pepper and Scott Keogh 2014: 1447), and the trees are usually less than 200 years old (Ogden 1981: 418). It is possible, however, that older wood or charcoal is more common in rock shelters due to anthropogenic activity, but the action of ubiquitous termites and fire greatly limit the abundance of old wood.

The source of the old carbon detected in the modern nest samples, is therefore, most likely to be old charcoal present in surface sediments. This is consistent with findings from studies of soil organic carbon where the average age of pyrogenic carbon is reported to be of the order of centuries or a few millennia, with charcoals in tropical soils at the shorter end of that scale (Graetz and Skjemstad 2003: 41, Hobley et al. 2014b: 751 and references therein, Hobley et al. 2014a).

With old carbon commonly present in the mud collected by wasps, how then can the radiocarbon age of incorporated charcoal be used to estimate the time of construction of the nest? One approach (Bronk Ramsey 2009b, Dee and Bronk Ramsey 2014: 83) notes that the age distribution of sampled charcoal is likely to be exponential (with most samples being young and the probability of selecting older samples diminishing as age increases). With a mean of 255 years (standard deviation of 370) from the 9 modern nest charcoal fractions dated (Table 2-2), an exponential age distribution would imply that 95% of samples have an inbuilt age of less than

764 years (from the cumulative distribution function  $P(X \leq x) = 1 - \exp(-\lambda x) = 0.95$  where  $\lambda$  is  $1/255$ ). Dates on further charcoal fractions would improve this estimate of the inbuilt age of charcoal in newly constructed nests, but a reasonable working hypothesis is that the age of carbon in modern nests is most likely to be less than 764 years, and usually much less.

### **2.6.2 Alternative Methods**

Alternative pretreatment methods were considered but the very small mass of carbon available in wasp nest samples means that most are not feasible. Old wasp nests measured had a carbon concentration of c. 0.2% and a median mass of 247 mg so a typical initial carbon mass is 0.5 mg. This is well below the more than 100 mg of well-preserved charcoal considered necessary for acid-base-oxidation-stepped combustion (ABOx-SC) processing (Higham et al. 2009a: 1265). The hydrogen pyrolysis (hypy) technique (Ascough et al. 2009, Ascough et al. 2010) also requires larger carbon masses and is not necessarily any more effective when the ages being measured are less than c. 25 ka (Higham et al. 2009b). The aim of pretreatment is to eliminate carbon-bearing minerals as well as organic contamination so techniques such as plasma oxidation offer no clear advantage over ABA in this application (Bird et al. 2010).

After standard ABA processing, the median carbon concentration is 0.022% (mean 0.077%) and for the modified ABA process, when HLS and 8/16M HCl is used, it is 0.019% (mean 0.022%). With some 90% of carbon being lost in chemical pretreatment, 10 nests were analysed to determine whether pollen, insect sclerites or other macroscopic carbon sources were viable targets, at least in very large samples. Even though these components are known to be in low abundance when the nest is constructed it may be that they are more able to survive pretreatment. Hydrofluoric acid was used to remove quartz from the largest samples (up to 7.7 g) after which the residue was microscopically inspected. None of these samples contained macroscopic particles and for those where pollen grains were evident their volume was minor compared to the volume of charcoal.

### **2.6.3 Sources of uncertainty**

The sandstone-dominated geology of the northern Kimberley region is entirely devoid of limestone or soil carbonates, so potential contamination risks are more likely to be from modern rather than ancient carbon. Bednarik (2014: 230) also noted that there is little chance of old carbon contamination in the absence of carbonates in the environment. It is possible that old, relatively insoluble, oxalate minerals may weather and mobilise across rock shelter surfaces by a process such as colloidal transport, but wasp nests are generally not built, or do not survive, on surfaces subject to run off. In the unlikely event that old oxalate minerals were mobilised onto wasp nests then they would be removed by strong acids during pretreatment. An important result of this study is thus that the identified contamination risks are such that true nest ages may be older than reported ages, but it is most unlikely that they are younger.

In the laboratory, the risk is also from modern carbon contamination as there are few sources of dead carbon contamination available, and these are generally known and controlled (e.g. grease from vacuum pumps). If the potential, uncontrolled, risks are predominantly from more modern carbon sources then the age estimates provided by wasp nests overlying rock art remain valid minimum ages: a contaminated sample may appear to be younger than the true age, but it will still be correct to state that the art must be older than the measured age of the nest.

The same is not true of under art nests: contamination from modern carbon could lead to an erroneous conclusion as the nest may now be measured to be younger than the art. This imposes an additional constraint on under art samples as they need to be such that any external surfaces can be thoroughly removed prior to ABA processing.

### **2.6.4 Anomalous results**

Even with the revised pretreatment protocol (section 2.5.2.3.2) there are significant age differences between the heavy and light fractions in 15 of the 16 heavy/light sample pairs analysed (Table 2-6). For all but 4 samples, density separation had the effect of sorting the older, more mineralised pyrogenic carbon into the heavy fraction while the younger, less mineralised charcoal floated into the light fraction.

Some of the samples, however, were single nests where all carbon should be of much the same age and yet the age differences were still significant. The greatest age differences occurred when it had not been possible to completely remove the outer surfaces prior to chemical processing, either because the sample pieces were too small or too friable. Samples where the outer surface was able to be thoroughly removed, such as DR015\_10-2, DR015\_14-4 and DR013\_06-1, produced fractions with the smallest age differences. This outcome suggests carbon in detrital material and accretions that form on the outer nest surfaces is not completely removed during chemical pretreatment alone, even with the most aggressive processes using strong acids.

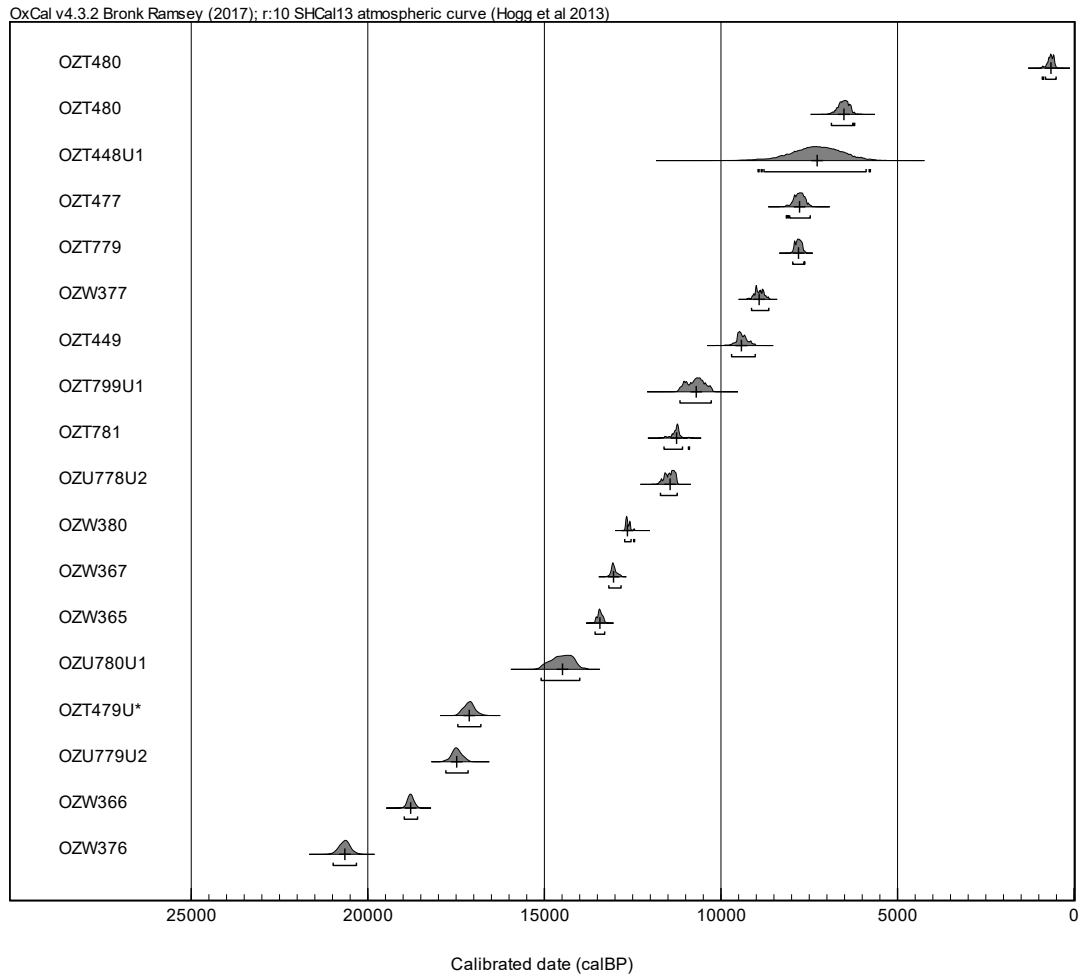
The most likely source of this highly recalcitrant carbon is fine charcoal blown into rock shelters after the frequent bushfires. Consequently, carbon in light fractions should always be younger than that in heavy fractions and this is usually the case, but for four samples the opposite was true. Three of the four samples (KG002\_02-1, KG021A\_02-2, KG028A\_03-1) are from the same river gorge area and are from sites that may, rarely, be flooded. It is possible that intermittent flooding acted to thoroughly bind younger detrital material to the mineral matrix so that it tended to sink during HLS, moving more of the younger carbon into the heavy fraction. All 4 samples were underneath pigment and the 3 with large age differentials between fractions were indurated nests well bonded to the underlying surface accretionary coating. Hence the sample included the older surface coating material as well as the original nest and subsequent accretionary deposits, all of which contain carbon of different ages. The age differential between fractions is plausible, even if the reason why the four light fractions are older is not certain.

### **2.6.5 Age distribution of dated nest samples**

The spread of ages from 75 radiocarbon dates of old wasp nests across 20,000 years implies that wasp nests were produced with some regularity throughout this period (Figure 2-9). While it is possible that changes to environmental conditions affected the rate of nest production and preservation, most significant age ranges are represented in the data. From these initial results, there appears to be no major bias (apart from the normal taphonomic one) in the age distribution of nests that would lead to under-representation of periods of art production. A possible exception is the

period 2 – 6 cal ka BP but that probably reflects some sampling bias toward older art styles and older nests. Given sufficient samples, dates on wasp nests should serve to constrain the age of all major art styles evident in this region over, at least, the last 20,000 years.

A reassuring result is the wide spread of ages of wasp nests from a single rock shelter site. If nest production was continuous rather than episodic (at a millennial scale) then there is a better chance that the age of any particular nest is close to the age of the underlying or overlying rock art. The single site with the largest number of dated nests is DR015 with 18 samples dated (Figure 2-10). Samples were not selected at random: if, based on colour, morphology, texture, and context, the nest appeared to be young then it was unlikely to be sampled. If multiple samples are taken from such a site then a single, very old, date may be considered anomalous whereas multiple old dates from multiple samples increases confidence that the results are accurate. The 4 oldest nests have ages in the range 17 – 21 cal ka BP. Another 7 nests have ages in the range of 10 – 15 cal ka BP so more than half the nests dated are older than 10 ka. The overall range of dates leaves little doubt that nests were being built at this site in each millennium from 6 to 21 ka with a possible gap around  $16 \pm 1$  ka.



**Figure 2-10** Calibrated ages for nests from site DR015 (95.4% probability range and median value)

## 2.7 Conclusion

The aim of this research has been to develop a robust approach to the radiocarbon dating of mud wasp nests to provide reliable bounding age estimates for rock art and other anthropogenic features on the surfaces of rock shelters.

The results establish that useful age estimates can be obtained when the following constraints are acknowledged:

- Charcoal is the carbon-bearing constituent most likely to provide a reliable radiocarbon age determination for old nests. Although some of the mud used to construct nests may contain a significant amount of old charcoal at the



time of construction, it is possible to characterise this inbuilt age to determine the impact on the accuracy of age estimates for old nests. The potential non-analytical sources of uncertainty identified here will mostly be small (<10%) compared to such ages.

- While old, mineralised nests are closed to contamination, accretions form on outer surfaces and can trap younger detrital material. The modified chemical pretreatment protocol will remove carbon-bearing minerals but younger carbon contamination from aeolian charcoal or biological processes may remain. Dates on nests overlying the feature to be dated therefore provide reliable minimum age estimates as residual carbon contamination will only be younger than the age of the nest. Any nests underlying the same feature will be somewhat less reliable unless all possible contamination on the outer surface is removed prior to chemical pretreatment.
- The physical and chemical pretreatment protocols adopted, as well as the mass of carbon used for AMS measurement, all have an impact on the reliability of the age estimate of the wasp nest sample. Although the impact is difficult to quantify, the reliability assessment reported here communicates the relative level of confidence that can be held in one age measurement compared to another.

The results from 101 radiocarbon age determinations, on 75 old mud wasp nests, represent an unprecedented survey of the age of wasp nests in rock shelters. Of all the old nests, 31 are older than 10 cal ka BP and 9 are older than 15 cal ka BP with the two oldest nests dated to just over 20 cal ka BP. The wide range of ages measured establishes that, at the millennial scale, wasp nests have been built quasi-continuously in the Kimberley over at least the last 20,000 years and are therefore, capable of providing age estimates for archaeological features and rock art throughout that period.

## 2.8 Acknowledgements

This research was funded by an Australian Research Council Linkage Projects LP130100501 and LP170100155 and co-funded by the Kimberley Foundation Australia and Dunkeld Pastoral Co Pty Ltd. DF is supported by an Australian Postgraduate Award and an AINSE Post Graduate Research Award.

We acknowledge and thank the Traditional Owners for permission to work on their country and for their support during fieldwork, particularly Augustine, Scott and Adrian Unghango, Ambrose Chalarimeri, Ian and Uriah Waina, Gareth, Ethan and Lucas Karadada on Balanggarra land and Donny and Kenny Woolagoodja and Wayne Rastus on Dambimangari land. Invaluable fieldwork support was provided by Helen Green, Cecilia Myers, Pauline Heaney, Susan Bradley, Paul Hartley, Nick Sundblom, Robin Maher, staff at Theda and Doongan Stations, Traudl Tan and Peter Kendrick. Special thanks also to the archaeologists who recorded the field context of our samples including Peter Veth, Sven Ouzman and Sam Harper.

It was only possible to visit so many remote sites in a relatively short time because modern day explorers, including Joc Schmiechen, the late Grahame Walsh, and the Kimberley Visions and Dunkeld Pastoral Co Pty Ltd Survey teams, have spent decades relocating and recording Kimberley rock art sites. We also received generous support from analytical technology experts from the University of Melbourne; Jon Woodhead, Alan Greig, Liz Goodall (XRD), Jay Black, Abaz Alimanovic and Graham Hutchinson, as well as Bin Yang (MCF), Alan Williams, Fiona Bertuch and the Radiocarbon Chemistry team at ANSTO. XRD measurements were performed at the Materials Characterisation and Fabrication Platform at the University of Melbourne. We acknowledge the help of radiocarbon laboratory staff and financial support for the Centre for Accelerator Science at ANSTO, through the Australian National Collaborative Research Infrastructure Strategy (NCRIS). We also thank two anonymous reviewers, whose comments led to substantial improvements to the manuscript.

## 2.9 References

- Armitage, R. A., J. E. Brady, A. Cobb, J. R. Southon and M. W. Rowe (2001). "Mass spectrometric radiocarbon dates from three rock paintings of known age." American Antiquity **66**(3): 471-480.
- Ascough, P. L., M. I. Bird, F. Brock, T. F. G. Higham, W. Meredith, C. E. Snape and C. H. Vane (2009). "Hydropyrolysis as a new tool for radiocarbon pre-treatment and the quantification of black carbon." Quaternary Geochronology **4**(2): 140-147.
- Ascough, P. L., M. I. Bird, S. M. Francis and T. Lebl (2011). "Alkali extraction of archaeological and geological charcoal: evidence for diagenetic degradation and formation of humic acids." Journal of Archaeological Science **38**(1): 69-78.
- Ascough, P. L., M. I. Bird, W. Meredith, R. E. Wood, C. E. Snape, F. Brock, T. F. G. Higham, D. J. Large and D. C. Apperley (2010). "Hydropyrolysis: Implications for radiocarbon pretreatment and characterization of black carbon." Radiocarbon **52**(3): 1336-1350.
- Aubert, M. (2012). "A review of rock art dating in the Kimberley, Western Australia." Journal of Archaeological Science **39**(3): 573-577.
- Bednarik, R. G. (2002). "The Dating of Rock Art: a Critique." Journal of Archaeological Science **29**(11): 1213-1233.
- Bednarik, R. G. (2014). "Mud-wasp Nests and Rock Art." Rock Art Research **31**(2): 225-231.
- Bird, M. I., P. L. Ascough, I. M. Young, C. V. Wood and A. C. Scott (2008). "X-ray microtomographic imaging of charcoal." Journal of Archaeological Science **35**(10): 2698-2706.
- Bird, M. I., P. D. J. Charville-Mort, P. L. Ascough, R. Wood, T. Higham and D. Apperley (2010). "Assessment of oxygen plasma ashing as a pre-treatment for radiocarbon dating." Quaternary Geochronology **5**(4): 435-442.
- Bird, M. I., J. G. Wynn, G. Saiz, C. M. Wurster and A. McBeath (2015). The Pyrogenic Carbon Cycle. Annual Review of Earth and Planetary Sciences, Vol 43. R. Jeanloz and K. H. Freeman. Palo Alto, Annual Reviews. **43**: 273-298.
- Bowman, D., G. K. Brown, M. F. Braby, J. R. Brown, L. G. Cook, M. D. Crisp, F. Ford, S. Haberle, J. Hughes, Y. Isagi, L. Joseph, J. McBride, G. Nelson and P. Y. Ladiges (2010). "Biogeography of the Australian monsoon tropics." Journal of Biogeography **37**(2): 201-216.
- Brock, F., D. G. Froese and R. G. Roberts (2010). "Low temperature (LT) combustion of sediments does not necessarily provide accurate radiocarbon ages for site chronology." Quaternary Geochronology **5**(6): 625-630.
- Brodowski, S., W. Amelung, L. Haumaier, C. Abetz and W. Zech (2005). "Morphological and chemical properties of black carbon in physical soil fractions as

revealed by scanning electron microscopy and energy-dispersive X-ray spectroscopy." Geoderma **128**(1–2): 116-129.

Bronk Ramsey, C. (2009a). "Bayesian analysis of radiocarbon dates." Radiocarbon **51**(1): 337-360.

Bronk Ramsey, C. (2009b). "Dealing with outliers and offsets in radiocarbon dating." Radiocarbon **51**(3): 1023-1045.

Bronk Ramsey, C. (2017). "Methods for Summarizing Radiocarbon Datasets." Radiocarbon: 1-25.

Dee, M. W. and C. Bronk Ramsey (2014). "High-Precision Bayesian Modeling of Samples Susceptible to Inbuilt Age." Radiocarbon **56**(1): 83-94.

Devries, H. L. and G. W. Barendsen (1954). "Measurements of age by the carbon-14 technique." Nature **174**(4442): 1138-1141.

Fink, D., M. Hotchkis, Q. Hua, G. Jacobsen, A. M. Smith, U. Zoppi, D. Child, C. Mifsud, H. van der Gaast, A. Williams and M. Williams (2004). "The ANTARES AMS facility at ANSTO." Nuclear Instruments and Methods in Physics Research Section B: Beam Interactions with Materials and Atoms **223–224**(0): 109-115.

Ford, B., I. MacLeod and P. Haydock (1994). "Rock Art Pigments from Kimberley Region of Western Australia: Identification of the Minerals and Conversion Mechanisms." Studies in Conservation **39**(1): 57-69.

Graetz, R. D. and J. Skjemstad (2003). The charcoal sink of biomass burning on the Australian continent, CSIRO Atmospheric Research.

Green, H., A. Gleadow and D. Finch (2017a). "Characterisation of mineral deposition systems associated with rock art in the Kimberley region of northwest Australia." Data in Brief.

Green, H., A. Gleadow, D. Finch, J. Hergt and S. Ouzman (2017b). "Mineral deposition systems at rock art sites, Kimberley, Northern Australia - Field observations." Journal of Archaeological Science-Reports **14**: 340-352.

Hatté, C., J. Morvan, C. Noury and M. Paterne (2001). "Is Classical Acid-Alkali-Acid Treatment Responsible for Contamination? An Alternative Proposition." Radiocarbon **43**(2A): 177-182.

Hattersley, P. W. (1983). "The distribution of C3 and C4 grasses in Australia in relation to climate." Oecologia **57**(1): 113-128.

Hedges, R. E. M., C. Bronk Ramsey, G. J. Van Klinken, P. B. Pettitt, C. Nielsen-Marsh, A. Etchegoyen, J. O. F. Niello, M. T. Bosch and A. M. Llamazares (1998). "Methodological issues in the C-14 dating of rock paintings." Radiocarbon **40**(1): 35-44.

- Higham, T., F. Brock, M. Peresani, A. Broglio, R. Wood and K. Douka (2009a). "Problems with radiocarbon dating the Middle to Upper Palaeolithic transition in Italy." Quaternary Science Reviews **28**(13-14): 1257-1267.
- Higham, T. F. G., H. Barton, C. S. M. Turney, G. Barker, C. B. Ramsey and F. Brock (2009b). "Radiocarbon dating of charcoal from tropical sequences: results from the Niah Great Cave, Sarawak, and their broader implications." Journal of Quaternary Science **24**(2): 189-197.
- Hobley, E., G. R. Willgoose, S. Frisia and G. Jacobsen (2014a). "Stability and storage of soil organic carbon in a heavy-textured Karst soil from south-eastern Australia." Soil Research **52**(5): 476-482.
- Hobley, E., G. R. Willgoose, S. Frisia and G. Jacobsen (2014b). "Vertical distribution of charcoal in a sandy soil: evidence from DRIFT spectra and field emission scanning electron microscopy." European Journal of Soil Science **65**(5): 751-762.
- Hogg, A. G., Q. Hua, P. G. Blackwell, M. Niu, C. E. Buck, T. P. Guilderson, T. J. Heaton, J. G. Palmer, P. J. Reimer, R. W. Reimer, C. S. M. Turney and S. R. H. Zimmerman (2013). "SHCal13 Southern Hemisphere calibration, 0–50,000 years cal BP." Radiocarbon **55**(4): 1889-1903.
- Hua, Q., G. E. Jacobsen, U. Zoppi, E. M. Lawson, A. A. Williams, A. M. Smith and M. J. McGann (2001). "Progress in radiocarbon target preparation at the ANTARES AMS Centre." Radiocarbon **43**(2A): 275-282.
- Hua, Q., U. Zoppi, A. A. Williams and A. M. Smith (2004). "Small-mass AMS radiocarbon analysis at ANTARES." Nuclear Instruments & Methods in Physics Research Section B-Beam Interactions with Materials and Atoms **223**: 284-292.
- Kershaw, A. P. (1986). "Climatic change and Aboriginal burning in north-east Australia during the last two glacial/interglacial cycles." Nature **322**(6074): 47-49.
- Klingner, S., F. Voigts, W. Viol and W. Maus-Friedrichs (2013). "Analysis of plasma degreased aluminium foil with XPS." Surface Engineering **29**(5): 396-401.
- Kuzyakov, Y. (2006). "Sources of CO<sub>2</sub> efflux from soil and review of partitioning methods." Soil Biology and Biochemistry **38**(3): 425-448.
- McWilliam, J. and K. Mison (1974). "Significance of the C<sub>4</sub> Pathway in *Triodia irritans* (Spinifex), a Grass Adapted to Arid Environments." Functional Plant Biology **1**(1): 171-175.
- Morwood, M., G. Walsh and A. L. Watchman (1994). "The dating potential of rock art in the Kimberley, NW Australia." Rock Art Research: The Journal of the Australian Rock Art Research Association (AURA) **11**(2): 79.
- Naumann, I. D. (1983). The biology of mud nesting Hymenoptera (and their associates) and Isoptera in rock shelters of the Kakadu region, Northern Territory. The Rock Art Sites of Kakadu National Park - Some Preliminary Research Findings for their Conservation and Management. D. Gillespie. Canberra, Australian National Parks and Wildlife Service: 127 - 189.

Ogden, J. (1981). "Dendrochronological Studies and the Determination of Tree Ages in the Australian Tropics." Journal of Biogeography **8**(5): 405-420.

Pepper, M. and J. Scott Keogh (2014). "Biogeography of the Kimberley, Western Australia: a review of landscape evolution and biotic response in an ancient refugium." Journal of Biogeography **41**(8): 1443-1455.

Polidori, C., L. Trombino, C. Fumagalli and F. Andrietti (2005). "The nest of the mud-dauber wasp, *Sceliphron spirifex* (Hymenoptera, Sphecidae): application of geological methods to structure and brood cell contents analysis." Italian Journal of Zoology **72**(2): 153-159.

Proske, U., D. Heslop and S. Haberle (2014). "A Holocene record of coastal landscape dynamics in the eastern Kimberley region, Australia." Journal of Quaternary Science **29**(2): 163-174.

Ridges, M., I. Davidson and D. Tucker (2000). The organic environment of paintings on rock. Advances in Dating Australian Rock-Markings: Papers from the First Australian Rock-Picture Dating Workshop, Lucas Heights, The Australian Rock Art Research Association.

Roberts, R., G. Walsh, A. Murray, J. Olley, R. Jones, M. Morwood, C. Tuniz, E. Lawson, M. Macphail, D. Bowdery and I. Naumann (1997). "Luminescence dating of rock art and past environments using mud-wasp nests in northern Australia." Nature **387**(6634): 696-699.

Roberts, R. G., G. L. Walsh, J. M. Olley, A. S. Murray, M. K. Macphail, I. D. Naumann, R. Jones and M. J. Morwood (2000). Rock-picture chronologies and palaeoenvironmental records from fossil mud-wasp nests: preliminary investigations using optical dating. Advances in Dating Australian Rock-Markings. First Australian Rock-Picture Dating Workshop. G. Ward and C. Tuniz. Lucas Heights, Australian Rock Art Research Association: 40-44.

Ross, J., K. Westaway, M. Travers, M. J. Morwood and J. Hayward (2016). "Into the Past: A Step Towards a Robust Kimberley Rock Art Chronology." PLoS ONE **11**(8): e0161726.

Taylor, R. E. and J. Southon (2012). "On the Resolution of <sup>14</sup>C Dating Anomalies: Case Studies from New World Archaeology." Radiocarbon **54**(3-4): 979-991.

Trumbore, S. (2009). "Radiocarbon and Soil Carbon Dynamics." Annual Review of Earth and Planetary Sciences **37**(1): 47-66.

Vigilante, T., D. Bowman, R. Fisher, J. Russell-Smith and C. Yates (2004). "Contemporary landscape burning patterns in the far North Kimberley region of north-west Australia: human influences and environmental determinants." Journal of Biogeography **31**(8): 1317-1333.

Watchman, A. (2000). "A review of the history of dating rock varnishes." Earth-Science Reviews **49**: 261 - 277.

Wilcken, K., M. Hotchkis, V. Levchenko, D. Fink, T. Hauser and R. Kitchen (2015). "From carbon to actinides: A new universal 1MV accelerator mass spectrometer at ANSTO." Nuclear Instruments & Methods in Physics Research Section B-Beam Interactions with Materials and Atoms **361**: 133-138.

Wooller, M. J., B. J. Johnson, A. Wilkie and M. L. Fogel (2005). "Stable isotope characteristics across narrow savanna/woodland ecotones in Wolfe Creek Meteorite Crater, Western Australia." Oecologia **145**(1): 100-112.

Yang, B. and A. M. Smith (2016). "Conventionally Heated Microfurnace for the Graphitization of Microgram-Sized Carbon Samples." Radiocarbon **59**(3): 859-873.

Yang, B., A. M. Smith and Q. Hua (2013). "A cold finger cooling system for the efficient graphitisation of microgram-sized carbon samples." Nuclear Instruments & Methods in Physics Research Section B-Beam Interactions with Materials and Atoms **294**: 262-265.

Yoshida, H., R. G. Roberts and J. M. Olley (2003). "Progress towards single-grain optical dating of fossil mud-wasp nests and associated rock art in northern Australia." Quaternary Science Reviews **22**(10-13): 1273-1278.

**Note:** Video file “Finch et al\_WaspCollectBuildProv\_30fpsNoAUDIO.mp4” is available online from the publisher at <https://doi.org/10.1016/j.quageo.2019.02.007>

## 2.10 Supplementary Information

### 2.10.1 Routine methods

#### 2.10.1.1 X-Ray Fluorescence (XRF)

Fourteen old wasp nest samples were prepared as fused glass disks using a mixed lithium metaborate/tetraborate flux and analysed on a SPECTRO Xepos energy dispersive XRF spectrometer in the School of Earth Sciences at the University of Melbourne. Calibrations were constructed using a wide variety of international certified reference materials (including United States Geological Survey (BCR-1, BCR-2, AGV-1, AGV-2, BIR-1, BHVO-1, BHVO-2, G-2, PCC-1), SARM (NIM-L, NIM-S, NIM-G, NIM-P), and the International Association of Geoanalysts (PM-S, WS-E)) and analyses of secondary reference materials suggest accuracy generally better than 1 - 2% for most elements. Analytical reproducibility is generally better than 1% for most elements with the exception of  $P_2O_5$  (up to 2%) and  $Na_2O$  (up to 4%).

#### 2.10.1.2 X-ray diffraction

X-ray diffraction (XRD): 41 old wasp nest samples were measured using a Bruker D8 Advance x-ray powder diffractometer, part of the Materials Characterisation and Fabrication Platform at the University of Melbourne. The D8 uses Ni-filtered Cu  $\alpha$  radiation with an incident beam divergence of  $0.26^\circ$  and a  $2.5^\circ$  soller slit in the diffracted beam. Intensities were measured between angles of at least  $5-85^\circ 2\theta$ , with a step size of  $0.02^\circ$  and a scan rate of 1.0 s per step. Mineral phases were identified and semi-quantified using Materials Data Inc. Jade 9.3 and Bruker EVA software linked to the ICDD PDF-2 and PDF- 4 databases with key phases established for each sample using standard search-matching procedures.

#### 2.10.1.3 Standard chemical pretreatment

The first acid treatment used a 2M HCl solution added to the sample in the centrifuge tube then placed in a  $60^\circ\text{C}$  shaking water bath for 2 hours after which it was rinsed in ultrapure water. The alkali treatment dissolves degraded organic material present in the form of humic acids (Ascough, Bird et al. 2011) as well as fats and proteins. NaOH,



starting at 0.5% concentration, was added and the tube returned to the water bath for 1 hour. If the solution was clear, then the alkali treatment was repeated a final time. If the sample was not clear, the process was repeated at double the concentration of NaOH, up to a maximum of 8%. After rinsing to a neutral pH, a 2M HCl acid solution was added then left to stand at room temperature for at least 2 hours. After rinsing, the sample was transferred into a glass vial and dried in an oven at 60°C.

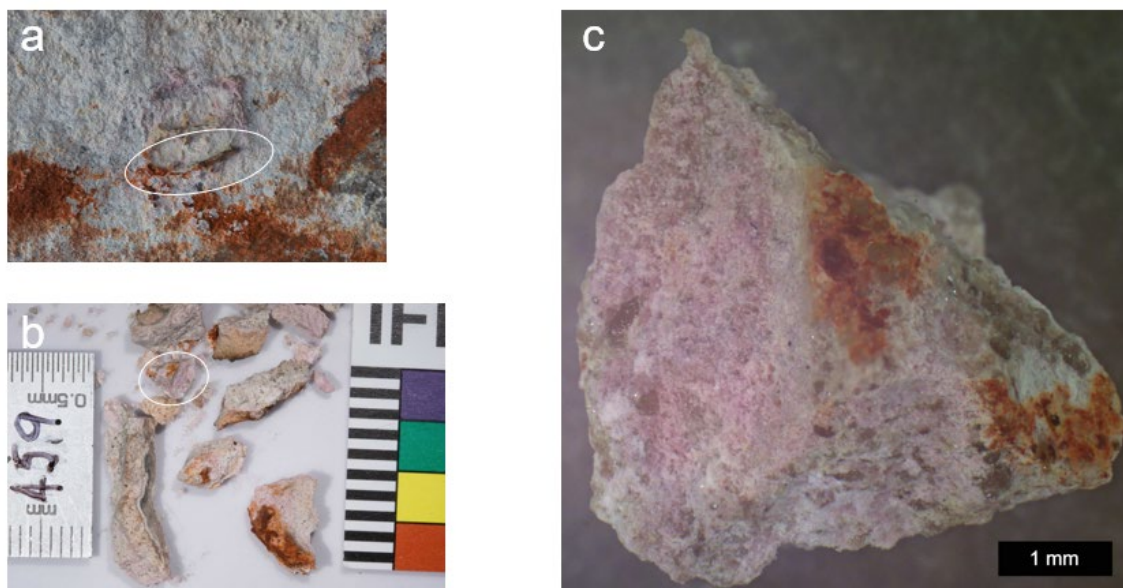
#### *2.10.1.4 Graphitisation and AMS measurement*

The standard process and equipment used to convert most pretreated samples into graphite targets for accelerator mass spectrometry (AMS) measurement is described by Hua et al (2001) and (2004). Some 33 samples used essentially this process to convert carbon dioxide to graphite but employing ANSTO's microconventional furnace (MCF) facility, developed to more efficiently graphitise ultra-small samples (Yang, Smith et al. 2013, Yang and Smith 2016). The carbon isotope ratios of the graphite targets were then measured in one of three of ANSTO's Accelerator Mass Spectrometers (AMS); 10MV ANTARES, 2MV STAR or 1MV VEGA (Fink, Hotchkis et al. 2004, Wilcken, Hotchkis et al. 2015) against OxI and Ox II International Radiocarbon Standards.

Where surplus graphite remained after AMS measurement, the  $\delta^{13}\text{C}$  value was measured using an Elementar varioMICRO CUBE Elemental Analyser coupled to a Micromass Isoprime IRMS and age determinations were corrected accordingly (following Stuiver and Polach 1977). Where all graphite was consumed during AMS measurement the  $\delta^{13}\text{C}$  value was assumed to be -25.0‰, consistent with other measured samples.

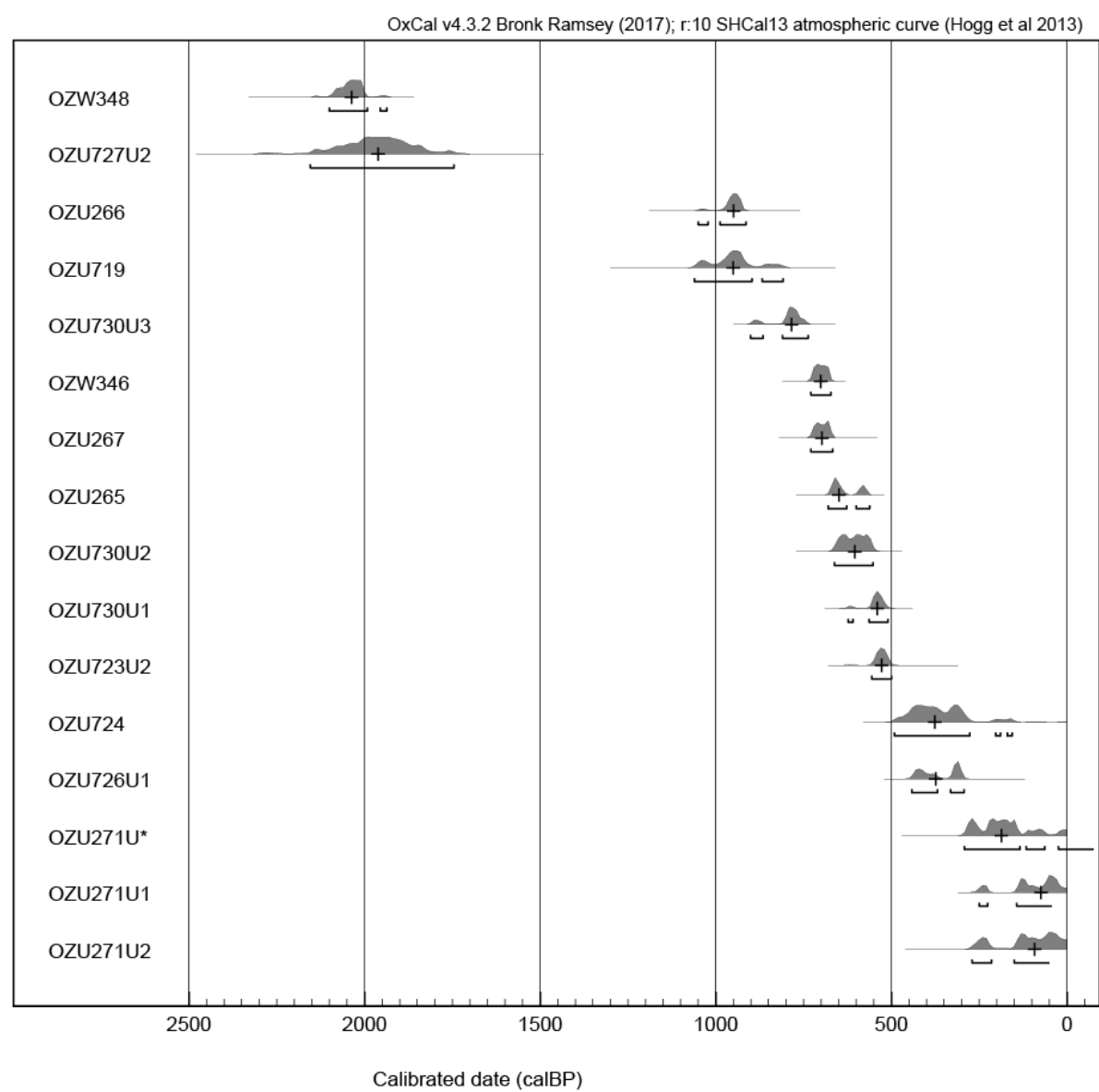
#### **2.10.2 Micro-CT scan of old wasp nest**

An example of a three-dimensional density model generated by a micro-CT scan of an old wasp nest sample (D459) is recorded as a video file (micro-CT scan D459.mp4, see note in 2.10.5). Each frame in the video represents a two-dimensional slice through the sample. Areas of highest density, such as pigment (rich in haematite), show up as white pixels and those of lowest density (air) as black pixels.



**Figure 2-S1** Mineralised wasp nest sample D459. (a) Pigment coated nest prior to sampling, (b) Sample as removed. Piece selected for scanning is circled, (c) plan view of scanned piece showing brown pigment coating.

2.10.3 Calibrated radiocarbon dates for modern wasp nest fractions



**Figure 2-S2** Calibrated radiocarbon date ranges (95.4%) and median for Modern Wasp Nests and associated mud sources.

## 2.10.4 Modern wasp nest AMS measurements

**Table 2-S1** Radiocarbon measurements for modern wasp nest and soil samples

Sample Code	Laboratory Code	C mass $\mu\text{g}$	$\delta^{13}\text{C}$ ‰	Error ( $1\sigma$ )	percent Modern Carbon	Error ( $1\sigma$ )
D202	OZU719	97			87.33	0.54
D202	OZU720	3,070	-23.9	0.1	109.48	0.79
D204	OZU721	55			104.97	0.78
D204	OZU722	1,830	-23.7	0.4	112.98	0.33
D206	OZU723U1	170	-20.9		100.98	0.36
D206	OZU723U2	200			93.39	0.39
D207	OZU724	42			96.00	0.66
D208	OZU265	114	-23.2		91.23	0.33
D208	OZU266	570	-21.3	0.1	87.29	0.32
D208	OZU267	950	-22.9	0.1	90.37	0.26
D208	OZU268	170			105.59	0.33
D208	OZU730U1	470	-25.3	0.1	93.05	0.36
D208	OZU730U2	121	-22.6		91.89	0.46
D208	OZU730U3	430	-21.5	0.3	89.02	0.22
D209	OZU725	800	-24.5	0.1	107.98	0.37
D210	OZU269	2,000	-18.3	0.1	107.21	0.3
D211	OZU726U1	1,740	-23.8	0.1	96.13	0.27
D211	OZU726U2	520	-22.5	0.1	100.98	0.34
D212	OZU727U1	45			101.64	0.76
D212	OZU727U2	17			77.55	0.76
D213	OZU270	4,700	-23.6	0.1	109.33	0.34
D215	OZU271U*	850	-18.2	0.2	97.54	0.37
D215	OZU271U1	250	-17.3	0.2	98.60	0.3
D215	OZU271U2	45			98.79	0.59
D216	OZU728U1	410			103.81	0.36
D216	OZU728U2	170	-21.3		105.40	0.38
D217	OZU729U1	2,630	-26.1	0.1	134.66	0.47
D217	OZU729U2	270	-23.9	0.4	112.48	0.39
D219	OZU272	1,500	-23.1	0.1	102.69	0.3
D500	OZW346	1,900	-25.2	0.1	90.27	0.2
D508	OZW344	740	-25.1	0.2	107.62	0.25
D514	OZW347	250	-24.2		100.35	0.34
D632	OZW349	1,000	-25.9	0.1	104.35	0.24
D670	OZW350	71			104.77	0.5
D699	OZW345	46	-25.0		105.36	0.57
D516	OZW348	860	-24.9	0.1	76.91	0.23
D700	OZW351	1,780	-24.8	0.2	108.84	0.31

		Site:	XRD Sample:																																								
			FWC003	FWC010	FWC010	FWC016	FWC014	FWC014	FWC014	FWC019	DRV009	DRV008	DRV012C	DRV012C	DRV013	DRV013	DRV013	DRV013	DRV013	DRV013	DRV013	DRV015	DRV015	DRV015	DRV015	DRV015	DRV015	DRV015	DRV015	DRV015	DRV018	DRV016	DRV016	DRV016	DRV006	DRV006	DRV006	DRV006	DRV037	DRV041	KGR021A	PC15	PC15
Mineral	Chemical Formula	D010	D018	D019	D020	D025	D026	D027a	D034	D105	D111	D118	D119	D129	D131	D134	D136	D139	D140a	D144	D147	D151	D152	D153	D154	D155	D335	D156A	D161A	D161B	D161C	D162	D164	D167B	D168	D348	D379	D459	PC15-01	PC15-02			
Carbonates																																											
Calcite	CaCO <sub>3</sub>							○										○																									
Nitrates																																											
Niter	KNO <sub>3</sub>																																			○							
Nitratine	NaNO <sub>3</sub>												○														○							○									
Oxalates																																											
Glushinskite	C <sub>2</sub> MgO <sub>4</sub> •2H <sub>2</sub> O				○																																						
Whewellite	Ca(C <sub>2</sub> O <sub>4</sub> )•H <sub>2</sub> O		○	●	○							○																															
Oxides																																											
Hematite/Iron Oxide	Fe <sub>2</sub> O <sub>3</sub>												○												○												○					○	
Phosphates, Arsenates																																											
Aluminum Ammonium Hydroxide Phosphate Hydrate	Al <sub>2</sub> (NH <sub>4</sub> )(OH)(PO <sub>4</sub> ) <sub>2</sub> (H <sub>2</sub> O) <sub>2</sub>																												○	○		○											
Leucophosphite	KFe <sub>2</sub> (PO <sub>4</sub> ) <sub>2</sub> (OH)(H <sub>2</sub> O) <sub>2</sub>													○										○																			
Taranakite	K <sub>2</sub> Al <sub>2</sub> (HPO <sub>4</sub> ) <sub>2</sub> (PO <sub>4</sub> ) <sub>2</sub> •18(H <sub>2</sub> O)											○		○		○								●		○									○					○			
Tinsleyite	KAl <sub>2</sub> (PO <sub>4</sub> ) <sub>2</sub> (OH)•2(H <sub>2</sub> O)															●		○								●							○		○								
Silicates																																											
Illite	K <sub>0.65</sub> Al <sub>2.2</sub> [Al <sub>0.65</sub> Si <sub>3.35</sub> O <sub>10</sub> ](OH) <sub>2</sub>														○												○																
Kaolinite	Al <sub>2</sub> (Si <sub>2</sub> O <sub>5</sub> )(OH) <sub>4</sub>		○				○		○											○							○																
Montmorillonite	(Na,Ca) <sub>0.33</sub> (Al,Mg) <sub>2</sub> (Si <sub>4</sub> O <sub>10</sub> )						○																																				
Muscovite	(K,Na)Al <sub>2</sub> (Si,Al) <sub>4</sub> O <sub>10</sub> (OH) <sub>2</sub>												○			○		○															○		○								
Quartz	SiO <sub>2</sub>	●	●	●	●	●	●	●	●	●	●	●	●	●	●	●	●	●	●	●	●	●	●	●	●	●	●	●	●	●	●	●	●	●	●	●	●	●	●	●	●	●	●
Sulphates																																											
Alunite	KAl <sub>3</sub> (SO <sub>4</sub> ) <sub>2</sub> (OH) <sub>6</sub>											○									○	○																●					
Anhydrite	CaSO <sub>4</sub>											○				○	○																										
Bassanite	CaSO <sub>4</sub> •0.5H <sub>2</sub> O																									○																	
Boussingaultite	(NH <sub>4</sub> ) <sub>2</sub> Mg(SO <sub>4</sub> ) <sub>2</sub> •6(H <sub>2</sub> O)													○																													
Gypsum	CaSO <sub>4</sub> •2H <sub>2</sub> O		●	●	○		○		●	●																																	
Polyhalite	K <sub>2</sub> Ca <sub>2</sub> Mg(SO <sub>4</sub> ) <sub>4</sub> •2H <sub>2</sub> O													○	○		○										○										○	●					
Schlossmacherite	(H <sub>2</sub> O) <sub>10.75</sub> Ca <sub>0.25</sub> Al <sub>2</sub> (AsO <sub>4</sub> ) <sub>2</sub> •5(SO <sub>4</sub> ) <sub>0.5</sub> (OH) <sub>6</sub>													○	○												○							○							○		
Key:																																											
Major phase (100 - 16%)		●																																									
Minor Phase (15 - 4%)		○																																									
Trace (<4%)		○																																									

Table 2-S2 Mineral composition of old wasp nests - XRD results

Key:

Major phase (100 - 16%) ●

Minor Phase (15 - 4%) ○

Trace (<4%) ○

Table 2-S2 Mineral composition of old wasp nests - XRD results

## 2.10.5 References

Ascough, P. L., M. I. Bird, S. M. Francis and T. Lebl (2011). "Alkali extraction of archaeological and geological charcoal: evidence for diagenetic degradation and formation of humic acids." Journal of Archaeological Science **38**(1): 69-78.

Fink, D., M. Hotchkis, Q. Hua, G. Jacobsen, A. M. Smith, U. Zoppi, D. Child, C. Mifsud, H. van der Gaast, A. Williams and M. Williams (2004). "The ANTARES AMS facility at ANSTO." Nuclear Instruments and Methods in Physics Research Section B: Beam Interactions with Materials and Atoms **223–224**(0): 109-115.

Hua, Q., G. E. Jacobsen, U. Zoppi, E. M. Lawson, A. A. Williams, A. M. Smith and M. J. McGann (2001). "Progress in radiocarbon target preparation at the ANTARES AMS Centre." Radiocarbon **43**(2A): 275-282.

Hua, Q., U. Zoppi, A. A. Williams and A. M. Smith (2004). "Small-mass AMS radiocarbon analysis at ANTARES." Nuclear Instruments & Methods in Physics Research Section B-Beam Interactions with Materials and Atoms **223**: 284-292.

Stuiver, M. and H. A. Polach (1977). "Reporting of  $^{14}\text{C}$  Data - Discussion." Radiocarbon **19**(3): 355-363.

Wilcken, K., M. Hotchkis, V. Levchenko, D. Fink, T. Hauser and R. Kitchen (2015). "From carbon to actinides: A new universal 1MV accelerator mass spectrometer at ANSTO." Nuclear Instruments & Methods in Physics Research Section B-Beam Interactions with Materials and Atoms **361**: 133-138.

Yang, B. and A. M. Smith (2016). "Conventionally Heated Microfurnace for the Graphitization of Microgram-Sized Carbon Samples." Radiocarbon **59**(3): 859-873.

Yang, B., A. M. Smith and Q. Hua (2013). "A cold finger cooling system for the efficient graphitisation of microgram-sized carbon samples." Nuclear Instruments & Methods in Physics Research Section B-Beam Interactions with Materials and Atoms **294**: 262-265.

**Note:** Supplementary Information Video file (micro-CT scan D459.mp4) is stored by the publisher online at <https://doi.org/10.1016/j.quageo.2019.02.007>

# **Chapter 3**

## **Radiocarbon age estimates for the Gwion Period**

This chapter is the author accepted version of the paper “12,000-year-old Aboriginal rock art from the Kimberley region, Western Australia” published in Science Advances on 5<sup>th</sup> February 2020 (Sci Adv **6** (6). DOI:10.1126/sciadv.aay3922). This paper provides an overview of the probabilistic model developed to derive chronological estimates for rock art periods. The model is fully developed in Chapter 6. The paper also introduces the method used in this study to classify motifs into one of Kimberly rock art styles. It goes on to apply these techniques to the ages determined for wasp nests in contact with motifs classified as being from the Gwion stylistic period, as an example.

Individual co-author contributions are as noted in the section 3.7.2 with the candidate contributing more than 90% to the content for this publication.

### **12,000-year-old Aboriginal rock art from the Kimberley region, Western Australia**

Damien Finch<sup>1</sup>, Andrew Gleadow<sup>1</sup>, Janet Hergt<sup>1</sup>, Vladimir A. Levchenko<sup>2</sup>, Pauline Heaney<sup>3</sup>, Peter Veth<sup>4</sup>, Sam Harper<sup>4</sup>, Sven Ouzman<sup>4</sup>, Cecilia Myers<sup>5</sup>, Helen Green<sup>1</sup>

<sup>1</sup> The School of Earth Sciences, The University of Melbourne

<sup>2</sup> Australian Nuclear Science and Technology Organisation, Sydney.

<sup>3</sup> Lettuce Create, Queensland, Australia

<sup>4</sup> Centre for Rock Art Research and Management, University of Western Australia

<sup>5</sup> Dunkeld Pastoral Co. Pty Ltd Theda Station, WA, Australia

### 3.1 Abstract:

The Kimberley region in Western Australia hosts one of the world's most substantial bodies of Indigenous rock art, thought to extend in a series of stylistic or iconographic phases from the present-day back into the Pleistocene. As with other rock art worldwide, the older styles have proven notoriously difficult to date quantitatively, requiring new scientific approaches. Here we present the radiocarbon ages of 24 mud wasp nests that were either over or under pigment from 21 anthropomorphic motifs of the Gwion style (previously referred to as "Bradshaws") from the middle of the relative stylistic sequence. We demonstrate that while one date suggests a minimum age of c. 17 ka for one motif, most of the dates support a hypothesis that these Gwion paintings were produced in a relatively narrow period around 12,000 years ago.



### 3.2 Introduction

Constraining the age of rock art older than 6 thousand years (ka) has remained a largely intractable scientific problem, particularly for rock engravings and for paintings where the paint no longer contains any original organic material (Bednarik 2002, Pike et al. 2012, Aubert et al. 2017, Jones et al. 2017). Although Pleistocene ages have been determined for exceptionally well protected rock art paintings in limestone caves, quantitative age constraints for only a very small number of earlier Holocene or Pleistocene motifs in open rock shelters have been obtained (Ruiz et al. 2012, David et al. 2013).

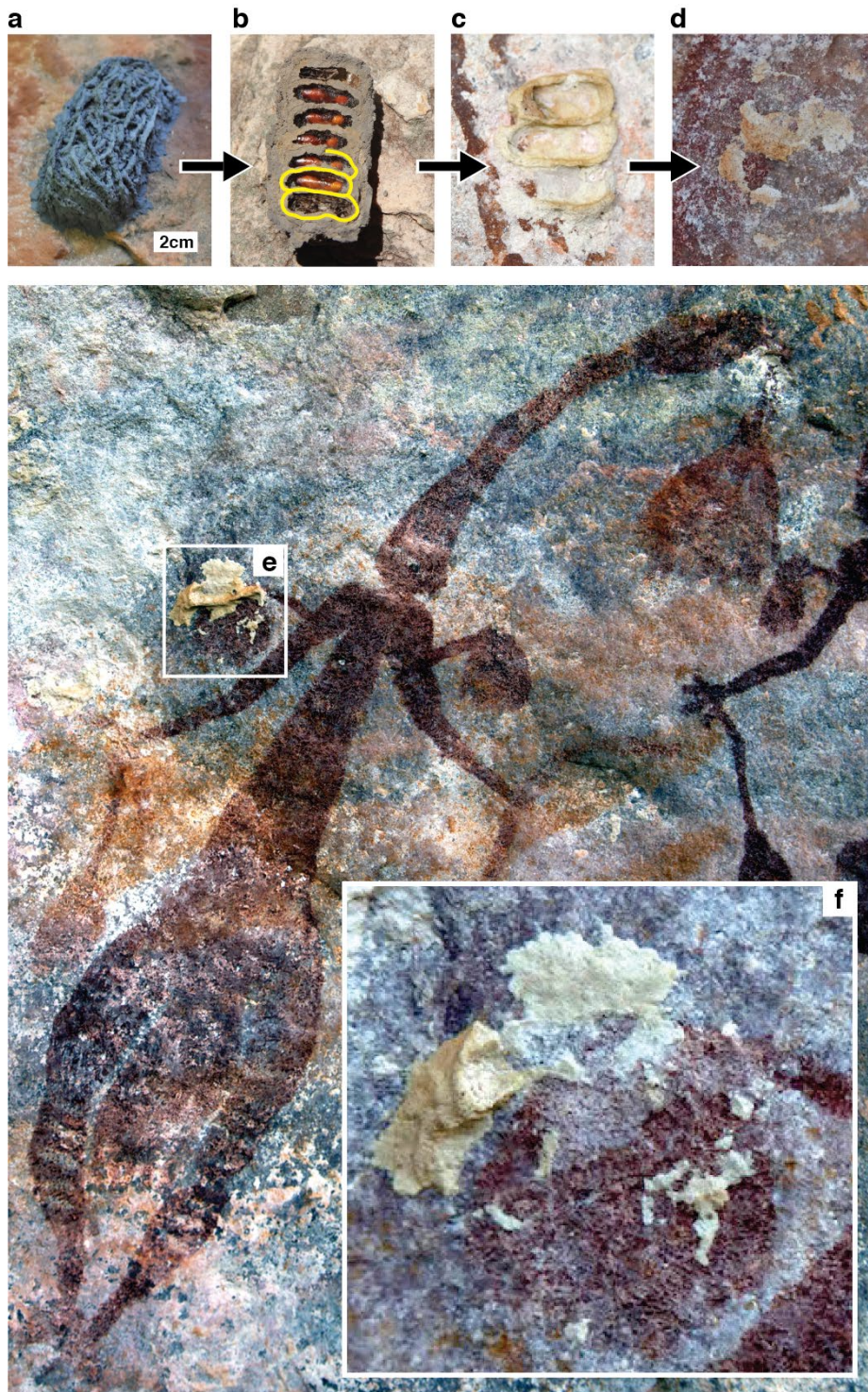
In many of the world's major rock art regions, the relative timing of different art 'styles' or iconographies has been proposed on the basis of analysis of motif superimpositions, weathering, and subject matter (Lewis 1988, Russell 2000, Walsh 2000, Sanz 2012, Garcia-Diez et al. 2013). However, until the ages of individual style phases within a rock art sequence are quantitatively dated, it is not possible to incorporate this powerful evidence of past human activity into the archaeological, palaeoenvironmental and, sometimes, ethnographic record with confidence. The definition of a "style", and the proposed stylistic sequences themselves, may be disputed as it can be difficult to verify the analysis on which they are based (Lewis 1988, Bednarik 1995, Sanz 2012, Sanz and Fiore 2014). Consequently, quantitative, radiometric dating of many stylistically distinct motifs is required both to confirm, or to refine, the proposed sequences and to constrain the absolute age intervals over which particular styles were produced (Hoffmann et al. 2016).

A well-defined stylistic sequence for Aboriginal rock art in the Kimberley region of Western Australia has been developed and comprehensively documented by researchers over the last 40 years (Crawford 1977, Welch 1993, Walsh 1994, Lewis 1997, Walsh 2000, Donaldson 2012), and ongoing research continues to refine this sequence. Apart from the most recent Wanjina phase, very few motifs from the earlier art periods have absolute age constraints. Only two Kimberley rock art motifs have provided age estimates older than the mid-Holocene (Roberts et al. 1997, Ross et al. 2016) and only one of these can be attributed to an identified style, but even this date has been the subject of much debate (Aubert 2012, David et al. 2013).

Notwithstanding this lack of direct evidence, it has long been thought that the older styles in the Kimberley sequence date back to the Pleistocene (e.g., Morwood et al. 1994, Veth et al. 2017). Here we report on radiocarbon dating of mud wasp nests, overlying (thereby providing minimum ages) or underlying (providing maximum ages) Kimberley rock art motifs, allowing this hypothesis to be thoroughly tested.

The development of the method to confidently date mud wasp nests is fully described elsewhere (Finch et al. 2019). This method relies on the identification of possible sources of carbon contamination in the environment of Kimberley rock shelters and pretreatment methods to remove them. This research also analysed newly constructed mud wasp nests to understand their initial carbon composition and identified charcoal as the target compound for accelerator mass spectrometry (AMS) dating. The inbuilt or inherited age of the different sources of carbon was measured, and while not trivial, it can be accommodated within the accuracy sought from this method.

In this study, we use 24 wasp nest dates to estimate the age of a renowned anthropomorphic style from one of the relatively older periods of the Kimberley rock art stylistic sequence. These 24 nests were either under or over motifs originally referred to as “Bradshaw” paintings but which are now generally referred to as “Gwion” figures (Donaldson 2014, Veth et al. 2017) while acknowledging that different Traditional Owner groups have their own preferred names (including Gwion Gwion, Kiro Kiro, or Kujon). The Gwion style is dominated by finely painted human figures in elaborate ceremonial dress (Welch 2007, Welch 2015) including long headdresses and accompanied by material culture including boomerangs and spears (e.g. Fig. 3-1).



**Figure 3-1.** Mud wasp nest samples and their development sequence. (a) A recently constructed *Sceliphron laetum* mud wasp nest. (b) Underside of the nest after removal from the rock surface with basal nest structure highlighted to show (c) the characteristic oval shape evident in weathered nests, leaving (d) just a remnant of mineralised mud over time. (e) a typical remnant mud wasp nest (DR006\_03-1) overlying pigment from a Gwion motif before removal, and (f) the remainder with pigment revealed underneath.

### 3.3 Results

#### 3.3.1 Age constraints for Gwion motifs

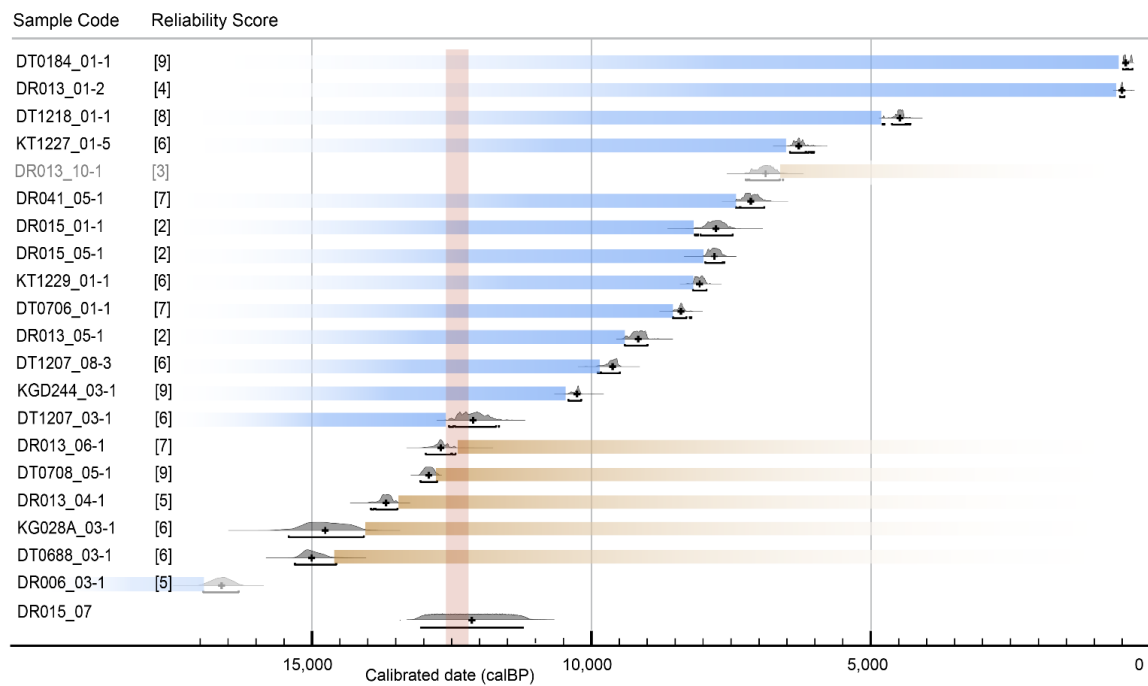
As part of a larger multiyear rock art dating project (Veth et al. 2017, Finch et al. 2019), nest samples associated with 21 different motifs of the distinctive Gwion style are reported here. All samples were obtained with Traditional Owner consent and participation. The motifs were identified as belonging to the Gwion style by PH and CM (see Materials and Methods 3.6.3). Detailed results are listed in Table 3-S1 and specific details of radiocarbon pretreatments are listed in Table 3-S2. Each age measurement is given a qualitative “Reliability Score” (described in detail elsewhere (Finch et al. 2019)), based on the carbon mass analysed, the physical cleaning of the sample and the chemical pretreatment applied. The Reliability Score is a relative measure that communicates the susceptibility of the age measurement to potential sources of contamination. Ages with scores of 3 or less are, thus, less reliable than the most robust measurements associated with scores of 8 or more. Most samples fall into the middle reliability range (4 to 7).

Usually, only a single dated nest was associated with a particular motif, but one motif, DR015\_01, had two overlying nests dated and another, DR015\_07, had two overlying and one underlying nest dated. Where there was more than one overlying nest on a motif, only the oldest is included in the subsequent analysis as its age will be closer to that of the motif. For the other 19 motifs, 6 had nests underlying pigment and 13 had nests overlying pigment. Fig. 3-S2 provides photographs and interpretative illustrations for the dated motifs.

The calibrated ages of the 12 oldest wasp nests overlying art are mostly in the range from 4.5 to 12.1 ka (median calibrated years before the present (median cal BP)) with one nest (DR006\_03) significantly older at 16.6 ka (median cal BP), with a Reliability Score of 5 out of 10 (Fig. 3-2) (Finch et al. 2019). Five of the 6 nests underlying pigment were dated to between 13 and 15 ka (median cal BP). The remaining nest, DR013\_10-1, was dated to 6.9 ka (median cal BP) but with a low Reliability Score of 3. The low score reflects both the small mass of carbon measured (23µg) and the small size of the sample pieces that restricted the potential for thorough cleaning of external

surfaces. Given the potential for younger carbon contamination, this age is treated as an outlier.

Uniquely, one motif, DR015\_07, had one nest underlying and two nests overlying pigment. The dates on these three nests together provide an age bracket of 11.3 to 13.0 ka (cal BP, 95% probability) (Fig. 3-2).



**Figure 3-2. Summary of Gwion related ages.** Calibrated dates for the oldest wasp nests and the associated Reliability Score (10 is the most reliable, and 1 is the least). The bar underneath each probability distribution plot indicates the 95% probability range with the median marked with a cross. The minimum age constraints provided by overlying nests (indicated with blue bars, starting just beyond the 95% probability range for the nest) and the maximum age constraints from underlying nests (brown bars), together with the age bracket for DR015\_07, suggest a narrow age range for production of most of these Gwion motifs around 12,400 years ago (cal BP) (red vertical bar), apart from DR013\_10-1 and DR006\_03-1.

## 3.4 Discussion

### 3.4.1 Theoretical determination of art periods

Dated wasp nests, over or under pigment, provide only minimum or maximum age limits for individual motifs. How then can these individual age limits be used to estimate the age range of the stylistic periods of Kimberley rock art?

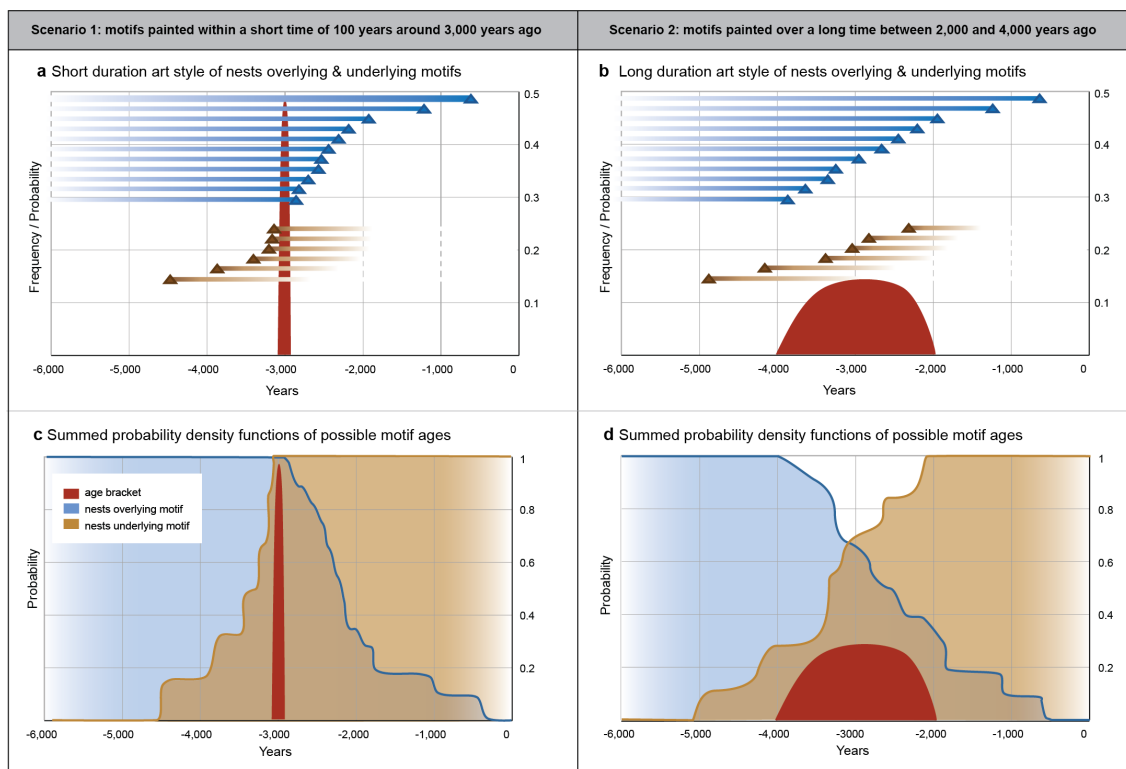
Weathering of the initially large surface area of mud wasp nests gives results in a rapid reduction in nest volume until the nest is reduced to a stump (Fig. 3-1) (Finch et al. 2019). Hence, the age distribution of all nests is likely to be broadly exponential with most nests being young and the probability of nests being preserved diminishes as age increases. Although it is possible that nest production rates fluctuated in response to changing environmental conditions over the past 30,000 years, the almost continuous sequence of ages measured on Kimberley wasp nests reported elsewhere (Finch et al. 2019), suggests a quasi-continuous nest production through time (Fig. 3-S1a).

If the age distribution of all wasp nests is exponential, or at least monotonically decreasing with time, then the age of the nests over-lying rock art will be biased towards younger values. The most probable age for any ‘over-art’ nest is, therefore, one that is closer to year 0, and the least probable ages for overlying nests are those closer to the age of the motif (Fig. 3-S1b). The opposite is true for nests underneath rock art in that the most likely nests are those closer in age to the age of the motif. With experience, it is often possible to identify and avoid more modern nests, thereby increasing the probability that the over-art sample age will be closer to the age of the motif. In general, however, an under-art nest is more likely to be closer in age to that of the motif (although it could sometimes be substantially older).

Only very occasionally will an individual motif have more than one overlying or underlying nest. It is thus rare to find multiple nests that will provide a narrow age bracket for a single figure, although one such motif is reported here. Consequently, a different methodology is required to constrain the age of a particular period. The approach taken here is to consider the ages of all nests associated with all motifs of a single style to estimate the time span for that graphic tradition.



Assuming, at one extreme (Fig. 3-3, Scenario 1), that motifs of a given style were all painted within a narrow age range, e.g.,  $3000 \pm 100$  years ago, then the expected age of nests overlying these motifs will be as illustrated by the blue triangles and the ages of underlying nests by the brown triangles (Fig. 3-3a). The bars to the left or right of each nest age (triangle) indicate the possible age range for the associated motif. In this case there can be minimal overlap ( $<200$  years) in the age ranges for overlying and underlying nests. The difference between the age of the oldest overlying nest and the age of the youngest underlying nest provides a useful estimate of when motifs in this style were painted.



**Figure 3-3.** Hypothetical ages of nests overlying (blue triangles) and underlying (brown triangles) motifs. Blue (brown) horizontal bars show the possible age range for the associated motif over (under) the nest. Scenario 1: all motifs were painted in a short period permitting no major overlap between the ages of underlying and overlying nests. Scenario 2: motifs were painted between 2000 and 4000 years ago so the ages of underlying and overlying nests will overlap significantly. The probability functions in (c) and (d) are the sum of the possible age ranges for motifs from overlying (blue curve) and underlying (brown curve) nests.

At the other extreme, in Scenario 2, we assume that motifs in this style were painted over a more extended period between 2000 and 4000 years ago (Fig. 3-3b). Here, the ages of the overlying and underlying nests may overlap significantly, by up to 2000 years. The age difference between the oldest over-art nest and the youngest under-art

nest still provides an estimate of the time span for the style. As the number of dated nests increases, the statistical distribution of the ages will provide a more precise and robust time span estimate for a given style phase.

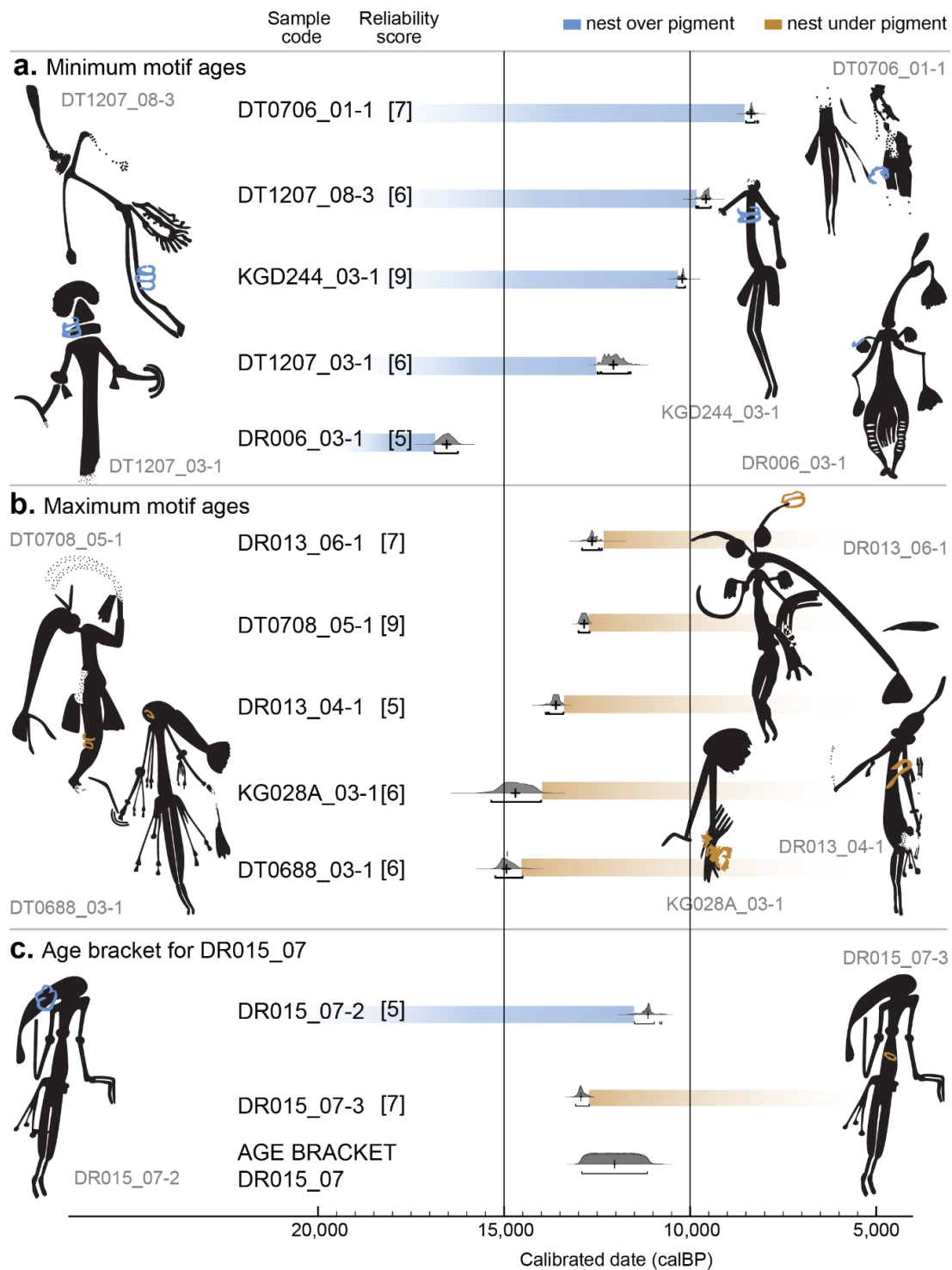
The summed probability functions for all the over-art nests (blue curves in Fig. 3-3c and 3-3d) show the probability that a motif has a minimum age of less than x years. Similarly, for under-art nests, the brown curves show the probability that the maximum age of a motif is greater than x years (see Materials and Methods).

### **3.4.2 Age range hypothesis for the Gwion style**

The lack of significant overlap between the probability distributions for maximum and minimum ages on 21 Gwion motifs (Fig. 3-2) suggests that they were painted over a short duration as modelled in Fig. 3-3a rather than a long duration as in Fig. 3-3b. All but one of the over-art nest ages are consistent with a hypothesis that Gwion motifs are older than ~12 ka cal BP (Fig. 3-4a) at least in the area studied. The under-art nest ages (excluding DR013\_10) are consistent with a hypothesis that Gwion motifs are younger than ~13 ka cal BP (Fig. 3-4b). The median of the age bracket for DR015\_07 falls between these two limits (Fig. 3-4c), supporting the proposition that the Gwion motifs in this study were painted between 12 and 13 ka cal BP.

While the 16.3 to 17.0 ka cal BP age for the nest overlying DR006\_03 has a mid-range Reliability Score of 5, we allow that although the rest of the data suggest a short period of production of Gwion motifs around 12.4 ka cal BP, it is possible some Gwion motifs may be more than 4,000 years older.

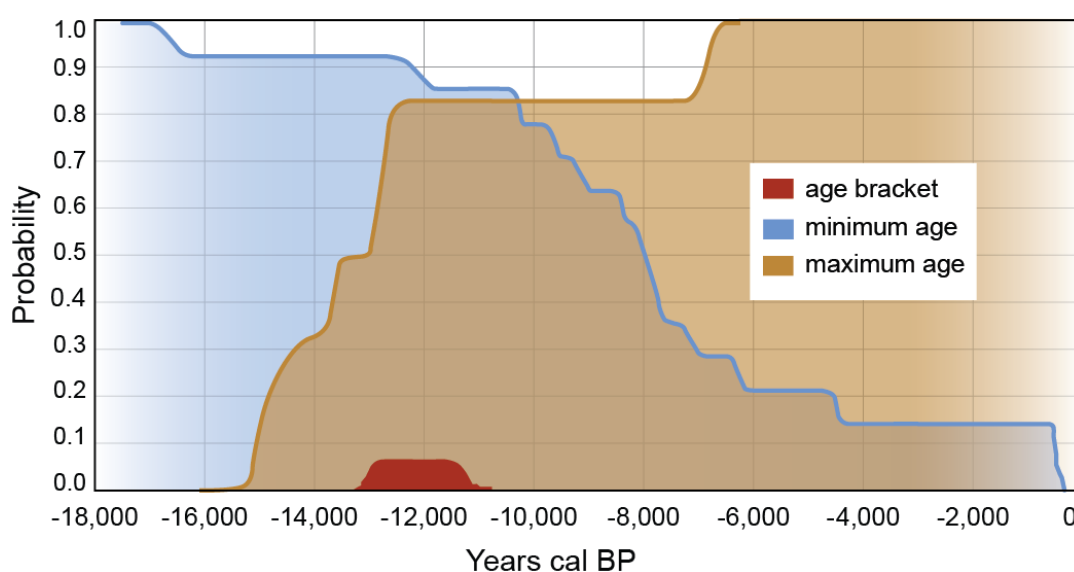




**Figure 3-4. Motif age ranges.** Calibrated dates for the oldest wasp nests with a Reliability Score of at least 5. (a) Nest over motif: Nest sample locations are indicated in blue on the black figures. (b) Nest under motif: Nest sample locations are indicated in brown. (c) Nests under and over the same motif DR015\_07 and the calculated age bracket for motif DR015\_07 using OxCal 4.3.2 software (Bronk Ramsey 2009a, 2017) and the code listed in the section 3.8.2. Illustrations: P.H.

The summed probability functions of the minimum ages (blue) and the maximum ages (brown) are plotted in Fig. 3-5. As the two outliers DR013\_10 and DR006\_03 are included, the overall shape of these curves is less like the short duration scenario depicted in Fig. 3-3C than it would be if they were excluded.

Even this unprecedented sample of ages on 21 Gwion motifs, collected from sites up to 100 km apart, may not fully represent the diversity present across the full geographic range of this style. The hypothesised age range for Gwion production is heavily influenced by a small number of age determinations with only one nest dated in the critical period from 10.5 to 12.5 ka. Nonetheless, this analysis serves to demonstrate how the theoretical model is applied. Additional samples from the earliest subphases in the Gwion style period and from the western half of the Kimberley will be sought in future studies. Many more nests, both over and under Gwion motifs, will need to be dated before the true age distribution of paintings in the Gwion style and substyles can be stated with greater confidence.



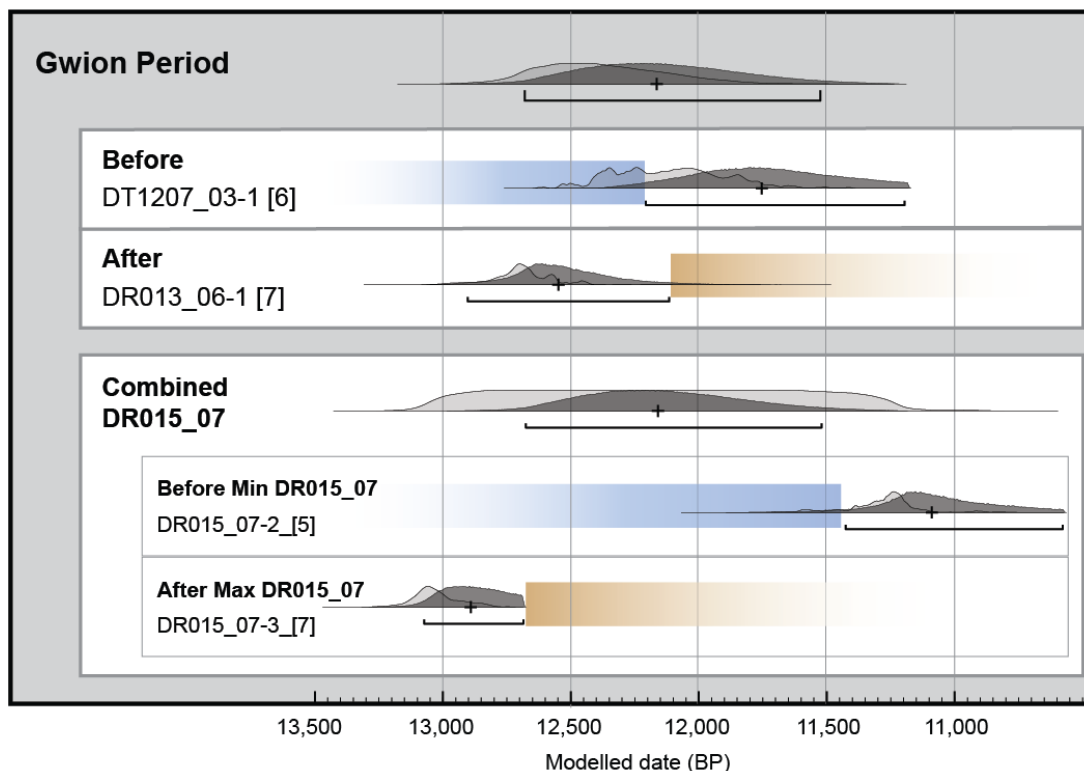
**Figure 3-5.** Probability distributions for the age constraints for Gwion motifs. Sum of the cumulative probability density functions for the ages of nests over (blue) and under (brown) pigment and the age bracket for motif DR015\_07 (red). The intersection of the blue and brown areas then represents the probability distribution for the age of Gwion motifs. The outliers, DR013\_10 and DR006\_03, are included.

### 3.4.3 Allowance for inbuilt age of charcoal

The main source of carbon in old mud wasp nests is from charcoal fragments in the mud collected by wasps at the time of nest construction (Finch et al. 2019). Frequent Kimberley bushfires burn relatively short-lived vegetation (especially grasses), such that most wasp nests do not contain very old charcoal when they are built. However, some recently constructed (i.e. modern) nests did contain charcoal up to ~1000 years old. Analysis of charcoal samples from 9 modern nests suggest a mean inbuilt age of 255 years (Finch et al. 2019), although the majority (six) contained only modern carbon.

If no correction is made for this inbuilt carbon age then, when the probability density functions for the maximum and minimum (excluding DR006\_03) age limits and the age bracket are combined, the implied duration of the Gwion period is 11,850 to 12,810 cal BP with a median of 12,400 cal BP (95% probability) (Fig. 3-6 light gray curves). This assumes that the oldest of the overlying nests (DT1207\_03) defines the minimum age for these Gwion paintings, and the youngest under-art nest (DR013\_06), defines the maximum age. While the age range is calculated from just two dates, these particular dates are end points in age distributions and it is the distributions (with a large number of samples, indeed the largest such sample ever dated for older Kimberley rock art) that provide confidence in the range calculated. If any one date was significantly removed from others (i.e. an outlier) then that would normally call for further evidence to support it.

The impact of old charcoal can be modelled assuming the inbuilt age follows an exponential distribution, with a mean of 255 years and a maximum possible value of 4000 years (Fig. 3-6 dark gray curves) (Bronk Ramsey 2009b). The effect is to shift the hypothesised age range of the Gwion style from 11,850 - 12,810 (median 12,400) cal BP to 11,520 – 12,680 (median 12,160) cal BP.



**Figure 3-6.** Hypothesised age range for the Gwion style (top graph), with (dark gray) and without (light gray) a correction for inbuilt charcoal age. Excluding the 2 possible outlier dates for DR013\_10 and DR006\_03, the Gwion style is defined temporally by combining the age distributions for the oldest over-art nest (DT1207\_03), the youngest under-art nest (DR013\_06), and the age bracket for DR015\_07. The bar under the curve is the 95% probability range and the cross marks the median of the corrected distribution. Modelled using OxCal v4.3.2 (Bronk Ramsey 2017); r:5 SHCal13 atmospheric curve (Hogg et al. 2013) and the code listed in section 3.8.2.

### 3.5 Results in context

The aim of this research was to demonstrate how multiple dates on mud wasp nests overlying and underlying rock art motifs of a particular style within a region can be used to estimate the age span of that style. A first estimate for an age span of Gwion style paintings (previously known as ‘Bradshaw’ paintings) is derived from radiocarbon age determinations on 24 mud wasp nests that were either under or over 21 motifs from 14 sites. If Gwion motifs were continually produced over a period of many thousands of years, then we would expect the ages of wasp nests under pigment to overlap significantly with those of nests on top of pigment. However, we found no overlap between the median calibrated ages of 13 overlying nests and 5 underlying nests, implying that most of these Gwion motifs were painted over a relatively narrow time span between 11,500 and 12,700 years ago. The closely bracketed age for motif

DR015\_07 supports this hypothesis, its age being constrained by two over- and one underlying nest to be between 11.3 and 13.0 ka cal BP.

However, two further results are outliers that do not support this hypothesis. The younger of these (DR013\_10) can be discounted as being of low reliability, but the other (DR006\_03) is of mid-range reliability and less readily discounted. The only other old minimum age determination on a proposed Gwion motif, reported in 1997 but still much debated, is also closer to 16 ka ( $16.4 \pm 1.8$  ka) (Roberts et al. 1997), so it is certainly possible that the initial depiction of Gwion motifs date from this period but that their production as the dominant anthropomorphic style proliferated by c. 12,000 BP. It has also been suggested that the anthropomorphic Datu Saman figures from Borneo are “notably similar” to Gwion motifs (Aubert et al. 2018). While there is only a single minimum age of 13.6 ka reported on one of these figures, it is a little older than the age suggested here for Gwion motifs but of the same order.

Most of the results presented here support a hypothesis that motifs of the Gwion rock art style of Australia’s north Kimberley were produced around 12,000 years ago with the proliferation of this phase likely occurring within a millennium; however one result points to the possibility that some motifs may be more than 4,000 years older. These results confirm that rock art was being produced in the Kimberley during the terminal Pleistocene. Notably, as the Gwion paintings are not the oldest in the relative stylistic sequence for this area, earlier styles must have an even greater antiquity.

## **3.6 Materials and Methods**

### **3.6.1 Sample collection**

Remnant mud wasp nest samples related to Gwion style paintings, were collected from 14 different rock art sites up to 100 kilometres apart in the Drysdale River and King George River catchments (Green et al. 2017) between 2015 and 2017. The median sample size of all samples collected is c. 250 mg. In keeping with the wishes of the Traditional Owners, the site locations are not disclosed here but have been fully documented in an access-controlled database (Green et al. 2017). Sampling was approved on site by relevant local Traditional Owners, who participated in this fieldwork, and under research permits from the Kimberley Land Council/Balanggarra Aboriginal Corporation and the Western Australian Department of Planning Lands and Heritage (formerly Department of Aboriginal Affairs).

All samples were photographed (including high resolution macro imaging) before and after they were removed to record the context of the sample in relation to the rock art. As others have noted (e.g., Aubert 2012, Hoffmann et al. 2016)), it is critical to establish a clear relationship between the art and the sample, but this is often challenging. Head-mounted, binocular magnifying glasses of varying magnification (x1.5 to x2.5) and bright light sources were particularly useful. Digital microscopes were also used but limited depth-of-field restricted their application on irregular rock surfaces. For nests overlying pigment, the expectation is that more pigment will be revealed when the sample is removed (see Fig. 3-1f). Commonly, however, part of the nest will remain adhered to the rock surface so it may not be absolutely clear that paint once overlay the nest and has simply weathered away. If there was any doubt, then the remaining nest was carefully abraded until pigment was revealed to confirm the inferred relationship.

Where approval was granted to remove samples underneath pigment, a different set of contextual challenges apply. In particular, it was necessary to establish that it was not possible for material younger than the nest to have been trapped in or behind the nest. Infrequently, signs of biogenic activity were evident when these samples were carefully inspected. These occur as thin, dark lines or accretions, usually between nest and rock surface. The introduction of modern carbon, following construction of the

nest, can invalidate maximum age estimates; therefore, if this material could not be removed during physical pretreatment, then the sample was rejected. A motif may have been repainted (rarely) or painted over by a separate motif (more commonly) after a nest was constructed over it resulting in pigment both over and under the nest. In all cases careful field observations were recorded photographically, on a custom field recording database and in field notes and discussions to confirm the relationships between the art and the sample.

Typically, only part of the nest occurs directly over or under pigment. Usually, only that part of the nest unambiguously in contact with the art was removed. However, when the available sample was small, the nest was critically examined to determine whether more of the nest could be included in the sample. The colour, texture and morphology of the nest were used to verify that it was all constructed at the same time (i.e. a single generation nest), with the practice progressively refined as hundreds of nests of all ages were studied (Finch et al. 2019). Given that new material can be added by wasps at the edge, or over an existing nest, only that part of the nest directly under the pigment or unequivocally part of the same construction episode was relied on.

### **3.6.2 Radiocarbon age measurements**

Initially (Laboratory Codes in the range OZT444 to OZU730), all stages of pretreatment were conducted using the Australian Nuclear Science and Technology Organisation (ANSTO) Radiocarbon Chemistry laboratory. Subsequently, samples with Laboratory Codes from OZU776 to OZW426 underwent physical pretreatment and part of the chemical pretreatment at the University of Melbourne. Complete details of the pretreatment methods are described elsewhere (Finch et al. 2019). All sample combustion and graphitisation were carried out at ANSTO. All samples were measured using the 10MV ANTARES (Australian National Tandem Research Accelerator) or 2MV STAR AMS at ANSTO. Although the mass of carbon analysed was mostly in the range 20 to 70  $\mu\text{g}$  (up to 159  $\mu\text{g}$ ), even the smallest samples (13-14  $\mu\text{g}$ ) are within the analytical capability previously established for this facility over the past 20 years with dedicated quality control procedures in place to monitor contamination in processing and possible fractionation in measurements (Hua et al. 2001, Hua et al. 2004, Yang and Smith 2016). In our measurements we have followed the protocols described in these papers. The carbon concentration of old wasp nests

varies greatly but is c. 0.22‰ before radiocarbon pretreatment (Finch et al. 2019).  $\delta^{13}\text{C}$  determinations were not performed for these samples because there was insufficient material. The typical charcoal value for  $\delta^{13}\text{C}$  (-25 ‰) was assumed. All radiocarbon ages were calibrated using SHCal13 (Hogg et al. 2013) in OxCal v4.3.2 (Bronk Ramsey 2017).

### **3.6.3 Motif classification**

Radiometric methods that quantitatively date older rock art almost always provide a maximum or minimum age for a single motif at a time. To determine the duration of Kimberley rock art styles or periods, we needed to classify motifs into a particular defined style. While objective classification is possible through attribute analysis, it is often a largely subjective decision, so it requires both expert opinion and an estimate of uncertainty.

Some motifs have the form and many of the elements that characterise a particular style and can be correctly and certainly classified by someone with minimal familiarity with Kimberley rock art typology. At the other extreme, some complete motifs were unable to be classified with any certainty because they lack clear defining characteristics. The most experienced observers can be expected to be able to classify a greater percentage of motifs, with a higher level of confidence, than those with less experience. However, even those with the greatest experience will be more or less confident in classifying a specific motif depending on the state of preservation and presence of defining characteristics. Notwithstanding the subjective component of the process, P.H. and C.M. classified 75 motifs into one of the 6 major Kimberley styles and nominated the level of confidence associated with each classification.

The claim to expertise in classifying Kimberley rock art is based on extensive field research, locating and recording rock art in field expeditions over a combined total of 27 years. P.H. and C.M. have contributed to the recording and digital cataloguing of more than 6,000 Kimberley rock art sites and more than 90,000 rock art images, over the past 30 years, as well as academic publications (Ouzman et al. 2017, Veth et al. 2017).



Each person classified a motif to one of the six main Kimberley rock art styles and nominated the probability that their decision was correct. Levels of confidence used in the classifications are as follows: “Certain” to indicate a probability of at least 99%, “Highly Likely” for at least 90%, “Likely” for 70%, “Possible” for 50%, “Uncertain” for 35% or “Unknown”. This terminology borrows from research into perceptions of probability terminology (e.g., MacLeod and Pietravalle 2017) and standard terms used by the Intergovernmental Panel on Climate Change (Budescu et al. 2009). So, if a motif is classified as “Highly likely” to be a “Gwion” then the expectation is that this interpretation would be correct for 90% of motifs of this form, with this set of characteristics.

All 21 Gwion motifs in this study were classed as “Gwion - Certain” by both P.H. and C.M. (Table 3-S2). Four further motifs were classed as “Gwion” by just one person and at a lower confidence level. They have, therefore, been excluded from this analysis. At the time of classification, neither person had knowledge of the age of the wasp nests related to the motifs.

#### **3.6.4 Probability functions for motif ages**

The possible age range for a motif was determined from the age of a nest that is either over or under the motif. This possible motif age range can be statistically expressed as a probability density function (pdf). For wasp nests overlying pigment, the pdf of the minimum age of the motif is the cumulative value of the pdf of the nest age, with a probability of 0 that the motif is older than ~50 ka (minimum age for the first arrival of people in Australia) and a probability of 1 that it is older than 0 years. Conversely, for wasp nests underlying pigment, the pdf of the maximum age of the motif is the cumulative value of the pdf of the nest age, with a probability of 1 that the motif is younger than 50 ka and a probability of 0 that it is younger than 0 years.

For each wasp nest dated, the OxCal (Bronk Ramsey 2009a) calibration program was used to generate a table showing the probability of the calibrated nest age at intervals of 5 years. To calculate the pdf for the minimum age of a motif, these values are accumulated (added), starting at a probability of 0 at 50 ka. For maximum age estimates, they accumulated starting at a probability of 0 at 0 years.

All the minimum motif age pdfs were then summed to derive the blue curves shown in Figs. 3-3 (c and d) and Fig. 3-5. Similarly, the maximum motif age pdfs were summed to derive the brown curves.

### **3.7 Acknowledgements**

We acknowledge and thank Balanggarra and Dambimangari Aboriginal Corporations, Rangers and Traditional Owners for permission to work on their Country and for their support during fieldwork. In particular, we thank Augustine Unghango and family, the Waina family, and Ambrose Chalarimeri on Balanggarra land, and Donny and Kenny Woolagoodja and Wayne Oobagooma on Dambimangari land. Fieldwork support was provided by Susan Bradley, Paul Hartley, Nick Sundblom, Robin Maher, Traudl Tan, Michi Maier and Peter Kendrick. The sites we visited were relocated and recorded over decades by Dunkeld Pastoral Co Pty Ltd and the *Kimberley Visions* Survey teams, Joc Schmiechen, and the late Grahame Walsh. Radiocarbon laboratory support from the Australian Nuclear Science and Technology Organisation was provided by Alan Williams, Fiona Bertuch and Bin Yang. Financial support for the Centre for Accelerator Science at ANSTO was provided by the Australian National Collaborative Research Infrastructure Strategy.

#### **3.7.1 Funding**

This research was funded by an Australian Research Council Linkage Projects LP130100501 and LP170100155 with funding partners the Kimberley Foundation Australia, with in-kind support from Dunkeld Pastoral Co Pty Ltd and Balanggarra Aboriginal Corporation especially for fieldwork. DF is supported by an Australian Postgraduate Award and an AINSE Post Graduate Research Award. The Kimberley Foundation Australia also provided a grant to DF to establish the radiocarbon pretreatment facility at the University of Melbourne.

#### **3.7.2 Author contributions**

This research is part of the multi-disciplinary Kimberley Rock Art Dating project conceived and led by AG who, with JH and VL, supervised this work as part of DF's PhD research project. Motif classification was by PH and CM. DF collected and pretreated the samples, designed and performed the experiments, and analysed and interpreted the results. Fieldwork was carried out by DF, PH, SH, SO, PV, CM, AG and HG. Illustrations were drawn by PH. VL conducted radiocarbon measurements

and raw data analyses. DF wrote the manuscript draft with key editing from JH and AG with further input from all authors.

### **3.7.3 Competing interests:**

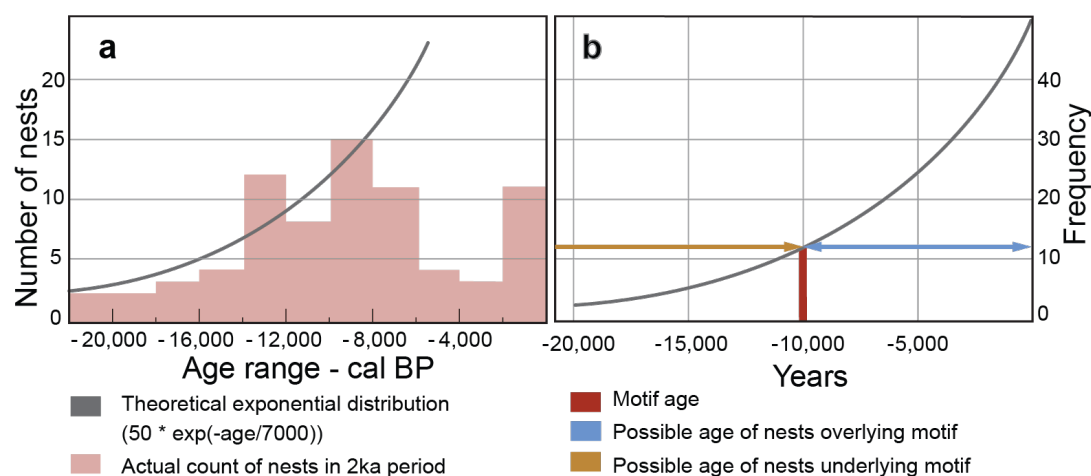
The authors declare that they have no competing interests.

### **3.7.4 Data and materials availability**

All data is available in the main text or the supplementary materials. OxCal code is included in Supplementary Materials section 3.8.2.

### 3.8 Supplementary Materials:

#### 3.8.1 Figure 3-S1 Relationship between age of nest and associated motif.



**Figure 3-S1.** (a) Histogram of ages of 75 mud wasp nests from (Finch et al. 2019) in 2ka intervals with a theoretical exponential age distribution for comparison. Note that the significantly fewer nests recorded from this study in the 2 - 6 ka period represents deliberate sampling bias towards the earliest surviving examples (b) Hypothetical age distribution of all possible nests overlying and underlying a 10,000-year-old motif.

#### 3.8.2 Text 3-S1. Calibrated age modelling code

The age bracket for motif DR015\_07 is calculated as follows. The calibrated ages of the overlying nests are used to define the distribution of possible ages for the motif using the BEFORE function in OxCal version 4.3.2 software (Bronk Ramsey 2009b, Bronk Ramsey 2017). Similarly, the calibrated age of the underlying nest (DR015\_07-3) uses the AFTER function to specify the maximum age range. The possible age range for the motif is then defined by applying the statistical COMBINE (or AND) function to the Before and After probability distributions. The motif's minimum age is solely constrained by nest sample DR015\_07-2 as nest DR015\_07-5 is younger.

The OxCal code used to generate parts of Figures 3-2 and 3-4 is listed below:

Options()

```
{ Curve="SHCal13.14c";
```

```
BCAD=FALSE; };
```

Plot()

```
{Combine("DR015_07")
```

```
{Before("Min DR015_07")
```

```
{R_Date("DR015_07-2_[5]", 9875, 85);
```

```
R_Date("DR015_07-5_[5]", 8094, 70);};
```

```
After("Max DR015_07")
```

```
{R_Date("DR015_07-3_[7]", 11220, 71);};};};
```

The OxCal code used to generate Fig. 3-6, showing the hypothesised Gwion period age range, with and without a correction for inbuilt charcoal age is listed below. The code applies a charcoal outlier model to each date (Bronk Ramsey 2009b).

Options()

```
{Curve="SHCal13.14c";
```

```
BCAD=FALSE;};
```

Plot()

```
{Outlier_Model("Charcoal",Exp(255,-4000,0));
```

```
{ Combine("Gwion")
```

```
{ Before() { R_Date("DT1207_03-1 [6] Min", 10353, 107)
```

```
{Outlier("Charcoal",1);};};
```

```
After() { R_Date("DR013_06-1 [7] Max", 10818, 120)
```

```
{Outlier("Charcoal",1);};};
```

```
Combine("DR015_07")
```

```
{Before("Min DR015_07") {R_Date("DR015_07-2_[5]", 9875, 85)
```

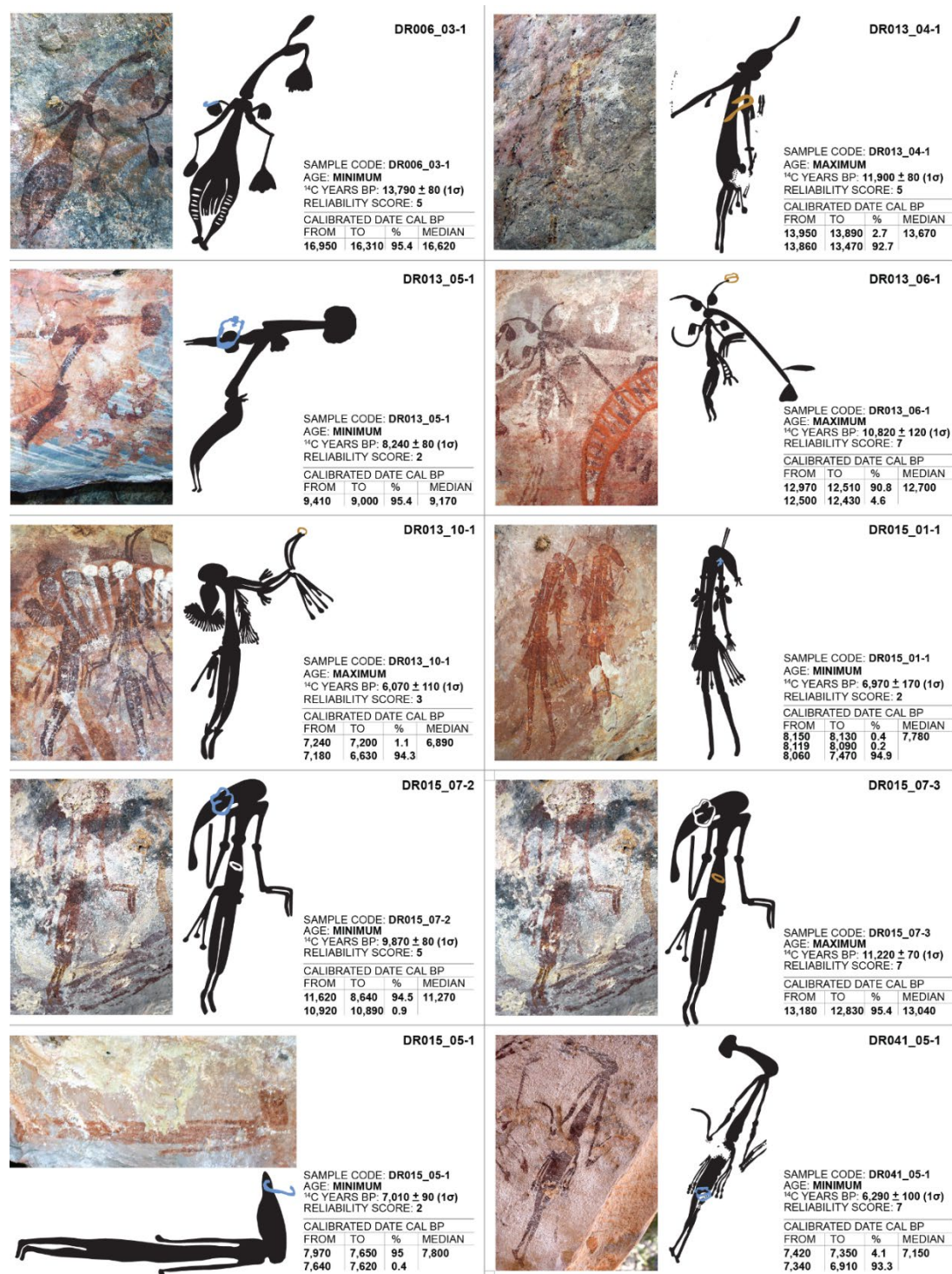
```
{Outlier("Charcoal",1);};};
```

```
After("Max DR015_07") {R_Date("DR015_07-3_[7]", 11220, 71)
```

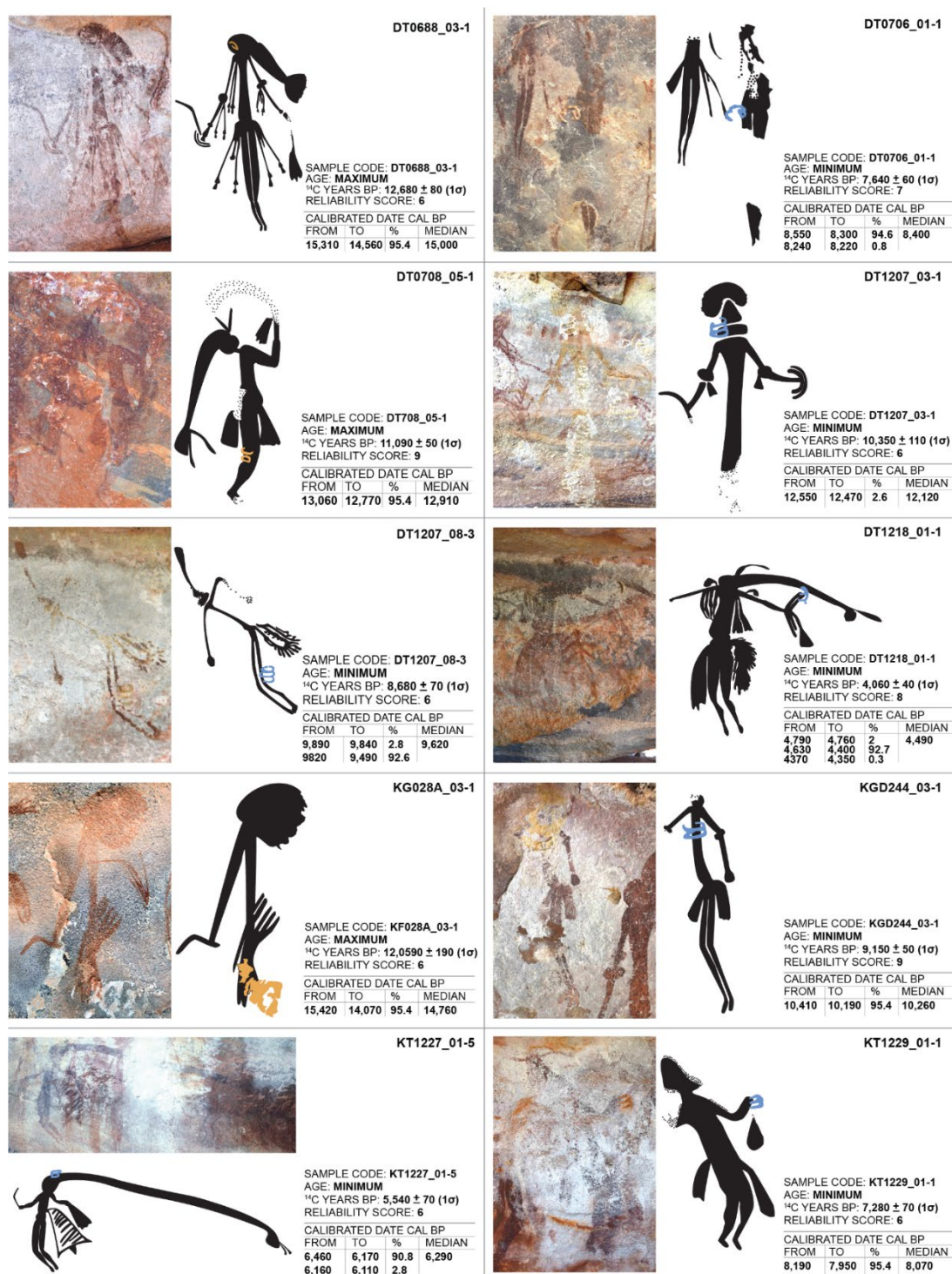
```
{Outlier("Charcoal",1);};};};
```

```
}; }; };
```

### 3.8.3 Figure 3-S2. Photograph and illustrative interpretation of dated Gwion motifs







**Figure 3-S2.** Photograph and illustrative interpretation of dated Gwion motifs showing sample location (blue for nests over pigment, brown for nests under pigment, in the illustrations). Four overlying nests, less than 1000 years old, are not shown, nor, therefore, is motif DR013\_01 as the data indicates, trivially, only that this motif is older than ~500 years. Photo Credit: D.F. Illustrations: P.H.



#### **3.8.4 Table 3-S1. Radiocarbon age determinations on wasp nests associated with Gwion motifs.**

The Sample Code is constructed from a short site identifier, followed by a number to identify the painted motif and then the number of the sample collected (on that motif, at that site) in the format “SITE\_MOTIF-NEST”. The “Min or Max age constraint” indicates the nest sample was respectively, either over or under the motif. For a complete description of the Pretreatment Sequence, Fractions, and Reliability Score refer (Finch et al. 2019). Calibrated using SHCal13(Hogg et al. 2013) in OxCal v4.3.2 (Bronk Ramsey 2009b).

**Table 3-S1**

Sample Code	Laboratory Code	C mass (µg)	<sup>14</sup> C years BP	Error (1σ) ± (yrs)	Calibrated date cal BP (95% probability range) (years)				Rel. Score	Min or Max age constraint for motif
					from	to	%	Median		
DR006_03-1	OZT791	58	13,790	80	16950	16310	95.4	16,620	5	Min
DR013_01-2	OZT787	41	510	40	560	470	95.4	510	4	Min
DR013_04-1	OZT775	24	11,900	80	13950 13860	13890 13470	2.7 92.7	13,670	5	Max
DR013_05-1	OZT776	22	8,240	80	9410	9000	95.4	9,170	2	Min
DR013_06-1	OZU776U1	27	10,820	120	12970 12500	12510 12430	90.8 4.6	12,700	7	Max
DR013_10-1	OZT462	23	6,070	110	7240 7180	7200 6630	1.1 94.3	6,890	3	Max
DR015_01-1	OZT477	13	6,970	170	8150 8110 8060	8130 8090 7470	0.4 0.2 94.9	7,780	2	Min
DR015_01-2	OZT492	14	740	110	900 810	860 510	2.2 93.2	660	1	Min*
DR015_05-1	OZT779	24	7,010	90	7970 7640	7650 7620	95.0 0.4	7,800	2	Min
DR015_07-2	OZT781	55	9,870	80	11620 10920	11080 10890	94.5 0.9	11,270	5	Min
DR015_07-3	OZW367	39	11,220	70	13180	12830	95.4	13,040	7	Max
DR015_07-5	OZW377	30	8,090	70	9140	8640	95.4	8,920	5	Min*
DR041_05-1	OZW368	28	6,290	100	7420 7340	7350 6910	4.1 91.3	7,150	7	Min
DT0184_01-1	OZW371	159	410	20	500 410	430 320	55.4 40.0	450	9	Min
DT0688_03-1	OZW421U2	34	12,680	80	15310	14560	95.4	15,000	6	Max
DT0706_01-1	OZW416U2	31	7,640	60	8550 8240	8300 8220	94.6 0.8	8,400	7	Min
DT0708_05-1	OZW392	70	11,090	50	13060	12770	95.4	12,910	9	Max
DT1207_03-1	OZW418U2	22	10,350	110	12550 12450	12470 11710	2.6 92.8	12,120	6	Min
DT1207_08-3	OZW386	22	8,680	70	9890 9820	9840 9490	2.8 92.6	9,620	6	Min
DT1218_01-1	OZW372	36	4,060	40	4790 4630 4370 4330	4760 4400 4350 4300	2.0 92.7 0.3 0.4	4,490	8	Min
KG028A_03-1	OZU785U1	25	12,590	190	15420	14070	95.4	14,760	6	Max
KGD244_03-1	OZW414U2	60	9,150	50	10410	10190	95.4	10,260	9	Min
KT1227_01-5	OZW420U2	36	5,540	70	6460 6160 6080 6050	6170 6110 6060 6020	90.8 2.8 0.6 1.3	6,290	6	Min
KT1229_01-1	OZW419U2	25	7,280	70	8190	7950	95.4	8,070	6	Min

**3.8.5 Table 3-S2. Radiocarbon pretreatment methods and age determinations (uncalibrated) on wasp nests associated with Gwion motifs.**

All motifs in this table were classified as "Certain" Gwion motifs by both PH and CM. The "Fraction" column indicates where Heavy Liquid Separation was used to separate the sample into low density (Light) and higher density (Heavy) fractions with "All" indicating the sample was not separated. The  $\delta^{13}\text{C}$  of all samples was not able to be reliably measured but is assumed to be -25‰ for the isotopic correction, based on an average for other similar samples. For a complete description of the Pretreatment Sequence, Fractions, and Reliability Score refer Finch et al. (2019).

**Table 3-S2**

Sample Code	Laboratory Code	Pretreatment Sequence	Fraction	C mass (µg)	<sup>14</sup> C years BP	Error (1σ) ± (yrs)	Reliability Score
DR006_03-1	OZT791	ABA	All	58	13,790	80	5
DR013_01-2	OZT787	ABA	All	41	510	40	4
DR013_04-1	OZT775	ABA	All	24	11,900	80	5
DR013_05-1	OZT776	ABA	All	22	8,240	80	2
DR013_06-1	OZU776U1	A-HLS-BA(8M)	Light	27	10,820	120	7
DR013_10-1	OZT462	ABA	All	23	6,070	110	3
DR015_01-1	OZT477	ABA	All	13	6,970	170	2
DR015_01-2	OZT492	ABA	All	14	740	110	1
DR015_05-1	OZT779	ABA	All	24	7,010	90	2
DR015_07-2	OZT781	ABA	All	55	9,870	80	5
DR015_07-3	OZW367	ABA(8M)	All	39	11,220	70	7
DR015_07-5	OZW377	ABA(8M)	All	30	8,090	70	5
DR041_05-1	OZW368	ABA(8M)	All	28	6,290	100	7
DT0184_01-1	OZW371	ABA(8M)	All	159	410	20	9
DT0688_03-1	OZW421U2	AB-HLS-A(16M)	Heavy	34	12,680	80	6
DT0706_01-1	OZW416U2	AB-HLS-A(16M)	Heavy	31	7,640	60	7
DT0708_05-1	OZW392	A-HLS-BA(8M)	Heavy	70	11,090	50	9
DT1207_03-1	OZW418U2	AB-HLS-A(16M)	Heavy	22	10,350	110	6
DT1207_08-3	OZW386	A-HLS-BA(8M)	Heavy	22	8,680	70	6
DT1218_01-1	OZW372	ABA(8M)	All	36	4,060	40	8
KG028A_03-1	OZU785U1	A-HLS-BA(8M)	Light	25	12,590	190	6
KGD244_03-1	OZW414U2	A-HLS-BA(8M)	Heavy	60	9,150	50	9
KT1227_01-5	OZW420U2	A-HLS-BA(16M)	Heavy	36	5,540	70	6
KT1229_01-1	OZW419U2	A-HLS-BA(8M)	Heavy	25	7,280	70	6

### 3.9 References

- Aubert, M. (2012). "A review of rock art dating in the Kimberley, Western Australia." Journal of Archaeological Science **39**(3): 573-577.
- Aubert, M., A. Brumm and P. S. C. Taçon (2017). "The Timing and Nature of Human Colonization of Southeast Asia in the Late Pleistocene: A Rock Art Perspective." Current Anthropology **58**(0): S553-S566.
- Aubert, M., P. Setiawan, A. A. Oktaviana, A. Brumm, P. H. Sulistyarto, E. W. Saptomo, B. Istiawan, T. A. Ma'rifat, V. N. Wahyuono, F. T. Atmoko, J. X. Zhao, J. Huntley, P. S. C. Tacon, D. L. Howard and H. E. A. Brand (2018). "Palaeolithic cave art in Borneo." Nature **564**(7735): 254-+.
- Bednarik, R. G. (1995). "Refutation of stylistic constructs in Palaeolithic rock art." Comptes rendus de l'Académie des Sciences **321**: 817-821.
- Bednarik, R. G. (2002). "First dating of Pilbara petroglyphs." Records of the Western Australian Museum **20**(4): 415-430.
- Bronk Ramsey, C. (2009a). "Bayesian analysis of radiocarbon dates." Radiocarbon **51**(1): 337-360.
- Bronk Ramsey, C. (2009b). "Dealing with outliers and offsets in radiocarbon dating." Radiocarbon **51**(3): 1023-1045.
- Bronk Ramsey, C. (2017). "Methods for Summarizing Radiocarbon Datasets." Radiocarbon **59**(6): 1809-1833.
- Budescu, D. V., S. Broomell and H. H. Por (2009). "Improving Communication of Uncertainty in the Reports of the Intergovernmental Panel on Climate Change." Psychological Science **20**(3): 299-308.
- Crawford, I. M. (1977). The relationship of Bradshaw and Wandjina art in north-west Kimberley. Form in indigenous art; schematisation in the art of Aboriginal Australia and prehistoric Europe. P. J. Ucko. Canberra, Australian Institute of Aboriginal Studies.
- David, B., J.-M. Geneste, F. Petchey, J.-J. Delannoy, B. Barker and M. Eccleston (2013). "How old are Australia's pictographs? A review of rock art dating." Journal of Archaeological Science **40**(1): 3-10.

Donaldson, M. (2012). Kimberley rock art, Volumes 1, 2, 3. Mount Lawley, W.A, Wildrocks Publications,.

Donaldson, M. (2014). "What's in a name? Towards a nomenclature for Gwions ('Bradshaws')." Rock art research **31**(1): 31-35.

Finch, D., A. Gleadow, J. Hergt, V. A. Levchenko and D. Fink (2019). "New developments in the radiocarbon dating of mud wasp nests." Quaternary Geochronology **51**: 140-154.

Garcia-Diez, M., D. L. Hoffmann, J. Zilhao, C. de las Heras, J. A. Lasheras, R. Montes and A. W. G. Pike (2013). "Uranium series dating reveals a long sequence of rock art at Altamira Cave (Santillana del Mar, Cantabria)." Journal of Archaeological Science **40**(11): 4098-4106.

Green, H., A. Gleadow, D. Finch, J. Hergt and S. Ouzman (2017). "Mineral deposition systems at rock art sites, Kimberley, Northern Australia - Field observations." Journal of Archaeological Science-Reports **14**: 340-352.

Hoffmann, D. L., A. W. G. Pike, M. García-Diez, P. B. Pettitt and J. Zilhão (2016). "Methods for U-series dating of CaCO<sub>3</sub> crusts associated with Palaeolithic cave art and application to Iberian sites." Quaternary Geochronology **36**: 104-119.

Hogg, A. G., Q. Hua, P. G. Blackwell, M. Niu, C. E. Buck, T. P. Guilderson, T. J. Heaton, J. G. Palmer, P. J. Reimer, R. W. Reimer, C. S. M. Turney and S. R. H. Zimmerman (2013). "SHCal13 Southern Hemisphere calibration, 0–50,000 years cal BP." Radiocarbon **55**(4): 1889-1903.

Hua, Q., G. E. Jacobsen, U. Zoppi, E. M. Lawson, A. A. Williams, A. M. Smith and M. J. McGann (2001). "Progress in radiocarbon target preparation at the ANTARES AMS Centre." Radiocarbon **43**(2A): 275-282.

Hua, Q., U. Zoppi, A. A. Williams and A. M. Smith (2004). "Small-mass AMS radiocarbon analysis at ANTARES." Nuclear Instruments & Methods in Physics Research Section B-Beam Interactions with Materials and Atoms **223**: 284-292.

Jones, T., V. A. Levchenko, P. L. King, U. Troitzsch, D. Wesley, A. A. Williams and A. Nayingull (2017). "Radiocarbon age constraints for a Pleistocene–Holocene transition rock art style: The Northern Running Figures of the East Alligator River region, western Arnhem Land, Australia." Journal of Archaeological Science: Reports **11**: 80-89.

Lewis, D. (1988). The Rock Paintings of Arnhem Land, Australia. Oxford, B.A.R.

Lewis, D. (1997). "Bradshaws: The View from Arnhem Land." Australian Archaeology **44**: 1 - 16.

- MacLeod, A. and S. Pietravallo (2017). "Communicating risk: variability of interpreting qualitative terms." EPPO Bulletin **47**(1): 57-68.
- Morwood, M., G. Walsh and A. L. Watchman (1994). "The dating potential of rock art in the Kimberley, NW Australia." Rock Art Research: The Journal of the Australian Rock Art Research Association (AURA) **11**(2): 79.
- Ouzman, S., P. Veth, C. Myers, P. Heaney and K. Kenneally (2017). Plants Before Animals?: Aboriginal Rock Art as Evidence of Ecoscaping in Australia's Kimberley. The Oxford Handbook of the Archaeology and Anthropology of Rock Art. B. David and I. J. McNiven, Oxford University Press.
- Pike, A. W., D. L. Hoffmann, M. Garcia-Diez, P. B. Pettitt, J. Alcolea, R. De Balbin, C. Gonzalez-Sainz, C. de las Heras, J. A. Lasheras, R. Montes and J. Zilhao (2012). "U-series dating of Paleolithic art in 11 caves in Spain." Science **336**(6087): 1409-1413.
- Roberts, R., G. Walsh, A. Murray, J. Olley, R. Jones, M. Morwood, C. Tuniz, E. Lawson, M. Macphall, D. Bowdery and I. Naumann (1997). "Luminescence dating of rock art and past environments using mud-wasp nests in northern Australia." Nature **387**(6634): 696-699.
- Ross, J., K. Westaway, M. Travers, M. J. Morwood and J. Hayward (2016). "Into the Past: A Step Towards a Robust Kimberley Rock Art Chronology." PLoS ONE **11**(8): e0161726.
- Ruiz, J. F., A. Hernanz, R. A. Armitage, M. W. Rowe, R. Viñas, J. M. Gavira-Vallejo and A. Rubio (2012). "Calcium oxalate AMS <sup>14</sup>C dating and chronology of post-Palaeolithic rock paintings in the Iberian Peninsula. Two dates from Abrigo de los Oculados (Henarejos, Cuenca, Spain)." Journal of Archaeological Science **39**(8): 2655-2667.
- Russell, T. (2000). "The Application of the Harris Matrix to San Rock Art at Main Caves North, Kwazulu-Natal." The South African Archaeological Bulletin **55**(171): 60-70.
- Sanz, I. D. (2012). A Theoretical Approach to Style in Levantine Rock Art. A Companion to Rock Art. J. McDonald and P. Veth. Malden, Wiley-Blackwell: 306-321.
- Sanz, I. D. and D. Fiore (2014). Style: Its Role in the Archaeology of Art. Encyclopedia of Global Archaeology. C. Smith. New York, NY, Springer New York: 7104-7111.
- Veth, P., C. Myers, P. Heaney and S. Ouzman (2017). "Plants before farming: The deep history of plant-use and representation in the rock art of Australia's Kimberley region." Quaternary International.

Walsh, G. L. (1994). Bradshaws, ancient rock paintings of north-west Australia. Carouge-Geneva, Switzerland, Edition Limitée for the Bradshaw Foundation.

Walsh, G. L. (2000). Bradshaw art of the Kimberley, Takarakka Nowan Kas Publications.

Welch, D. (2007). Bradshaw art of the Kimberley. Rock art of the Kimberley. M. Donaldson and K. F. Kenneally. Perth, Western Australia, Kimberley Society: 81-100.

Welch, D. M. (1993). Stylistic change in the Kimberley rock art, Australia. Rock art studies: the post-stylistic era or where do we go from here?, Cairns, Oxbow Monograph.

Welch, D. M. (2015). Aboriginal Paintings of Drysdale River National Park, Kimberley, Western Australia. Coolalinga, Northern Territory, David M. Welch.

Yang, B. and A. M. Smith (2016). "Conventionally Heated Microfurnace for the Graphitization of Microgram-Sized Carbon Samples." Radiocarbon **59**(3): 859-873.



# **Chapter 4**

## **Radiocarbon age estimates for the Irregular Infill Animal Period**

This chapter is the manuscript “Ages for Australia’s oldest rock paintings” initially submitted on 13<sup>th</sup> July 2020 for publication in Nature Human Behaviour. As at December 2020, the paper has been accepted for publication, "in principle".

The individual author contributions are as noted in section 4.6.2 with the candidate contributing more than 90% to the content for this publication.

### **Ages for Australia’s oldest rock paintings**

Damien Finch<sup>1</sup>, Andrew Gleadow<sup>1</sup>, Janet Hergt<sup>1</sup>, Pauline Heaney<sup>3</sup>, Helen Green<sup>1</sup>, Cecilia Myers<sup>4</sup>, Peter Veth<sup>2</sup>, Sam Harper<sup>2</sup>, Sven Ouzman<sup>2</sup>, Vladimir A. Levchenko<sup>5</sup>

<sup>1</sup> The School of Earth Sciences, The University of Melbourne, Australia.

<sup>2</sup> Centre for Rock Art Research and Management, University of Western Australia.

<sup>3</sup> Lettuce Create, Strathpine, Queensland, Australia.

<sup>4</sup> Dunkeld Pastoral Co. Pty Ltd Theda Station, Western Australia.

<sup>5</sup> Australian Nuclear Science and Technology Organisation, Sydney, Australia

#### **4.1 Abstract:**

Naturalistic depictions of animals are a common subject for the world's oldest dated rock art, including wild bovids in Indonesia, and lions in France's Chauvet Cave. The oldest known Australian Aboriginal figurative rock paintings also commonly depict naturalistic animals but, until now, none had been quantitatively dated. Here we present 27 radiocarbon dates on mud wasp nests that constrain the ages of 16 motifs from this earliest known phase of rock painting in the Australian Kimberley region. These initial results suggest paintings in this style proliferated between 17,000 and 13,000 years ago. Notably, one painting of a kangaroo is securely dated to between 17,500 and 17,100 years cal BP based on the ages of 3 overlying and 3 underlying wasp nests. This is the oldest radiometrically dated, *in situ*, rock painting so far reported in Australia.

## 4.2 Introduction

Throughout the world, rock art records some of the earliest attempts at complex human communication. In regions where conditions do not favour preservation of organic material, evidence of past human activity is largely restricted to micromorphological evidence, stone tools and rock art. Stone tool usage is placed on the absolute timescale of human development using radiometric dating of the context where such material is found in the layers of an archaeological excavation (Clarkson et al. 2017, Vannieuwenhuyse et al. 2017, Maloney et al. 2018). Unfortunately, radiometric dating techniques are only rarely applicable to older rock art, so the age of this aspect of human creative expression is not as well constrained. Consequently, we cannot correlate records of changes in climate, sea-level, food sources, and population, for example, with the subjects that people chose to depict in their rock art, leaving the archaeological record incomplete.

In the absence of reliable methods to directly date rock art, researchers have used extensive observations of motif superimpositions and state of preservation to determine relative age sequences for groups of motifs that share common characteristics. In many of the major rock art regions, style and superimposition analysis have been used to hypothesise relative stylistic periods. However, stylistic groupings are not necessarily chronologically discrete. Furthermore, the practical difficulties in precisely defining particular styles and reliably determining superimposition sequences for the oldest, faded, pigments add uncertainty to this approach (Lewis 1988, Hoffmann et al. 2016, Jones et al. 2017a, Jones et al. 2017b). Absolute or well-constrained dates on individual motifs are essential to test these hypotheses and to confirm or refine the common characteristics used to define a given style.

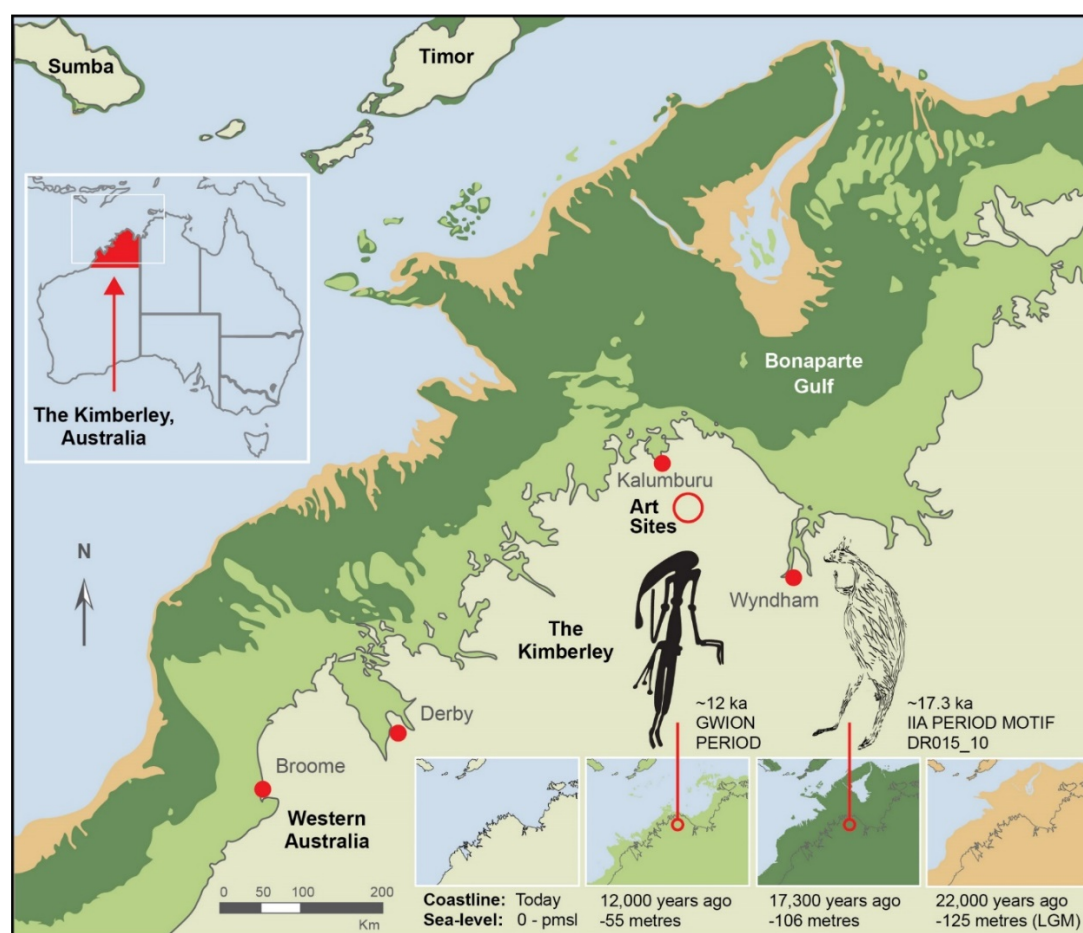
With rare exceptions, for example in France where charcoal pigmented art is preserved in deep caves (Quiles et al. 2016, Valladas et al. 2017), the remaining pigment in paintings from the Pleistocene period (older than c. 11,500 years) contains no materials that can be dated directly. Occasionally, rock fragments with some pigment on one surface are found in archaeological excavations with the stratigraphic context providing an age estimate for the time of burial. In Australia, two excavations have yielded such fragments, one estimated to be c. 28,000 years old (David et al. 2012) and the other c. 40 ka (O'Connor and Fankhauser 2001)

but neither are unambiguously classified as painted rock art motifs (Aubert et al. 2017) and, in any event, are unable to be classified to a particular style. In this study, we rely on the fortuitous occurrence of dateable mud wasp nests overlying or underlying rock art to provide minimum or maximum age limits for individual motifs. Such techniques, using wasp nests or surface mineral accretions, have provided Pleistocene age constraints for figurative rock paintings in Spain (Pike et al. 2012), Indonesia (Aubert et al. 2014, Aubert et al. 2017, Aubert et al. 2018, Aubert et al. 2019) and Australia (Roberts et al. 1997, Ross et al. 2016, Finch et al. 2020). Results from these limited examples support the proposition that ‘realistic’ paintings of animals dominate the oldest figurative rock art in different continents (Taçon et al. 2010, Aubert et al. 2014, Quiles et al. 2016, Valladas et al. 2017, Aubert et al. 2018, Aubert et al. 2019). In two of the most extensive provinces for painted rock art in Australia, the Kimberley (Fig. 4-1) and Arnhem Land, naturalistic animals are the most common subjects in the oldest stylistic period in each region (Chaloupka 1993, Welch 1993, Walsh 1994b, Chippindale and Tacon 1998, Walsh 2000, Welch 2015) based on superimposition analysis, but there is debate about their antiquity and the adequacy of the definitions of these earliest styles (Lewis 1988, Lewis 1997, Jones et al. 2017a, Taçon and Webb 2017). The same or similar animals are also depicted in more recent art periods, but using different stylistic techniques (e.g. solid or regular infill rather than irregular infill and solid infill of the extremities of the head, tail and limbs), so further evidence is required to test these ideas as no old, radiometric, age constraints have been published for any of these motifs.

In the Kimberley it is now known that paintings from the superimposed, and inferred to be more recent, Gwion stylistic period proliferated around 12,000 years ago (Finch et al. 2020) so the generally agreed relative rock art sequence predicts that the earlier paintings of naturalistic animals should be older than this. In the Kimberley rock art stylistic sequence these naturalistic animals belong to the earliest phase of painted rock art, the Irregular Infill Animal Period (IIAP). Notwithstanding the abovementioned debate about the classification of similar motifs in the Arnhem Land region (some 700 km to the east), we adopt the comprehensive definition of the Kimberley IIAP by Walsh (2000, 2019) and Welch (1993, 2015) as a starting hypothesis. This definition of IIAP motifs includes some styles of hand stencils, hand prints, stencils of boomerangs and other objects, and some freehand depictions of

plants (e.g. yams), animals (particularly kangaroos but also echidna, birds, goannas, fish, and possum) and, more rarely, anthropomorphs (see (Walsh and Kimberley-Foundation 2019) for examples).

Here we report radiocarbon ages determined from 27 mud wasp nests, collected from 8 separate sandstone rock shelters (Fig. 4-1), that serve to constrain the ages of 16 IIAP motifs (Table 4-S1). Fifteen nests overlay 10 IIAP motifs and six nests were underneath a further 5 motifs. Importantly, 3 overlying and 3 underlying nests were dated from one further IIAP motif, thereby providing a bracketed age constraint for that individual painting.



**Figure 4-1.** Map of Kimberley region in Western Australia showing the general location of the 8 rock art sample sites and the coastline (Whiteway 2009) at 12ka (Williams et al. 2018) around the time of the Gwion period (Finch et al. 2020) and at 17.3 ka when IIAP motif DR015\_10 was painted. The present mean sea level (pmsl) and the coastline during the Last Glacial Maximum (LGM) (125 m below pmsl at 22 ka) are shown for comparison. Illustrations: PH.

### 4.3 Results

As part of a broader multi-year program to date Kimberley rock art, a total of 75 remnant mud wasp nests either under or over pigment from north-east Kimberley rock art motifs of various styles have been radiocarbon dated (Finch et al. 2019). Of these, 27 nests were in contact with 16 different rock art motifs that are classified as “Certain” or “Highly Likely” to be in the IIAP style (see Table 4-S2). Other dated nests are associated with motifs that are less certainly IIAP, so they are not reported here.

Each age determination is given a Reliability Score (RS) in a range from 1 (least reliable) to 10 (most reliable) to communicate a qualitative assessment of several factors that can influence the accuracy of the result in addition to the analytical precision. The score is a relative measure based on the carbon mass of the sample measured, the degree to which physical cleaning was possible, and the chemical pretreatment applied. This approach is described in detail elsewhere (Finch et al. 2019, Finch et al. 2020) but it is worth noting here that even a sample with a very low score may still provide a useful age constraint for an underlying motif while one with a mid-range score may be rejected. For example, a mid-range score on a nest under a motif may be rejected if it has a significant risk of modern carbon contamination even after pretreatment. Lower scores serve to identify samples where the sample context and the risk of any potential contamination may influence the accuracy of the age constraint inferred from the date of the nest sample. Another important conclusion was that any possible residual contamination risk would be from more modern rather than ancient carbon in this setting of ancient sandstones devoid of organic carbon or carbonates. Consequently, any age determinations impacted by contamination would represent a minimum age for nest construction.

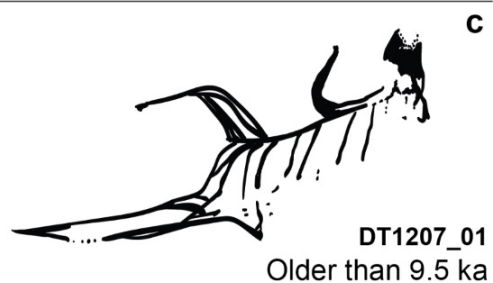
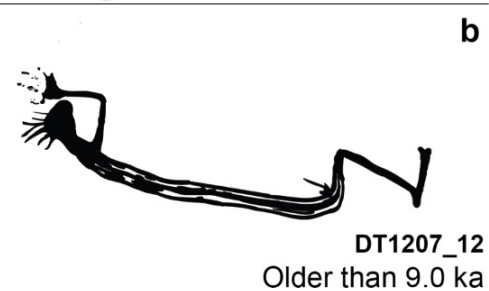
The results are presented below in three main sections beginning with the ages of nests overlying pigment giving minimum ages for the motifs, followed by a summary of the results for nests underlying pigment (maximum ages for the motifs), and finally, by a section detailing a single motif with both underlying and overlying nests.

### 4.3.1 Minimum age constraints

Calibrated ages for 15 wasp nests overlying pigment from 10 IIAP motifs (“Certain” or “Highly Likely” to be of the IIAP style), from 6 different rock art sites, are summarized in Fig. 4-2 (details in Tables 4-S1 and 4-S2). Three of the 10 motifs have more than one overlying wasp nest that has been dated. For nests overlying pigment, we take the younger limit of the 95.4% probability range for the calibrated age of the oldest overlying nest as the relevant minimum age constraint for the motif. So, for the macropod (i.e. kangaroo or wallaby) motif DR015\_04 where there are two overlying nests with median ages of c. 7.3 ka and 11.4 ka, we determine the painting must be older than 11.2 cal kBP (being the lower end of the 95.4% probability, radiocarbon calibrated age in thousands of years Before Present, which is taken to be 1950 by convention). Another macropod motif, DR016\_01, has 4 overlying nests, with median dates of 4.3, 9.4, 11.6 and 13.0 cal kBP. While the oldest of these nests has a relatively low RS of 2, the age determination is credible given the other 3 dates on nests overlying the same motif. As noted above, the contamination risk reflected in the low RS for this sample is such that, if anything, the nest, and therefore the motif, would be even older than 13 cal kBP if so affected. The third motif with more than one overlying nest, DT1207\_01 also depicts a macropod. The two overlying nests are of similar age and we conclude this motif is older than 9.5 cal kBP.

Of the other 7 motifs with overlying nests, 4 are at least of mid-Holocene age with minimum nest dates in the range 6.2 to 9.7 cal kBP (Fig. 4-2f). The other 3 dated nests are younger and therefore provide little by way of age constraints for the related motifs. The age of DR006\_05-1, for example, indicates, only that the motif is older than c. 100 years.





f Sample Code	Nest Age cal BP (95.4% probability)		Reliability Score
	Range	Median	
DR006_05-1	280 - ...	90	2
DR008_02-1	8560 - 8010	8,300	1
DR015_04-1	8960 - 5760	7,280	1
DR015_04-2	11750 - 11230	11,440	8
DR015_08-1	9710-9030	9,420	3
DR015_11-1	6890-6210	6,520	1
DR016_01-1	13300 - 12720	13,010	2
DR016_01-2	4800 - 3970	4,320	2
DR016_01-3	12370 - 11200	11,630	3
DR016_01-5	9540 - 9250	9,420	6
DR018_03-2	1830-1360	1,580	3
DR018_04-1	5290-4410	4,760	1
DT1207_01-1	7830-7570	7,670	6
DT1207_01-2	9890 - 9460	9,590	7
DT1207_12-1	9410-9000	9,170	6



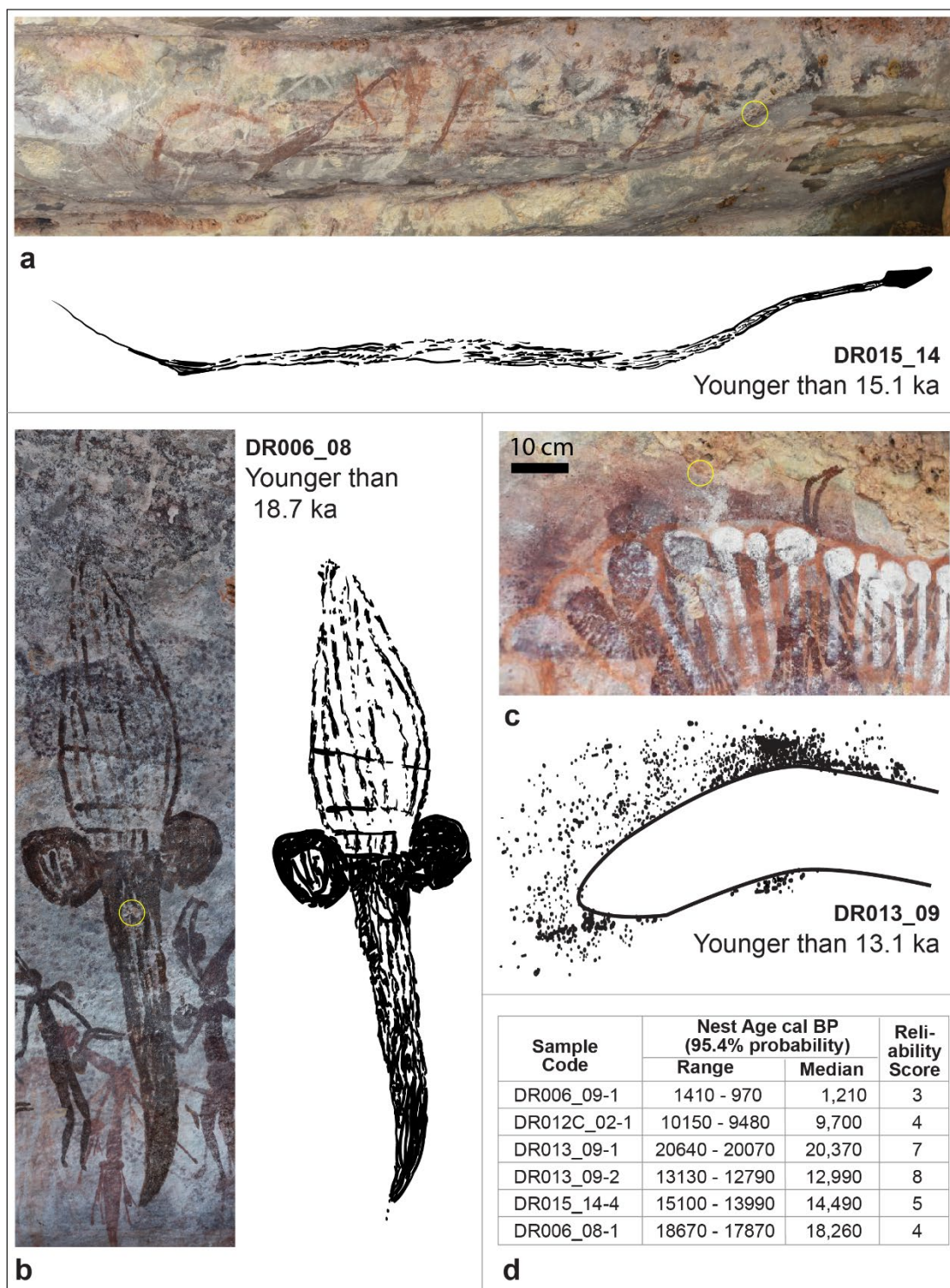


**Figure 4-2. Minimum ages for 10 motifs from 15 overlying wasp nest ages.** The five oldest motifs are illustrated: (a) (showing Traditional Owner Ian Waina inspecting motif DR016\_01), (c), and (e) are interpreted as macropods, (b) as a rare depiction of an IIAP human figure reclining and (d) as a lizard-like figure. Scale bars, where shown, are 10 cm. Sample locations marked are with a yellow circle. See Fig. 4-S1 for images of the other motifs. The Sample Code is constructed from a short site identifier, a number to identify the painted motif and the number of the sample collected from that motif, in the format “SITE\_MOTIF-NEST”. Full details of the radiocarbon dates are in table 4-S1. Credits: Photos DF, PV, Illustrations PH

### 4.3.2 Maximum age constraints

Calibrated radiocarbon ages measured for 6 mud wasp nests underlying 5 different motifs are summarized in Fig. 4-3 (see Table 4-S1 for details). All motifs are classified as IIAP (Table 4-S2) although DR006\_08 may have been repainted, at least in the lower part (Fig. 4-3b), hence, conservatively, the age of the nest serves as a maximum age for the repainted section of 18.7 cal kBP.

The boomerang stencil motif, DR013\_09, has two nests where paint spray was visible on the outer surfaces. The younger nest provides a maximum age of 13.1 cal kBP for this stencil. While there is some debate around the classification of some boomerang stencils as IIAP motifs (e.g. Lewis 1997), in this case, the stencil pigment was subsequently overpainted by Gwion figures (see Fig. 4-S2) thereby providing further support for the IIAP classification. DR015\_14, interpreted as a snake motif, had a single underlying nest providing a maximum age of 15.1 cal kBP.



**Figure 4-3. Maximum ages for 5 motifs from 6 underlying was nest ages.** Motifs with the three oldest dates are illustrated: (a) is interpreted as a snake, 3 m long, (b) is indeterminate, 1.1 m long, and (c) is a boomerang stencil (overpainted with Gwion then Wanjin motifs) with the illustration showing the interpreted position of the boomerang used to make the stencil (see Fig. S2). Sample locations marked are with a yellow circle. Credits: Photos DF, Illustrations PH

### 4.3.3 Reliability considerations

The 6 nests underlying 5 separate motifs have median ages in the range of 1.2 to 20.4 cal kBP. If all of these motifs are correctly classified as IIAP and the age estimates are all correct, then the youngest age of 1.2 cal kBP (DR006\_09-1) implies at least some IIAP motifs may have been painted relatively recently. At the other extreme, the 18.3 cal kBP age for DR006\_08-1 indicates others may be as much as 17 ka older, in which case motifs in this style may have been painted over almost 17,000 years. Critical to the interpretation of this age interval, however, is the observation that the two youngest nest ages are of comparatively low reliability. The reliability score is particularly important for under-art nests because, as noted earlier, the potential sources of contamination are from more modern carbon. Hence the contamination risk for low reliability score under-art samples is such that the measured nest age may be younger, perhaps much younger, than the true age of construction, so any such results require further scrutiny.

Nest DR006\_09-1, dated to c. 1.2 ka, underlies an animal motif with dotted infill (see Fig. 4-S1). While the dotted infill is not common for IIAP motifs it has other attributes that make its IIAP classification "highly likely". Importantly, the IIAP motif is also superimposed by motifs that belong to the more recent Gwion stylistic period. A Gwion motif (DR006\_03-1) from the same site has a measured minimum age of c. 16.3 ka and ages determined for other Gwion motifs are around 12 cal kBP (Finch et al. 2020). Consequently, either the age of <1.2 ka for DR006\_09-1 is incorrect, or the overlying Gwion motifs must also be anomalously young (< 1.2 ka). The DR006\_09-1 sample comprised a number of small, friable pieces with external surfaces that could not be thoroughly cleaned. As one of the samples processed in the first batch of wasp nests dated in 2016, it also had an early form of chemical pretreatment that may not have removed all contamination (Finch et al. 2019). Both factors contribute to the relatively low Reliability Score of 3 even though the carbon mass dated (40 µg) is above average. The same limitations apply to DR012C\_02-1; although obvious contamination from debris built up behind the nest was removed prior to chemical pretreatment the presence of this debris represents a higher risk of contamination. These, and some other early inconsistent results, led to further experimentation and refinement of both sample selection and processing methods as described elsewhere

(Finch et al. 2019). Consequently, the results from DR006\_09 and DR012C\_02 are considered unreliable and are excluded from subsequent discussion.

The other 3 under-art samples underwent the more advanced pretreatment protocols and are considered more reliable. These nest dates suggest that a boomerang stencil (DR013\_09) is younger than c. 12.8 cal kBP and that a snake motif (DR015\_14) is younger than c. 14.0 ka.

#### 4.3.4 Age bracket for macropod motif

The large IIAP macropod motif, DR015\_10, was painted on the sloping ceiling in a rock shelter housing many thousands of fossilized mud wasp nests (Fig. 4-4). Three nests overlying the motif and a further three nests under the motif were radiocarbon dated with results summarized in Table 4-1 (for details, see Table 4-S1). The six samples were collected in 3 separate field trips in 2015, 2016 and 2017 and underwent pretreatment in 4 different batches at two different laboratories (at the University of Melbourne and ANSTO).

**Table 4-1. Calibrated radiocarbon ages for macropod motif DR015\_10**

Sample Code	Laboratory Code	Fraction	Nest Age cal BP (95.4% probability)		Reliability Score	Over/Under Pigment
			Range	Median		
DR015_10-7	OZW379	Light	5590 - 5050	5,380	2	Over
DR015_10-7	OZW380	Heavy	12740 - 12440	12,650	4	Over
DR015_10-3	OZW365	All	13570 - 13280	13,430	7	Over
DR015_10-2	OZU779U1	Light	17570 - 16870	17,230	9	Over
DR015_10-2	OZU779U2	Heavy	17790 - 17160	17,480	8	Over
DR015_10-1	OZT479U*	All	17450 - 16790	17,130	4	Under
DR015_10-4	OZW366	All	18970 - 18590	18,790	8	Under
DR015_10-6	OZW376	All	20980 - 20320	20,650	7	Under





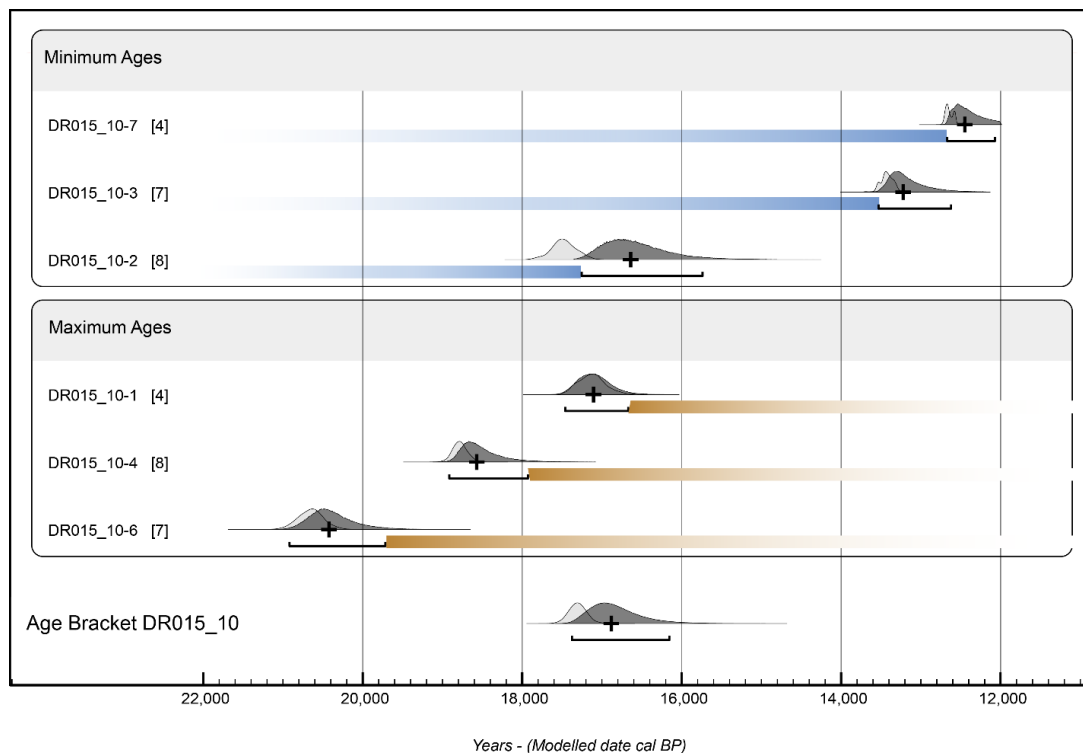
**Figure 4-4. Macropod motif DR015\_10 dated to c. 17,300 years.** Showing (a) upper part of Site DRY015 with (b) the location of motif 10 on the ceiling as indicated by the arrow, (c) composite image of macropod motif from 39 photographs, and (d) motif illustration in same orientation as (c). The motif is c. 2 metres long. See Fig.4-S3 for sample locations and images. Credits: Photos DF, Illustration PH.

Two samples (10-7 and 10-2) were sufficiently large to use heavy liquid separation to produce “light” (density  $<2.2 \text{ g/cm}^3$ ) and “heavy” fractions ( $>2.2 \text{ g/cm}^3$ ) (see Finch et al. (2019) for details and rationale) both of which contained enough carbon for AMS measurement (Table 4-1). The ages determined for the two fractions of DR015\_10-2 have high reliability scores and are both close to 17 cal kBP. The age on the heavy fraction of

17.8 – 17.2 cal kBP (95.4% probability) provides a minimum age constraint of c. 17.2 cal kBP for the underlying painting (taking the youngest limit of the 95.4% probability range). However, the two fractions for sample DR015\_10-7 are of very different ages (Light at c. 5.4 cal kBP and Heavy at 12.7 cal kBP) with lower reliability scores of 2 and 4. The outer surfaces of this sample were too small to be removed prior to chemical pretreatment so the young age for the light fraction most likely reflects the inclusion of more modern carbon in the mineral accretion coating the nest. This fraction also has an extremely low carbon mass (11µg) so even a tiny amount of modern carbon contamination will significantly reduce the measured age.

The age of the oldest over-art nest (10-2) fraction implies the motif is older than c. 17.2 cal kBP and the age of the youngest under-art nest, DR015\_10-1, (17.5 – 16.8 cal kBP) implies it is younger than c. 17.5 cal kBP. While DR015\_10-1 has a mid-range RS of 4 reflecting the less than ideal pretreatment, the higher than average carbon mass dated (37µg) means that it is somewhat less susceptible to significant contamination and is therefore difficult to discount. The possible age range for the motif, modelled using OxCal radiocarbon calibration software (Bronk Ramsey 2009b, 2009a) (Fig. 4-5, light gray probability distribution graphs), is in the range 17.5 – 17.1 cal kBP with a median value of 17.3 cal kBP (95.4% probability range).

It has been shown that charcoal incorporated into mud wasp nests may have a not-insignificant inherited or inbuilt age at the time of construction but, in our research area, the mean inbuilt age based on studies of modern nests is determined to be ~255 years (Finch et al. 2019). The effects of any possible contamination of this kind can be accommodated when calculating the possible age range for this motif (see Finch et al. (2020) and 4.7.4). Applying a correction for an inbuilt charcoal age of this magnitude reduces the possible age of motif DR015\_10 to be in the range 17.4 – 16.2 cal kBP with a median of 16.9 cal kBP (95.4% probability) (Fig. 4-5, dark gray probability distribution graph). However, based on the analysis of modern wasp nests (Finch et al. 2019), the uncorrected age bracket is likely to be more accurate.



**Figure 4-5. Calibrated ages for 6 nests used to constrain an age range for motif DR015\_10.** Light and dark gray probability distribution graphs for each sample illustrate (i) the calibrated age range determined for the nest and (ii) the effect of the correction on that distribution for any potential inbuilt charcoal age, respectively. The bar under the dark gray curve shows the 95.4% probability range and the cross marks the median of the corrected distribution. The coloured horizontal bars, starting just beyond the 95.4% range (for clarity), show the possible age range for the motif. That is, art painted over the nest must be younger than the age of the nest (brown bars) and art underlying the nest must be at least as old as the nest (blue bars). The Age Bracket (lower graph) is constrained by nests underlying and overlying the motif and has been modelled using OxCal (v4.3.2 (Bronk Ramsey 2017a); r:5 SHCal13 atmospheric curve (Hogg et al. 2013)) using the software code listed in 4.7.4.

#### 4.4 Hypothesised IIAP age range

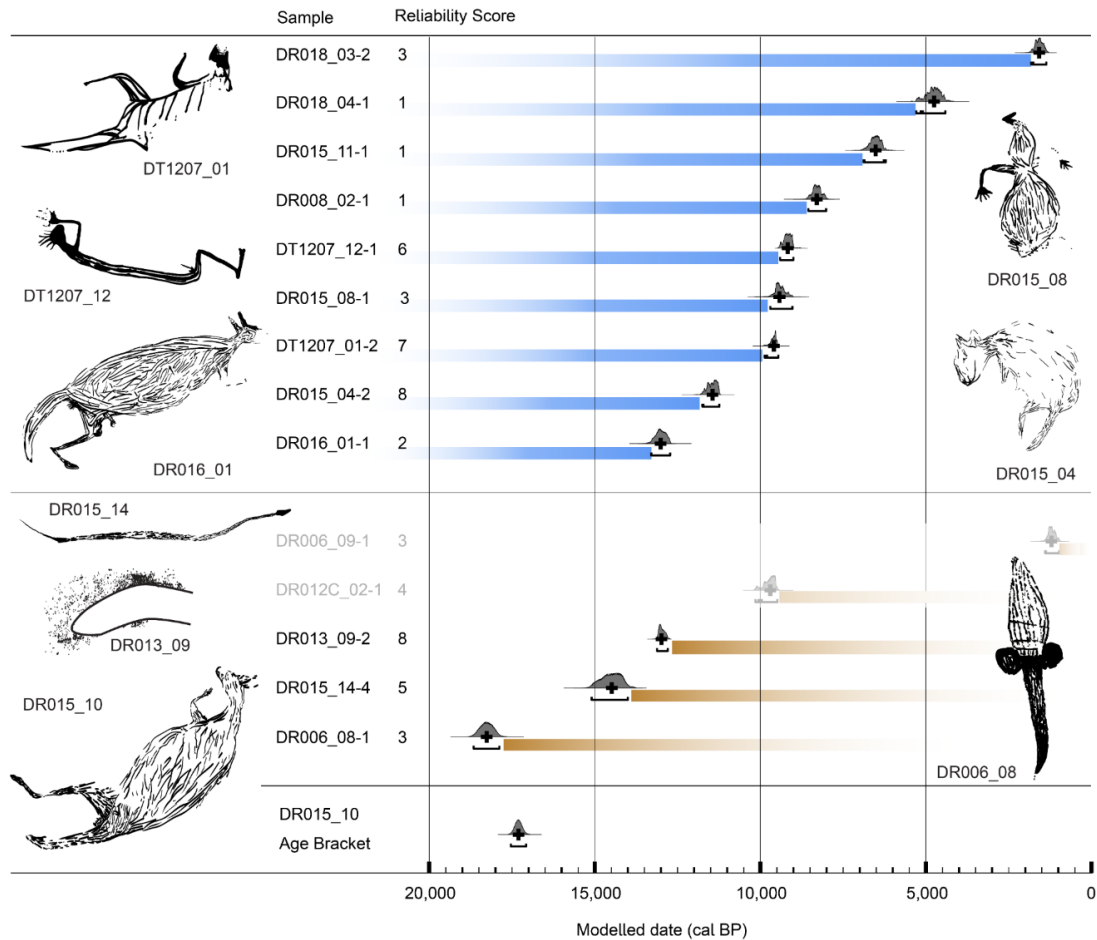
Ultimately, the aim of the rock art dating program is to determine the age distribution for the different Kimberley styles described from numerous superimposition sequences and for sub-styles less amenable to superimposition analysis. In the case of the Gwion style, even with just 24 ages on wasp nests over or under 21 different motifs it was possible to justify an initial hypothesis that paintings in this style proliferated around 12,000 years ago (Finch et al. 2020). The age distribution for all but two nests associated with Gwion motifs revealed that 15 over-art nests are younger than c. 12 ka and do not overlap with ages of 6 under-art nests that are all older than c. 13 ka (Finch et al. 2020). In contrast, the results

presented here, for IIAP motifs, do not support a similar, relatively short period of proliferation. The overlapping ages between over- and under-art nest ages (Fig. 4-6) are more consistent with production over an extended period, as argued below.

The method developed to infer the chronology of rock art stylistic periods from maximum and minimum age constraints is described elsewhere (Finch et al. 2020). An estimate for the extent of the art period is provided by the period between the age of the oldest over-art nest and the age of the youngest under-art nest (Finch et al. 2020). Therefore, these data suggest that IIAP motifs were produced over the timespan from, at least, 17.2 to 13.1 cal kBP (using 95.4% probability ranges for calibrated age measurements).

This analysis, however, does not take into account the fact that some of the over-art and under-art nests relate to the same motif, DR015-10. The additional evidence provided by the age bracket for this macropod motif (17.5 – 17.1 cal kBP with a median age of 17.3 cal kBP (95.4% probability)) strongly supports a starting age of 17.2 cal kBP for the IIAP, at the latest. The end date of 13.1 ka is derived from the maximum age of the boomerang stencil DR013\_09. In his first major publication on Kimberley rock art, Walsh (1994) argues that some boomerang stencils are appropriately classified as IIAP motifs based on observed superimpositions of such motifs by tasselled human figures, generally accepted as the earliest of the Gwion style variants (Welch 1993, Walsh 2000). Lewis (1997) disputed this classification, arguing that boomerang stencils were more likely to be contemporary with Gwion figures. Walsh (2000, Plates 142 and 353/4) subsequently published two further examples of tasselled Gwion motifs painted over boomerang stencils to support his inclusion of some boomerang stencils as IIAP motifs. The stencil DR013\_09 is another example that is overpainted by tassel Gwion motifs (see Fig. 4-S2) and, as such, supports Walsh's argument. Nonetheless, the results so far are not definitive for all boomerang stencils. It is still possible that boomerang stencils are younger than other IIAP motifs and closer in age to Gwion motifs, but further dates are required to resolve the absolute chronology. If the DR013\_09 stencil was not accepted as an IIAP motif then the estimated age range for the IIAP period would be reduced to 17.2 to 15.1 cal kBP.





**Figure 4-6. Age constraints for IIAP motifs.** The top panel summarises the ages of nests that have been constructed over IIAP artwork. Thus, the ages of the IIAP motifs must be older (blue bars). The middle panel shows the ages of nests underlying IIAP motifs thereby requiring the artwork to be younger than the nest age (brown bars). The bottom panel identifies the age bracket derived from ages of three overlying and three underlying wasp nests from the single macropod motif DR015\_10. For motifs with more than one nest dated, the oldest over-art nest age and/or the youngest under-art nest age are used. Illustrations: PH

## 4.5 Conclusions

Kimberley IIAP motifs share similar stylistic characteristics (parsimonious infill, colour of pigment, anatomical detail, close to life-size figures) with naturalistic animal motifs elsewhere in the world (Aubert et al. 2014, Tacon et al. 2014, Hodgson and Watson 2015, Hodgson and Pettitt 2018). Of the motifs that have been radiometrically dated, there is a very wide spread of ages from less than 5,000 years (e.g. in China (Tacon et al. 2016)), to the oldest dated figurative motifs from the Southeast Asian islands of Sulawesi (a pig motif, painted before 44 ka (Aubert et al. 2019)) and Borneo (an unidentified animal, older than 40 ka (Aubert et al. 2018)). Ages determined for

similar European (mostly Franco-Cantabrian) figurative motifs suggest some may be as old as 35 ka but the directly dated charcoal drawings at Chauvet range in age from 34 – 29 ka (Quiles et al. 2016) and throughout the period from 33 to 12 ka more generally in the region (Pike et al. 2012, Pettitt and Bahn 2015).

The age estimates for 27 mud wasp nests in contact with 16 different rock paintings of the Kimberley IIAP style suggest these motifs were painted between 17.2 and 13.1 cal kBP. The age of one IIAP macropod motif is well-constrained by six radiocarbon dates on three overlying and three underlying wasp nests to be between 17.5 and 17.1 cal kBP, corresponding to the middle of the age range for the European figurative motifs.

This is a period when sea levels in the nearby Joseph Bonaparte Gulf began to rise from a low of ~125m below present sea levels during the Last Glacial Maximum (LGM) ( $21\pm3$  ka) but mostly before the rapid rise in sea levels between 14.6 and 8 ka (Meltwater Pulse 1a) (Williams et al. 2018) (see Fig. 4-1). By 12 ka, the coastline to the north-west had advanced by around 300 km over the continental shelf toward the area in which our study was undertaken. Many generations of Kimberley coastal Aboriginal populations experienced continuing loss of territory over these millennia. At around the same time, from 14 to 13 ka, a paleoenvironmental record from a nearby mound spring and other Kimberley climate proxies indicate an improving climate with an increase in monsoonal activity and precipitation (Field et al. 2017). It was just after this time, 12,000 years ago, that paintings in the Gwion style proliferated in the northern Kimberley (Finch et al. 2020). The dominant subjects in IIAP paintings are animals and, to a lesser degree, plants. This was replaced by an almost complete focus on decorated human figures during the Gwion period (Ouzman et al. 2017, Veth et al. 2017). The coincidence between these marked changes in painted rock art styles and prevailing environmental conditions suggests that the shift from the IIAP to the Gwion period may reflect social and cultural changes in the region. For example, the change in the style of artwork may have been a response to increasing territoriality and population growth supported by an improving climate (Williams et al. 2018).

These first Pleistocene ages for naturalistic animal motifs from the earliest known period of Australian rock painting position this creative human activity at the end of

the Last Glacial Maximum. The initial results from 8 rock art sites in the north-eastern Kimberley suggest an extended period for the Irregular Infill Animal style, from 17,000 to 13,000 years ago. Many more dates from this period are required before the full chronological extent of the paintings still visible today can be determined. For now, a robustly dated, c. 17,300-year-old painting of a kangaroo is the oldest *in situ* rock painting radiometrically dated in Australia.

## **4.6 Acknowledgements:**

We acknowledge and thank the Balanggarra Aboriginal Corporation, Rangers and Traditional Owners for permission to work on their Country and for their support during fieldwork. In particular, we thank Augustine Unghango and family, the Waina family, and A Chalarimeri. Fieldwork support was provided by S Bradley, P Hartley, N Sundblom, R Maher, T Tan, M Maier and P Kendrick. The sites we visited were relocated and recorded over decades by Dunkeld Pastoral Co Pty Ltd and the Kimberley Visions Survey teams, J Schmiechen, and the late G Walsh. Radiocarbon measurements and laboratory support from the Australian Nuclear Science and Technology Organisation (ANSTO) was provided by A Williams, F Bertuch and B Yang. Financial support for the Centre for Accelerator Science at ANSTO was provided by the Australian National Collaborative Research Infrastructure Strategy. DF thanks AINSE Ltd for providing financial assistance through a Post Graduate Research Award to enable work on the radiocarbon analyses.

### **4.6.1 Funding**

This research was funded by an Australian Research Council Linkage Projects LP130100501 and LP170100155 with funding partners the Kimberley Foundation Australia, with in-kind support from Dunkeld Pastoral Co Pty Ltd and Balanggarra Aboriginal Corporation especially for fieldwork. DF is supported by an Australian Postgraduate Award. The Kimberley Foundation Australia also provided a grant to DF to establish the radiocarbon pretreatment facility at the University of Melbourne.

### **4.6.2 Authors contributions:**

This research is part of the multi-disciplinary Kimberley Rock Art Dating project conceived and led by AG who, with JH, supervised this work as part of DF's PhD research project. Motif classification was by PH and CM. DF collected and pretreated the samples, designed, and performed the experiments, and analysed and interpreted the results. Fieldwork was carried out by DF, PH, SH, SO, PV, CM, AG and HG. Illustrations were drawn by PH. Radiocarbon measurements and initial data reduction were performed by VL. DF wrote the manuscript draft with key editing from JH and AG with further input from all authors.

**Competing interests:** The authors declare that they have no competing interests.

#### **4.6.3 Data and materials availability**

All data is available in the manuscript or the supplementary materials and two earlier publications (Finch et al. 2019, Finch et al. 2020). At the request of Balangarra Aboriginal Traditional Owners of the land where the samples were collected, the data does not include exact locations of rock art sites.

## **4.7 Methods:**

The methodology developed to radiocarbon date mud wasp nests is described in Finch et al. (2019). Methods developed to derive estimates for the age of rock art stylistic periods are described in Finch et al. (2020). The following sections provide specific detail for the IIAP motifs.

### **4.7.1 Sample Collection**

Mud wasp nest samples related to IIAP paintings were collected between 2015 and 2017 from 8 rock art sites up to 16 km apart in the Drysdale River National Park, an area known to be particularly rich in IIAP paintings (Welch 2015). Sampling was approved on site with the consent and participation of local Traditional Owners and under research permits from the Kimberley Land Council/ Balanggarra Aboriginal Corporation, the Western Australian Department of Biodiversity and Attractions and Department of Planning Lands and Heritage (Section 16 Permits 558, 567). The Balanggarra Traditional Owners have requested that the site locations are not disclosed here but locations have been fully documented in an access-controlled database (Green et al. 2017b).

### **4.7.2 Motif Classification**

The subject matter of most IIAP motifs, such as macropods and plants, also appear in later stylistic periods of the Kimberley rock art sequence. The classification of a motif as IIAP requires familiarity with the sometimes-subtle differences in the way such subjects are depicted in different periods. Given the subjective nature of the classification process, the most experienced researchers of Kimberley rock art can be expected to provide the most accurate classifications. The motif classifications reported here (Table 4-S2) were determined by P.H. and C.M. whose qualifications are described elsewhere (Finch et al. 2020). Only motifs "Highly Likely" or "Certain" to belong to the IIAP are reported here.

### **4.7.3 Sample Preparation and Age Measurement**

Initially, mud wasp nest samples underwent all stages of pretreatment using the Australian Nuclear Science and Technology Organisation (ANSTO) Radiocarbon Chemistry laboratory (Laboratory Codes in the range OZT448 to OZT801).

Subsequently, samples with Laboratory Codes from OZU777 to OZW417 underwent physical pretreatment and part of the chemical pretreatment at the University of Melbourne. Complete details of the pretreatment methods are described elsewhere (Finch et al. 2019) but, in short, after mechanical cleaning, where possible, samples were ground before undergoing a version of the acid-base-acid (ABA) charcoal pretreatment protocol. Heavy liquid separation (HLS) was used on some of the larger samples to create fractions labelled as "Light" (density < ~2.0 g/cm<sup>3</sup>) and "Heavy" (density > ~2.0 g/cm<sup>3</sup>) in Table 4-S1. Fractions labelled as "All" did not undergo HLS. All sample combustion and graphitisation was carried out at ANSTO. All samples were measured using the 10MV ANTARES (Australian National Tandem Research Accelerator) or 2MV STAR (Small Tandem for Applied Research) AMS at ANSTO. All radiocarbon ages were calibrated using SHCal13 (Hogg et al. 2013) in OxCal v4.3.2 (Bronk Ramsey 2009a)

#### 4.7.4 Statistical Model and Code

The radiocarbon calibration program, OxCal (version 4.3, SHCal13) was used to calibrate all carbon isotope measurements (Bronk Ramsey 2009a, Bronk Ramsey 2009b, Hogg et al. 2013). The software code used to generate Fig. 4-5 is listed below:

```
Options()
{ Resolution=10;
  Curve="SHCal13.14c";
  BCAD=FALSE; };
Plot()
{Outlier_Model("Charcoal",Exp(255,-4000,0));
  Combine("DR015_10")
  {Before("Minimum Ages")
    {R_Date("DR015_10-7_[4]", 10730, 70){Outlier("Charcoal",1);};
    R_Date("DR015_10-3_[7]", 11640, 80){Outlier("Charcoal",1);};
    R_Date("DR015_10-2_[8]", 14390, 100){Outlier("Charcoal",1);};};
  After("Maximum Ages")
    {R_Date("DR015_10-1_[4]", 14130, 100){Outlier("Charcoal", 1);};
    R_Date("DR015_10-4_[8]", 15570, 90){Outlier("Charcoal", 1);};
    R_Date("DR015_10-6_[7]", 17160, 120){Outlier("Charcoal", 1);};};
  }; }
```

The software code used in OxCal to generate Fig. 4-6 is:

```
Options()
{ Curve="SHCal13.14c";
  BCAD=FALSE; };
Plot()
{Sum("Minimum Ages")
{BEFORE() { R_DATE("DR018_03-2 [3] Min", 1713, 98); };
BEFORE() { R_DATE("DR018_04-1 [1] Min", 4264, 149); };
BEFORE() { R_DATE("DR015_11-1 [1] Min", 5750, 145); };
BEFORE() { R_DATE("DR008_02-1 [1] Min", 7535, 138); };
BEFORE() { R_DATE("DT1207_12-1 [6] Min", 8243, 76); };
BEFORE() { R_DATE("DR015_08-1 [3] Min", 8484, 135); };
BEFORE() { R_DATE("DT1207_01-2 [7] Min", 8645, 75); };
BEFORE() { R_DATE("DR015_04-2 [8] Min", 10011, 70); };
BEFORE() { R_DATE("DR016_01-1 [2] Min", 11201, 157); };
BEFORE() { R_DATE("DR015_10-2 [8] Min", 14392, 96); };
};
line();
Sum("Maximum Ages")
{ AFTER() { R_DATE("DR013_09-2 [8] Max", 11172, 71); };
AFTER() { R_DATE("DR015_14-4 [5] Max", 12415, 146); };
AFTER() { R_DATE("DR015_10-1 [4] Max", 14126, 88); };
AFTER() { R_DATE("DR006_08-1 [3] Max", 15070, 171); };
};
};
```



## 4.8 Supplementary Information

- All Figures exclude the result for sample DR006\_05-1 as it returned a modern age and therefore provides no useful constraint on the age of the motif.

**Table 4-S1. Radiocarbon age measurements on wasp nests associated with IIAP motifs.**

Sample Code	Laboratory Code	Pretreatment sequence	Fraction	C mass (µg)	Conventional Radiocarbon Age		Calibrated age (cal BP, 95.4% probability range)			R S
					years BP	± 1σ error	From (yrs)	To (yrs)	% of range	
DR006_05-1	OZT801U2	ABA - HLS	Light	18	-		280 150	210 ...	16.8 78.6	2
DR006_08-1	OZT453x	ABA	All	26	15,070	180	18670	17870	95.4	3
DR006_09-1	OZT769U*	ABA	All	40	1,350	110	1410 1380	1390 970	0.6 94.8	3
DR008_02-1	OZT458	ABA	All	17	7,540	140	8560	8010	95.4	1
DR012C_02-1	OZT795U*	ABA	All	33	8,720	110	10150 9960	9980 9480	8.3 87.2	4
DR013_09-1	OZT797U2	ABA - HLS	Light	110	16,930	100	20640	20070	95.4	7
DR013_09-2	OZU777U2	A-HLS-BA(8M)	Heavy	40	11,170	80	13130	12790	95.4	8
DR015_04-1	OZT448U1	ABA - HLS	Light	18	6,440	680	8960 8870 8780 5790	8920 8830 5890 5760	0.2 0.2 94.9 0.1	1
DR015_04-2	OZU778U2	A-HLS-BA(8M)	Heavy	51	10,010	80	11750 11720	11730 11230	0.6 94.8	8
DR015_08-1	OZT449	ABA	All	14	8,480	140	9710	9030	95.4	3
DR015_10-1	OZT479U*	ABA	All	37	14,130	100	17450	16790	95.4	4
DR015_10-2	OZU779U2	A-HLS-BA(8M)	Heavy	47	14,390	100	17790	17160	95.4	8
DR015_10-3	OZW365	ABA(8M)	All	31	11,640	80	13570	13280	95.4	7
DR015_10-4	OZW366	ABA(8M)	All	46	15,570	90	18970	18590	95.4	8
DR015_10-6	OZW376	ABA(8M)	All	35	17,160	120	20980	20320	95.4	7
DR015_10-7	OZW380	A-HLS-BA(8M)	Heavy	33	10,730	70	12740 12470	12540 12440	92.6 2.8	4
DR015_11-1	OZT480	ABA	All	12	5,750	150	6890 6250	6260 6210	94.2 1.2	1
DR015_14-4	OZU780U1	A-HLS-BA(8M)	Light	11	12,420	150	15100	13990	95.4	5
DR016_01-1	OZT495	ABA	All	18	11,200	160	13300	12720	95.4	2
DR016_01-2	OZT451	ABA	All	19	3,940	120	4800 4690 4650	4760 4670 3970	1.5 0.3 93.6	2
DR016_01-3	OZT496	ABA	All	23	10,100	150	12370 12270 12110	12340 12220 11200	0.5 0.8 94.1	3
DR016_01-5	OZW375	ABA(8M)	All	42	8,440	70	9540	9250	95.4	6
DR018_03-2	OZT494	ABA	All	35	1,710	100	1830	1360	95.4	3
DR018_04-1	OZT768U*	ABA	All	14	4,260	150	5290	4410	95.4	1
DT1207_01-1	OZW383	A-HLS-BA(8M)	Heavy	21	6,870	70	7830	7570	95.4	6
DT1207_01-2	OZW417U2	A-HLS-BA(16M)	Heavy	39	8,650	80	9890 9820	9840 9460	1.0 94.4	7
DT1207_12-1	OZW389	A-HLS-BA(8M)	Heavy	22	8,240	80	9410	9000	95.4	6

The Sample Code is constructed from a short site identifier, a number to identify the motif and the number of the sample collected, in the format “SITE\_MOTIF-NEST”. For a complete description of the Pretreatment Sequence, Fractions, and Reliability Score (RS) refer Finch et al. (2019). The  $\delta^{13}\text{C}$  of DR013\_09-1 was measured to be -22.5‰ but all other samples contained too little carbon for this ratio to be measured directly. The typical charcoal value for  $\delta^{13}\text{C}$  (-25 ‰) was assumed for all other samples. Calibrated using SHCal13 (Hogg et al. 2013) in OxCal v4.3.2. (Bronk Ramsey 2009a)

**Table 4-S2. Stylistic classification of motifs associated with wasp nest samples**

Sample Code	Median age calBP (years)	Over/ Under Pigment	Reliability Score	Confidence in motif classification	
				PH	CM
DR006_05-1	90	Over	2	Certain	Highly likely
DR008_02-1	8,300	Over	1	Certain	Certain
DR015_04-1	7,280	Over	1	Certain	Certain
DR015_04-2	11,440	Over	8	Certain	Certain
DR015_08-1	9,420	Over	3	Certain	Certain
DR015_11-1	6,520	Over	1	Certain	Certain
DR016_01-1	13,010	Over	2	Certain	Certain
DR016_01-2	4,320	Over	2	Certain	Certain
DR016_01-3	11,630	Over	3	Certain	Certain
DR016_01-5	9,420	Over	6	Certain	Certain
DR018_03-2	1,580	Over	3	Certain	Certain
DR018_04-1	4,760	Over	1	Certain	Certain
DT1207_01-1	7,670	Over	6	Certain	Highly likely
DT1207_01-2	9,590	Over	7	Certain	Highly likely
DT1207_12-1	9,170	Over	6	Certain	Highly likely
DR006_08-1	18,260	Under	3	Certain	Highly likely
DR006_09-1	1,210	Under	3	Highly likely	Highly likely
DR012C_02-1	9,700	Under	4	Certain	Highly likely
DR013_09-1	20,370	Under	7	Certain	Certain
DR013_09-2	12,990	Under	8	Certain	Certain
DR015_14-4	14,490	Under	5	Certain	Highly likely

“Over/ Under Pigment” indicates the nest sample was respectively, either over or under the motif. The confidence level in the expert identification of motifs as of the IIAP style is listed in the two columns on the right side. DR015\_10 was classed as a "Certain" IIAP motif by both PH and CM.

**DR006\_05-1**

Minimum Age

Nest Age (95.4% cal BP)

From	To	%
280	210	16.8
150	...	78.6

Median (cal BP): 90

Reliability Score 2

**DR013\_09-2**

Maximum Age

Nest Age (95.4% cal BP)

From	To	%
13130	12790	95.4

Median (cal BP): 12,990

Reliability Score 8

**DR006\_09-1**

Maximum Age

Nest Age (95.4% cal BP)

From	To	%
1410	1390	0.6
1380	970	94.8

Median (cal BP): 1,210

Reliability Score 3

**DR015\_04-1**

Minimum Age

Nest Age (95.4% cal BP)

From	To	%
8960	8920	0.2
8870	8830	0.2
8780	5890	94.9
5790	5760	0.1

Median (cal BP): 7,280

Reliability Score 1

**DR008\_02-1**

Minimum Age

Nest Age (95.4% cal BP)

From	To	%
8560	8010	95.4

Median (cal BP): 8,300

Reliability Score 1

**DR015\_04-2**

Minimum Age

Nest Age (95.4% cal BP)

From	To	%
11750	11730	0.6
11720	11230	94.8

Median (cal BP): 11,440

Reliability Score 8

**DR012C\_02-1**

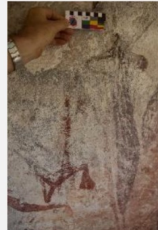
Maximum Age

Nest Age (95.4% cal BP)

From	To	%
10150	9980	8.3
9960	9480	87.2

Median (cal BP): 9,700

Reliability Score 4

**DR015\_08-1**

Minimum Age

Nest Age (95.4% cal BP)

From	To	%
9710	9030	95.4

Median (cal BP): 9,420

Reliability Score 3

**DR013\_09-1**

Maximum Age

Nest Age (95.4% cal BP)

From	To	%
20640	20070	95.4

Median (cal BP): 20,370

Reliability Score 7

**DR015\_11-1**

Minimum Age











Nest Age (95.4% cal BP)

From	To	%
6890	6260	94.2
6250	6210	1.2

Median (cal BP): 6,520

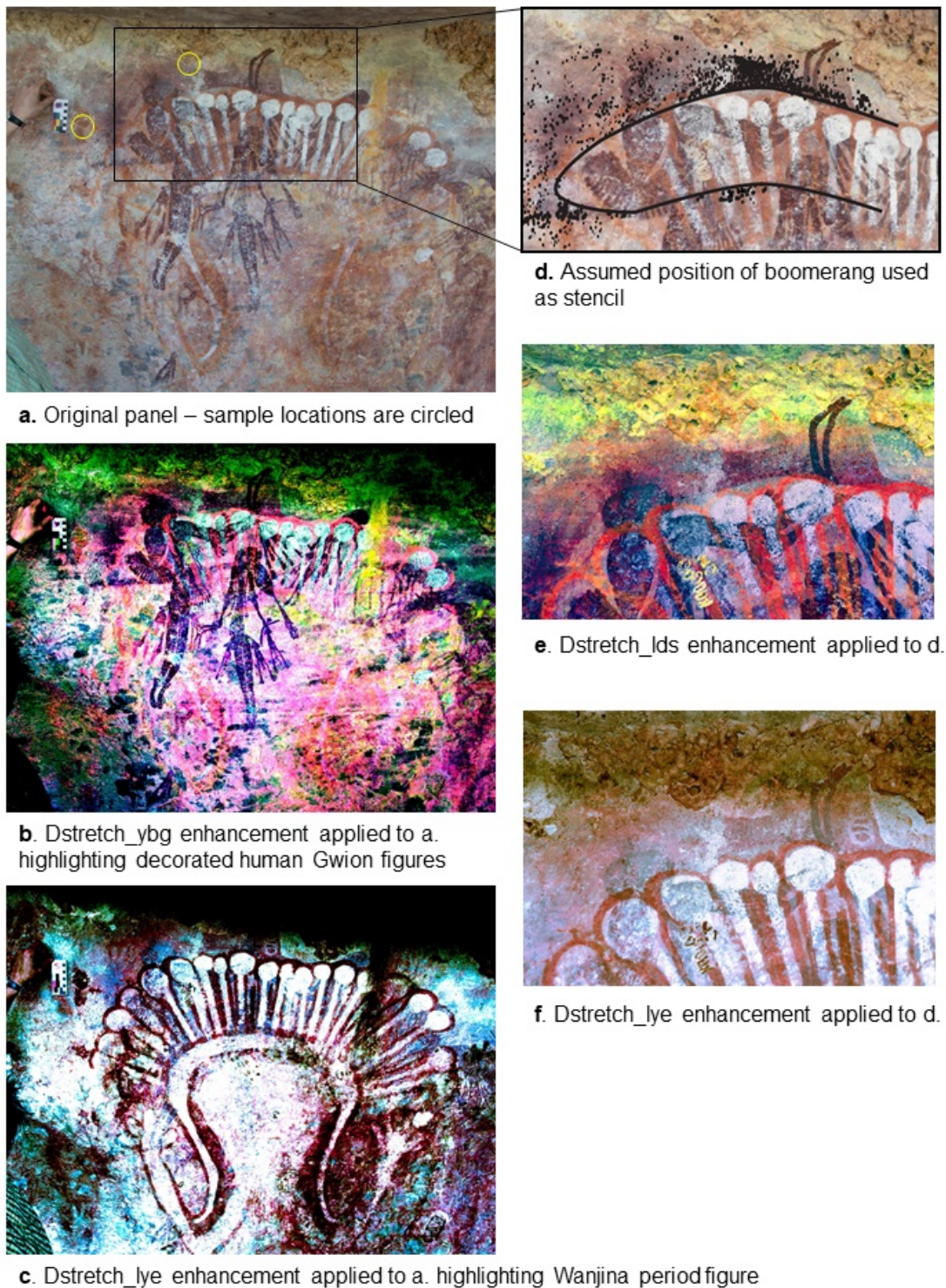
Reliability Score 1



<b>DR015_14-4</b> Maximum Age Nest Age (95.4% cal BP) From To % 15100 13990 95.4  Median (cal BP): 14,490 Reliability Score 5		<b>DR018_03-2</b> Minimum Age Nest Age (95.4% cal BP) From To % 1830 1360 95.4  Median (cal BP): 1,580 Reliability Score 3	
<b>DR016_01-1</b> Minimum Age Nest Age (95.4% cal BP) From To % 13300 12720 95.4  Median (cal BP): 13,010 Reliability Score 2		<b>DR018_04-1</b> Minimum Age Nest Age (95.4% cal BP) From To % 5290 4410 95.4  Median (cal BP): 4,760 Reliability Score 1	
<b>DR016_01-2</b> Minimum Age Nest Age (95.4% cal BP) From To % 4800 4760 1.5 4690 4670 0.3 4650 3970 93.6  Median (cal BP): 4,320 Reliability Score 2		<b>DT1207_01-1</b> Minimum Age Nest Age (95.4% cal BP) From To % 7830 7570 95.4  Median (cal BP): 7,670 Reliability Score 6	
<b>DR016_01-3</b> Minimum Age Nest Age (95.4% cal BP) From To % 12370 12340 0.5 12270 12220 0.8 12110 11200 94.1  Median (cal BP): 11,630 Reliability Score 3		<b>DT1207_01-2</b> Minimum Age Nest Age (95.4% cal BP) From To % 9890 9840 1 9820 9460 94.4  Median (cal BP): 9,590 Reliability Score 7	
<b>DR016_01-5</b> Minimum Age Nest Age (95.4% cal BP) From To % 9540 9250 95.4  Median (cal BP): 9,420 Reliability Score 6		<b>DT1207_12-1</b> Minimum Age Nest Age (95.4% cal BP) From To % 9410 9000 95.4  Median (cal BP): 9,170 Reliability Score 6	

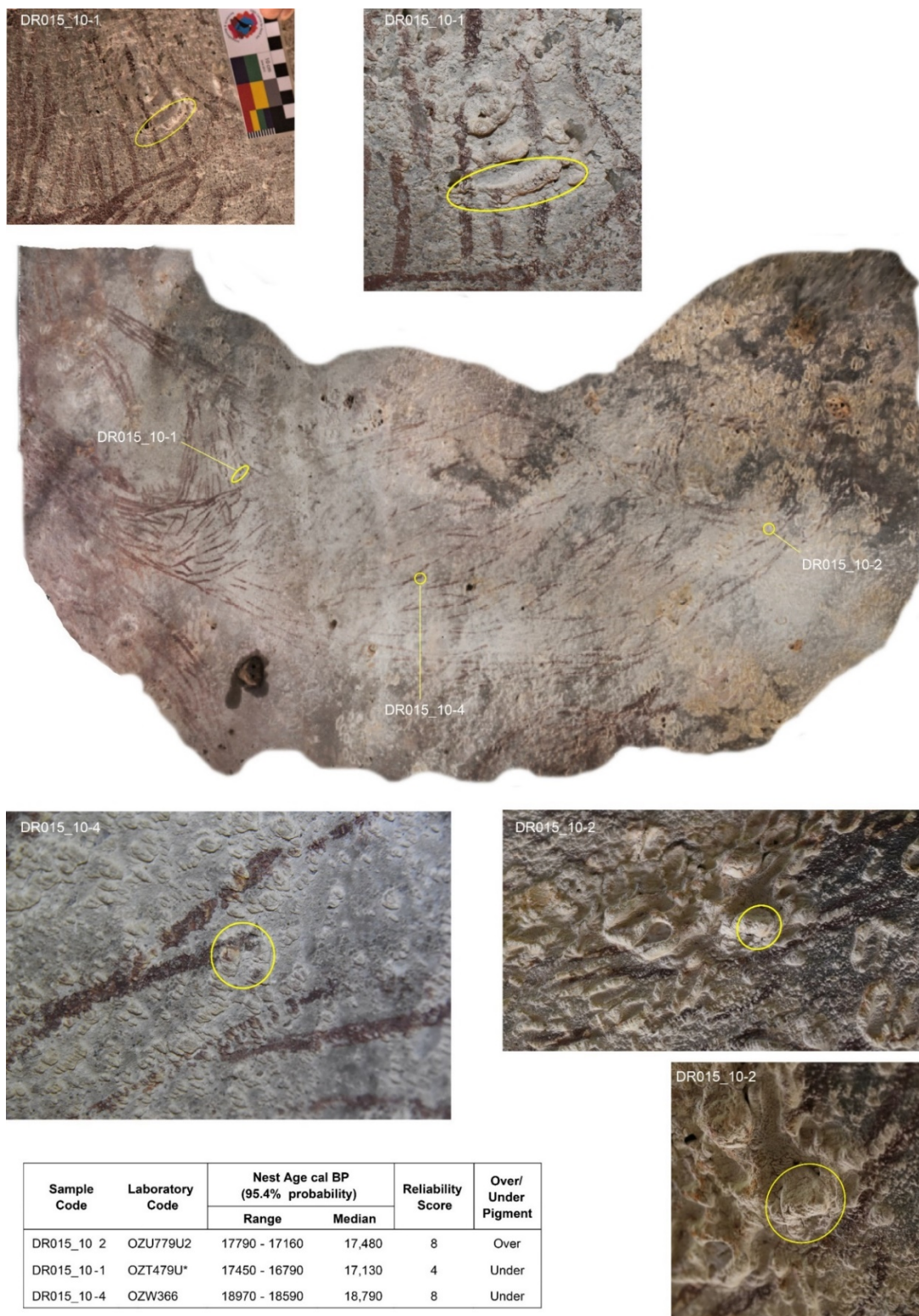
**Figure 4-S1. Dated IIAP motifs (excluding DR015\_10)**





**Figure 4-S2. Context for boomerang stencil motif DR013-09**(a) shows the original photograph. (b) and (c) are D Stretch (Harman 2005, Harman 2020) enhanced, false colour versions of the same photograph to highlight the superimposed paintings over the boomerang stencil. (d) illustrates the assumed position of the boomerang stencil with enhancements applied in (e) and (f).





**Figure 4-S3. Macropod motif DR015\_10 sample locations.**

Wasp nest locations and sample images, prior to sampling, for the oldest over-art sample and the two youngest under-art samples.

## 4.9 References

- Aubert, M., A. Brumm, M. Ramli, T. Sutikna, E. W. Saptomo, B. Hakim, M. J. Morwood, G. D. van den Bergh, L. Kinsley and A. Dosseto (2014). "Pleistocene cave art from Sulawesi, Indonesia." Nature **514**(7521): 223-227.
- Aubert, M., A. Brumm and P. S. C. Taçon (2017). "The Timing and Nature of Human Colonization of Southeast Asia in the Late Pleistocene: A Rock Art Perspective." Current Anthropology **58**(0): S553-S566.
- Aubert, M., R. Lebe, A. A. Oktaviana, M. Tang, B. Burhan, Hamrullah, A. Jusdi, A. B. Hakim, B. Hakim, J. X. Zhao, I. M. Geria, P. H. Sulistyarto, R. Sardi and A. Brumm (2019). "Earliest hunting scene in prehistoric art." Nature **576**(7787): 442-+.
- Aubert, M., P. Setiawan, A. A. Oktaviana, A. Brumm, P. H. Sulistyarto, E. W. Saptomo, B. Istiawan, T. A. Ma'rifat, V. N. Wahyuono, F. T. Atmoko, J. X. Zhao, J. Huntley, P. S. C. Tacon, D. L. Howard and H. E. A. Brand (2018). "Palaeolithic cave art in Borneo." Nature **564**(7735): 254-+.
- Bronk Ramsey, C. (2009a). "Bayesian analysis of radiocarbon dates." Radiocarbon **51**(1): 337-360.
- Bronk Ramsey, C. (2009b). "Dealing with outliers and offsets in radiocarbon dating." Radiocarbon **51**(3): 1023-1045.
- Bronk Ramsey, C. (2017). "Methods for Summarizing Radiocarbon Datasets." Radiocarbon: 1-25.
- Chaloupka, G. (1993). Journey in time: the 50,000-year story of the Australian Aboriginal rock art of Arnhem Land. Sydney, Reed New Holland.
- Chippindale, C. and P. S. C. Tacon (1998). The many ways of dating Arnhem Land rock-art, north Australia. The Archaeology of Rock-Art. C. Chippindale and P. S. C. Tacon. Cambridge, Cambridge University Press: 90-111.
- Clarkson, C., Z. Jacobs, B. Marwick, R. Fullagar, L. Wallis, M. Smith, R. G. Roberts, E. Hayes, K. Lowe, X. Carah, S. A. Florin, J. McNeil, D. Cox, L. J. Arnold, Q. Hua, J. Huntley, H. E. A. Brand, T. Manne, A. Fairbairn, J. Shulmeister, L. Lyle, M. Salinas, M. Page, K. Connell, G. Park, K. Norman, T. Murphy and C. Pardoe (2017). "Human occupation of northern Australia by 65,000 years ago." Nature **547**(7663): 306-310.
- David, B., B. Barker, F. Petchey, J.-J. Delannoy, J.-M. Geneste, C. Rowe, M. Eccleston, L. Lamb and R. Wheat (2012). "A 28,000 year old excavated painted rock from Nawarla Gabarnmang, northern Australia." Journal of Archaeological Science.



Field, E., H. A. McGowan, P. T. Moss and S. K. Marx (2017). "A late Quaternary record of monsoon variability in the northwest Kimberley, Australia." Quaternary International **449**: 119-135.

Finch, D., A. Gleadow, J. Hergt, V. A. Levchenko and D. Fink (2019). "New developments in the radiocarbon dating of mud wasp nests." Quaternary Geochronology **51**: 140-154.

Finch, D., A. Gleadow, J. Hergt, V. A. Levchenko, P. Heaney, P. Veth, S. Harper, S. Ouzman, C. Myers and H. Green (2020). "12,000-Year-old Aboriginal rock art from the Kimberley region, Western Australia." Science Advances **6**(6): eaay3922.

Green, H., A. Gleadow, D. Finch, J. Hergt and S. Ouzman (2017). "Mineral deposition systems at rock art sites, Kimberley, Northern Australia - Field observations." Journal of Archaeological Science-Reports **14**: 340-352.

Harman, J. (2005). Using decorrelation stretch to enhance rock art images. American Rock Art Research Association Annual Meeting, <http://www.dstretch.com>.

Harman, J. (2020). "DStretch Rock Art Digital Enhancement." Retrieved 21/4/2020, 2020.

Hodgson, D. and P. Pettitt (2018). "The Origins of Iconic Depictions: A Falsifiable Model Derived from the Visual Science of Palaeolithic Cave Art and World Rock Art." Cambridge Archaeological Journal **28**(4): 591-612.

Hodgson, D. and B. Watson (2015). "The visual brain and the early depiction of animals in Europe and Southeast Asia." World Archaeology: 1-16.

Hoffmann, D. L., A. W. G. Pike, M. García-Diez, P. B. Pettitt and J. Zilhão (2016). "Methods for U-series dating of CaCO<sub>3</sub> crusts associated with Palaeolithic cave art and application to Iberian sites." Quaternary Geochronology **36**: 104-119.

Hogg, A. G., Q. Hua, P. G. Blackwell, M. Niu, C. E. Buck, T. P. Guilderson, T. J. Heaton, J. G. Palmer, P. J. Reimer, R. W. Reimer, C. S. M. Turney and S. R. H. Zimmerman (2013). "SHCal13 Southern Hemisphere calibration, 0–50,000 years cal BP." Radiocarbon **55**(4): 1889-1903.

Jones, T., V. Levchenko and D. Wesley (2017a). How old is X-ray art? Minimum age determinations for early X-ray rock art from the 'Red Lily' (Wulk) Lagoon rock art precinct, western Arnhem Land. The archaeology of rock art in Western Arnhem Land, Australia. B. David, P. S. C. Taçon, J.-J. Delannoy and M. Geneste. Canberra. A.C.T., ANU Press. **Terra Australis: no. 47**: 129 - 143.

Jones, T., V. A. Levchenko, P. L. King, U. Troitzsch, D. Wesley, A. A. Williams and A. Nayingull (2017b). "Radiocarbon age constraints for a Pleistocene–Holocene

transition rock art style: The Northern Running Figures of the East Alligator River region, western Arnhem Land, Australia." Journal of Archaeological Science: Reports **11**: 80-89.

Lewis, D. (1988). The Rock Paintings of Arnhem Land, Australia. Oxford, B.A.R.

Lewis, D. (1997). "Bradshaws: The View from Arnhem Land." Australian Archaeology **44**: 1 - 16.

Maloney, T., S. O'Connor, R. Wood, K. Aplin and J. Balme (2018). "Carpenters Gap 1: A 47,000 year old record of indigenous adaption and innovation." Quaternary Science Reviews **191**: 204-228.

O'Connor, S. and B. Fankhauser (2001). Art at 40,000 bp? One step closer: an ochre covered rock from Carpenter's Gap Shelter 1, Kimberley Region, Western Australia. Histories of old ages: essays in honour of Rhys Jones. A. Anderson, I. Lilley and S. O'Connor. Canberra, Pandanus Books, Research School of Pacific and Asian Studies The Australian National University: 287-300.

Ouzman, S., P. Veth, C. Myers, P. Heaney and K. Kenneally (2017). Plants Before Animals?: Aboriginal Rock Art as Evidence of Ecoscaping in Australia's Kimberley. The Oxford Handbook of the Archaeology and Anthropology of Rock Art. B. David and I. J. McNiven, Oxford University Press.

Pettitt, P. and P. Bahn (2015). "An alternative chronology for the art of Chauvet cave." Antiquity **89**(345): 542-553.

Pike, A. W., D. L. Hoffmann, M. Garcia-Diez, P. B. Pettitt, J. Alcolea, R. De Balbin, C. Gonzalez-Sainz, C. de las Heras, J. A. Lasheras, R. Montes and J. Zilhao (2012). "U-series dating of Paleolithic art in 11 caves in Spain." Science **336**(6087): 1409-1413.

Quiles, A., H. Valladas, H. Bocherens, E. Delque-Kolic, E. Kaltnecker, J. van der Plicht, J. J. Delannoy, V. Feruglio, C. Fritz, J. Monney, M. Philippe, G. Tosello, J. Clottes and J. M. Geneste (2016). "A high-precision chronological model for the decorated Upper Paleolithic cave of Chauvet-Pont d'Arc, Ardeche, France." Proceedings of the National Academy of Sciences of the United States of America **113**(17): 4670-4675.

Roberts, R., G. Walsh, A. Murray, J. Olley, R. Jones, M. Morwood, C. Tuniz, E. Lawson, M. Macphall, D. Bowdery and I. Naumann (1997). "Luminescence dating of rock art and past environments using mud-wasp nests in northern Australia." Nature **387**(6634): 696-699.

Ross, J., K. Westaway, M. Travers, M. J. Morwood and J. Hayward (2016). "Into the Past: A Step Towards a Robust Kimberley Rock Art Chronology." PLoS ONE **11**(8): e0161726.

Taçon, P. S. and S. Webb (2017). Art and megafauna in the Top End of the Northern Territory, Australia: Illusion or reality? The Archaeology of Rock Art in Western Arnhem Land, Australia. B. David, P. Tacon, J. J. Delannoy and J. M. Geneste. Acton ACT, ANU Press. **47**: 145.

Taçon, P. S. C., L. Gang, Y. Decong, S. K. May, L. Hong, M. Aubert, J. Xueping, D. Curnoe and A. I. R. Herries (2010). "Naturalism, Nature and Questions of Style in Jinsha River Rock Art, Northwest Yunnan, China." Cambridge Archaeological Journal **20**(01): 67.

Tacon, P. S. C., N. H. Tan, S. O'Connor, X. Ji, G. Li, D. Curnoe, D. Bulbeck, B. Hakim, I. Sumantri, T. Heng, S. Im, S. Chia, K.-N. Khuon and K. Soeung (2014). "The global implications of the early surviving rock art of greater Southeast Asia." Antiquity **88**(342): 1050-1064.

Tacon, P. S. C., H. S. Tang and M. Aubert (2016). "Naturalistic Animals And Hand Stencils In The Rock Art Of Xinjiang Uyghur Autonomous Region, Northwest China." Rock Art Research **33**(1): 19-31.

Valladas, H., A. Quiles, M. Delque-Kolic, E. Kaltnecker, C. Moreau, E. Pons-Branchu, L. Vanrell, M. Olive and X. Delestre (2017). "Radiocarbon Dating of the Decorated Cosquer Cave (France)." Radiocarbon **59**(2): 621-633.

Vannieuwenhuyse, D., S. O'Connor and J. Balme (2017). "Settling in Sahul: Investigating environmental and human history interactions through micromorphological analyses in tropical semi-arid north-west Australia." Journal of Archaeological Science **77**: 172-193.

Veth, P., C. Myers, P. Heaney and S. Ouzman (2017). "Plants before farming: The deep history of plant-use and representation in the rock art of Australia's Kimberley region." Quaternary International.

Walsh, G. and Kimberley-Foundation. (2019). "Irregular Animal Infill Period." Kimberley Rock Art Sequence Retrieved 12 September 2019, 2019, from [www.kimberleyfoundation.org.au/kimberley-rock-art/rock-art-sequence/irregular-animal-infill-period/](http://www.kimberleyfoundation.org.au/kimberley-rock-art/rock-art-sequence/irregular-animal-infill-period/).

Walsh, G. L. (1994). Bradshaws, ancient rock paintings of north-west Australia. Carouge-Geneva, Switzerland, Edition Limitée for the Bradshaw Foundation.

Walsh, G. L. (2000). Bradshaw art of the Kimberley, Takarakka Nowan Kas Publications.

Welch, D. M. (1993). Stylistic change in the Kimberley rock art, Australia. Rock art studies: the post-stylistic era or where do we go from here?, Cairns, Oxbow Monograph.

Welch, D. M. (2015). Aboriginal Paintings of Drysdale River National Park, Kimberley, Western Australia. Coolalinga, Northern Territory, David M. Welch.

Whiteway, T. (2009). Australian bathymetry and topography grid. G. Australia. Canberra, Department of Industry, Tourism & Resources. **GeoCat # 67703**: 46.

Williams, A. N., S. Ulm, T. Sapienza, S. Lewis and C. S. M. Turney (2018). "Sea-level change and demography during the last glacial termination and early Holocene across the Australian continent." Quaternary Science Reviews **182**: 144-154.

## **Chapter 5**

### **Radiocarbon age estimates for the Cupule and more recent art periods**

#### **5.1 Introduction**

Preceding chapters report radiocarbon ages for 24 mud wasp nests constructed over or under 21 Gwion motifs and 27 nests preserved over or under 16 IIAP motifs. These ages were used to propose absolute chronologies for the two oldest periods of painted Kimberley rock art based on superimposition. This chapter reports on the remaining 24 wasp nests that make up the total of 75 old wasp nests dated for this study. These 24 nests were in contact with 24 motifs that either could not confidently be categorised to any style or were from one of the four other main Kimberley rock art stylistic periods: Cupules, Static Polychrome, Painted Hand or Wanjina. Where possible, age constraints on motifs of less certain classification are used to infer the most likely stylistic period.

In this chapter, samples belonging to each of the main stylistic periods (Table 5-1) are considered in order of decreasing age as suggested by the relative chronology of the Kimberley stylistic sequence. Details of the radiocarbon pretreatment and measurements for the 24 nest samples are listed in Supplementary Data Table 5-2.

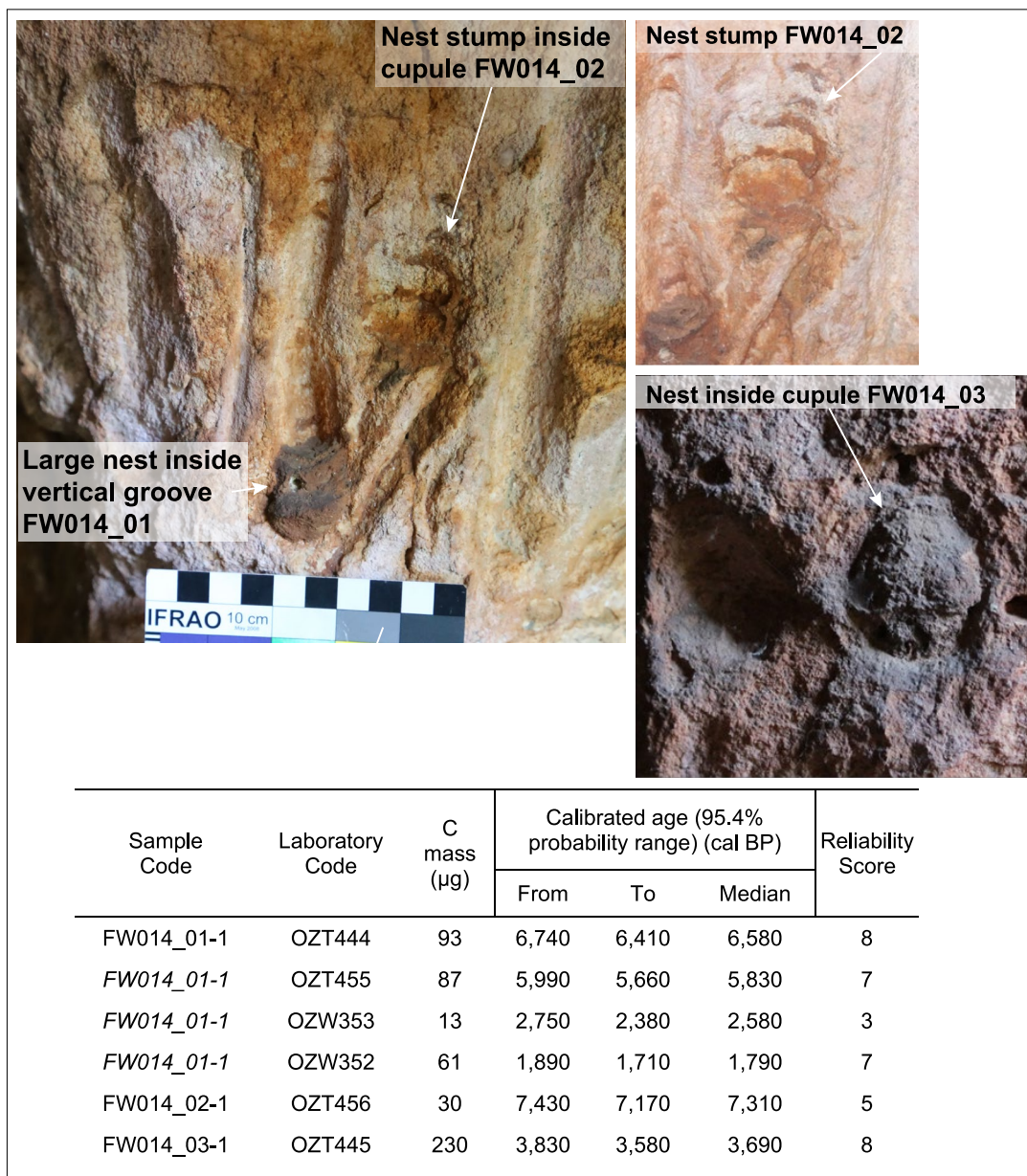
**Table 5-1** Stylistic classification of 24 motifs. “NA” indicates the classification was by the author

Sample Code	Style Classification	Expert Classification	
		PH	CM
FW014_01-1	Cupule/Groove	NA	NA
FW014_02-1	Cupule/Groove	NA	NA
FW014_03-1	Cupule/Groove	NA	NA
DR008_01-2	IIAP?	Possible	Likely
KG020_08-1	IIAP?	Possible	Likely
KG020_08-4	IIAP?	Possible	Likely
KG021A_05-1	IIAP?	Likely	Uncertain
KGD236_01-1	IIAP?	Possible	Likely
DR015_06-1	IIAP or Gwion?	Gwion - Possible	IIAP - Uncertain
DR007_03-1	Gwion?	Uncertain	Uncertain
KG071_01-1	Static Polychrome?	Likely	Possible
DR009_02-1	Static Polychrome	Certain	Certain
DR108_01-2	Static Polychrome	Likely	Highly Likely
KG002_02-1	Static Polychrome?	Likely	Possible
FW010_06-1	Painted Hand	Highly Likely	Highly Likely
DR007_04-1	Painted Hand?	Likely	Possible
DR031_24-1	Painted Hand?	Possible	Likely
FW010_02-1	Painted Hand?	Possible	Possible
KG021A_06-1	Painted Hand or Wanjina?	Painted Hand - Possible	Wanjina - Possible
FW004_11-1	Wanjina	NA	Certain
FW016_02-1	Wanjina	NA	Certain
FW002_02-1	Wanjina?	NA	Likely
KG021A_01-2	Unknown	Unknown	Unknown
KG021A_04-1	Unknown	Unknown	Unknown

## 5.2 Cupules and Grooves

Cupules and abraded grooves have been assigned to the earliest Archaic Period of the Kimberley rock art sequence although some dispute their classification as “art” (Walsh 2000: 99, Welch 2015: 166). Walsh reports evidence suggesting that some cupules may also have been produced or at least modified in more recent times because they do not have the “highly patinated surfaces” evident on older cupules (2000: 100). To date, there is insufficient evidence to establish whether the Cupules & Abraded Grooves period and IIAP paintings are at least partly contemporaneous or are discrete, sequential phases.

One wasp nest over an abraded groove and two nests from within cupules were dated. All samples were taken from the same Western Kimberley coastal site FWC014, located 180 km NNE of Derby.



**Figure 5-1** Mud wasp nests inside grooves and cupules. The white arrows show the sample locations. The arrow for FW014\_01 (lower left) also indicates a lighter coloured exit hole in the nest

Sample FW014\_01-1 (Figure 5-1) is a large wasp nest taken from within the lower part of a vertical groove. The more horizontal outer areas of the mineralised nest had a dark accretion. The light colour of the exit hole suggests the nest has been reused by a different species of wasp or bee and may, therefore, contain organic material younger than that contained in the original nest. Four radiocarbon age measurements

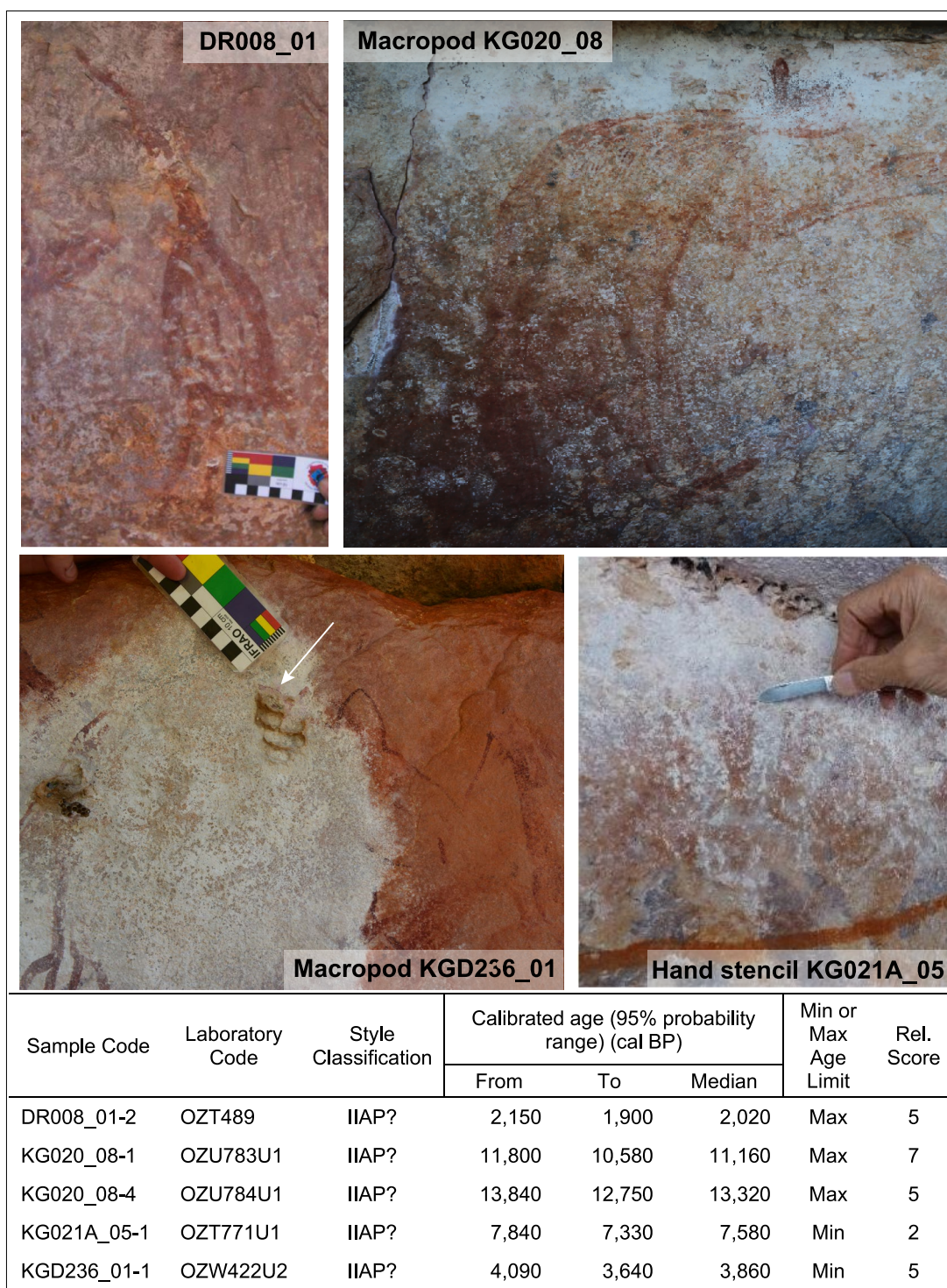
on 3 different sub-samples using three different pretreatment methods established that the age of carbon in the nest ranged from at least 6.7 – 1.7 cal kBP (Figure 5-1). The source of the younger carbon is probably pyrogenic carbon in the dark accretion and, potentially, more modern organic material introduced when the nest was reused. The oldest dated sub-sample, with a Reliability Score of 8, establishes that this feature, from the Abraded Groove stylistic phase is at least 6,400 years old.

The ages of two other nests constructed inside cupules (FW014\_02 and \_03, Figure 5-1) show that one is older than 7.2 ka and the other is older than 3.6 ka. With just three motifs dated and no under-art samples available we can only hypothesise, broadly, that some cupules and grooves at this site are older than ~7.2 ka but others may be as young as 3.6 ka.

### **5.3 Possible IIAP motifs**

Four motifs that were classified as only “Possibly” or “Likely” to be IIAP (Table 5-1) were not included in the analysis in Chapter 4. Here, the dates measured on 5 nests in contact with these 4 motifs are used to test the idea that the age constraints provided by wasp nest dates can be used to determine the art period that the motif belongs to. This is one of the main long-term objectives for the rock art dating program: to use age constraints on motifs to infer the art period where this is not obvious and, therefore, to revise or confirm stylistic attributes used to define rock art styles.





**Figure 5-2** Possible IIAP motifs and associated age constraints

DR008\_01 is a bird-like motif with irregular infill. The pigment colour is similar to that evident on old hand stencils on the same panel. PH classified it as possibly IIAP or Gwion period while CM suggests it is likely to be IIAP (Table 5-1). Either interpretation is at odds with the maximum age of c. 2 ka based on the age of an underlying nest (Figure 5-2). The Reliability Score of 5 reflects the fact that an early

radiocarbon pretreatment was used, and, in this case, it may be that younger carbon contamination on the external surface of the nest sample was not completely removed. As this is an under-art sample, significant contamination may invalidate any maximum age determination for the motif. Without further constraints, we cannot therefore rule out the possibility that the motif may still be IIAP or Gwion.

Two nests underlying a macropod motif KG020\_08 were dated. PH and CM noted the unusual ear/head detail as the reason for less confidence in an IIAP classification. The two dates provide good support for a maximum age of 10.6 ka for this motif, so it is more likely to be of the Gwion period than the IIAP. Consequently, the rounded ear attribute evident in KG020\_08 is probably a characteristic of Gwion period macropods.

KG021A\_05 is a hand stencil, older than 7.3 ka. It may be IIAP, but the dated nest establishes only that it is older than mid-Holocene.

KGD236\_01 is a weathered macropod motif determined only to be older than 3.6 ka so it may still be Gwion or IIAP.

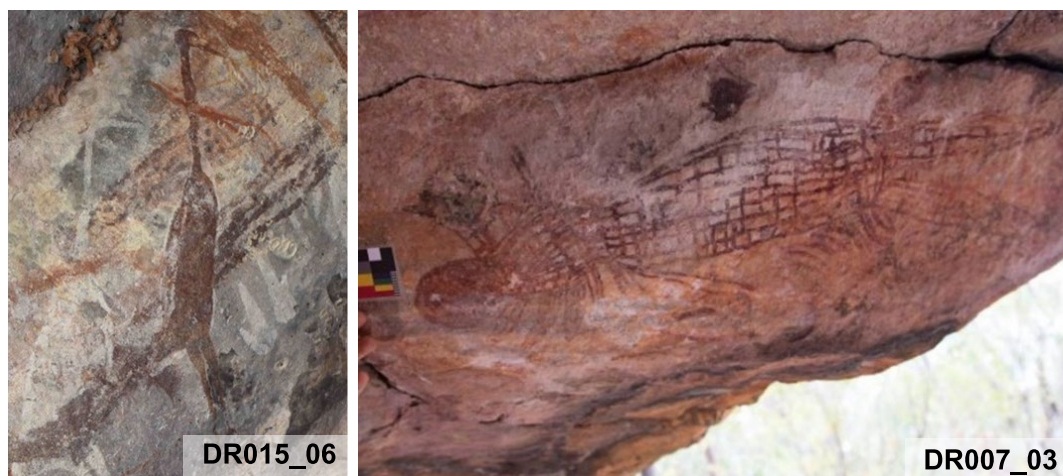
The dates determined for KG020\_08 provide potentially useful insights into the defining characteristics of Gwion macropods, but the results on the other 3 motifs provide little new information. Many more dated nests will be required to refine the attributes used to define specific styles. The probability of obtaining a useful age constraint on an atypical motif is greatly enhanced if multiple nest samples can be dated.

## **5.4 Possible Gwion motifs**

Nests overlying two possible Gwion motifs were dated. DR015\_06 is one of a series of brolga motifs (Welch 2015: 129) and is older than 10.3 ka (Figure 5-3). The extremely low Reliability Score of 1 reflects the higher risk of more modern carbon contamination so, if anything, the nest may be older than the measured age. This motif is superimposed on a 3-metre-long IIAP snake motif, DR015\_14, known to be younger than 15.1 ka (Chapter 4). PH classified the motif as “possibly” Gwion while CM noted that it was possibly overlain by a separate Gwion figure. So, the brolga

motif must be between 15.1 and 10.3 ka and therefore may have been painted in either the IIAP or earlier in the Gwion period.

The nest overlying DR007\_03 was close to modern in age and provides no useful minimum age limit for the motif.



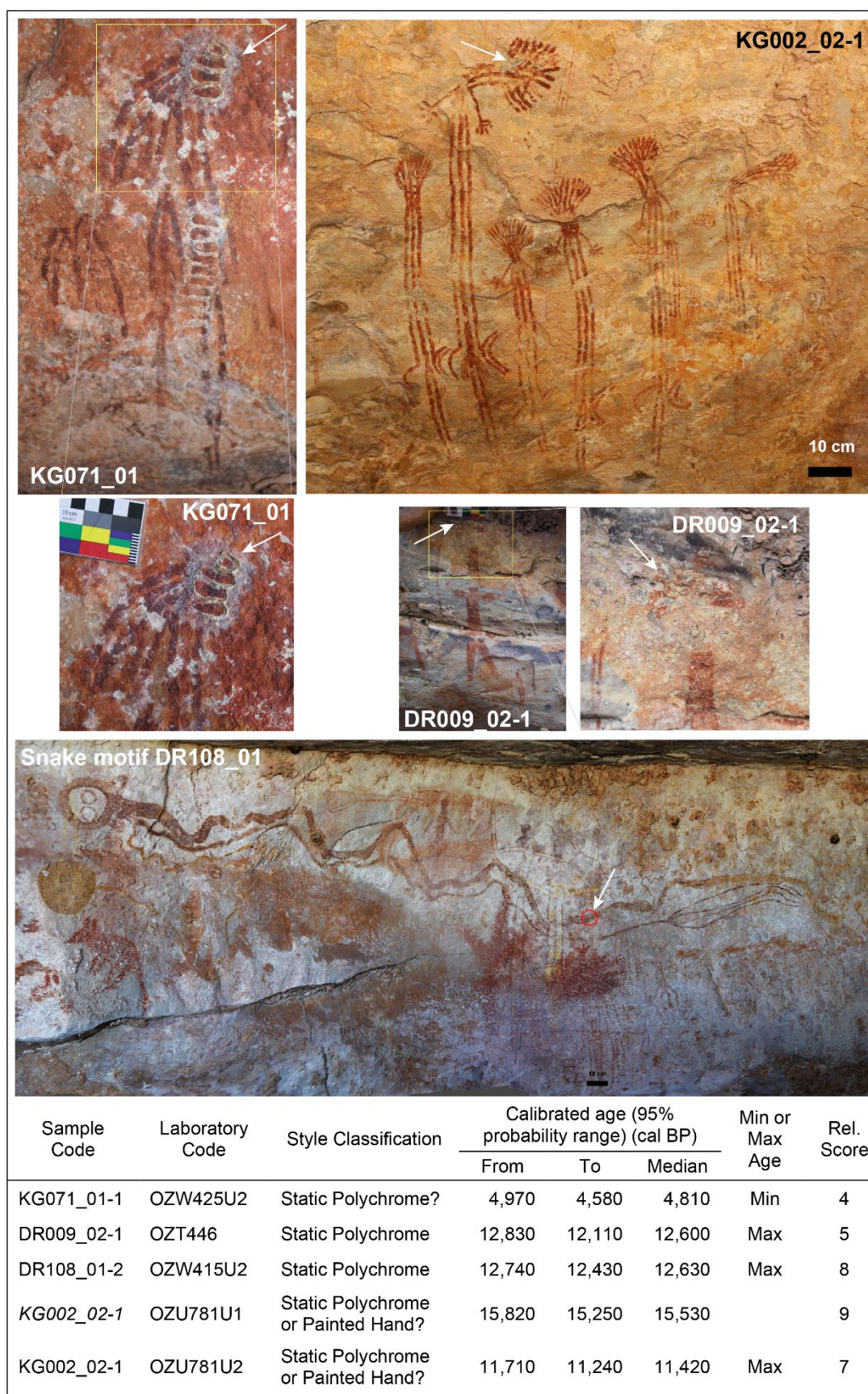
Sample Code	Laboratory Code	Style Classification	Calibrated age (95% probability range) (cal BP)			Min or Max Age Limit	Rel. Score
			From	To	Median		
DR015_06-1	OZT799U1	IIAP or Gwion?	11,170	10,270	10,700	Min	1
DR007_03-1	OZT793U2	Gwion?	310	...	140	Min	2

**Figure 5-3** Possible Gwion motifs and associated age constraints

## 5.5 Static Polychrome motifs

Nests underlying two motifs confidently classified as Static Polychrome were dated (motifs DR009\_02 and DR108\_01) as were two fractions from another nest under a less certain Static Polychrome motif (KG002\_02) and one nest overlying another likely Static Polychrome motif (KG071\_01).





**Figure 5-4** Static Polychrome possible motifs - sample locations (white arrows) and calibrated ages.

KG071\_01-1 has some attributes of a “watusi” or dreadlock headdress Gwion but is more likely a transition stick figure in the Static Polychrome style (Walsh, 2000: 179, 203, 270). The age of an overlying nest indicates only that the motif is older than 4.6 ka (Figure 5-4). DR108\_01 is interpreted to be a Static Polychrome Rainbow Serpent motif c. 3.5 m long that has been repainted or added to at least once. The sample location is marked with a red circle in Figure 5-4. The date on the underlying nest establishes a reliable maximum age of 12.7 ka for the motif.

Motif KG002\_02 was classified as likely or possibly, Static Polychrome. Walsh (2000: 353 Fig 590) describes this group of figures holding boomerangs as Stick Static Polychrome variants (“Stick Clothes Peg Figure”). Whilst distinctive, some attributes of these stick figures may be shared with motifs from other styles hence classification can be problematic. The figures were painted on the ceiling of a rock shelter in a narrow gorge of the King George river. The relatively smooth ceiling was c. 13 metres above the dry season river level but is likely to be occasionally flooded. Agglomerations of wasp nests were evident on the ceiling but were of low relief and rounded as though weathered. Two fractions (Light and Heavy) from an under-art nest sample were dated with the younger age of the Heavy fraction (OZU781U2) providing a maximum age constraint of 11.7 ka for the motif (Figure 5-4). This maximum age is slightly younger than the hypothesised Gwion period providing some support for the Static Polychrome classification but also allowing that they may be of a transitional style, in between the two main periods.

Apart from the possibly Static Polychrome motif KG071\_01 with a minimum age of 4.6 ka, no nests overlying paintings from the Static Polychrome period were successfully dated. The 3 maximum age constraints on 3 motifs from 3 different sites all fall in the range 12.7 – 11.7 ka. As it is statistically more likely that the age of these under-art nests is closer to the age of the motif (as discussed in Chapter 3), these data suggest the Static Polychrome period is younger than, but close to, the Gwion period although we cannot rule out an overlap between the two periods without further evidence.

## 5.6 Painted Hand motifs

One fish-like motif highly likely to be from the Painted Hand period (FW010\_06) and a further four likely, or possibly, Painted Hand motifs were dated including two further fish-like motifs, a radial star motif and a linear motif (Fig.5-5).

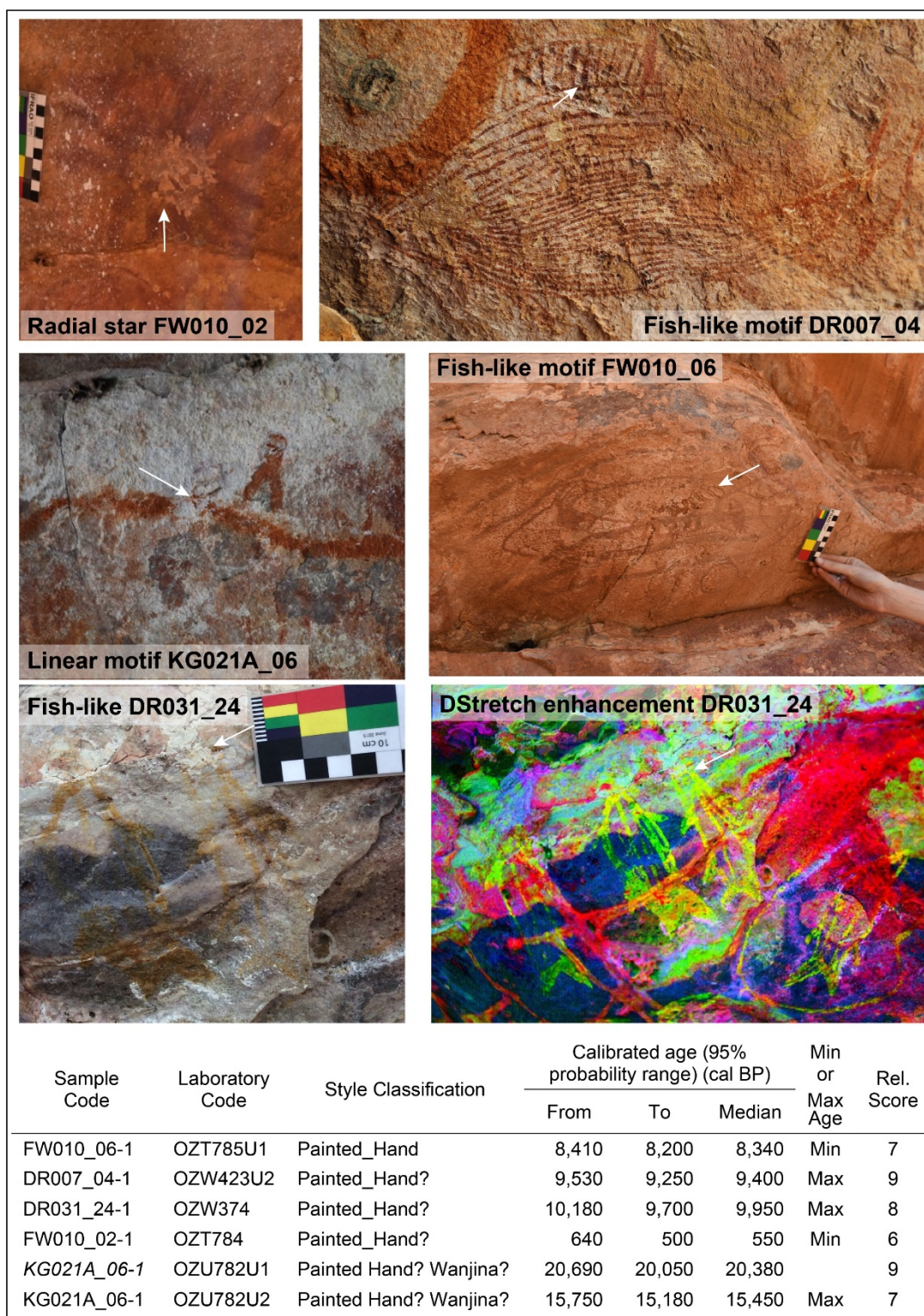
The nest overlying FW010\_06 provides a minimum age of 8.2 ka for this motif. Another fish-like motif, DR007\_04, was classified as possibly (PH) or likely (CM) to be Painted Hand. The date of an underlying nest sample establishes that this motif is less than 9,500 years old.

Another fish-like motif, DR031\_24, is one of a group of similar yellow motifs possibly (PH) or likely (CM) to be from the Painted Hand period. The wasp nest underlying DR031\_24 indicates that this fish-like motif is younger than 10.2 ka

Motif FW010\_02-1 is a radial, star shaped motif with overlying nest stump dated to 640 - 500 cal BP. The motif is possibly (PH) Painted Hand but the very young minimum age constraint of 500 years (cal BP) does not support any specific stylistic classification.

Two fractions from a nest underlying the long undulating linear motif KG021A\_06 were dated. The motif is possibly Painted Hand (CM) or Wanjina (PH). The maximum age of 15.8 ka does not constrain it to either period.



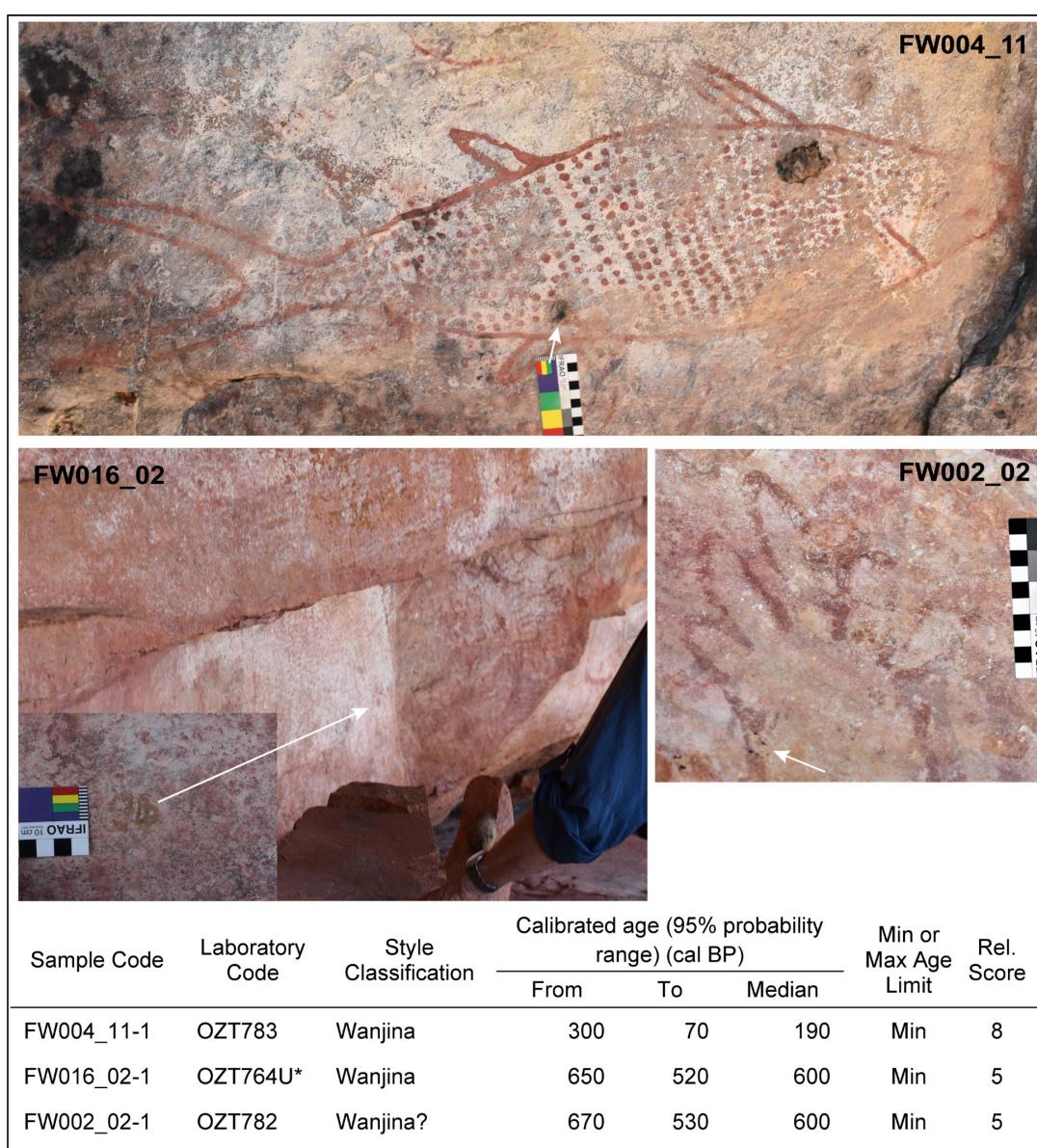


**Figure 5-5** Painted Hand possible motifs - sample locations (arrows) and associated calibrated age constraints. Motif DR031\_24 is shown with DStretch (Harman 2005, 2020) colour enhancement to highlight the yellow pigment.



## 5.7 Wanjina motifs

As illustrated in Figure 5-6, three nests overlying three motifs from the most recent Wanjina period provide minimum age constraints of 70 years for one (sample FW004\_11-1 over a fish-like motif) and ~500 years for the other two (Wanjina motif FW016\_02 and hand-like motif FW002\_02). No under-art nests were dated but even these few ages confirm that this “recent” style includes paintings that are at least 500 years old.

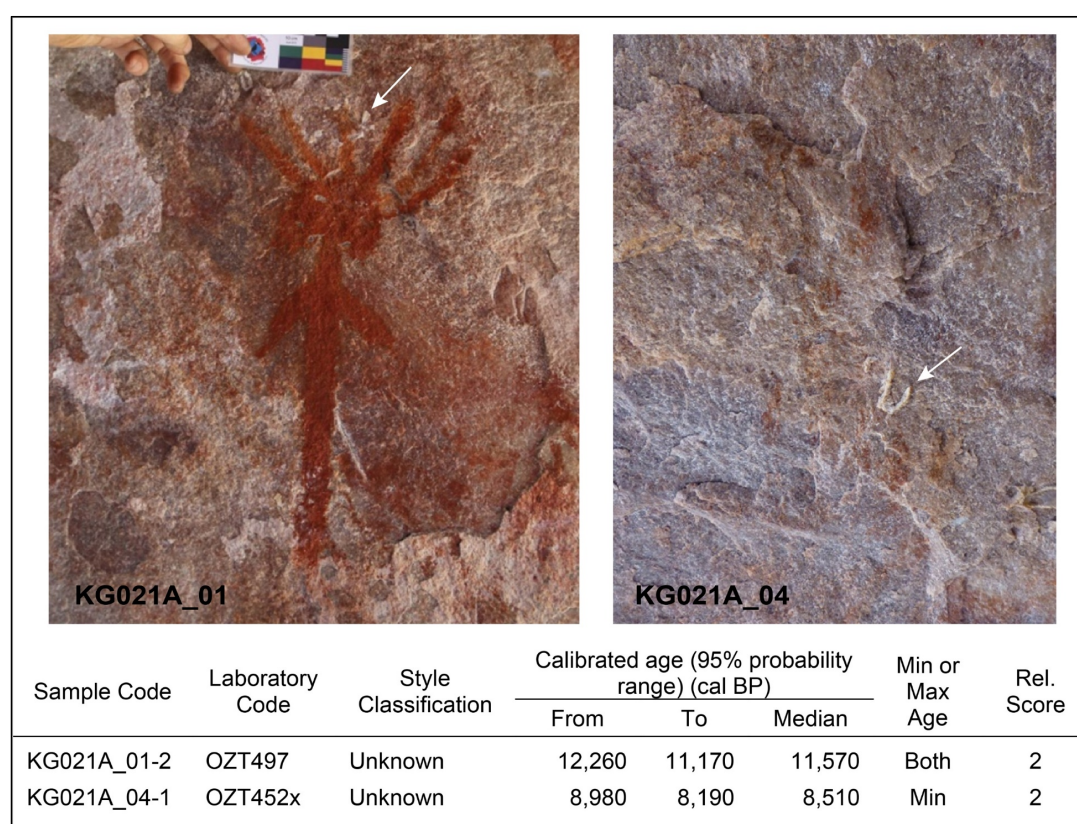


**Figure 5-6** Wanjina motifs - sample locations (arrows) and associated calibrated age constraints.



## 5.8 Motifs of indeterminate style

Two motifs could not be classified to a particular style. KG021A\_04-1 is a very faded motif determined to be older than 8.2 ka. The nest underlying the figure KG021A\_01 had pigment on its under surface and clearly also overlies a broad area of very faded brown pigment so the figure is younger than 12.3 ka and the faded painting underneath is older than 11.2 ka. Some remnant and indeterminate motifs were sampled to test for the possibility that the very oldest Kimberley paintings may be of an as yet unidentified style, predating the IIA period, but no such evidence was found in this study.



**Figure 5-7** Motifs of indeterminate style - sample locations (arrows) and associated calibrated age constraints.

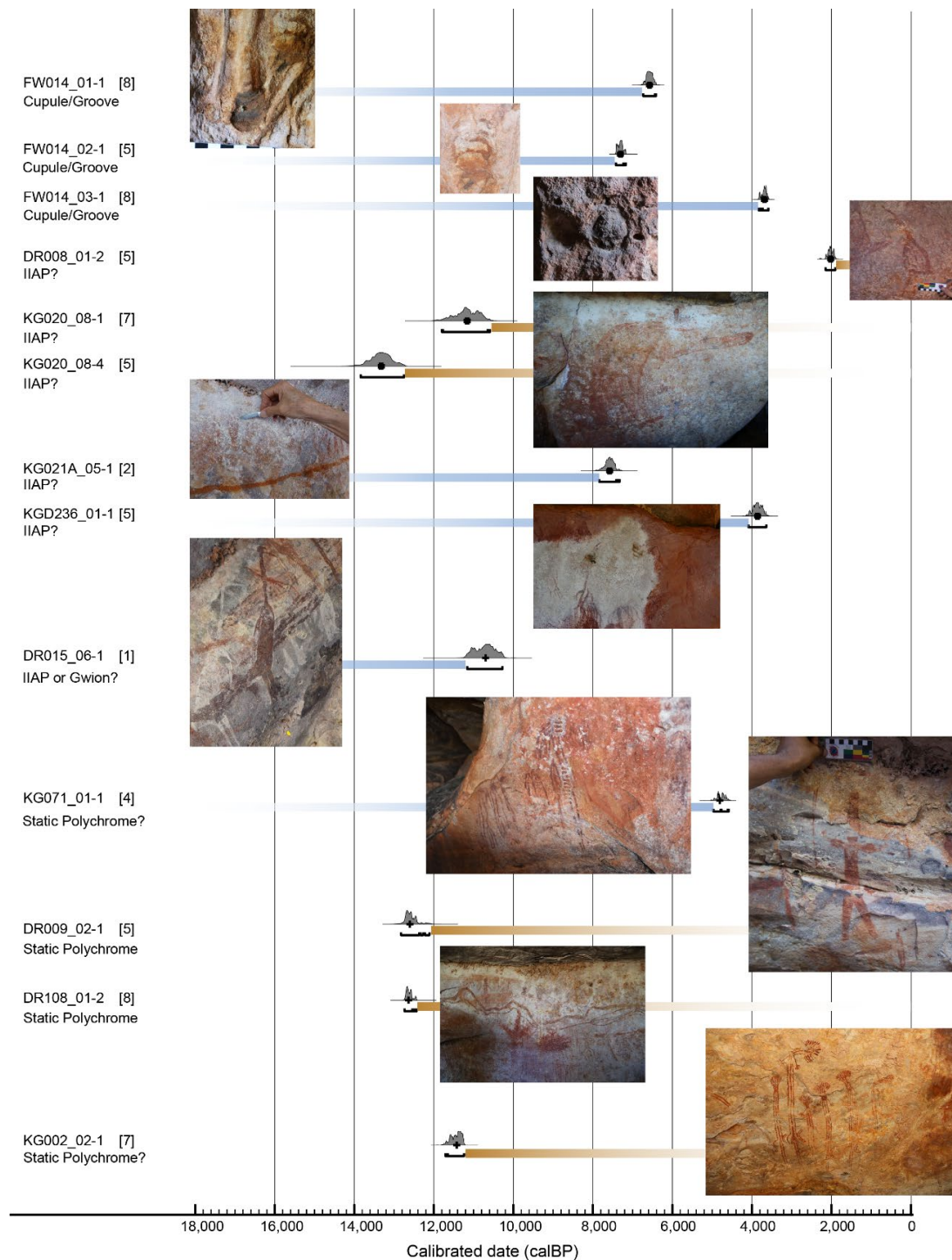
## 5.9 Conclusion

The age constraints reported above are summarised in Figure 5-8 and Figure 5-9 and raise the question “How does this new evidence support or contradict the proposed stylistic definition and relative chronology of the Kimberley rock art sequence?” The

data for each of the main periods is considered below, in turn, from oldest to youngest. The three minimum age constraints relating to pecked cupules and abraded grooves of 3.6 ka, 6.4 ka and 7.2 ka are a useful addition to the very few radiometrically dated motifs in this style; however, they are not sufficient to substantiate the proposed position of this style as the earliest phase in the Kimberley rock art sequence. Of the more than 150 Kimberley rock art sites visited between 2015 and 2017 only one site yielded dateable samples from cupules or grooves. It will require significantly more exploratory fieldwork, or a new dating technique, to establish the chronology of the Cupules style.

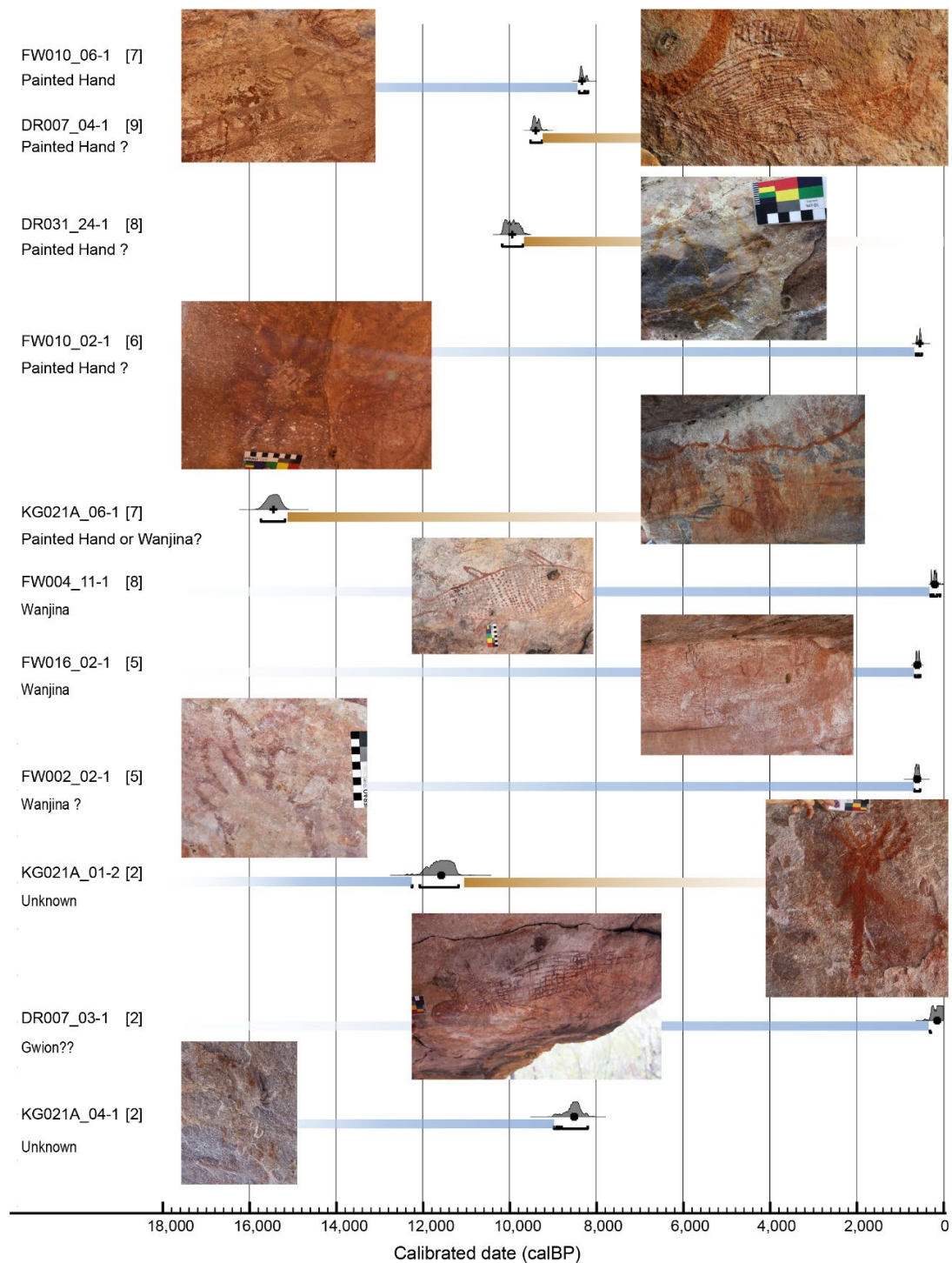
In this study, ~80% of nest samples collected were associated with either IIAP or Gwion motifs. Of the 75 wasp nest radiocarbon dates reported here 77% related to either Gwion or IIAP motifs (including those at least “possibly” belonging to these styles) and these two styles accounted for 72% of the 60 motifs with one or more age constraints. The relatively large number of age constraints determined for IIAP (16 dates) and Gwion motifs (20 dates) provide a useful estimate of the absolute chronology for these periods. This potentially permits age constraints determined for motifs of uncertain classification to be used to refine the definition of the individual styles. The maximum age of 11.8 ka determined for the macropod motif KG020\_08 is an example. The unusual ear detail can now be taken to indicate that a macropod motif is not from the IIAP but is from a more recent period. Notwithstanding this useful result, the age constraints for other motifs of less certain classification demonstrate the limitations of this approach. Generally, a single over-art nest does not provide the required diagnostic precision to allow classification to a specific style. A single under-art nest, however, is more likely to provide a useful age constraint as demonstrated, in particular, by the results for the Static Polychrome and Painted Hand motifs. All three dates relating to Wanjina period motifs are single, over-art samples providing little new chronological information for this recent art style.

The following chapter considers how these age constraints on individual motifs can be used to propose an absolute chronology for the main Kimberley art styles together with an assessment of the reliability of such estimates.



**Figure 5-8** Age constraints for older motif styles. The small gray graphs are the probability distribution of the calibrated nest age where the bar underneath each plot indicates the 95.4% probability range, with the median marked with a cross. The brown and blue bars, representing the possible motif age range, pass under a photograph of the relevant motif.





**Figure 5-9** Age constraints for younger motif styles. The small gray graphs are the probability distribution of the calibrated nest age where the bar underneath each plot indicates the 95.4% probability range, with the median marked with a cross. The brown and blue bars, representing the possible motif age range, pass under a photograph of the relevant motif.

## 5.10 Supplementary Data

**Table 5-2** Radiocarbon pretreatment methods and carbon isotope measurements on wasp nests

Sample Code	Laboratory Code	Pretreatment Sequence	Fraction	C mass (µg)	percent Modern Carbon	1σ error ±	Rel. Score
FW014_01-1	OZT444	ABA	All	93	48.46	0.38	8
<i>FW014_01-1</i>	OZT455	ABA	All	87	52.65	0.39	7
<i>FW014_01-1</i>	OZW353	A-HF-HLS-BA(8M)	Heavy	13	72.72	0.57	3
<i>FW014_01-1</i>	OZW352	A-HF-HLS-BA(8M)	Light	61	78.97	0.36	7
FW014_02-1	OZT456	ABA	All	30	45.01	0.32	5
FW014_03-1	OZT445	ABA	All	230	64.89	0.24	8
DR008_01-2	OZT489	ABA	All	40	77.06	0.44	5
KG020_08-1	OZU783U1	A-HLS-BA(8M)	Light	28	29.51	0.66	7
KG020_08-4	OZU784U1	A-HLS-BA(8M)	Light	10	23.86	0.78	5
KG021A_05-1	OZT771U1	ABA - HLS	Heavy	16	43.15	0.69	2
KGD236_01-1	OZW422U2	A-HLS-BA(8M)	Heavy	14	63.82	0.64	5
DR015_06-1	OZT799U1	ABA - HLS	Heavy	12	30.78	0.63	1
<i>DR015_06-1</i>	OZT799U*	ABA	All	24	75.5	0.9	3
KG071_01-1	OZW425U2	ABA(16M)	Heavy	26	58.59	0.41	4
DR009_02-1	OZT446	ABA	All	24	26.31	0.42	5
DR108_01-2	OZW415U2	AB-HLS-A(16M)	Heavy	35	26.31	0.27	8
KG002_02-1	OZU781U1	A-HLS-BA(8M)	Light	120	19.75	0.19	9
<i>KG002_02-1</i>	OZU781U2	A-HLS-BA(8M)	Heavy	44	28.77	0.21	7
FW010_06-1	OZT785U1	A(conc)	AcidSol	3470	39.03	0.2	7
DR007_04-1	OZW423U2	A-HLS-BA(8M)	Heavy	46	35.04	0.24	9
DR031_24-1	OZW374	ABA(8M)	All	32	33.05	0.25	8
FW010_02-1	OZT784	ABA - HLS	Light	84	92.9	0.5	6
KG021A_06-1	OZU782U1	A-HLS-BA(8M)	Light	56	12.14	0.17	9
<i>KG021A_06-1</i>	OZU782U2	A-HLS-BA(8M)	Heavy	47	19.9	0.2	7
FW004_11-1	OZT783	ABA - HLS	Light	180	97.43	0.25	8
FW016_02-1	OZT764U*	ABA	All	68	92.47	0.44	5
FW002_02-1	OZT782	ABA - HLS	Light	43	92.14	0.65	5
KG021A_01-2	OZT497	ABA	All	16	28.58	0.53	2
DR007_03-1	OZT793U2	ABA - HLS	Light	19	98.25	1.14	2
KG021A_04-1	OZT452x	ABA	All	14	38.19	0.68	2

Notes: The Sample Code is constructed from a short site identifier, followed by a number to identify the painted motif and then the number of the sample collected

(on that motif, at that site) in the format "SITE\_MOTIF-NEST". The "Fraction" column indicates where Heavy Liquid Separation was used to separate the sample into low density (Light) and higher density (Heavy) fractions with "All" indicating the sample was not separated. The  $\delta^{13}\text{C}$  of all samples was not able to be reliably measured but is assumed to be -25‰ for the isotopic correction, based on an average for other similar samples. For a complete description of the Pretreatment Sequence, Fractions, and Reliability Score refer Chapter 2.

## 5.11 References

Harman, J. (2005). Using decorrelation stretch to enhance rock art images. American Rock Art Research Association Annual Meeting, <http://www.dstretch.com>.

Harman, J. (2020). "DStretch Rock Art Digital Enhancement." Retrieved 21/4/2020, 2020.

Walsh, G. L. (2000). Bradshaw art of the Kimberley, Takarakka Nowan Kas Publications.

Welch, D. M. (2015). Aboriginal Paintings of Drysdale River National Park, Kimberley, Western Australia. Coolalinga, Northern Territory, David M. Welch.

# **Chapter 6**

## **Modelling the chronology of the Kimberley rock art sequence**

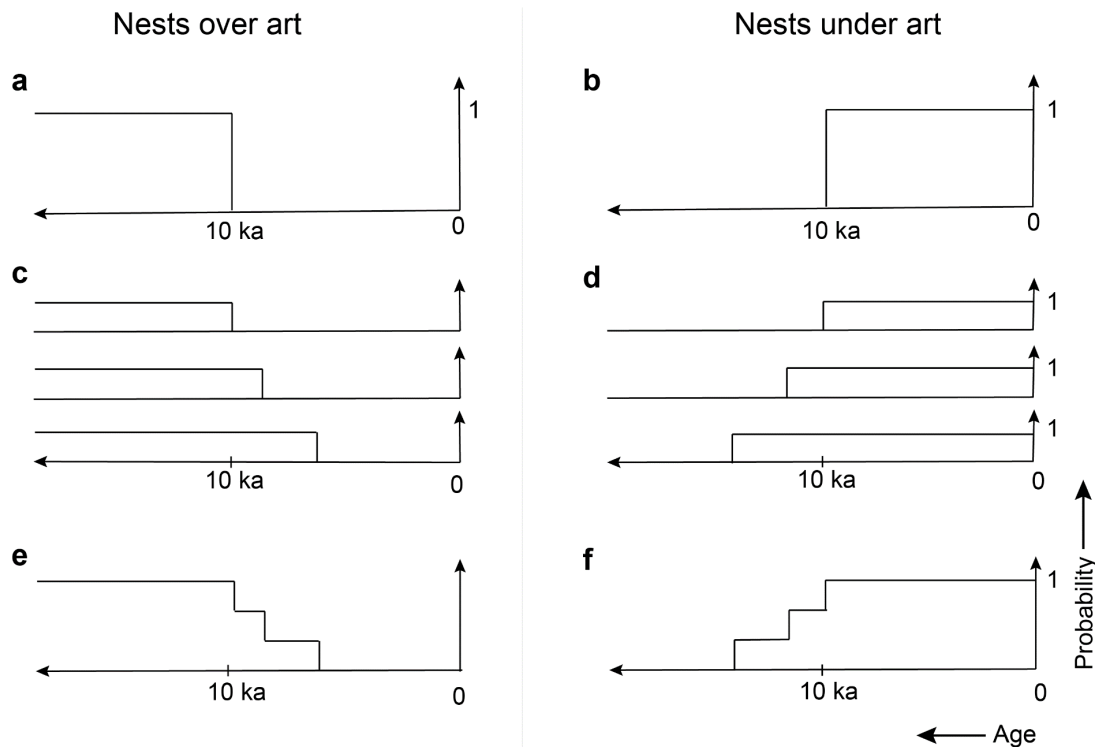
### **6.1 Modelling art period chronologies**

Very few techniques have been developed that provide age constraints for rock paintings when the pigment itself cannot be dated. Those that do invariably provide just a few successful ages. It is also uncommon to have available a thoroughly researched and documented rock art stylistic sequence based on detailed observations at thousands of sites. There is, therefore, no established probabilistic method that can be used to derive absolute age ranges for individual art periods from a large number of wasp nest dates. The method developed in this study, described very briefly in Chapter 3, is fully developed below.

#### **6.1.1 Using wasp nest dates as age constraints**

If we consider an example of a mud wasp nest that is exactly 10,000 years old (zero error) then any underlying painting must be older than 10 ka and any overlying painting must be younger than 10 ka. The probability density functions (pdfs) for the possible age of the motif in these two cases are represented in Figure 6-1a (overlying) and 6-1b (underlying).





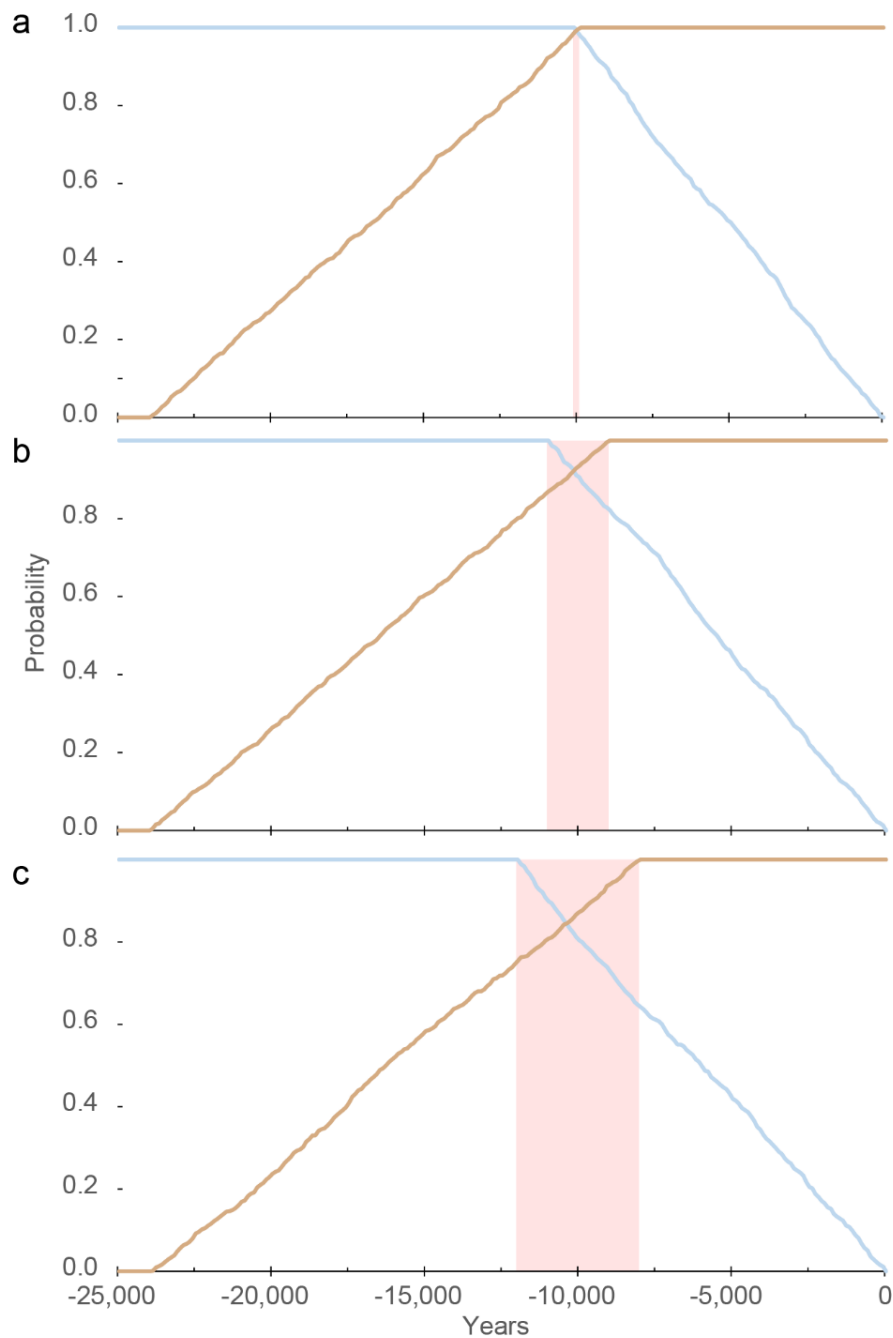
**Figure 6-1** (a) is the probability density function (pdf) representing the range of possible ages for a motif underneath a 10 ka old wasp nest. (b) is the equivalent pdf when the nest is underneath the motif. When two further nests from two different motifs are dated as in (c) and (d) the individual pdfs are summed to produce the minimum and maximum age summed probability distribution functions (Spdfs) in (e) and (f) respectively.

Where a group of motifs can be determined to belong to a single class, we want to use the age constraints provided by multiple wasp nest dates to estimate the absolute time-period over which motifs of that class were painted. The classes analysed here are the 6 main Kimberley rock art stylistic periods, but other classes could be all motifs that include a boomerang, all depictions of kangaroos, or all motifs of a particular colour for example.

If the ages of three nests overlying three motifs of the same style were as indicated in Figure 6-1c then the sum of the individual pdfs (normalised back to a maximum of 1) would have the distribution in Figure 6-1e. This graph then shows the probability that a motif has a minimum age of less than  $x$  years (based on the 3 dates), where  $x$  is any value (in years) on the horizontal age axis. Similarly, for 3 under-art nests (Fig. 6-1d), their normalised sum (Fig. 6-1f) is a graph of the probability that the maximum age of a motif is greater than  $x$  years.

To understand what these two summed probability distributions tell us about the age distribution of motifs of a particular style, consider three stylistic periods of varying durations of 200, 2000 and 4000 years, all centred on 10 ka (Fig. 6-2). In this simplified case we assume a uniform distribution of paintings throughout the period and a uniform age distribution of suitable wasp nest samples from 24 ka to the present. The oldest nest successfully dated in this study is ~21 ka so 24 ka is taken as a practical limit for illustrative purposes, but this number has no material impact on the methodology.

When the art period is as short as 200 years the possible age range for wasp nests overlying these 10 ka paintings, is between 10.1 ka and 0. Similarly, underlying nest ages may range from 24 ka to 9.9 ka. When 1000 ages are randomly generated in the over-art 10.1 – 0 ka range, the normalised sum of the pdfs (Spdfs), representing the possible age range for each of the 1000 underlying motifs, is approximately linear (Fig. 6-2a, blue curve), increasing to 1 at 10.1 ka. A corresponding set of 1000 random ages in the under-art range of 24 – 9.9 ka produce a Spdf (Fig 6-2a, brown curve) that intersects the blue curve at around 10 ka, and a probability of ~0.99. Repeating this process with hypothetical periods of 2000 years (Fig 6-2b) and 4000 years (Fig 6-2c) shows that the age at which these plots reach a probability of 1 establishes the upper and lower limit for the art period.



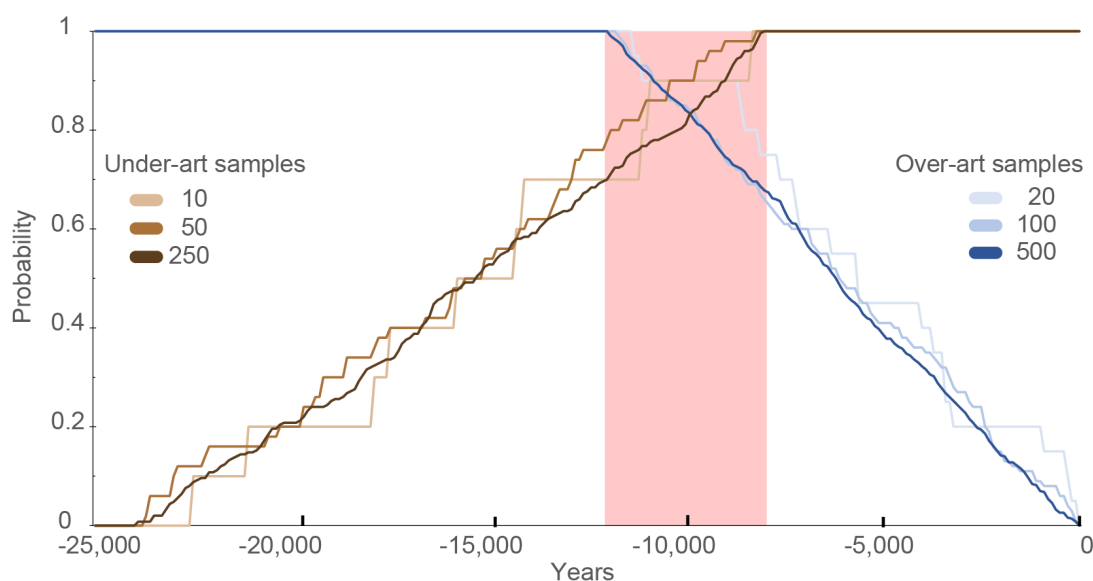
**Figure 6-2** Spdfs derived from randomly generated ages of 1000 nests under (brown curve) and 1000 nests over (blue) motifs of the same style. Three different art periods, all centred on -10,000 years, are assumed with different durations (red vertical bar): (a) 200 years, (b) 2000 years, and (c) 4000 years. The age at which the two Spdfs first reach maximum probability serve as accurate estimates for the start and end of the actual art period.

Thus, as the length of the art period increases, the probability level at which the two curves intersect will decrease: if the art period uniformly spanned the period from 24 – 0 ka (not shown) the two Spdfs would intersect at a probability around 0.5 but for a very brief period of 1 year the Spdfs would only intersect at a probability of  $\sim 1$ . Given

sufficient samples, the shape of the plots within the art period (within the red bars in Fig. 6-2) reflects the rate of art production at different times: the approximately straight lines in Figure 6-2 reflect the assumption of uniform production throughout the period.

### **6.1.2 Modelling different sample sizes**

In this study, the number of dated nests in any one art period is very much less than 2000 and there are about half as many dates determined for under-art nests as there are for those constructed over-art. This ratio of 1:2 is used in the model in Figure 6-3 where the number of randomly generated dates for over-art nests is reduced to 500, 100 and 20 and half that number for the under-art scenarios. While the plots for the 500, 100 (over-art) and 250 (under-art) sample scenarios do not deviate greatly from the plots for 1000 samples, the 50, 20 and 10 sample plots show significant variation. This modelling suggests, for runs with 100 or more samples, the shape of the Spdf within the art period (12 – 8 ka in this case) is likely to provide reliable information about the changing rate of art production. For all of these scenarios, however, the age at which the Spdf reaches 1 (100 % probability) is a useful estimate of the youngest or oldest limit of the art period. As the number of samples increases, the art period duration estimated from the youngest and oldest limit will more closely approximate the actual duration of the period.

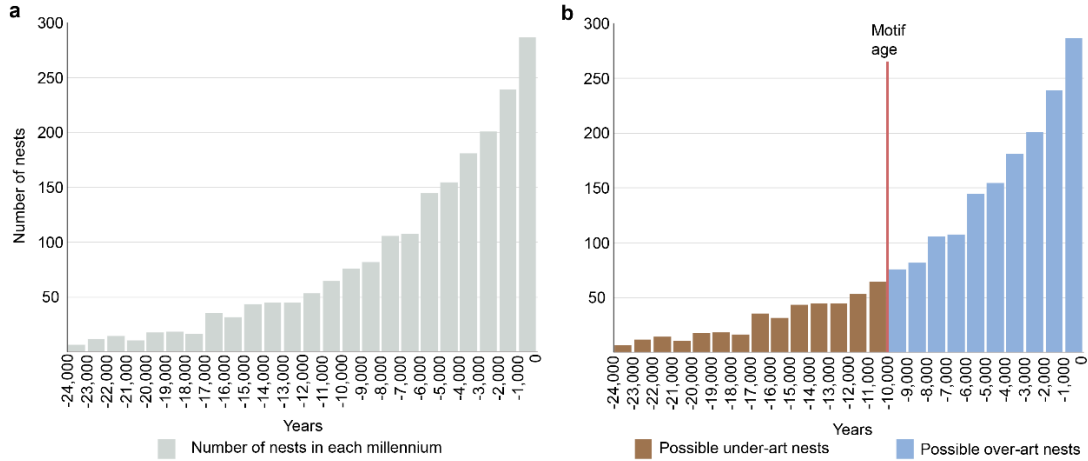


**Figure 6-3** Spdfs derived from different sized sets of randomly generated wasp nest ages constrained to be under (brown) or over (blue) motifs from an art period spanning 12 – 8 ka. The number of over-art samples is twice that of under-art samples to simulate the situation in this study.

### 6.1.3 Modelling for declining nest volume with age

The model can be refined to incorporate other observations from the data collected in this study. As demonstrated in Chapter 3, because weathering causes mud wasp nests to reduce in volume over time, the number of wasp nests that can be successfully dated decreases with age hence their age distribution will be biased toward younger ages. When the age distribution of the 75 nests dated in this study is plotted, the curve of best fit for these data is approximated by the function  $\exp(\text{Age}/7000)$  (Chapter 3, Fig. S1). An example of the age distribution of 2000 wasp nest ages, randomly generated and weighted according to this function, is depicted in Figure 6.4a where the number of nests in each millennium to 24 ka is plotted. With this large number of ages, the shape of the histogram approximates the function  $\exp(\text{Age}/7000)$ . Every nest sampled is drawn from a population with this distribution of ages, so younger nests always have a higher probability of being selected than older nests just because there are more of them. For example, for a 10,000 year old motif, the age distribution of all possible nests overlying the motif is represented by the blue bars in Figure 6-4b and the possible ages of under-art motifs are represented by the brown bars. It is evident that the greater number of young nests means that any over-art nest sampled at random is more likely to be closer to zero years old than it is to the 10 ka age of the motif. Importantly, the

opposite is true for under-art nests where **the bias toward younger nests ensures that any under-art nest sampled is more likely to be closer to the 10 ka age of the motif.** This is an important insight from this investigation.



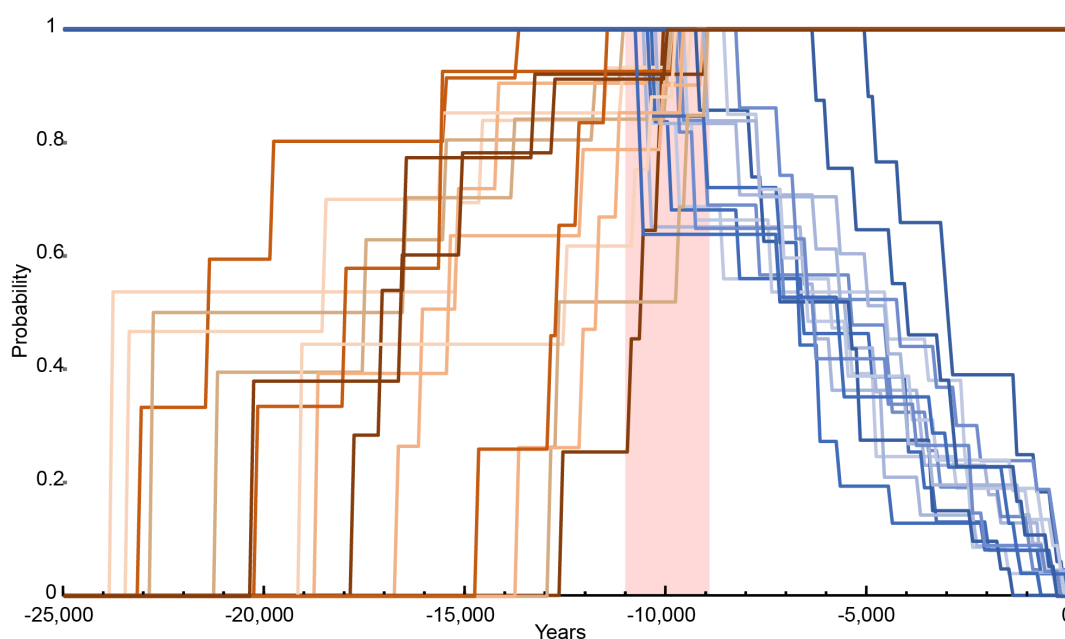
**Figure 6-4** (a) Age distribution of 2000 nests with ages randomly generated and weighted by the function  $\exp(\text{Age}/7000)$  to approximate the actual age distribution of the 75 nests dated in this study. (b) Age distribution of nests over and under a 10,000 year old motif.

To reflect this known age distribution for old nests in the model we firstly generate an appropriately biased set of random ages by applying the inverse function  $(7000 * \ln(\text{probability}))$  to a randomly generated value of probability. As before, an oldest age limit of -24,000 years is applied (for illustrative purposes) so the range of random probabilities generated is restricted to be between 0.0324 (i.e.  $\exp(-24000/7000)$ ) and 1. The set of ages produced by this method will, therefore, more accurately represent ages for wasp nests sampled.

Recognising that nest samples will be biased toward those of younger age it is appropriate to apply a correction to give greater statistical weighting to older nests and lesser weight to younger samples in subsequent analysis. This is done when calculating the Spdf by multiplying the pdf for each age measurement by the inverse factor,  $\exp(\text{Age}/7000)$ , and then normalising the sum of pdfs by dividing the Spdf by the sum of the sample weighting factors. In summary, the model is modified to firstly generate nest ages according to the observed age distribution and then the inverse of the same function is used when calculating the Spdf to reverse the bias.

#### 6.1.4 Modelling with a small number of wasp nest ages

When this revised model is used with sample sizes more typical of those available in this study for the IIAP and Gwion periods it provides a visual representation of the possible differences between the estimated chronology of an art period and the actual chronology. Figure 6-5 illustrates the model output for 15 sets of randomly generated wasp nest dates where each set includes 12 ages for over-art nests and 5 ages for under-art nests and an assumed uniform art period from 11 – 9 ka. The Spdfs exhibit wide variability between their upper and lower limits (0 and 1) and clearly the shape of these curves within the art period (red vertical bar) will provide no reliable information about the changing rate of art production. However, the age at which the maximum motif age Spdfs (brown) and the minimum age Spdfs (blue) reach a probability value of 1 (denoted as  $P(S_{max}) = 1$ , and  $P(S_{min}) = 1$  respectively) often falls within, or close to, the known art period and should therefore provide usefully accurate estimates of the upper and lower age extent.

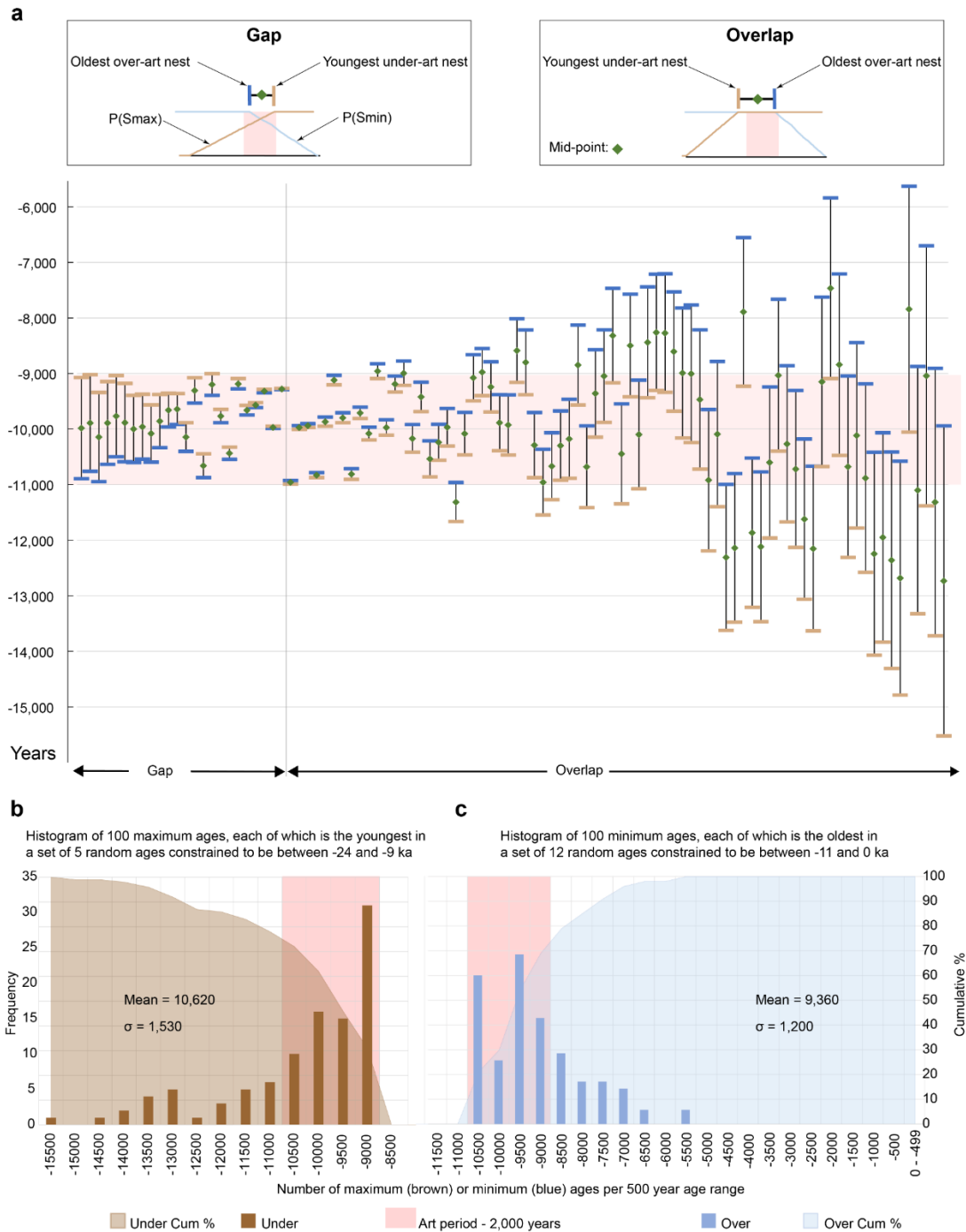


**Figure 6-5** Fifteen sets of Spdfs each derived from ages of 12 over-art (blues) and 5 under-art (browns) wasp nests assuming by an art period spanning 11 – 9 ka, using a model weighted to correct under-representation of older nests.

To quantify this accuracy when just 17 nest ages (12 over-art and 5 under) are used to estimate the extent of an art period, 100 randomly generated sets of nest ages were analysed. The age at which the minimum age Spdf (blue) reaches a probability of 1 (i.e.  $P(S_{min}) = 1$ ) is the age of the youngest over-art nest. Similarly, the age of the oldest under-art nest is the equivalent point for the maximum age Spdf (brown) (i.e.

$P(S_{max}) = 1$ ). When the age of the youngest over-art nest is subtracted from the age of the oldest under-art nest the difference is negative if the two plots overlap and positive if there is a gap (see Figure 6-6a). For the 100 simulations of 17 nest ages, 24% of the differences result in a gap and 76% in an overlap that varies in duration from 65 to 5580 years (Figure 6-6a). We know that when a very large number of nest samples are measured this difference is a gap with lower and upper ages that are a very close estimate for the start and end dates for the art period (Fig. 6-2). We can therefore conclude that overlaps are indicative of a dataset less likely to represent the actual art period chronology. Even so, the youngest under-art age in each run falls within the 2 ka art period in 72% of cases (Figure 6-6b). The oldest over-art age is within the art period in 69% of runs (Figure 6-6c). In all 100 runs, at least one end of the gap/overlap period falls within the actual art period and 47% of the time both ends fall within this 11 – 9 ka period. When there is a gap rather than an overlap, the gap always falls wholly within the actual art period. The mean of the mid-points of the gaps/overlaps ( $((P(S_{max}) = 1) + (P(S_{min}) = 1))/2$ ) is -9,986 years and the standard deviation,  $\sigma$ , is 1099 years so the single standard deviation range is close to the actual art period of  $-10,000 \pm 1,000$  years. The estimated mid-point is within 10% of the actual mid-point in 69% of runs. The average length of the gap/overlap for these data is -1261 years with a standard deviation of -1662 years.

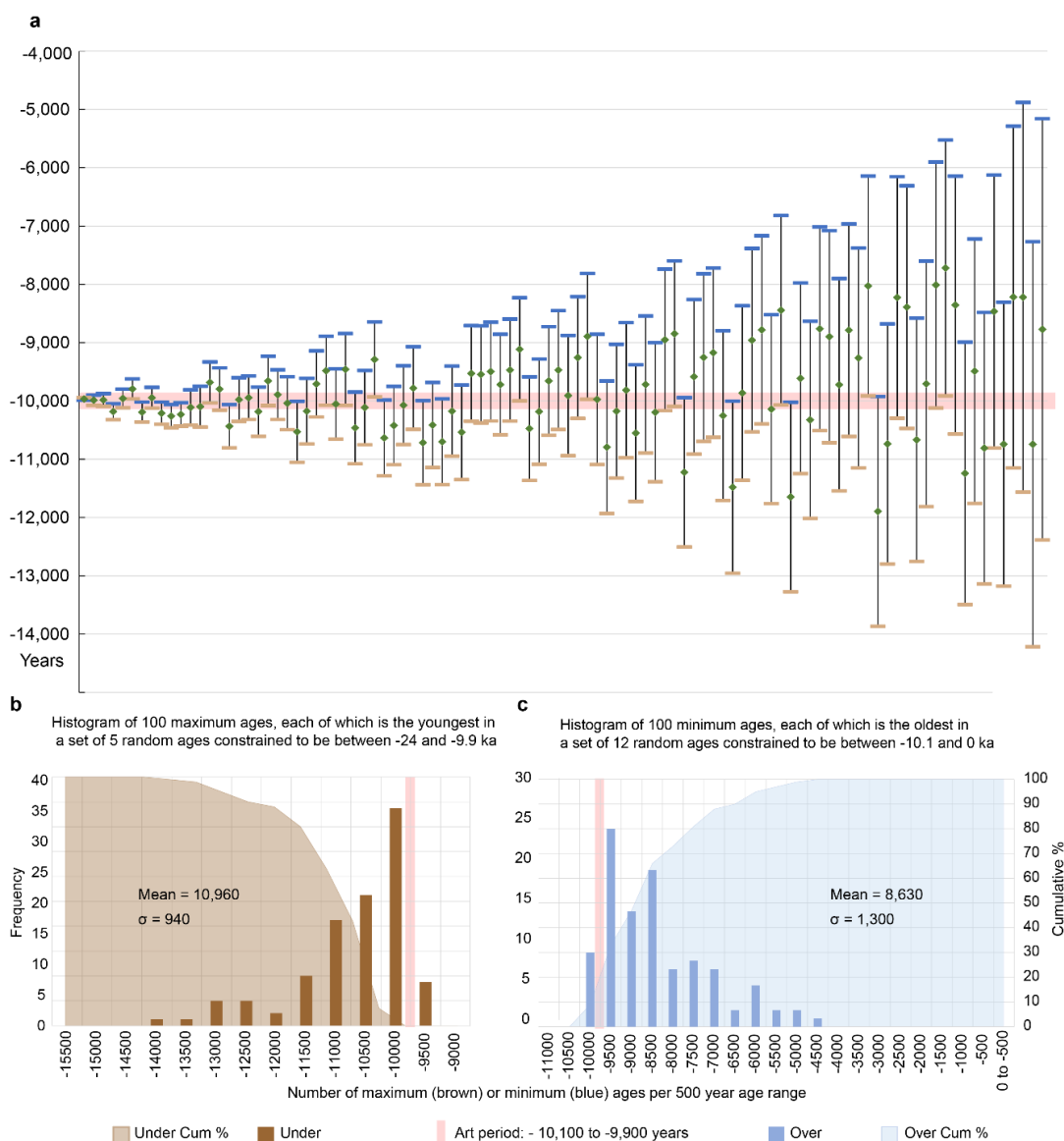




**Figure 6-6** (a) Gaps/overlaps from 100 simulations (each with 12 over-art and 5 under-art wasp nests, assuming an art period spanning 11 – 9 ka, using a weighted model) sorted left to right by gap size. The difference between the age of the youngest under-art nest (short brown bar) and the oldest over-art nest (short blue bar) is positive for a “gap” (24 of the runs), and negative for an “overlap” (76 runs). A green diamond marks the mid-point between the two. (b) Histogram of the age of the youngest under-art sample from each of 100 runs and the corresponding cumulative density function. (c) Histogram of the oldest under-art samples from each run.

When the art period is reduced to 200 years, again centred on 10 ka, the estimated mid-point is within 10% of the actual mid-point in 75% of these 100 runs (Figure 6-7).

The mean of the 100 mid-points is -9797 years and the standard deviation is 814 years. The gap/overlap falls entirely within the narrow art period in only 3% of runs but the youngest under-art age in each run falls within the 200-year art period in 15% of runs (Figure 6-7b). The oldest over-art age is also within the art period in 15% of runs (Figure 6-7c).



**Figure 6-7** Gaps/overlaps from 100 simulations (12 over-art and 5 under-art wasp nests and, assuming an art period spanning 200 years from 10.1 – 9.9 ka, using a weighted model). The difference between the age of the youngest under-art nest (short brown bar) and the oldest over-art nest (short blue bar) is negative (an “overlap”) for all but one simulation. Histograms of the 100 maximum ages (b), and 100 minimum ages (c) with corresponding cumulative distributions.

This model assumes zero age measurement uncertainty and perfect classification of motifs to the particular style. Typically, an actual calibrated age determination for a 10,000 year old nest will have an analytical uncertainty span of about 500

years for the 95.4% probability range. The effect on the Spdf plots is to smooth the inflection points over time but the overall shape of the Spdfs is retained. For a real dataset, the estimates of the upper and lower limits of the art period are particularly dependent on the accuracy of the age for the youngest under-art nest and the oldest over-art nest so these should be most critically reviewed.

#### **6.1.5 What is a “good” estimate?**

The aim of this study is to use the ages of wasp nests underlying and overlying rock art to estimate the start, end, and median age of the previously defined art periods. The foregoing analysis of randomly generated wasp nest ages suggests that the oldest over-art wasp nest and the youngest under-art nest can provide a useful estimate for the timing of an actual art period. The accuracy of the estimate improves with sample size but as few as 100 over and 100 under-art nests will provide both an accurate estimate of the art period start and end points as well as information regarding relative rates of production within that period.

As sample sizes reduce to the actual numbers available in this study for the IIAP and Gwion periods, the estimated extent of the art period will fall within the range of the actual art period about half the time. Importantly, if the age of the youngest under-art nest is younger than the age of the oldest over-art nest (i.e a gap rather than overlap between the two Spdf curves at a probability of 1) then those two points will always fall within the actual art period so we determine that art in that style was produced, at least, between those two ages.

If, on the other hand, the age of the youngest under-art nest is older than the age of the oldest over-art nest (i.e the two Spdf curves overlap at a probability of 1) then the mid-point between these two ages is the more useful estimate. At worst, the mid-point is an estimate of the median age of the art period and will be within ~10% of the actual median in ~70% of cases using 12 over-art and 5 under-art nest ages.

### **6.2 A hypothesis for the chronology of the Kimberley rock art sequence**

When motifs that are at least rated as “likely” to belong to a particular period are included, the numbers of dates that can be used to develop a hypothesis for the overall

chronology are listed in Table 6-1. Where more than one nest has been dated for a single motif only the oldest over-art and/or the youngest under-art nest are included. As described above, the hypothesis is based on the summed probability density functions for the ages of the nests and, in particular, the age of the oldest over-art nest, the youngest under-art nest and the mid-point between the two.

**Table 6-1** Number of nests dated and key ages (in years, median, cal BP) for each of the main stylistic periods

Period	Overlying nests	Underlying nests	Oldest Over-art Nest	Youngest Under-art Nest	Mid-point
Cupule/Groove	3	-	7,310	-	-
IIAP	12	4	17,480	12,990	15,230
Gwion	14	6	12,120	12,700	12,410
Static Polychrome	1	3	4,810	11,420	8,120
Painted Hand	2	2	8,340	9,400	8,870
Wanjina	3	-	600	-	-

For the purported oldest period in the Kimberley sequence, the Cupule/Abraded Groove period, the three minimum ages on two cupules and an abraded groove, all from the same rock art panel, indicate only that at least one motif in this style is older than ~7.2 ka. At the other end of the scale, the three minimum dates relating to the recent Wanjina period motifs confirm only that some of these motifs are at least 500 years old. While the number of samples associated with engravings is limited by their rarity, the small number of Wanjina samples is more a result of the focus in this study toward the older art styles.

Just 4 dates are available for each of the Static Polychrome and Painted Hand periods, so the estimated chronology for these will be of much lower reliability. These low numbers again largely reflect the lower abundance of motifs in these styles in the areas studied. Nonetheless, the data suggest the Painted Hand period is centred around 8.9 ka, and spans the period from 9,400 to 8,300 cal BP (Figure 6-7). Similarly, the mid-point for the Static Polychrome data is ~8.1 ka with a broad span from 5 – 11 ka. This apparent overlap is at variance with the expected sequence of these two styles but is very poorly defined owing to the limited sample numbers. If, in the absence of evidence to the contrary, we accept the additional constraints imposed by the relative

Kimberley stylistic sequence, then we constrain the Static Polychrome period to be older than Painted Hand period. The modified hypothesis is then that the Static Polychrome period occurred at around 11,000 to 9,000 years ago followed by the Painted Hand period around 8,500 to 9,000 years ago. Modelling suggests a large uncertainty associated with this hypothesis as it is based on just 8 wasp nest ages so further dates are required to refine this chronology.

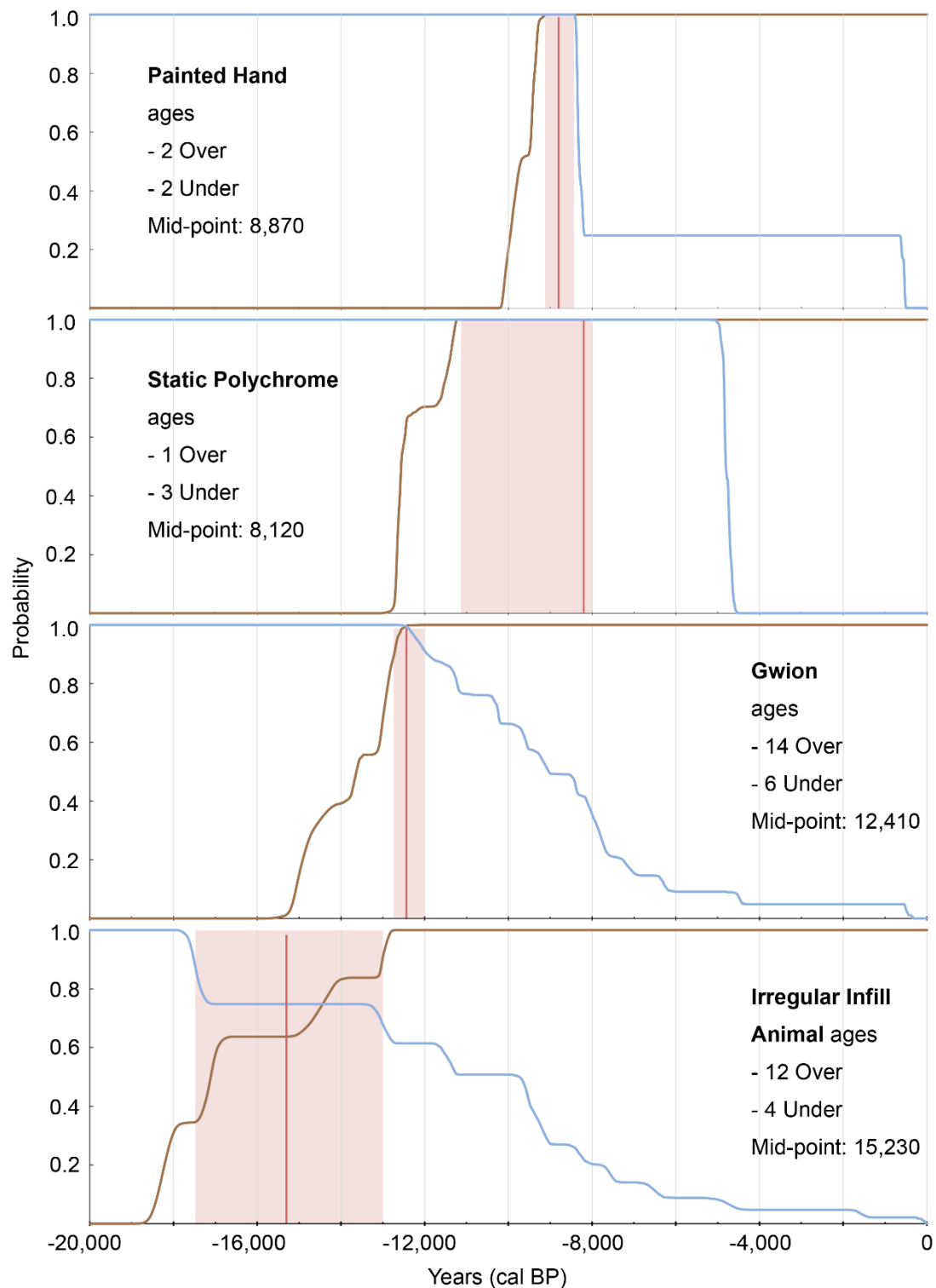
The hypothesis derived from the Gwion related dates, however, is more robust using 20 age constraints for Gwion motifs but excluding one low reliability minimum age of ~7ka on DR013\_10 and a minimum age of ~17 ka for DR006\_03 for reasons outlined in Chapter 3. The estimated mid-point at 12.4 ka is highly likely (with a probability of around 70%) to be within 10% of the median of the actual age distribution of all Gwion motifs in the area surveyed. These data also suggest a period of proliferation for the Gwion period between 13 – 12 ka albeit with the possibility of some older Gwion motifs such as DR006\_03 at more than 17 ka. The Gwion motif DR015\_07 is one of only two motifs in this study where both underlying and overlying nests were successfully dated. The age bracket for this motif of 12.7 – 11.5 ka provides further support for the proposed Gwion period chronology.

A total of 27 radiocarbon dates on 16 IIAP motifs were used to infer the chronology for this period. The calculated mid-point of the IIAP is 15.2 ka and modelling suggests this will be within ~10% of the actual median for this period with a probability of ~70%. Importantly, the oldest over-art nest (17.5 ka cal BP median) is older than the youngest under-art nest (13 ka cal BP) so the IIAP can be interpreted with some confidence to span the period from 17 – 13 ka cal BP, at least. The most securely dated motif in this study is the IIAP macropod painting DR015\_10 whose age is constrained by 6 radiocarbon dates to be between 17,500 and 17,100 years old, within the earlier part of this period.

These results suggest that the Gwion period followed the IIAP but the sample sizes are small so, without further evidence, we cannot rule out the possibility that these two styles were in use concurrently. From the limited results for Static Polychrome and Painted Hand motifs it seems these two periods were also closer together in time, if not overlapping, then followed by a long break of some 4,000 years before the start

of the Wanjina period around 4 ka, as reported by others (Welch 2015, Veth et al. 2017)

In summary, the hypothesis derived from these data for the chronology of the Kimberley rock art styles is that the IIAP style was in use from at least 17,000 to 13,000 years ago. It was followed by the Gwion period from 13,000 – 12,000 years ago and then the Static Polychrome period 11,000 to 9,000 years ago. The Painted Hand period followed at around 8,500 to 9,000 years ago.



**Figure 6-8** Hypothesised chronology of the Kimberley rock art sequence. Blue curves are the sum of the minimum age pdfs (from nests over art). Brown curves are the maximum age pdfs (nests under art). The red line is the mid-point between the ages of the oldest over-art nest and the youngest under-art nest. The broad red bar is the hypothesised extent of the art period.

### 6.3 References

Veth, P., C. Myers, P. Heaney and S. Ouzman (2017). "Plants before farming: The deep history of plant-use and representation in the rock art of Australia's Kimberley region." Quaternary International.

Welch, D. M. (2015). Aboriginal Paintings of Drysdale River National Park, Kimberley, Western Australia. Coolalinga, Northern Territory, David M. Welch.

Veth, P., C. Myers, P. Heaney and S. Ouzman (2017). "Plants before farming: The deep history of plant-use and representation in the rock art of Australia's Kimberley region." Quaternary International.



## **Chapter 7**

### **Conclusion**

The main findings from this study are summarised below and recommendations are made for future work to build on these results. Chapter 2 detailed the outcomes from the analysis of both modern and old mud wasp nests using a range of established geochemical techniques. This investigation guided the iterative development of physical and chemical pretreatment methods to improve the carbon yield for radiocarbon dating and to explain some unexpected results. In Chapters 3, 4 and 5 the 101 radiocarbon age determinations derived from 75 old wasp nests are grouped into one of the six main Kimberley rock art stylistic periods. The method used to derive an estimate for the duration of a stylistic period from the maximum and minimum age constraints provided by dated wasp nests is introduced in Chapter 3 using samples relating to the Gwion period as an example. The method is fully developed in Chapter 6. Monte Carlo statistical experiments are employed to study the accuracy and precision of chronological models derived from age constraints. Finally, the statistical model is used to refine a chronological hypothesis for the main periods in the Kimberley rock art sequence and to estimate its reliability based on the number of samples available.

#### **7.1 Mud wasp nests - observations**

##### **7.1.1 Modern mud wasp nests**

Observations of wasps collecting mud and building nests were made during two Wet season field trips in 2016 and 2017. Thirty freshly constructed nests were collected. Analysis of these established that they were composed mostly of quartz sand with the average carbon concentration in 5 nests measured at just 1.2% by weight. Disaggregation of 13 modern nests revealed the main sources of carbon to be charcoal and plant material in roughly equal volumes with much smaller volumes of insect sclerites and even less pollen. Unlike plant material, charcoal is likely to persist for millennia and was selected as the target for radiocarbon pretreatment and dating.

One risk with using the age of charcoal as a proxy for the time of wasp nest construction is that it is known that charcoal found on or near the surface in some places may be thousands of years old. Hence the inbuilt or inherited age of charcoal at the time it is collected by the mud wasp may be similarly old. However, there are good reasons to believe this is a rare occurrence. Environmental conditions in the Kimberley do not favour preservation of dead wood due to the action of termites and frequent bushfires, and trees in the region are usually less than 200 years old (Ogden 1981, Vigilante et al. 2004). Carbon isotope measurements on 5 modern nests suggest that much of the pyrogenic carbon they contain is from short-lived, abundant grasses (such as spinifex) and sedges rather than longer lived trees (McWilliam and Mison 1974, Hattersley 1983). Radiocarbon measurements on components extracted from 19 modern wasp nests confirmed that although most nests contain only modern carbon, some do preserve a significant inbuilt age. The mean age of charcoal in 9 modern nests was measured to be 255 cal years. Therefore, the radiocarbon age measured for any old nest will have some additional uncertainty due to the possible inbuilt age of the charcoal. Importantly, at less than a few hundred years on average, this uncertainty is only about 2-3% of the ages of most interest in this study.

### **7.1.2 Old mud wasp nests**

Having determined the composition of nests at the time of their construction, older nests from more than 150 rock shelters were studied to understand how both nest morphology and composition change over time. The great majority of old nests are preserved as thoroughly mineralised residual stumps of those parts of the nest that are in close contact with the rock surface. Individual remnant cells of the nest have a characteristic oval shape that aids their recognition on the rock shelter surfaces even when only a fraction of the material remains. The median sample mass of all old nests collected is ~250 mg and most have a maximum length in the range of 2 – 4 cm.

Inspection of polished sections of mounted samples confirmed that many old nests have outer surfaces coated with a mineral accretion that, in some cases, contained microscopic dust or charcoal particles. X-ray diffraction (XRD) and X-ray fluorescence (XRF) spectrometry techniques were used to analyse the mineral composition of old nests and to identify potential sources of exogenous carbon contamination. Minerals in a total of 39 old nests and 82 mineral accretions (Green et

al. 2017a, Green et al. 2017b) were identified. The carbon bearing calcium oxalate minerals (particularly whewellite) were commonly found in accretions but the only other carbon source identified was from carbonates, and these are rare.

The average carbon concentration in old nests was measured to be 0.2%, (c.f. 1.2% in modern nests) but is highly variable.

### **7.1.3 Field sampling**

Between 2015 and 2017, more than 500 mud wasp nest samples were recorded and removed from 125 of the more than 150 Kimberley rock shelters visited. This represents an unprecedented level of close observations of wasp nests of all ages and the context they share with rock art. Based on this experience, the most critical aspect of the sampling process is to unambiguously establish the relationship between the sample to be removed and the rock art and then to record that evidence at a high resolution. A useful practice is to have at least two people on-site making independent assessments of the sample context. They then arrive at a consensus before the sample is removed. They should also agree beforehand as to what they expect to see after the sample is removed to confirm the assumed context. Often this amounts to agreeing that it appears a nest overlies pigment, in which case removal of the nest should expose further pigment still adhered to the rock surface or on the base of the sample removed.

Another important lesson from extensive field observations is an understanding of how nest morphology changes over time. This makes it possible to identify possibly problematic samples where the original nest has been subsequently reworked by a different species of wasp or bee or where nests constructed at different times may be mistaken as a single, multi-cell nest. In both cases the problem is that different parts of the sample will have different ages so only that part of the sample directly over or under pigment should be dated (Chapter 3).

## **7.2 Radiocarbon pretreatment**

The investigations described above guided the development of methods to remove potential carbon contamination from the wasp nest sample while preserving as much of the original charcoal as possible. It became clear that it was particularly important to remove any modern carbon contamination from under-art samples, whereas for

over-art samples, the risk of such contamination can be tolerated if the yield is significantly improved, as it will not invalidate the interpretation as a minimum age.

### **7.2.1 Physical pretreatment**

Given that surface mineral accretions are found on many old wasp nests it is always desirable to mechanically remove the exposed outer surface of a sample where possible. High speed Dremel type drills are often unsuitable for this purpose as it is difficult to secure the sample against the high energy imparted by the drill. Variable speed drills, set on very low speeds, are more suitable when fitted with small cylindrical or disk-shaped diamond coated bits. With experience, it is possible to remove the sample from the rock surface as larger pieces, more readily cleaned in this way with a drill. If the sample pieces are smaller than about 5 mm then they should be cleaned ultrasonically by being placed in an ultrasonic bath inside a beaker of ultrapure water.

### **7.2.2 Chemical pretreatment**

Experimentation using variations on the established ABA (acid-base-acid) charcoal pretreatment protocol included the use of hydrofluoric acid (HF) and heavy liquid separation (HLS). HF was tried as a way to increase the carbon concentration by dissolving the quartz that makes up most of the nest sample. It was found to be unsuitable as it tended to also dissolve the older charcoal and remove it along with the quartz. HLS treatment was useful as an investigative tool but did not improve the yield by concentrating all charcoal in a light fraction, as intended. Significant amounts of (heavily indurated) charcoal were still found to be present in heavy fractions after such treatment. There was evidence to suggest that the concentration of hydrochloric acid (HCl) normally used in ABA pretreatment was inadequate to ensure complete removal of the oxalate minerals so later pretreatment always used more concentrated (8 or 16 M) HCl.

### **7.2.3 Reliability Score**

Given that physical and chemical pretreatment protocols evolved as the study progressed, a method was sought to communicate the degree to which some of the dated samples had a higher risk of including carbon contamination than others. For

example, samples treated with concentrated HCl have a lower risk of including carbon of unknown age from oxalate minerals, so their radiocarbon age is more reliable. Another significant factor is the mass of carbon available for dating. A small amount of carbon contamination will have a greater adverse impact on a low carbon mass sample than one with a high mass of original carbon. Hence, all else being equal, a radiocarbon age is more reliable if a larger carbon mass is available for measurement. These and other semi-quantitative factors are combined into a Reliability Score with a value between 1 (least reliable) and 10 (most reliable). Half of the score weight is based on the carbon mass, 30% on the physical pretreatment employed and 20% on the chemical pretreatment. As a relative scale, the Reliability Score serves to identify samples more or less likely to have an anomalous radiocarbon age.

An important result from the foregoing discussion is that any residual carbon contamination, still in the sample after pretreatment, is most unlikely to be older than the carbon in the nest when it was constructed. Hence any anomalous radiocarbon age may well be younger than the true age of the nest, but it is most unlikely to be older.

### **7.3 Radiocarbon age measurements**

For this study, 175 sample fractions were prepared from 120 old mud wasp nests. The initial pretreatment protocol resulted in about 40% of prepared sample fractions containing too little carbon (usually,  $< 12 \mu\text{g}$ ) to permit AMS measurement. The yield improved following changes to pretreatment processes. Ultimately, 75 of the 120 old nests were successfully radiocarbon dated with the ages ranging from modern to just over 20,000 years. Of these, 31 are more than 10,000 years old and 9 are older than 15,000 years. The distribution of ages suggests nests were built quasi-continuously over, at least, the last 20,000 years in the northern Kimberley and are, therefore, capable of providing age constraints for rock art throughout that period.

### **7.4 Motif classification**

Although the number of age constraints generated during this study is very large compared to most previous studies of the chronology of Australian rock art, as few as 3 and only a maximum of 20 dates are available for each of the main Kimberley stylistic periods. Hence any one date may significantly change the estimated

chronology for a single period. It is most important, therefore, to ensure that motifs are correctly classified to the appropriate stylistic period.

The ability to classify a greater percentage of motifs, with greater accuracy, increases with experience. Two co-authors of the published papers based on Chapters 3 and 4, Pauline Heaney and Cecilia Myers, classified the motifs represented in this study. Both are eminently well qualified for the task with experience gathered in a total of 27 years of recording and classifying Kimberley rock art. Classifications were carried out before either had any knowledge of the dates relating to the motifs. As classification is a subjective process both were asked to nominate the probability that their decision was correct. This is a measure of the level of confidence in the classification that will vary depending on the state of preservation of the motif and the distinguishing characteristics of the particular style that are present or absent.

## **7.5 Modelling rock art periods from wasp nest dates**

There is no established method to derive absolute age ranges for individual rock art periods from age constraints provided by wasp nests, or other dateable material, found over- or underlying rock art. One possible analogy is the challenge of determining when the various stone tool traditions were in use, based on the age of charcoal or other dateable material in the same excavated stratigraphic context as individual stone tools. Within a single excavation, the minimum and maximum depth at which stone tools are found can be translated into a chronological period if there is suitable dateable material at the relevant depths. This process also requires that individual stone tools be classified into a previously defined typology by a subject matter expert. Recognising that human use of any one site may have been episodic rather than continuous, it is necessary to combine evidence from many excavated sites to be confident that the full extent of the period of use of any one stone tool tradition is captured.

The probabilistic method outlined in Chapter 3, and fully developed in Chapter 6, is used to generate estimates for the beginning and end of individual rock art stylistic periods. When many more age constraints become available, the method will also indicate relative rates of art production within the period. Monte Carlo type simulations are used to understand the accuracy provided by the method used to

combine age estimates. Simulations based on the ideal case, when thousands of age estimates are available, are compared to those generated in this study where only much smaller sample numbers exist. Modelling also reveals how the results vary when the duration of the stylistic period varies from 200 years to 4,000 years. A useful observation from these simulations is that if the age of the youngest under-art nest is younger than the age of the oldest over-art nest then those two points will always fall within the actual art period so we know that art in that style was produced, at least, between those two ages. Alternatively, when the age of the youngest under-art nest is older than the age of the oldest over-art nest, the mid-point between these two ages is a more useful estimate. This estimate will be within ~10% of the actual median age of the art period ~70% of the time with sample sizes as small as 12 over-art and 5 under-art ages.

It is worth noting here that all estimates apply only to those motifs and styles still visible today. Motifs executed using less durable pigments, or in sites less favourable for preservation, may have been very much more common than is evident now.

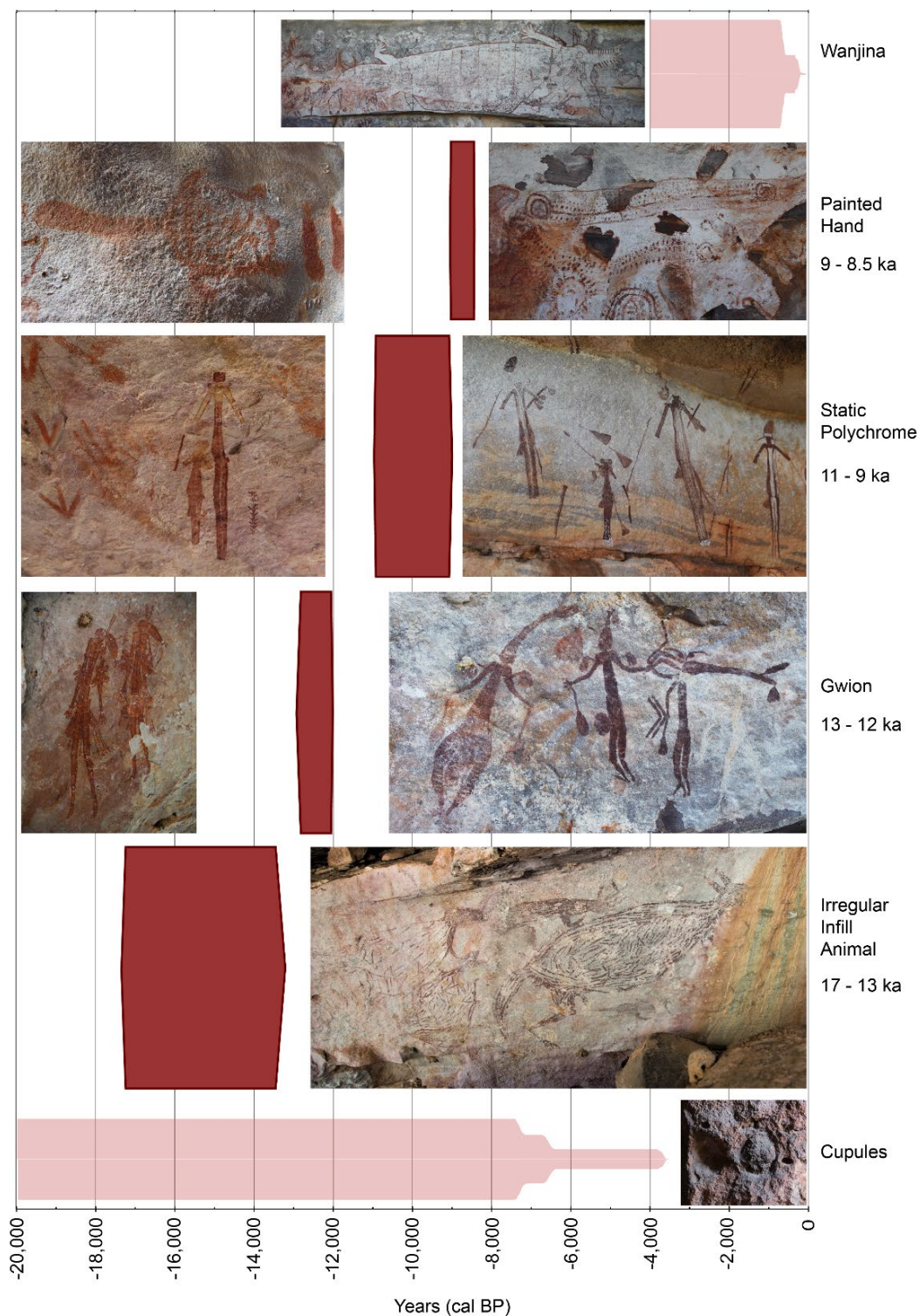
## **7.6 Hypothesised Kimberley rock art sequence chronology**

With just three overlying nests dated from inside cupules and abraded grooves from a single site there is insufficient evidence for or against the prevailing hypothesis that the Cupule/Abraded Groove period is the earliest in the Kimberley sequence. This study found only that at least one motif in this style is older than ~7.2ka. Similarly, the 3 minimum age constraints for Wanjina period motifs indicate only that some of these motifs are at least 500 years old, consistent with previous estimates.

The 4 dates available for each of the Static Polychrome and Painted Hand periods permit a very tentative hypothesis for their chronology as described in Chapter 6. They are recorded here as a starting point to which future evidence can be added. The hypotheses developed for the IIAP and Gwion periods are significantly more secure. The middle of the Gwion period is estimated to be at  $12.4 \pm 1.2$  ka with a probability of ~70%. The mid-point of the IIAP is calculated to be at  $15.2 \pm 1.5$  ka with a probability of ~70%.

The hypothesis for the chronology of the Kimberley rock art sequence based on this evidence is summarised in Figure 7-1. A major conclusion from this study is that the results are generally consistent with the previously proposed sequence of the main rock art styles, particularly for the older IIAP and Gwion periods.





**Figure 7-1** Hypothesised chronology of the Kimberley rock art sequence. The dark red bars are the hypothesised extent of the four art periods. The lighter red bars indicate the possible age range for the Wanjina and Cupule periods based on 3 minimum age constraints for each style. The maximum age indicated for the Wanjina period reflects results published by others (see section 6.2)

## 7.7 Future work

This study has established an important foundation for further research to establish a definitive chronology for Kimberley rock art and for other Aboriginal rock art across northern Australia. The geographic extent of the sites visited is largely limited to Balanggarra country in the northern Kimberley. The known range of the older styles of Kimberley rock art extends to the coast in the west (Gamberre, Wunambal and Worora country) and far to the south (Ngarinyin country) so only a fraction of this potential area is covered in this study. Some hundreds of dated samples from these other regions will be required before the proposed chronology can be considered to fully represent the age of Kimberley rock art. Part of the research required in these new areas will include analysis of more modern nests to determine if the inbuilt age of charcoal is consistent with that measured in this study.

Even when the scale of the present research is extended to the known geographic range of the Kimberley rock art styles there are many categories of archaeological questions that can only be answered with hundreds and perhaps thousands of further dates, each defining maximum and minimum ages for particular motifs. The hypothesised chronology is, at best, probably accurate to one or two millennia. So, it is not yet possible to answer questions about the extent of any postulated gaps or overlaps between the 6 main art periods. Nor is it yet possible to confirm or refute the relative timing of sub-styles such as sash and tassel Gwion variants. Greater chronological resolution is also required to understand if a given style proliferated at different times in different parts of the Kimberley, particularly when environmental conditions changed, and sea levels rose rapidly after the Last Glacial Maximum.

As more samples are collected from more sites throughout the Kimberley the number of motifs that cannot reliably be classified to a single style will increase. Some researchers also dispute the typology defined by Walsh (1994, 2000). These issues, and others, would benefit from automated algorithms to classify motifs. Research on similar problems where general shapes, such as outline drawings of animals, are classified by computer algorithm, is underway (Wilder et al. 2018). A key prerequisite for any such development is the availability of a large number of classified images that can be used to train the algorithm. The Walsh archive, Takarakka database and

associated motif illustrations are resources ideally suited for this purpose; probably uniquely so for the scientific study of rock art.

Only 3 dates relating to the Wanjina period are reported here. This style is more common in the areas yet to be covered by the Dating project and is an obvious target for future work. As the most recent of the 6 main Kimberley art styles it is of great cultural importance to current Traditional Owners. Hence any work on these specific motifs will require even closer engagement with these communities. Sampling and pretreatment techniques will also require further development to take advantage of the stratified layers of charcoal pigment evident in some Wanjina motifs.

With around 40% of samples producing too little carbon to be reliably dated, further experimentation with pretreatment methods is justified. Currently, about 90% of carbon in the original sample is lost during the aggressive pretreatment process. Less carbon will be lost if there are fewer steps in the process as each step requires multiple rinses that remove at least some part of the wanted carbon. As long as the process continues to reliably remove contaminating carbon older than the age of the nest, a less aggressive chemical protocol can be tested, particularly for over-art samples. The use of stepped-combustion may also deliver a yield improvement. Carbon can be extracted from the sample as CO<sub>2</sub> gas at different temperatures with the CO<sub>2</sub> from oxalate minerals only being released at higher temperatures. The technique may have an overall yield benefit if it means that significantly less of the wanted carbon is removed prior to combustion.

This study has established that radiocarbon dating can be used to reliably date mud wasp nests. It has also shown that suitably sized nests can be found from all millennia in the past 20,000 years. Probabilistic methods have been developed to then translate age constraints on single rock art motifs into chronological estimates for rock art stylistic periods. Future research that builds on this foundation has a very good chance of making important contributions to Australian archaeology.

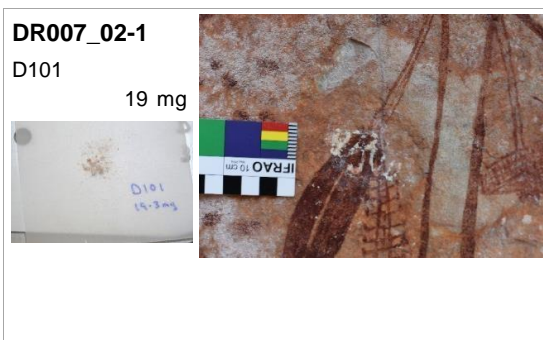
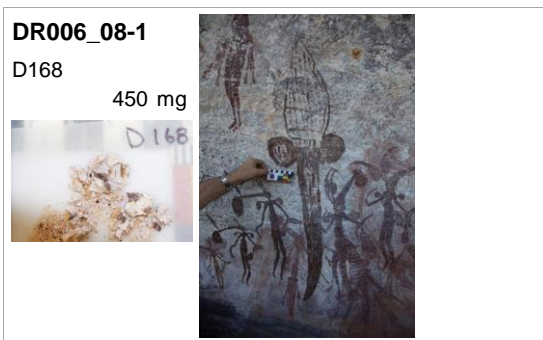
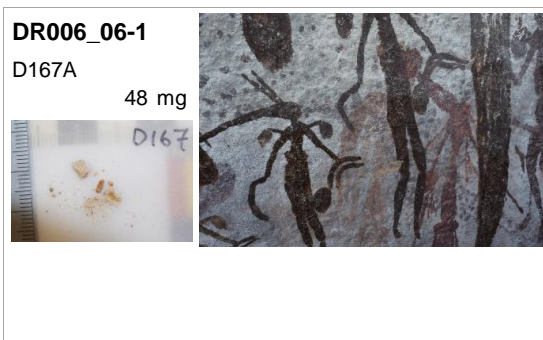
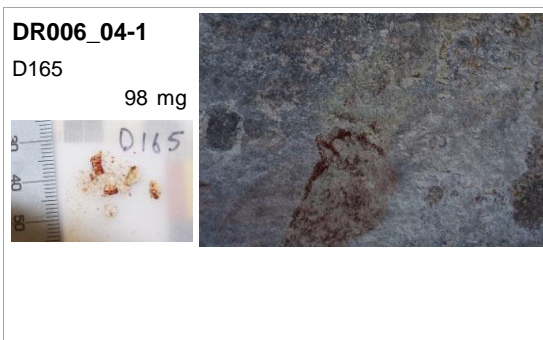
## 7.8 References

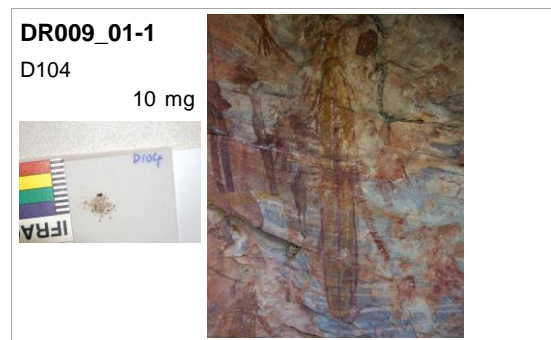
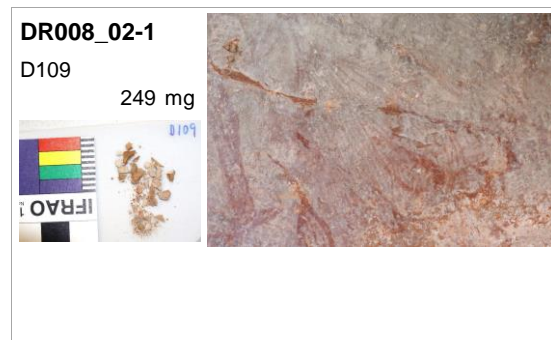
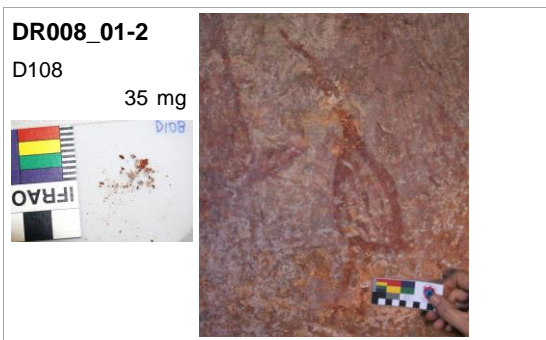
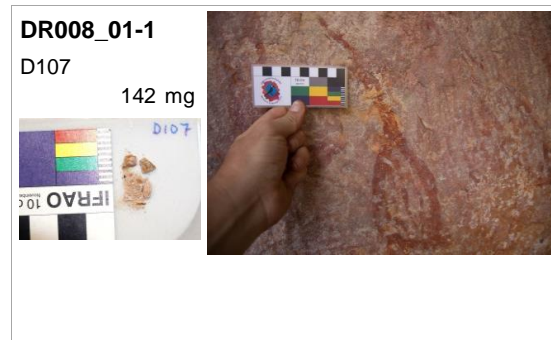
- Green, H., A. Gleadow and D. Finch (2017a). "Characterisation of mineral deposition systems associated with rock art in the Kimberley region of northwest Australia." Data in Brief.
- Green, H., A. Gleadow, D. Finch, J. Hergt and S. Ouzman (2017b). "Mineral deposition systems at rock art sites, Kimberley, Northern Australia - Field observations." Journal of Archaeological Science-Reports **14**: 340-352.
- Hattersley, P. W. (1983). "The distribution of C3 and C4 grasses in Australia in relation to climate." Oecologia **57**(1): 113-128.
- McWilliam, J. and K. Mison (1974). "Significance of the C4 Pathway in *Triodia irritans* (Spinifex), a Grass Adapted to Arid Environments." Functional Plant Biology **1**(1): 171-175.
- Ogden, J. (1981). "Dendrochronological Studies and the Determination of Tree Ages in the Australian Tropics." Journal of Biogeography **8**(5): 405-420.
- Vigilante, T., D. Bowman, R. Fisher, J. Russell-Smith and C. Yates (2004). "Contemporary landscape burning patterns in the far North Kimberley region of north-west Australia: human influences and environmental determinants." Journal of Biogeography **31**(8): 1317-1333.
- Walsh, G. L. (1994). Bradshaws, ancient rock paintings of north-west Australia. Carouge-Geneva, Switzerland, Edition Limitée for the Bradshaw Foundation.
- Walsh, G. L. (2000). Bradshaw art of the Kimberley, Takarakka Nowan Kas Publications.
- Wilder, J., I. Fruend and J. H. Elder (2018). "Frequency tuning of shape perception revealed by classification image analysis." Journal of Vision **18**(8): 21.

# Appendix 1







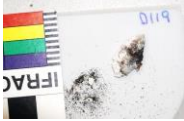









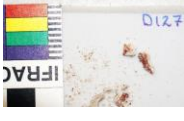
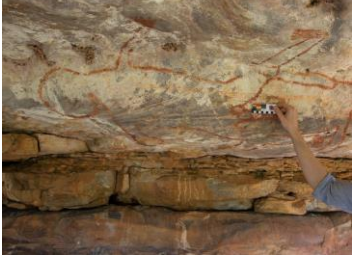
Photographs of the sampled motifs, the sample as removed and the sample mass collected.









<p><b>DR009_02-1</b> D105 5,656 mg</p>  	<p><b>DR009_03-1</b> D106 15 mg</p>  
<p><b>DR012C_01-1</b> D118 176 mg</p>  	<p><b>DR012C_02-1</b> D119 444 mg</p>  
<p><b>DR012D_03-1</b> D120 82 mg</p>  	<p><b>DR013_01-1</b> D123 120 mg</p> 
<p><b>DR013_01-2</b> D124 63 mg</p>  	<p><b>DR013_01-3</b> D125 25 mg</p>  
<p><b>DR013_02-1</b> D126 318 mg</p> 	<p><b>DR013_03-1</b> D127 200 mg</p>  



**DR013\_03-2**

D128

385 mg



**DR013\_04-1**

D129

388 mg



**DR013\_05-1**

D130

164 mg



**DR013\_06-1**

D131

8,461 mg



**DR013\_07-1**

D132

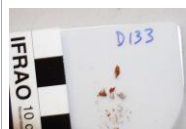
92 mg



**DR013\_08-1**

D133

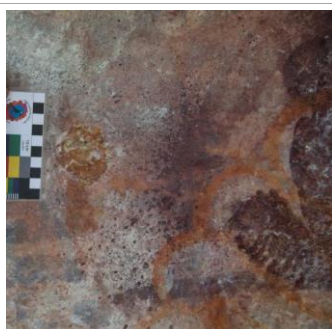
32 mg



**DR013\_09-1**

D134

10,187 mg



**DR013\_09-2**

D136

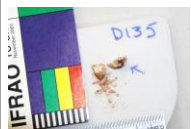
28,300 mg



**DR013\_10-1**

D135

143 mg



**DR013\_12-1**

D137A

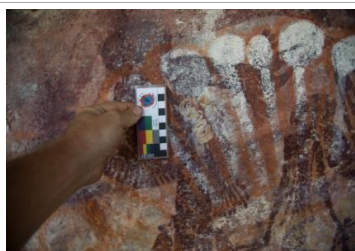
93 mg



**DR013\_12-2**

D137B

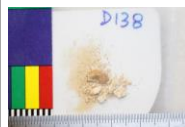
69 mg



**DR013\_13-1**

D138

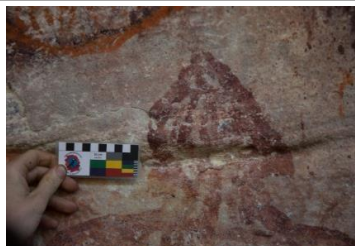
24 mg



**DR013\_13-2**

D139

383 mg



**DR015\_01-1**

D141

198 mg



**DR015\_01-2**

D142

72 mg



**DR015\_04-1**

D144

662 mg



**DR015\_04-2**

D331

963 mg



**DR015\_05-1**

D145

146 mg



**DR015\_06-1**

D147

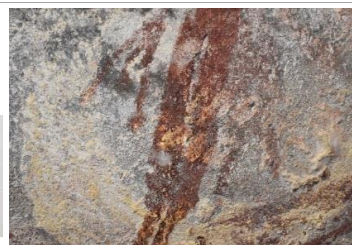
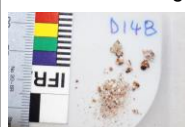
1,156 mg



**DR015\_07-1**

D148A

135 mg





**DR015\_07-2**

D148B

121 mg



**DR015\_07-3**

D370

418 mg



**DR015\_07-5**

D372

176 mg



**DR015\_08-1**

D149

456 mg



**DR015\_09-1**

D150

103 mg



**DR015\_09-2**

D151

494 mg



**DR015\_10-1**

D152

640 mg



**DR015\_10-2**

D335

2,165 mg



**DR015\_10-3**

D336

371 mg



**DR015\_10-4**

D358

439 mg



**DR015\_10-6**

D360

454 mg



**DR015\_10-7**

D600

1,052 mg



**DR015\_10-8**

D601

683 mg



**DR015\_11-1**

D153

488 mg



**DR015\_14-4**

D367

1,055 mg



**DR015\_98-1**

D155

56,000 mg



**DR015\_99-1**

D154

29,000 mg



**DR016\_01-1**

D161A

483 mg



**DR016\_01-2**

D161B

1,324 mg



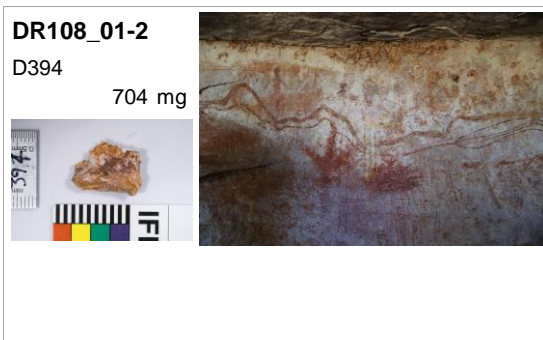
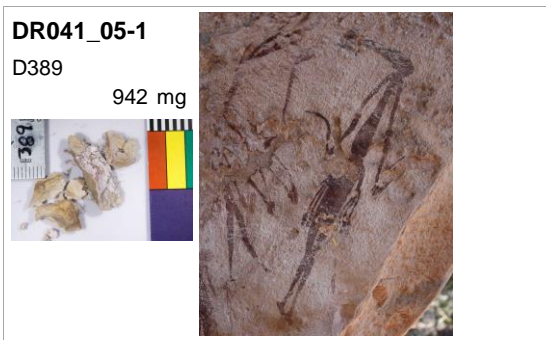
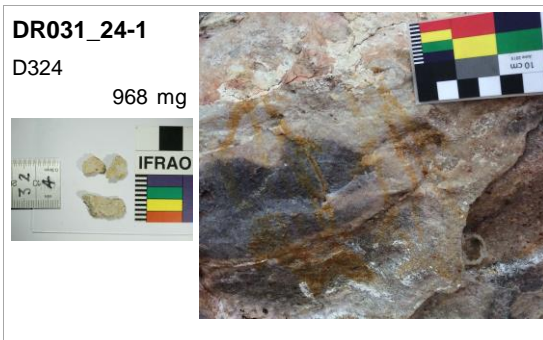
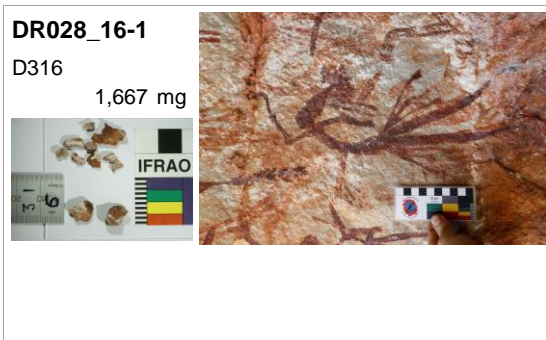
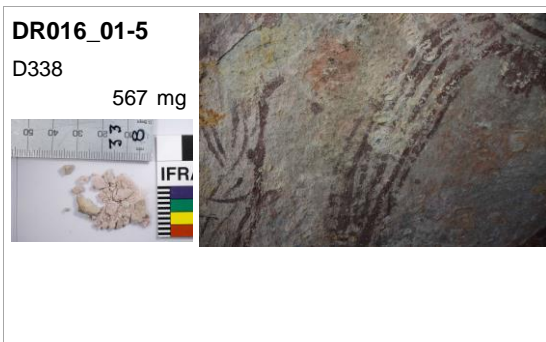
**DR016\_01-3**

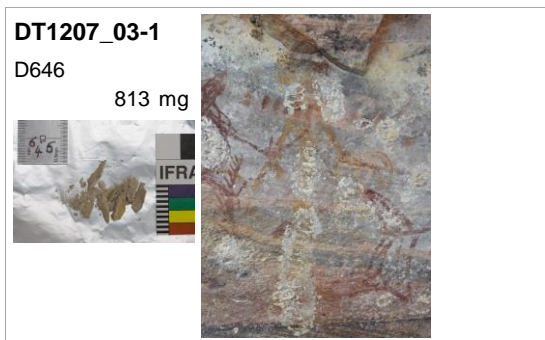
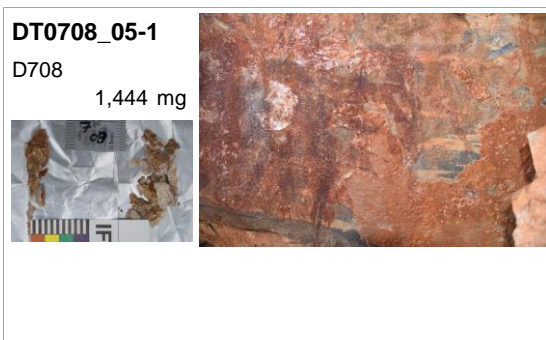
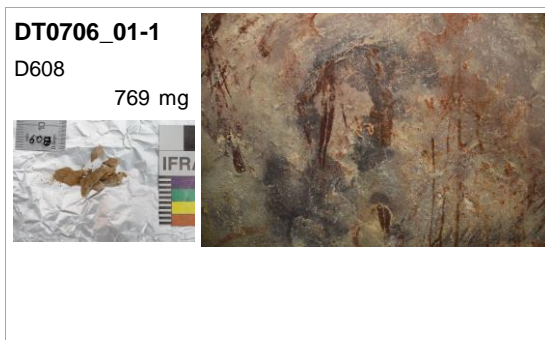
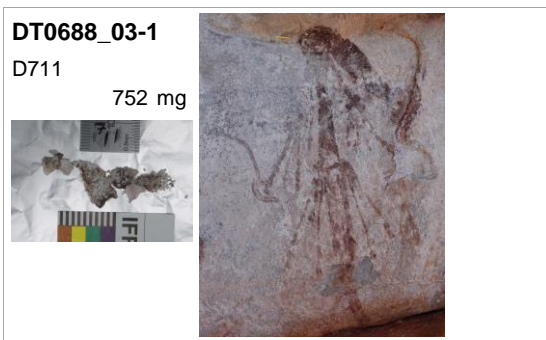
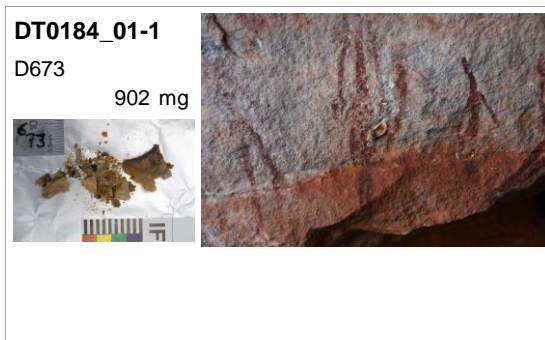
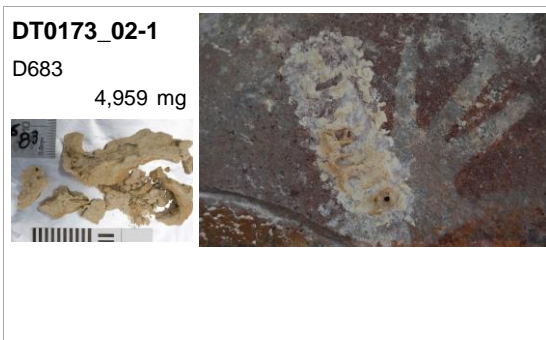
D161C

233 mg

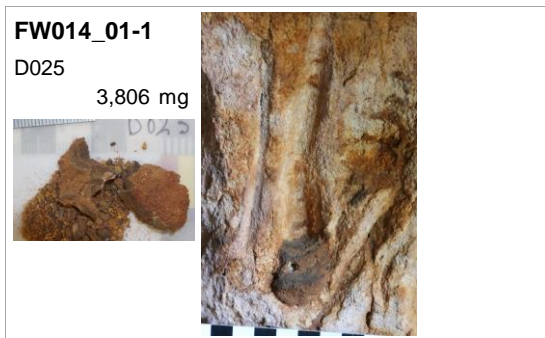
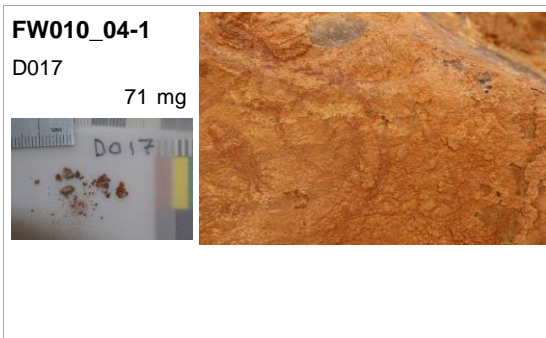
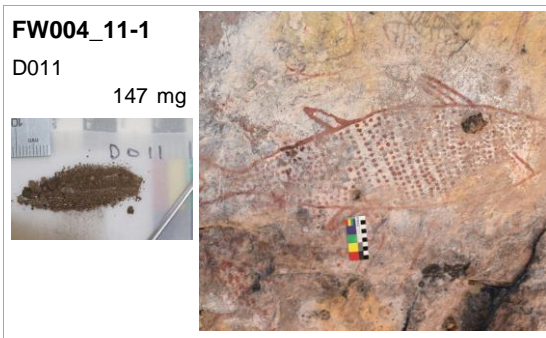
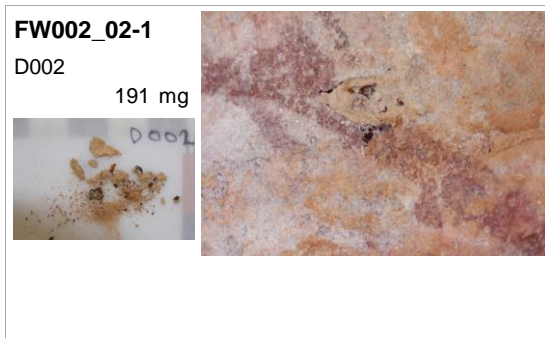
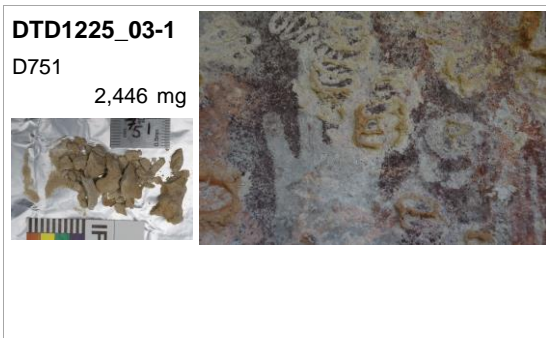
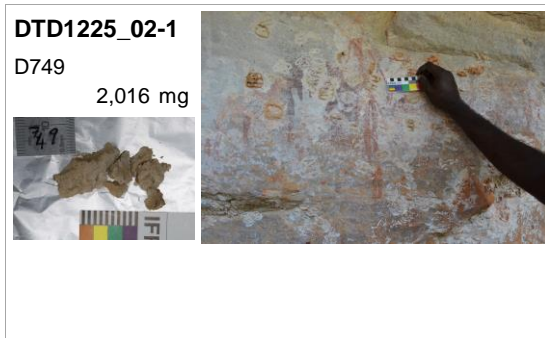
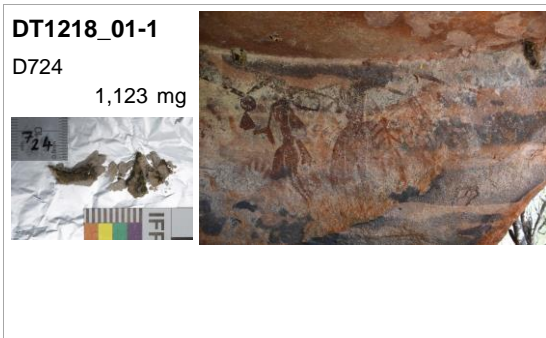


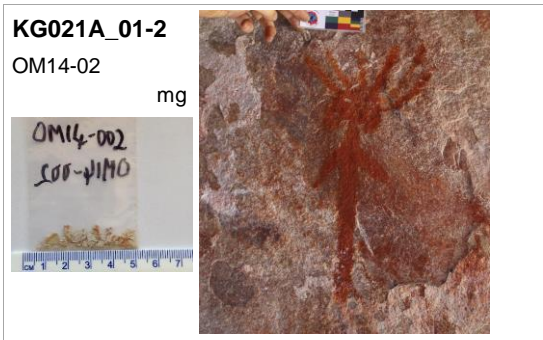
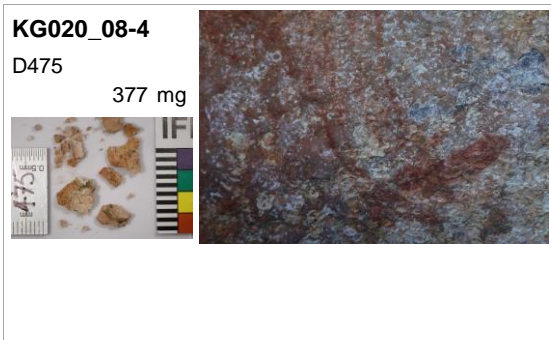
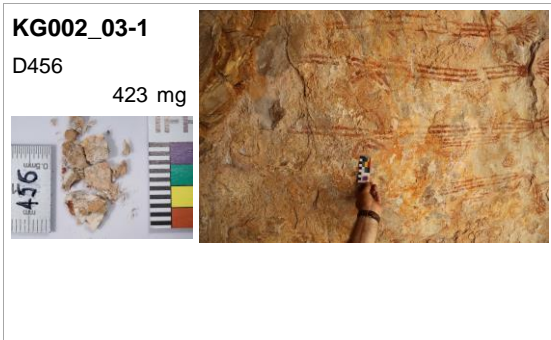
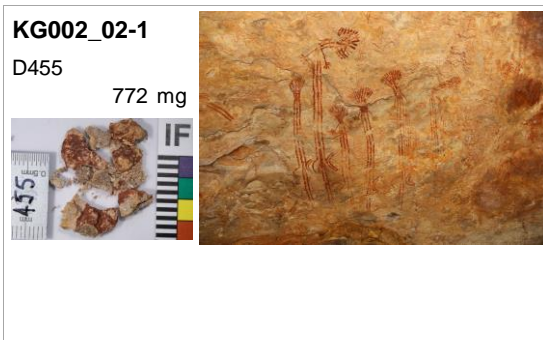
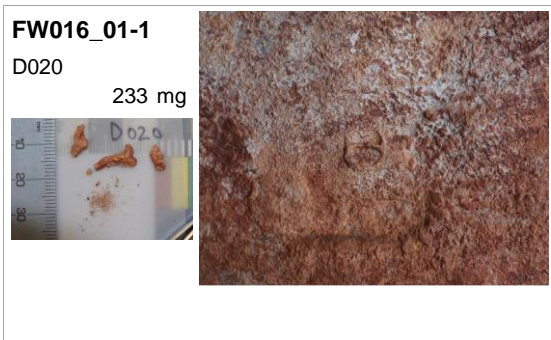
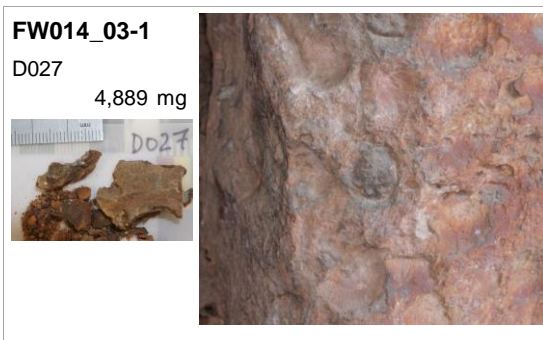
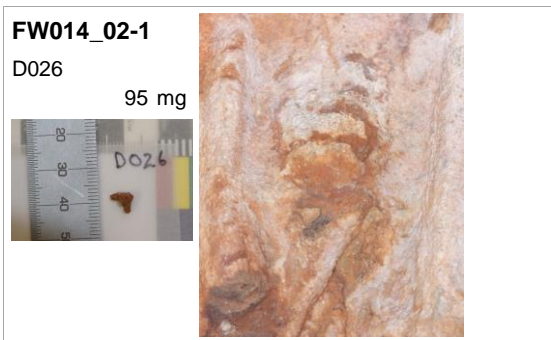




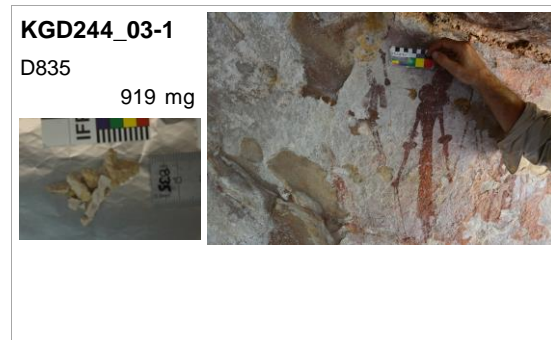
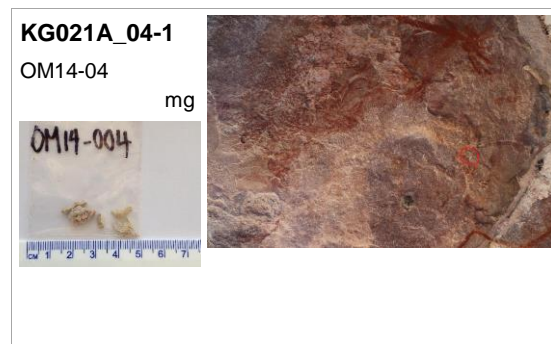
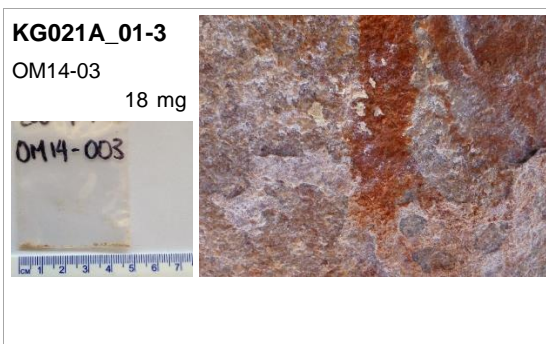












## Appendix 2

Table 1: Listing of all old wasp nest samples prepared for radiocarbon dating, with measured, uncalibrated ages and associated carbon mass. The terms used are fully described in chapter 2.

Table 2 Calibrated age ranges for old wasp nests listed in table 1

**Table 1 Old wasp nest samples prepared for radiocarbon dating**

Sample Code	Sample ID	Laboratory Code	Pretreatment Sequence	Fraction	C mass $\mu$ g	$^{14}\text{C}$ years BP	Error $1\sigma$ (years)	Rel. Score
DR006_01-1	D162	OZT789	ABA - HLS	Light	5.1	NA	NA	1
DR006_02-1	D163	OZT790	ABA	All	13.7	NA	NA	1
DR006_03-1	D164	OZT791	ABA	All	58.0	13,800	90	5
DR006_04-1	D165	OZT463	ABA	All	5.7	NA	NA	0
DR006_05-1	D166	OZT801U2	ABA - HLS	Light	18.4	-		2
DR006_05-1	D166	OZT801U1	ABA - HLS	Heavy	13.2	3,110	140	1
DR006_06-1	D167A	OZT481	ABA	All	4.4	NA	NA	0
DR006_06-2	D167B	OZT482	ABA	All	7.4	NA	NA	0
DR006_08-1	D168	OZT453x	ABA	All	25.6	15,070	180	3
DR006_09-1	D169	OZT769U*	ABA	All	39.5	1,350	110	3
DR007_02-1	D101	OZT488	ABA	All	6.3	NA	NA	0
DR007_03-1	D102	OZT793U2	ABA - HLS	Light	19.3	140	100	2
DR007_03-1	D102	OZT793U1	ABA - HLS	Heavy	7.9	NA	NA	0
DR007_03-2	D103	OZT794U2	ABA - HLS	Light	12.2	-		2
DR007_03-2	D103	OZT794U1	ABA - HLS	Heavy	6.7	NA	NA	0
DR007_04-1	D755	OZW423U2	A-HLS-BA(8M)	Heavy	46.0	8,420	60	9
DR007_04-1	D755	OZW423U1	A-HLS-BA(8M)	AcidSol	7.7	NA	NA	
DR008_01-1	D107	OZT457	ABA	All	6.1	NA	NA	0
DR008_01-2	D108	OZT489	ABA	All	40.3	2,095	50	5
DR008_02-1	D109	OZT458	ABA	All	16.5	7,540	140	1
DR008_02-2	D110	OZT459	ABA	All	7.3	NA	NA	0
DR008_03-1	D112	OZT473	ABA	All	8.0	NA	NA	0
DR008_03-2	D113	OZT474	ABA	All	8.1	NA	NA	0
DR009_01-1	D104	OZT765U1	ABA - HLS	Heavy	2.2	NA	NA	0
DR009_01-1	D104	OZT765U2	ABA - HLS	Light	7.0	NA	NA	1
DR009_02-1	D105	OZT446	ABA	All	23.5	10,730	130	5
DR009_03-1	D106	OZT766U1	ABA - HLS	Heavy	2.0	NA	NA	0
DR009_03-1	D106	OZT766U2	ABA - HLS	Light	2.6	NA	NA	1
DR012C_01-1	D118	OZT460	ABA	All	6.9	NA	NA	0
DR012C_02-1	D119	OZT795U*	ABA	All	32.6	8,720	110	4
DR012D_03-1	D120	OZT767U1	ABA - HLS	Heavy	5.0	NA	NA	1
DR012D_03-1	D120	OZT767U2	ABA - HLS	Light	6.3	NA	NA	1
DR013_01-1	D123	OZT461	ABA	All	87.9	NA	NA	5
DR013_01-2	D124	OZT787	ABA	All	40.6	510	40	4
DR013_01-3	D125	OZT796U*	ABA	All	8.4	NA	NA	0
DR013_02-1	D126	OZT772	ABA - HLS	Light	5.0	NA	NA	1
DR013_03-1	D127	OZT773	ABA	All	23.3	993		2
DR013_03-2	D128	OZT774	ABA - HLS	Light	2.0	NA	NA	1
DR013_04-1	D129	OZT775	ABA	All	23.9	11,900	90	5
DR013_05-1	D130	OZT776	ABA	All	22.2	8,240	80	2
DR013_06-1	D131	OZU776U1	A-HLS-BA(8M)	Light	26.5	10,820	120	7
DR013_06-1	D131	OZU776U2	A-HLS-BA(8M)	Heavy	33.1	11,340	90	7
DR013_06-1	D131	OZT447	ABA	All	14.6	15,350	200	3
DR013_07-1	D132	OZT475	ABA	All	7.6	NA	NA	0

Sample Code	Sample ID	Laboratory Code	Pretreatment Sequence	Fraction	C mass $\mu$ g	$^{14}\text{C}$ years BP	Error $1\sigma$ (years)	Rel. Score
DR013_08-1	D133	OZT490	ABA	All	4.8	NA	NA	0
DR013_09-1	D134	OZT797U*	ABA	All	48.5	11,530	80	5
DR013_09-1	D134	OZT797U1	ABA - HLS	Heavy	26.5	15,940	160	3
DR013_09-1	D134	OZT797U2	ABA - HLS	Light	110.0	16,930	100	7
DR013_09-2	D136	OZU777U1	A-HLS-BA(8M)	Light	42.6	1,370	610	8
DR013_09-2	D136	OZT798U2	ABA - HLS	Light	50.9	4,920	80	7
DR013_09-2	D136	OZW355	A-HF-HLS-BA(8M)	Heavy	13.5	10,190	110	5
DR013_09-2	D136	OZU777U2	A-HLS-BA(8M)	Heavy	40.1	11,170	80	8
DR013_09-2	D136	OZT798U1	ABA - HLS	Heavy	20.2	11,350	150	3
DR013_09-2	D136	OZW354	A-HF-HLS-BA(8M)	Light	11.1	15,780	200	5
DR013_09-2	D136	OZT798U*	ABA - HLS	All	8.9	NA	NA	0
DR013_10-1	D135	OZT462	ABA	All	22.5	6,070	120	3
DR013_12-1	D137A	OZT476	ABA	All	11.7	NA	NA	0
DR013_12-2	D137B	OZT491	ABA	All	5.4	NA	NA	0
DR013_13-1	D138	OZT777	ABA - HLS	Light	15.1	NA	NA	2
DR013_13-2	D139	OZT778	ABA - HLS	Light	2.8	NA	NA	3
DR015_01-1	D141	OZT477	ABA	All	13.4	6,970	170	2
DR015_01-2	D142	OZT492	ABA	All	14.4	740	120	1
DR015_04-1	D144	OZT448U1	ABA - HLS	Light	18.0	6,440	680	1
DR015_04-1	D144	OZT448	ABA	All	11.1	NA	NA	0
DR015_04-2	D331	OZU778U1	A-HLS-BA(8M)	Light	16.8	7,010	90	5
DR015_04-2	D331	OZU778U2	A-HLS-BA(8M)	Heavy	51.4	10,010	80	8
DR015_05-1	D145	OZT779	ABA	All	24.0	7,010	100	2
DR015_06-1	D147	OZT799U*	ABA	All	24.2	2,260	100	3
DR015_06-1	D147	OZT799U1	ABA - HLS	Heavy	12.4	9,460	170	1
DR015_06-1	D147	OZT799U2	ABA - HLS	Light	9.6	NA	NA	0
DR015_07-1	D148A	OZT780	ABA	All	57.9	NA	NA	5
DR015_07-2	D148B	OZT781	ABA	All	55.2	9,880	90	5
DR015_07-3	D370	OZW367	ABA(8M)	All	39.1	11,220	80	7
DR015_07-5	D372	OZW377	ABA(8M)	All	30.2	8,090	70	5
DR015_08-1	D149	OZT449	ABA	All	14.1	8,480	140	3
DR015_09-1	D150	OZT478	ABA	All	6.7	NA	NA	0
DR015_09-2	D151	OZT450	ABA	All	8.8	NA	NA	0
DR015_09-2	D151	OZT450U1	ABA	Light	6.8	NA	NA	0
DR015_10-1	D152	OZT479U*	ABA	All	37.2	14,130	100	4
DR015_10-2	D335	OZU779U1	A-HLS-BA(8M)	Light	41.5	14,200	110	9
DR015_10-2	D335	OZU779U2	A-HLS-BA(8M)	Heavy	46.5	14,390	100	8
DR015_10-3	D336	OZW365	ABA(8M)	All	31.5	11,640	80	7
DR015_10-4	D358	OZW366	ABA(8M)	All	45.6	15,570	90	8
DR015_10-6	D360	OZW376	ABA(8M)	All	34.8	17,160	120	7
DR015_10-7	D600	OZW379	A-HLS-BA(8M)	Light	10.9	4,690	90	2
DR015_10-7	D600	OZW380	A-HLS-BA(8M)	Heavy	33.3	10,730	70	4
DR015_10-7	D600	OZW381	A-HLS-BA(8M)	AcidSol	7.8	NA	NA	
DR015_10-8	D601	OZW370	A-HLS-HF-BA(8M)	All	2.3	NA	NA	
DR015_11-1	D153	OZT480	ABA	All	12.2	5,750	150	1
DR015_11-1	D153	OZT480U1	ABA - HLS	Light		NA	NA	

Sample Code	Sample ID	Laboratory Code	Pretreatment Sequence	Fraction	C mass $\mu$ g	$^{14}\text{C}$ years BP	Error $1\sigma$ (years)	Rel. Score
DR015_14-4	D367	OZU780U1	A-HLS-BA(8M)	Light	11.2	12,420	150	5
DR015_14-4	D367	OZU780U2	A-HLS-BA(8M)	Heavy	49.2	13,450	90	8
DR015_98-1	D155	OZW358	A-HF-HLS-BA(8M)	Light	15.7	2,010	60	6
DR015_98-1	D155	OZW359	A-HF-HLS-BA(8M)	Heavy	5.0	NA	NA	
DR015_99-1	D154	OZW356	A-HF-HLS-BA(8M)	Light	6.5	NA	NA	
DR015_99-1	D154	OZW357	A-HF-HLS-BA(8M)	Heavy	0.0	NA	NA	
DR016_01-1	D161A	OZT495	ABA	All	18.3	11,200	160	2
DR016_01-2	D161B	OZT451	ABA	All	19.3	3,940	120	2
DR016_01-3	D161C	OZT496	ABA	All	22.7	10,100	150	3
DR016_01-5	D338	OZW375	ABA(8M)	All	41.8	8,440	70	6
DR018_01-1	D156A	OZT800U2	ABA - HLS	Light	5.0	NA	NA	0
DR018_02-1	D157	OZT788	ABA	All	9.4	NA	NA	0
DR018_03-1	D158A	OZT493	ABA	All	11.8	NA	NA	0
DR018_03-2	D158B	OZT494	ABA	All	35.5	1,710	100	3
DR018_04-1	D159	OZT768U*	ABA	All	14.0	4,260	150	1
DR028_16-1	D316	OZW364	A-HLS-HF-BA(8M)	All	3.0	NA	NA	
DR031_24-1	D324	OZW374	ABA(8M)	All	32.3	8,890	70	8
DR041_05-1	D389	OZW368	ABA(8M)	All	27.6	6,290	100	7
DR108_01-2	D394	OZW415U2	AB-HLS-A(16M)	Heavy	35.0	10,730	90	8
DR108_01-2	D394	OZW415U1	AB-HLS-A(16M)	Light	3.3	NA	NA	0
DR108_01-2	D394	OZW415U3	AB-HLS-A(16M)	AcidSol	3.3	NA	NA	
DT0173_02-1	D683	OZW360	A-HF-BA(8M)	All	1.0	NA	NA	
DT0184_01-1	D673	OZW371	ABA(8M)	All	159.5	405	25	9
DT0688_03-1	D711	OZW421U1	AB-HLS-A(16M)	Light	12.1	8,930	130	3
DT0688_03-1	D711	OZW421U2	AB-HLS-A(16M)	Heavy	34.0	12,680	90	6
DT0688_03-1	D711	OZW421U3	AB-HLS-A(16M)	AcidSol	2.4	NA	NA	
DT0706_01-1	D608	OZW416U2	AB-HLS-A(16M)	Heavy	31.0	7,640	70	7
DT0706_01-1	D608	OZW416U1	AB-HLS-A(16M)	Light	2.6	NA	NA	
DT0706_01-1	D608	OZW416U3	AB-HLS-A(16M)	AcidSol	2.5	NA	NA	
DT0708_05-1	D708	OZW392	A-HLS-BA(8M)	Heavy	69.6	11,090	60	9
DT0708_05-1	D708	OZW391	A-HLS-BA(8M)	Light	5.5	NA	NA	
DT0708_05-1	D708	OZW393	A-HLS-BA(8M)	AcidSol	7.3	NA	NA	
DT1207_01-1	D638	OZW382	A-HLS-BA(8M)	Light	16.6	2,380	80	5
DT1207_01-1	D638	OZW383	A-HLS-BA(8M)	Heavy	20.9	6,870	70	6
DT1207_01-1	D638	OZW384	A-HLS-BA(8M)	AcidSol	6.3	NA	NA	
DT1207_01-2	D639	OZW417U2	A-HLS-BA(16M)	Heavy	39.4	8,650	80	7
DT1207_01-2	D639	OZW417U1	A-HLS-BA(16M)	AcidSol	3.9	NA	NA	
DT1207_03-1	D646	OZW418U1	AB-HLS-A(16M)	Light	10.4	4,970	120	4
DT1207_03-1	D646	OZW418U2	AB-HLS-A(16M)	Heavy	22.0	10,350	110	6
DT1207_03-1	D646	OZW418U3	AB-HLS-A(16M)	AcidSol	2.9	NA	NA	
DT1207_08-3	D662	OZW386	A-HLS-BA(8M)	Heavy	21.9	8,680	80	6
DT1207_08-3	D662	OZW385	A-HLS-BA(8M)	Light	8.0	NA	NA	
DT1207_08-3	D662	OZW387	A-HLS-BA(8M)	AcidSol		NA	NA	
DT1207_12-1	D668	OZW388	A-HLS-BA(8M)	Light	14.6	5,260	80	5
DT1207_12-1	D668	OZW389	A-HLS-BA(8M)	Heavy	22.1	8,240	80	6
DT1207_12-1	D668	OZW390	A-HLS-BA(8M)	AcidSol	4.1	NA	NA	

Sample Code	Sample ID	Laboratory Code	Pretreatment Sequence	Fraction	C mass $\mu\text{g}$	$^{14}\text{C}$ years BP	Error $1\sigma$ (years)	Rel. Score
DT1218_01-1	D724	OZW372	ABA(8M)	All	36.2	4,100	60	8
DTD1225_02-1	D749	OZW373	A-HLS-HF-BA(8M)	All	6.1	NA	NA	0
DTD1225_03-1	D751	OZW361	A-HF-BA(8M)	All	1.6	NA	NA	
FW002_02-1	D002	OZT782	ABA - HLS	Light	43.5	660	60	5
FW004_11-1	D011	OZT783	ABA - HLS	Light	180.0	210	25	8
FW010_02-1	D015	OZT784	ABA - HLS	Light	84.2	590	45	6
FW010_04-1	D017	OZT762U*	ABA	All	8.3	NA	NA	0
FW010_06-1	D019	OZT785U1	A(conc)	AcidSol	3470.0	7,560	45	7
FW010_06-1	D019	OZT785U*	A(conc)BA	Residue	58.4	NA	NA	7
FW014_01-1	D025	OZW352	A-HF-HLS-BA(8M)	Light	60.8	1,895	40	7
FW014_01-1	D025	OZW353	A-HF-HLS-BA(8M)	Heavy	13.5	2,560	70	3
FW014_01-1	D025	OZT455	ABA	All	86.8	5,150	70	7
FW014_01-1	D025	OZT444	ABA	All	92.6	5,820	70	8
FW014_02-1	D026	OZT456	ABA	All	30.1	6,410	60	5
FW014_03-1	D027	OZT445	ABA	All	230.0	3,475	30	8
FW016_01-1	D020	OZT763U1	ABA - HLS	Light	8.0	NA	NA	1
FW016_02-1	D021	OZT764U*	ABA	All	68.0	630	40	5
KG002_01-1	D453	OZW378	ABA(8M)	All	52.4	NA	NA	
KG002_02-1	D455	OZU781U2	A-HLS-BA(8M)	Heavy	43.9	10,010	60	7
KG002_02-1	D455	OZU781U1	A-HLS-BA(8M)	Light	120.0	13,030	80	9
KG002_03-1	D456	OZW369	A-HLS-HF-BA(8M)	All	5.0	NA	NA	
KG020_08-1	D472	OZU783U1	A-HLS-BA(8M)	Light	28.2	9,800	180	7
KG020_08-4	D475	OZU784U1	A-HLS-BA(8M)	Light	9.9	11,510	270	5
KG021A_01-2	OM14-02	OZT497	ABA	All	16.0	10,060	150	2
KG021A_01-3	OM14-03	OZT770U*	ABA	All	5.2	NA	NA	0
KG021A_04-1	OM14-04	OZT452x	ABA	All	14.2	7,730	150	2
KG021A_05-1	OM14-05	OZT771U1	ABA - HLS	Heavy	15.6	6,750	130	2
KG021A_05-1	OM14-05	OZT771U2	ABA - HLS	Light	6.3	NA	NA	2
KG021A_06-1	D459	OZU782U2	A-HLS-BA(8M)	Heavy	46.5	12,970	80	7
KG021A_06-1	D459	OZU782U1	A-HLS-BA(8M)	Light	56.0	16,940	120	9
KG028A_03-1	D480	OZU785U2	A-HLS-BA(8M)	Heavy	40.7	11,750	80	7
KG028A_03-1	D480	OZU785U1	A-HLS-BA(8M)	Light	24.7	12,590	200	6
KG071_01-1	D855	OZW425U2	ABA(16M)	Heavy	25.7	4,300	60	4
KG071_01-1	D855	OZW425U1	ABA(16M)	AcidSol	7.4	NA	NA	
KGD236_01-1	D825	OZW422U2	A-HLS-BA(8M)	Heavy	14.1	3,610	90	5
KGD236_01-1	D825	OZW422U1	A-HLS-BA(8M)	AcidSol	6.0	NA	NA	
KGD244_03-1	D835	OZW414U2	A-HLS-BA(8M)	Heavy	60.2	9,145	50	9
KT1227_01-5	D821	OZW420U2	A-HLS-BA(16M)	Heavy	35.7	5,540	80	6
KT1227_01-5	D821	OZW420U1	A-HLS-BA(16M)	AcidSol	4.8	NA	NA	
KT1229_01-1	D814	OZW419U2	A-HLS-BA(8M)	Heavy	25.5	7,280	70	6
KT1229_01-1	D814	OZW419U1	A-HLS-BA(8M)	AcidSol	7.6	NA	NA	

Note: Codes and abbreviations are described in Chapter 2. All dates are uncalibrated. NA indicates the radiocarbon measurement failed or was not attempted because the carbon mass was too small. The  $\delta^{13}\text{C}$  of all samples was not able to be reliably measured but is assumed to be -25‰ for the isotopic correction, based on an average for other similar samples.

**Table 2 Calibrated age ranges for old wasp nests**

Sample Code	Laboratory Code	percent Modern Carbon	Error (1 $\sigma$ )	Calibrated date cal BP (95.4% probability range)			On Art?	Rel. Score
				from	to	Median		
DR006_03-1	OZT791	17.96	0.19	16,980	16,380	16,680	Over	5
DR006_05-1	OZT801U2	102.39	1.35	270	...	90	Over	2
DR006_05-1	OZT801U1	67.87	1.11	3,580	2,880	3,260	Over	1
DR006_08-1	OZT453x	15.32	0.33	18,750	17,980	18,410	Under	3
DR006_09-1	OZT769U*	84.53	1.09	1,410	960	1,210	Under	3
DR007_03-1	OZT793U2	98.25	1.14	310	...	140	Over	2
DR007_03-2	OZT794U2	108.29	1.50	...	-10	10	Over	2
DR007_04-1	OZW423U2	35.04	0.24	9,540	9,150	9,410	Under	9
DR008_01-2	OZT489	77.06	0.44	2,130	1,890	2,020	Under	5
DR008_02-1	OZT458	39.14	0.68	8,590	8,010	8,290	Over	1
DR009_02-1	OZT446	26.31	0.42	12,970	12,100	12,660	Under	5
DR012C_02-1	OZT795U*	33.77	0.46	10,150	9,480	9,710	Under	4
DR013_01-2	OZT787	93.83	0.47	560	460	510	Over	4
DR013_04-1	OZT775	22.72	0.24	14,020	13,500	13,720	Under	5
DR013_05-1	OZT776	35.87	0.34	9,420	8,990	9,170	Over	2
DR013_06-1	OZU776U1	26.01	0.39	13,070	12,480	12,750	Under	7
DR013_06-1	OZU776U2	24.36	0.26	13,410	13,080	13,220	Under	7
DR013_06-1	OZT447	14.79	0.35	18,940	18,230	18,590	Under	3
DR013_09-1	OZT797U*	23.81	0.24	13,570	13,180	13,370	Under	5
DR013_09-1	OZT797U1	13.74	0.27	19,550	18,880	19,210	Under	3
DR013_09-1	OZT797U2	12.15	0.15	20,720	20,140	20,420	Under	7
DR013_09-2	OZU777U1	84.31	6.32	2,770	150	1,360	Under	8
DR013_09-2	OZT798U2	54.18	0.48	5,900	5,460	5,630	Under	7
DR013_09-2	OZW355	28.13	0.36	12,440	11,270	11,760	Under	5
DR013_09-2	OZU777U2	24.89	0.22	13,190	12,850	13,060	Under	8
DR013_09-2	OZT798U1	24.33	0.44	13,500	12,920	13,230	Under	3
DR013_09-2	OZW354	14.03	0.33	19,490	18,710	19,050	Under	5
DR013_10-1	OZT462	46.97	0.67	7,250	6,630	6,890	Under	3
DR015_01-1	OZT477	42.00	0.88	8,170	7,430	7,780	Over	2
DR015_01-2	OZT492	91.16	1.28	910	500	660	Over	1
DR015_04-1	OZT448U1	44.87	3.78	8,980	5,890	7,280	Over	1
DR015_04-2	OZU778U1	41.76	0.45	7,980	7,620	7,810	Over	5
DR015_04-2	OZU778U2	28.76	0.25	11,720	11,230	11,460	Over	8
DR015_05-1	OZT779	41.77	0.47	7,980	7,620	7,810	Over	2
DR015_06-1	OZT799U*	75.50	0.90	2,490	1,930	2,210	Over	3
DR015_06-1	OZT799U1	30.78	0.63	11,180	10,280	10,710	Over	1
DR015_07-2	OZT781	29.25	0.31	11,640	10,880	11,260	Over	5
DR015_07-3	OZW367	24.74	0.22	13,250	12,920	13,120	Under	7
DR015_07-5	OZW377	36.51	0.32	9,260	8,640	8,920	Over	5
DR015_08-1	OZT449	34.78	0.59	9,730	9,020	9,430	Over	3
DR015_10-1	OZT479U*	17.23	0.19	17,390	16,930	17,160	Under	4

Sample Code	Laboratory Code	percent Modern Carbon	Error (1σ)	Calibrated date cal BP (95.4% probability range)			On Art?	Rel. Score
				from	to	Median		
DR015_10-2	OZU779U1	17.06	0.23	17,690	16,940	17,230	Over	9
DR015_10-2	OZU779U2	16.67	0.20	17,860	17,130	17,510	Over	8
DR015_10-3	OZW365	23.47	0.21	13,600	13,310	13,470	Over	7
DR015_10-4	OZW366	14.39	0.16	19,000	18,670	18,830	Under	8
DR015_10-6	OZW376	11.81	0.17	20,930	20,430	20,680	Under	7
DR015_10-7	OZW379	55.77	0.59	5,590	5,050	5,390	Over	2
DR015_10-7	OZW380	26.30	0.22	12,750	12,490	12,690	Over	4
DR015_11-1	OZT480	48.88	0.89	6,890	6,210	6,520	Over	1
DR015_14-4	OZU780U1	21.32	0.39	15,090	14,040	14,520	Under	5
DR015_14-4	OZU780U2	18.73	0.20	16,440	15,860	16,160	Under	8
DR015_98-1	OZW358	77.85	0.49	2,050	1,750	1,920	No	6
DR016_01-1	OZT495	24.80	0.49	13,340	12,760	13,080	Over	2
DR016_01-2	OZT451	61.26	0.87	4,800	3,980	4,320	Over	2
DR016_01-3	OZT496	28.44	0.53	12,440	11,190	11,620	Over	3
DR016_01-5	OZW375	34.96	0.28	9,540	9,140	9,430	Over	6
DR018_03-2	OZT494	80.80	0.99	1,830	1,350	1,580	Over	3
DR018_04-1	OZT768U*	58.81	1.10	5,290	4,410	4,770	Over	1
DR031_24-1	OZW374	33.05	0.25	10,190	9,690	9,960	Under	8
DR041_05-1	OZW368	45.71	0.56	7,420	6,900	7,150	Over	7
DR108_01-2	OZW415U2	26.31	0.27	12,770	12,480	12,680	Under	8
DT0184_01-1	OZW371	95.07	0.29	500	320	450	Over	9
DT0688_03-1	OZW421U1	32.89	0.52	10,250	9,550	9,970	Under	3
DT0688_03-1	OZW421U2	20.62	0.21	15,330	14,540	15,060	Under	6
DT0706_01-1	OZW416U2	38.64	0.29	8,550	8,210	8,400	Over	7
DT0708_05-1	OZW392	25.14	0.17	13,100	12,840	12,990	Under	9
DT1207_01-1	OZW382	74.36	0.65	2,710	2,140	2,370	Over	5
DT1207_01-1	OZW383	42.50	0.36	7,840	7,570	7,680	Over	6
DT1207_01-2	OZW417U2	34.09	0.32	9,890	9,460	9,600	Over	7
DT1207_03-1	OZW418U1	53.86	0.78	5,930	5,330	5,690	Over	4
DT1207_03-1	OZW418U2	27.56	0.37	12,610	11,730	12,140	Over	6
DT1207_08-3	OZW386	33.93	0.31	9,900	9,490	9,630	Over	6
DT1207_12-1	OZW388	51.96	0.49	6,270	5,750	6,000	Over	5
DT1207_12-1	OZW389	35.84	0.34	9,420	9,000	9,180	Over	6
DT1218_01-1	OZW372	60.36	0.33	4,800	4,300	4,490	Over	8
FW002_02-1	OZT782	92.14	0.65	670	530	600	Over	5
FW004_11-1	OZT783	97.43	0.25	290	100	200	Over	8
FW010_02-1	OZT784	92.90	0.50	640	500	550	Over	6
FW010_06-1	OZT785U1	39.03	0.20	8,410	8,190	8,340	Over	7
FW014_01-1	OZW352	78.97	0.36	1,880	1,700	1,790	Over	7
FW014_01-1	OZW353	72.72	0.57	2,760	2,360	2,580	Over	3
FW014_01-1	OZT455	52.65	0.39	6,000	5,660	5,840	Over	7
FW014_01-1	OZT444	48.46	0.38	6,740	6,400	6,580	Over	8
FW014_02-1	OZT456	45.01	0.32	7,430	7,160	7,300	Over	5



Sample Code	Laboratory Code	percent Modern Carbon	Error (1 $\sigma$ )	Calibrated date cal BP (95.4% probability range)			On Art?	Rel. Score
				from	to	Median		
FW014_03-1	OZT445	64.89	0.24	3,830	3,580	3,700	Over	8
FW016_02-1	OZT764U*	92.47	0.44	660	520	600	Over	5
KG002_02-1	OZU781U2	28.77	0.21	11,710	11,240	11,450	Under	7
KG002_02-1	OZU781U1	19.75	0.19	15,790	15,280	15,550	Under	9
KG020_08-1	OZU783U1	29.51	0.66	11,840	10,590	11,170	Under	7
KG020_08-4	OZU784U1	23.86	0.78	14,010	12,840	13,380	Under	5
KG021A_01-2	OZT497	28.58	0.53	12,430	11,170	11,570	Both	2
KG021A_04-1	OZT452x	38.19	0.68	8,990	8,190	8,510	Over	2
KG021A_05-1	OZT771U1	43.15	0.69	7,840	7,330	7,580	Over	2
KG021A_06-1	OZU782U2	19.90	0.20	15,730	15,220	15,460	Under	7
KG021A_06-1	OZU782U1	12.14	0.17	20,770	20,130	20,420	Under	9
KG028A_03-1	OZU785U2	23.17	0.21	13,770	13,430	13,570	Under	7
KG028A_03-1	OZU785U1	20.86	0.50	15,450	14,090	14,800	Under	6
KG071_01-1	OZW425U2	58.59	0.41	4,980	4,580	4,820	Over	4
KGD236_01-1	OZW422U2	63.82	0.64	4,150	3,640	3,870	Over	5
KGD244_03-1	OZW414U2	32.03	0.20	10,490	10,180	10,270	Over	9
KT1227_01-5	OZW420U2	50.20	0.47	6,490	6,010	6,300	Over	6
KT1229_01-1	OZW419U2	40.38	0.33	8,190	7,930	8,070	Over	6

Note: Dates calibrated using OxCal v4.4.2 Heaton (2020); r:5 Bronk Ramsey, C. (2009), Atmospheric data from Hogg et al (2020)

## References

Bronk Ramsey, C. (2009). Bayesian analysis of radiocarbon dates. *Radiocarbon*, 51(1), 337–360.

Heaton, T., Blaauw, M., Blackwell, P., Bronk Ramsey, C., Reimer, P., & Scott, M. (2020). The IntCal20 approach to radiocarbon calibration curve construction: a new methodology using Bayesian splines and errors-in-variables. *Radiocarbon*, 62.

Hogg, A., Heaton, T., Hua, Q., Palmer, J., Turney, C., Southon, J., Bayliss, A., Blackwell, P., Boswijk, G., Bronk Ramsey, C., Petchey, F., Reimer, P., Reimer, R., & Wacker, L. (2020). SHCal20 Southern Hemisphere calibration, 0–55,000 years cal BP. *Radiocarbon*, 62.

## Appendix 3

### Additional published work

The candidate contributed to three publications related to the present work.

The first was published by the Journal of Archaeological Science: Reports on 18th July 2017. The present author performed the mineralogical analysis of the X-ray Diffraction data. The mineralogical analysis of rock shelter accretions identified those carbon-bearing minerals that may contaminate old wasp nest samples as described in Chapter 2.

#### **Mineral deposition systems at rock art sites, Kimberley, Northern Australia - Field observations.**

Green, H., A. Gleadow, **D. Finch**, J. Hergt and S. Ouzman  
Journal of Archaeological Science-Reports 14: 340-352, (2017).  
[doi: 10.1016/j.jasrep.2017.06.009](https://doi.org/10.1016/j.jasrep.2017.06.009)

#### Abstract

Mineral coatings, fringes, glazes and skins forming on the surfaces of sandstone rock shelters in Western Australia's Kimberley region offer the potential to provide datable materials to bracket ages of rock art motifs with which they are often spatially associated. These mineral deposition systems, which occur at the interface between the atmosphere and host rock, have never been characterised specifically and their overall formation mechanisms have yet to be completely established. This study serves to increase the understanding of complex processes behind the formation and long-term preservation potential of these mineral deposition systems. This is achieved by combining field observations with multiple mineralogical and geochemical characterisation techniques. Using both wet and dry season field observations and 94 mineral accretion samples collected from three different areas of the Kimberley, we identify four separate mineral deposition systems; polychrome fringes, dispersed wall coatings, floor glazes and silica skins. Detailed observations of the different characteristics of each deposition system are used to assess their suitability for the application of radiometric dating methods. Coherent internal stratigraphies are identified in polychrome fringe accretions, essential for the reliable application of uranium-series dating techniques, whilst floor glaze mineralogy, identified as dominated by carbon-bearing calcium oxalate minerals, provides radiocarbon dating opportunities. Consequently, this study provides a rigorous basis for establishing targeted sampling and analysis strategies essential for reliable and replicable rock art dating as well as having implications for rock art conservation.

The second paper was published by Data in Brief on 18th July 2017. The present author provided the mineralogical analysis of the XRD data. This paper provides additional detail to that provided in the first paper.

## **Characterisation of mineral deposition systems associated with rock art in the Kimberley region of north west Australia.**

Green, H., A. Gleadow and **D. Finch**

Data in Brief, (2017).

[doi: 10.1016/j.dib.2017.08.029](https://doi.org/10.1016/j.dib.2017.08.029)

### Abstract

This data article contains mineralogical and chemical data from mineral accretions sampled from rock art shelters in the Kimberley region of north west Australia. The accretions were collected both on and off pigment and engraved rock art of varying styles observed in the Kimberley with an aim of providing a thorough understanding of the formation and preservation of such materials in the context of dating [1]. This contribution includes processed powder X-ray Diffraction data, Scanning Electron Microscopy energy dispersive spectroscopy data, and Laser Ablation ICP-MS trace element mapping data.

The third paper was published by the Journal of Archaeological Method and Theory on 2nd August 2020. The present author identified a suitable wasp nest sample under relevant rock art, collected the sample (D755, OZW423U2), performed sample pretreatment and interpreted the radiocarbon age. Further details of this sample are discussed in Chapter 5.

## **Investigating the Anthropic Construction of Rock Art Sites Through Archaeomorphology: the Case of Boroloka, Kimberley, Australia.**

Delannoy, J.-J., B. David, K. Genuite, R. Gunn, **D. Finch**, S. Ouzman, H.

Green, P. Veth, S. Harper and R. J. Skelly

Journal of Archaeological Method and Theory: 1-39, (2020).

[doi: org/10.1007/s10816-020-09477-4](https://doi.org/10.1007/s10816-020-09477-4)

### Abstract

Archaeologists usually see, and understand, rock shelters as taphonomically active, but pre-existing, physical structures onto which people undertake a variety of actions including rock art. Our aim in this paper is not only to document the changes undergone by rock shelters but also to identify traces of anthropic actions that have intentionally led to these changes. Recent research in northern Australia provides empirical evidence that for thousands of years, Aboriginal peoples altered the physical shape of rock shelters by removing masses of rock to create alcoves, restructure internal spaces and create stoneworked furniture. Through archaeomorphological research, this paper presents evidence from Boroloka in Australia's Kimberley region, where hard quartzite monoliths were shaped and engaged as architectural designs by Aboriginal people prior to painting many surfaces, making us rethink what have traditionally been distinguished as natural versus cultural dimensions of archaeological landscapes and rock art sites.